FURTHER DEVELOPMENT, UPDATING AND ASSESSMENT OF THE SCS-SA MODEL FOR DESIGN FLOOD ESTIMATION IN SOUTH AFRICA USING A CONTINUOUS SIMULATION APPROACH

Report
to the Water Research Commission

by

JC Smithers[1,2], TJ Rowe[1], RE Schulze[1], N Mabila[1],
NS Dlamini[1], U Maharaj[1,2], R Ramlall[1]

[1]Centre for Water Resources Research
[2]College of Agriculture, Engineering and Science,
University of KwaZulu-Natal Pietermaritzburg

Report No. 2926/1/22
ISBN 978-0-6392-0462-8

August 2022

WATER
RESEARCH
COMMISSION

Obtainable from:

Water Research Commission

Private Bag X03

Gezina, 0031

orders@wrc.org.za or download from www.wrc.org.za

EXECUTIVE SUMMARY

The assessment of flood risk by associating a flood event with the probability of an exceedance or return period is the standard approach to design flood estimation (DFE) in most countries (Smithers, 2012; Kang et al., 2013). These design flood estimates are essential for designing hydraulic infrastructure such as dams, bridges, culverts and other drainage structures (Lamb et al., 2016). A National Flood Studies Programme (NFSP) has been initiated to overhaul DFE procedures used in South Africa (Smithers et al., 2016). Some of the recommendations in the NFSP include the further development and assessment of a continuous simulation modelling (CSM) approach to DFE in South Africa, and updating and modernising the SCS-SA method.

Motivation for a CSM approach to DFE in South Africa includes the following:

- Rainfall records are generally more numerous, accurate and spatially representative in comparison to streamflow records
- The continuous simulation modelling approach has the potential to overcome many of the limitations of event-based rainfall-runoff methods
- Local and international trends promote the application of continuous simulation modelling approaches to design flood estimation
- The method has significant potential to account for land-use change, climate change and operational systems (e.g. dams) within the catchment, which impact on design flood estimates, thus making the approach more robust and providing greater confidence in the results

In addition to the CSM approach, the SCS-SA event-based approach (Schmidt and Schulze, 1987; Schulze et al., 1992; 2004) is widely used in practice in South Africa for DFE. The method is, however, outdated and was developed using the limited data available at the time.

Reasonable results have been obtained through several pilot research studies applying the agrohydrological model of the Agricultural Catchments Research Unit (ACRU) for DFE in South Africa (Smithers et al., 1997; 2001; 2007; 2013; Chetty and Smithers, 2005; Rowe, 2015). However, several aspects of the ACRU CSM approach that require further development and refinement have been identified, including the estimation of peak discharge, e.g. improving the estimation of catchment lag (Gericke and Smithers, 2016), the further investigation of appropriate temporal rainfall distributions and disaggregation of daily rainfall, methods to generate or stochastically extend rainfall records, the updating of land-cover information and rainfall records, and the further refinement of flood-routing methods (Smithers et al., 2013).

AIMS AND OBJECTIVES

The aims of this project were the following:

- Refine and update the SCS-SA model for design flood estimation to account for antecedent moisture conditions and the joint association of rainfall and runoff using the results and methodology from a CSM system
- Compare the performance of the CSM system to the traditional and updated SCS-SA models
- Further develop and assess the CSM approach, including the potential incorporation and assessment of improved daily rainfall disaggregation methods to account for the temporal distribution of daily rainfall
- Compare the performance of the ACRU CSM system that was developed to simpler, parameter-sparse CSM methods applied internationally

Hence, this project contributes directly to the objectives of the NFSP by updating and modernising DFE methods for South Africa.

In order to meet the above aims, the following objectives were set:

- Assess the performance of published and derived SCS curve numbers for DFE in South Africa
- Further develop and assess the ACRU CSM system for DFE in South Africa
- Assess the performance of existing methods, or develop a new or improved method to more adequately disaggregate daily rainfall within the ACRU model
- Select and assess the performance in South Africa of a simpler, parameter-sparse CSM used internationally and compare the performance with the ACRU CSM that was developed
- Investigate the potential to incorporate a joint probability approach (JPA) into the updated version of the SCS-SA model
- Develop, configure and assess the CSM system and incorporate the results into an updated SCS-SA model

Five studies to address the first five objectives were undertaken as postgraduate research projects, as summarised in chapters 2 to 6. The development and assessment of the SCS-CSM model that was developed in the study are detailed in 0.

AN ASSESSMENT OF THE PERFORMANCE OF PUBLISHED AND DERIVED SCS CURVE NUMBERS FOR DESIGN FLOOD ESTIMATION IN SOUTH AFRICA

The South African adaptation to the SCS-CN model (SCS-SA) is a commonly used event-based rainfall-runoff method for DFE on small catchments (< 30 km^2). The model is simple to use and only requires the selection of a curve number (CN) from a published CN table and daily design rainfall as input to simulate runoff volume. The SCS-CN runoff equation was originally developed to transform a daily rainfall depth to a runoff depth, which is used to estimate peak discharge. The published CNs were derived from observed data from catchments in the USA for selected land-cover and soil classes (Mishra and Singh, 2003). The published CNs are widely used internationally. However, the accuracy of the CN values that were published by the Soil Conservation Service (SCS) are unknown.

The use of published CNs limits the application of the SCS-SA model on catchments with land-cover classes and hydrological soil groups (HSGs) specific to South Africa. In addition, numerous studies have concluded that data-derived CNs result in better runoff estimates. In the SCS-SA model, the coefficient of initial abstraction (c) value (0.2) is not consistent with the c value used to calculate the published CNs (0.1), thus increasing the uncertainty related to the estimated runoff depths. The aim of this component of the study was therefore to investigate whether published CNs from the SCS-SA manual or data-derived CNs result in better runoff estimates, and to propose a CN-derivation technique that may be suitable for use in South Africa with results from a CSM.

A literature review indicated that the long periods of observed and simulated rainfall-runoff (P-Q) data could be used to assess available CN-derivation techniques. The approach used in this study was to investigate whether the published CNs could be replicated using observed or simulated P-Q data from small South African catchments. Various CN-derivation techniques were tested, and the derived CNs were compared to the published CNs. In addition, the current published CNs were evaluated to determine if they result in good DFE. The data-derived CNs determined using different methods were also evaluated to determine if they result in better DFE compared to the use of published CN values. Based on the results that were obtained, the CNs derived using observed annual maximum P-Q events and c = 0.1 were closest to the published CNs.

Subsequently, the methods that resulted in CNs similar to the published CNs were applied using simulated runoff from the ACRU model. The simulated annual maximum runoff depths from ACRU were parameterised using the rules developed by Rowe (2019) ($ACRU_{TR\text{-}P}$). This resulted in derived CNs that were more similar to the published CNs than the CNs derived using observed P-Q data.

The published CNs were then assessed to determine whether the design runoff estimated using the SCS-CN equation ($Q_{T,S}$), applied with published CN values, resulted in good estimates of design-observed runoff depths ($Q_{T,O}$).

The results of the analysis of published CNs indicated that the published CNs resulted in poor estimates of $Q_{T,O}$. However, the CNs calculated with c = 0.1 and design-observed P-Q depths for the 10-year return period ($CN_{10,0.1}$) resulted in good estimates of $Q_{T,O}$. Similarly, the $CN_{10,0.1}$ derived using runoff depths simulated with $ACRU_{TR\text{-}P}$ ($S\text{-}CN_{10,0.1}$) also resulted in improved estimates of $Q_{T,O}$ compared to the published CNs. The $S\text{-}CN_{10,0.1}$ values derived using Q values simulated using the conventional ACRU ($ACRU_{CON\text{-}P}$) parameterisation resulted in poorer estimates of $Q_{T,O}$. However, when the design peak discharges were calculated using the SCS-SA model, the $S\text{-}CN_{10,0.1}$ ($ACRU_{CON\text{-}P}$) generally resulted in the lowest mean average error between the observed and design peak discharge values.

Numerous different CN-derivation methods have been reported in the literature, but no single method has been universally accepted to derive CNs. In this study, CN values were calculated for study sites in South Africa using both observed P-Q data and simulated Q depths. The statistical comparisons between $Q_{T,O}$ and $Q_{T,S}$ that were done in this study have highlighted the poor performance of the use of published CN values in South Africa. The results from this study also indicate that an improvement in the use of published CNs is to use local P-Q values and frequency-matched P-Q pairs to determine CNs as a function of the return period. The improved performance of the SCS-CN model when using CNs derived with simulated Q depths from $ACRU_{TR\text{-}P}$ implies that the study could potentially be extended to different regions without observed Q data using the simulated Q values. It is, therefore, recommended that the currently used published CN tables be updated using the frequency-matching method to include land-cover classes that are unique to South Africa, and hence to remove the subjective interpolation when selecting a CN for a land cover and an HSG combination that is not included in the published CN tables.

DEVELOPMENT AND ASSESSMENT OF AN IMPROVED CONTINUOUS SIMULATION MODELLING SYSTEM FOR DESIGN FLOOD ESTIMATION IN SOUTH AFRICA USING THE ACRU MODEL

The methods used to estimate design floods in South Africa are outdated and in need of revision. A National Flood Studies Programme was initiated to overhaul DFE procedures in South Africa. One of the recommendations of the NFSP is the further development and assessment of a CSM approach to DFE for South Africa. Consequently, the aim of this component of the study was to further develop and assess the performance of an improved comprehensive CSM system to estimate design flood discharges consistently and reliably in small catchments (0–100 km^2) in South Africa using the ACRU model.

The CSM approaches that are applied locally and internationally for DFE were reviewed to identify research gaps and serve as a guideline for the development of an enhanced CSM system for DFE in South Africa. The literature review highlighted that the CSM approach to DFE has many advantages over traditional event-based rainfall-runoff DFE techniques. The literature review includes a list of recommendations and steps to develop and adopt a CSM approach for DFE. The first critical step that was identified and required was the development of a comprehensive CSM system using the ACRU model. This included the structure of the system and how to implement it, including an enhanced land-cover and soil classification to apply with the system, and default input information and databases to use with the system.

Subsequently, a comprehensive CSM system for DFE using the ACRU model was developed and described in detail. Based on similarities in the runoff-generation equation in ACRU and the SCS-SA models, and the fact that the SCS-SA model is relatively simple and widely applied in practice, the CSM system was adapted to be consistent with the land-cover classification used in the SCS-SA model. The performance of the CSM system that was developed was assessed and verified using observed data.

Through the assessments and verifications performed, an inconsistency between daily simulated stormflow volumes and the volume of stormflow used in the daily stormflow peak discharge equation used in the ACRU model was identified. Therefore, a revision was introduced, which is more conceptually correct, with only stormflow leaving the catchment on a given day contributing to the peak discharge on the day. The revision corrected the inconsistency and significantly improved the results, thereby providing an improved methodology to estimate peak discharges more accurately in ACRU.

Despite the improvement in the results, a general over-simulation of peak discharges was still evident. Thus, further investigation of the ACRU stormflow peak discharge computation was performed to identify an approach that provided the most acceptable results. This included a performance assessment of both the SCS single unit hydrograph (UH) approach and the incremental UH approach. The performance of each approach was assessed using both estimated parameters and parameters derived from observed data. Comparison of the results from the two approaches indicated that more accurate results are obtained when applying the incremental UH approach using either estimated or observed parameter inputs. In terms of the incremental UH approach, the approach was identified to be more sensitive to the use of synthetic daily rainfall distributions compared to estimated lag times.

The impact of model configuration on the performance of the developed ACRU CSM system was assessed to propose a final CSM system for DFE in South Africa. Results when using site-specific land-cover and soil information were compared to those obtained when different sources of input information were used. In addition, the most appropriate current databases to use with the CSM system were defined, providing users with the most appropriate default information currently available for use in the absence of site-specific information.

Lastly, the performance of the revised ACRU CSM system was compared to the widely applied SCS-SA model using the same input information. The performance of the revised ACRU CSM system in terms of DFE was found to be better than the SCS-SA model. In addition, several advantages of the ACRU CSM system over the traditional SCS-SA approaches were identified. Recommendations were made to further improve on the CSM system developed in this study.

ASSESSING THE PERFORMANCE OF TECHNIQUES FOR DISAGGREGATING DAILY RAINFALL FOR DESIGN FLOOD ESTIMATION IN SOUTH AFRICA

As indicated above, the temporal distribution of rainfall has a significant impact on the magnitude and timing of flood peak discharges. In order to improve DFE methods based on event-based or continuous simulation rainfall runoff models, it is generally necessary to use sub-daily timestep rainfall hyetographs as input. However, the number of recording rain gauges, which provides sub-daily timestep rainfall in South Africa, is relatively low compared to those that provide daily data. Rainfall temporal disaggregation (RTD) techniques can be used to produce finer-resolution data from coarser-resolution data. Several RTD approaches have been applied in South Africa. However, the application of RTD approaches locally is relatively limited, both in terms of the diversity of approaches and cases of application, compared to those developed and applied internationally. Therefore, a need exists to further assess the performance of locally applied RTD approaches, as well as to update the list of available approaches through the inclusion of internationally developed and used RTD techniques. This component of the study contains an overview of the application of selected RTD approaches on different sets of rainfall data in South Africa and the performance of the methods. An extensive literature review was conducted on approaches used for disaggregating rainfall data, both internationally and locally.

Suitable approaches were identified based on an examination of case studies of their application and on simplicity of application, data requirements and performance in regions with similar climates to South Africa. A pilot study was performed in which selected local and international RTD approaches were applied to disaggregate daily rainfall data. Some approaches were applied in their original form, while others were modified. Rainfall days with total depths less than 10 mm were excluded from the assessment.

Temporal distributions of rainfall were represented by dimensionless Huff curves, which served as the basis for the comparison of observed and disaggregated rainfall. It was found that, for daily rainfall, the SCS3, SCS4 and Knoesen model approaches performed considerably better than the other approaches at the pilot study site. The RTD approaches were further assessed using data from 14 additional rainfall stations located in different homogenous rainfall regions. For the additional stations, the Knoesen semi-stochastic model's disaggregated depths provided the most realistic temporal distributions overall, followed by the SCS-SA distributions. In additional, an adapted form of the triangular distribution was found to show potential for disaggregation when a generalised value for the timing of the peak was utilised.

AN ASSESSMENT OF SIMPLE CONTINUOUS SIMULATION MODELLING APPROACHES FOR DESIGN FLOOD ESTIMATION IN SOUTH AFRICA

Continuous simulation modelling has been investigated and has received increasing attention in the local and international literature as an approach with potential for DFE. In South Africa, the ACRU CSM has been used successfully in pilot studies for DFE. However, the model is comprehensive, and the input data requirements, time and expertise required to set up the model remain a challenge. Therefore, there is a need to evaluate the use of simpler continuous simulation (CS) models for DFE, which have fewer parameters, are easy to apply, and are less data demanding. The aim of this component of the study was to assess the performance of simple CS models for DFE in South Africa. Simple CS models from local and international literature were reviewed and the Modèle du Génie Rural à Quatre Paramètres Journalier (GR4J) (daily timestep model) and Génie Rural à Quatre Paramétres Horaires (GR4H) (hourly timestep model), developed by airGR and available as open-source software in the R programming language, were selected. Their performance was assessed on six catchments in South Africa. The models were set up and calibrated for three scenarios at both daily and hourly simulation timesteps, and an additional calibration scenario was included for the hourly simulation timestep. Due to rainfall data limitations and errors in the data, only three of the six catchments were simulated at both daily and hourly timesteps. A sensitivity analysis was also conducted, which assessed the impact of different daily rainfall disaggregation techniques on flow simulations. A comparison was undertaken of the GR4J's performance in the larger and smaller catchments to analyse the effect of catchment size on model performance. In general, the models were found to perform reasonably well at both daily and hourly timesteps. However, the daily timestep model was found to produce better results. At both timesteps, the design peak discharges were generally under-simulated for both calibration and validation. Only a small improvement in the design flood peak discharge estimates was obtained for the hourly timestep simulations (GR4H) compared to the daily timestep simulations (GR4J). However, in most cases, the improvement was insignificant and strongly dependent on the quality of the data. The use of disaggregation techniques to generate hourly hyetographs from daily rainfall data resulted in adequate simulated and observed flows, and demonstrated their usefulness in areas where the availability of hourly data is limited, despite further under-simulation of design peak discharges. The daily model performed acceptably in both small and large catchments. The potential for the use of a simple CSM for DFE in South Africa has been shown in this study. However, a further assessment of the models is recommended, including improved calibration techniques using a multi-criteria objective function and the development of a method to estimate model parameters at ungauged sites.

DEVELOPMENT AND ASSESSMENT OF AN ENSEMBLE JOINT PROBABILITY APPROACH USING THE SCS-SA MODEL

The DFE methods in South Africa are based on the statistical analysis of streamflow data and rainfall-based methods. Given the limited availability of observed streamflow and that rainfall data has longer records from a spatially denser network than streamflow records, rainfall-based DFE methods are widely used at ungauged sites. A key assumption in rainfall event-based methods for DFE is that the exceedance probability of the estimated flood is the same as the input design rainfall. This equality of rainfall and flood return periods is generally not true given the use of model parameters that represent average conditions in the catchment and the impact of antecedent moisture conditions on hydrological responses.

Hence, a joint probability approach is used, where the key input model parameters, and not only the input design rainfall, are treated probabilistically to address the limitations associated with rainfall event-based DFE methods. The underlying approach to a JPA is that, instead of the use of a single combination of input variables to determine flood characteristics, the method uses multiple likely combinations of flood-producing parameters to determine the flood characteristics. In this component of the study, a JPA was applied using the SCS-SA model.

The modelling framework used to determine the derived flood frequency curve is based on three principal elements: defining the key model inputs with their respective probability distributions and correlations, using a stochastic model to synthesise sequences of the selected variables, and selecting an appropriate deterministic hydrological model to simulate the flood-generation process. The ensemble of the simulated outputs is used to derive the flood distribution. To evaluate the performance of the Ensemble SCS-SA model, the results were compared to design values computed from the observed streamflow data. A statistical analysis was conducted in conjunction with graphs to assess the performance of the model. The Nash-Sutcliff efficiency (NSE) value, absolute relative difference and mean absolute relative error (MARE) were used to evaluate the model's performance. Using readily available data, probability distributions were derived for one-day design rainfall, time to peak (TP), antecedent moisture conditions and the temporal distribution of daily rainfall. The results produced from applying the Ensemble SCS-SA model indicated that the model was performing relatively poorly in terms of estimating both the observed design runoff volume and the design peak discharge for all the selected test catchments. The use of rainfall duration (TP) in conjunction with the probability distributions of the other key input variables in the Ensemble SCS-SA model resulted in significantly improved estimated design runoff volume and peak discharges for all the test catchments. The Ensemble SCS-SA model has also shown potential and flexibility to deal with uncertainty by accounting for the distributed nature of the input variables and taking on values across the full range of their distribution in the modelling process, thus avoiding the potential of bias that can occur when adopting a single set of predetermined input values. This study has shown the potential and flexibility of the Ensemble SCS-SA model to deal with uncertainty, providing opportunity for the expanded application of the model.

DEVELOPMENT AND ASSESSMENT OF THE SCS-SA CSM SYSTEM FOR DESIGN FLOOD ESTIMATION IN SOUTH AFRICA

CSM for DFE is an emerging approach in design hydrology and overcomes many shortcomings of event-based models, but requires complex rainfall-runoff models and the availability of long continuous and reliable observed or stochastically generated rainfall and climate data series. CSM is the most comprehensive tool to account for joint probabilities in flood frequency estimation. The motivation for using a CSM approach includes better representation of physical processes, and overcomes the restrictive assumptions required for the application of other methods. However, the cost of using a CSM approach is greater than other approaches and needs to be offset against the advantages of the CSM approach. Advantages of the CSM approach include the estimation of design flows at any simulation point and not just at the catchment outlet.

No assumptions need to be made about the design event and hydrograph shapes. Antecedent moisture conditions are explicitly accounted for, and actual or projected land-cover and climate conditions can be simulated. Sources of uncertainty when using a CSM approach include rainfall data, parameter uncertainty and the calibration metric used. In South Africa, the ACRU agrohydrological model has been used in a number of pilot studies on design flood estimation using a CSM approach. It has been further developed in this project.

The SCS-SA CSM system developed in this study uses Excel as a front-end graphical user interface (GUI) to input user information, and Visual Basic code to run compiled executable Fortran code. This extracts the required parameters, configures and runs the ACRU CSM, imports results and generates design peak discharges and hydrographs.

The evaluation of the SCS-SA CSM incorporated a number of configuration and simulation scenarios for design peak discharge estimation, which includes catchment-specific soils, soils for the dominant quinary in the catchment, or each quinary falling in the catchment modelled as a hydrological response unit (HRU) using the quinary soil information for the HRU; one-day duration design rainfall or short-duration rainfall equivalent to time to peak; the “CELRUN” or “DSTORM” design volumes simulated by the ACRU model; and land cover specific to the catchment in the study. The model assessment was performed on 19 catchments.

The following conclusions are drawn from the general trends in the performance of the SCS-SA CSM on all catchments and for each simulation scenario: generally better performance is evident when using DSTORM compared to CELRUN volumes; generally better performance is evident when using time to peak compared to using a one-day duration; and generally better performance is evident when quinary catchments simulated as HRUs and quinary catchments’ soil information are used, compared to using the soil information from the dominant quinary catchment.

COMPARISON OF RESULTS OBTAINED IN THE STUDY

The performance of the models used and developed in this project were compared. The standard and Ensemble SCS-SA were applied to 19 catchments. The SCS-SA CSM model was applied to 19 catchments. The ACRU model was applied to 11 catchments. The GR4J was applied to five catchments. In order to apply the Ensemble SCS-SA model at sites where no observed time to peak data is available, generalised equations were developed using the limited TP data available to estimate TP at sites that do not have observed TP data.

The best performance in terms of design peak discharge estimation was obtained by the Ensemble SCS-SA (time to peak) model, followed by the SCS-SA CSM (time to peak duration, quinary soils, DSTORM volume), standard SCS-SA model (time to peak) and Ensemble SCS-SA (regional equation duration) models, all of which have similarly good performance. The good performance of the Ensemble SCS-SA (regional equation duration) model, despite the limited datasets used in the derivation of the regionalised equations to estimate time to peak, is encouraging and requires further refinement. It is encouraging to note that some of the models developed in this study (the Ensemble SCS-SA and SCS-CSM models) perform better than the standard SCS-SA (one-day duration) model, which is currently used in practice.

DISCUSSION, CONCLUSIONS AND RECOMMENDATIONS

The aims of the project have been met and exceeded. The performance of the Ensemble SCS-SA model and SCS-SA CSM has resulted in major improvements in the estimation of design peak discharges compared to the standard SCS-SA model as currently used in practice.

Some significant findings and developments from this study are as follows:

- The best approaches have been identified to determine CNs for the SCS-SA model for South African catchments, and South African land-cover and soil classifications using observed rainfall and either observed or simulated runoff
- The use of data-derived catchment-specific CNs resulted in improved performance in the SCS-SA model
- The performance of the standard SCS-SA (one-day duration) model for DFE is improved when the time to peak rainfall duration is used
- The Ensemble approach improved the performance of the SCS-SA model and enables the uncertainty to be estimated; it can also tentatively be applied at ungauged sites in South Africa
- The semi-stochastic Knoesen model and SCS-SA distributions have been found to perform acceptably well to disaggregate daily rainfall
- The use a simple, parameter-sparse CSM for DFE has been shown to have potential, but significant further development is required to apply the model at ungauged sites
- Refinements and improvements to the ACRU model for peak discharge estimation have been undertaken and links to parameterise the model using national land-cover and soil classifications have been established
- A SCS-SA CSM system for DFE has been developed, which incorporates many of the results obtained in the study, and has been shown to perform reasonably well
- The models developed in this study (refined ACRU CSM, Ensemble SCS-SA and SCS-CSM) for DFE perform better than the standard SCS-SA (D = one day) model currently used in practice

The following recommendations are made:

- The performance of the models assessed in this study should be expanded to include design volume estimation, and inconsistencies in the performance of the models for transforming a design volume into a design peak discharge should be investigated and resolved
- The beta version of the SCS-SA CSM system should be further developed to include the Knoesen semi-stochastic daily rainfall disaggregation model
- The Ensemble SCS-SA model should be further developed and refined for use in practice
- The ensemble approach should be expanded to include other event-based flood estimation models used in South Africa.

CAPACITY BUILDING

This project has contributed to supporting five postgraduate students. This has resulted in one PhD, one MSc Engineering and three MSc studies being completed and degrees awarded.

ACKNOWLEDGEMENTS

The funding of the project by the Water Research Commission and the contribution of the members of the Reference Group are gratefully acknowledged.

Mr W Nomquphu	Water Research Commission (Chairman)
Mr C Brooker	Chris Brooker and Associates
Mr M Braune	Bio Eng
Mr JP Calitz	eThekwini Municipality
Dr D Dlamini	Department of Water and Sanitation
Mr S Dunsmore	Fourth Element
Prof JA Du Plessis	University of Stellenbosch
Dr OJ Gericke	Central University of Technology
Dr TR Kjeldsen	University of Bath, UK
Ms I Loots	University of Pretoria
Dr S Lorentz	SRK Consulting
Mr B Masombuka	Department of Water and Sanitation
Mr J Naidoo	Department of Water and Sanitation
Prof J Ndiritu	University of the Witwatersrand
Mr E Oakes	Department of Water and Sanitation
Mr JPJ Pietersen	Central University of Technology
Mr M Parak	South African National Roads Agency Limited
Mr P Rademeyer	Department of Water and Sanitation
Prof RE Schulze	University of KwaZulu-Natal
Mr TA Thobejane	Department of Water and Sanitation
Mr D van der Spuy	Department of Water and Sanitation
Mr M van Dijk	University of Pretoria

TABLE OF CONTENTS

LIST OF FIGURES

LIST OF TABLES

LIST OF ACRONYMS

ABM	Alternating Block Method
ACRU	Agricultural Catchments Research Unit
ADD	Average Daily Discharge
ADPD	Actual Daily Peak Discharge
AMC	Antecedent Moisture Conditions
AMS	Annual Maximum Series
ARC	Agricultural Research Council
ASCE	American Society of Civil Engineers
AVM	Average Variability Method
AVM-B	Modified Average Variability Method
BLRP	Bartlett-Lewis Rectangular Pulse
BLRPG	Bartlett-Lewis Rectangular Pulse Gamma
c	Coefficient
CN	Curve Number
COIAM	Coefficient of Initial Abstraction
CS	Continuous Simulation
CSIR	Council for Scientific and Industrial Research
CSM	Continuous Simulation Modelling
CWRR	Centre for Water Resources Research
D	Duration
DFE	Design Flood Estimation
DRE	Design Rainfall Estimation
DWS	Department of Water and Sanitation
EX-HYD	Flood Hydrograph Extraction Software
FEH	Flood Estimation Handbook
GEV	Generalised Extreme Value
GR4H	Hourly Timestep Simulation

GR4J	Daily Timestep Simulation
GUI	Graphical User Interface
HAT	Hydrograph Analysis Tool
HEC-HMS	Hydrologic Modelling System
HPD	Hourly Peak Discharge
HRU	Hydrological Response Unit
HSG	Hydrological Soil Group
Ia	Initial Abstraction
IIM	Instantaneous Intensity Method
L	Lag Time
JAM	Joint Association Method
JPA	Joint Probability Approach
MAP	Mean Annual Precipitation
MARE	Mean Absolute Relative Error
MBLRPG	Modified Bartlett-Lewis Rectangular Pulse Gamma
MCM	Median Condition Method
MOF	Method of Fragments
NEH	National Engineering Handbook
NFSP	National Flood Studies Programme
NLC	National Land Cover
NRCS	National Resource Conservation Service
MRE	Mean Relative Error
NSE	Nash-Sutcliff Efficiency
NSRP	Neyman-Scott Rectangular Pulse
OTD	On the Day
P	Rainfall/Precipitation
PDM	Probability Distributed Model
Q	Runoff/Stormflow
P-Q	Rainfall-runoff

QFRESP	Quick-flow Response Coefficient
QPEAK	Peak Discharge
R^2	Coefficient of Determination
RBLM	Randomised Bartlett-Lewis Model
RFL	Rainfall/Precipitation
RLMA&SI	Regional Linear Moment Algorithm and Scale Invariance
RMC	Random Multiplicative Cascade
RP	Return Period
RTD	Rainfall Temporal Disaggregation
S	Soil Water Deficit
S&S	Schmidt and Schulze (1984)
SANRAL	South African National Roads Agency Limited
SAWS	South African Weather Service
SCS	Soil Conservation Service
SD	Standard Deviation
SHYREG	Simulation of Hydrographs for Flood Frequency Estimation - REGionalised
SMDDEP	Critical Hydrological Response Depth of the Soil
SOR	Sum of Rank
STORMF	Stormflow
T_c	Time of Concentration
TP	Time to Peak
UH	Unit Hydrograph
UKZN	University of KwaZulu-Natal
UQFLOW	Same-day Response Fraction
USFLOW	Total Simulated Streamflow
USDA	United States Department of Agriculture
VBA	Visual Basic for Application

CHAPTER 1: INTRODUCTION

The assessment of flood risk by associating a flood event with the probability of an exceedance or return period is the standard approach to design flood estimation in most countries (Smithers, 2012; Kang et al., 2013). These design flood estimates are essential to design hydraulic infrastructure such as dams, bridges, culverts and other drainage structures (Lamb et al., 2016).

A National Flood Studies Programme was initiated to overhaul DFE procedures used in South Africa (Smithers et al., 2016). Some of the recommendations in the NFSP include the further development and assessment of a continuous simulation modelling approach to DFE in South Africa, and updating and modernising the SCS-SA method.

Motivation for a CSM approach to DFE in South Africa includes the following:

- Rainfall records are generally more numerous, accurate and spatially representative in comparison to streamflow records
- The continuous simulation modelling approach has the potential to overcome many of the limitations of event-based rainfall-runoff methods
- Local and international trends promote the application of continuous simulation modelling approaches to design flood estimation
- The method has significant potential to account for land-use change, climate change and operational systems (e.g. dams) within the catchment, which impact on design flood estimates, thus making the approach more robust and providing greater confidence in the results

In addition to the CSM approach, the SCS-SA event-based approach (Schmidt and Schulze, 1987; Schulze et al., 1992; 2004) is widely used in practice in South Africa for DFE. The method is, however, outdated and was developed using the limited data available at the time.

In addition, due to computational limitations and limited databases on catchment characteristics, such as land cover and soil, simplified soil moisture adjustment procedures were developed for the median condition method (Nathan and McMahon, 1990) and the joint association method (JAM). For example, CSM using the ACRU model was performed for only 30 days prior to the five largest rainfall events in each year, and moisture adjustments were performed for only 712 homogenous zones defined for South Africa based on a simple 3 x 3 x 3 matrix of soil depths, vegetation density and soil texture. Currently, significantly more data is available to update the SCS-SA soil moisture adjustment procedures, which can easily be updated using a significantly longer record of rainfall and other climate variables (50 years or more, depending on data availability from organisations such as the South African Weather Service (SAWS); a much finer division of the country into homogeneous zones, where the country has been delineated into 1 946 quaternary catchments and 5 838 quinary catchments; and detailed information on soil and land cover, with national soil and land-cover maps of both natural and current land cover currently available.

Reasonable results have been obtained through several pilot research studies applying the ACRU agrohydrological model for DFE in South Africa (Smithers et al., 1997; 2001; 2007; 2013; Chetty and Smithers, 2005; Rowe, 2015). However, several aspects of the ACRU CSM approach that require further development and refinement have been identified, including the estimation of peak discharge, e.g. improving the estimation of catchment lag (Gericke and Smithers, 2016), further investigation of appropriate temporal rainfall distributions and disaggregation of daily rainfall, methods to stochastically generate extended periods of rainfall, the updating of land-cover information and rainfall records, and further refinement of flood-routing methods (Smithers et al., 2013).

Rowe (2015) investigated a methodology to include land management and hydrological condition classes used in the SCS-SA model in the ACRU land-cover classification. Further development of and investigation into the approach was recommended, including the analysis of additional land-cover classes, further independent verification at different geographical locations, and verification of the simulated results against observed data in terms of both runoff volumes and peak discharges. In addition, further development of a CSM system for DFE for South Africa was recommended.

The aims of this project are the following:

- Refine and update the SCS-SA model for DFE to account for antecedent moisture conditions and the joint association of rainfall and runoff using the results and methodology from a CSM system
- Compare the performance of the CSM system to the traditional and updated SCS-SA models
- Further develop and assess the CSM approach, including the potential incorporation and assessment of improved daily rainfall disaggregation methods to account for the temporal distribution of daily rainfall
- Compare the performance of the ACRU CSM system developed to simpler, parameter-sparse CSM methods applied internationally

Hence, this project will contribute directly to the objectives of the NFSP by updating and modernising DFE methods for South Africa.

The following objectives were set to meet the above aims:

- Assess the performance of published and derived SCS curve numbers for DFE in South Africa
- Further develop and assess the ACRU CSM system for DFE in South Africa
- Assess the performance of existing methods, or develop a new or improved method to more adequately disaggregate daily rainfall within the ACRU model
- Select and assess the performance in South Africa of a simpler, parameter-sparse CS model applied internationally and compare the performance with the ACRU CSM that was developed
- Investigate the potential to incorporate a joint probability approach into the updated version of the SCS-SA model
- Develop, configure and assess the CSM system and incorporate the results into an updated SCS-SA model

Studies to address the first five objectives have been undertaken as postgraduate studies, which are summarised in chapters 2 to 6. These chapters are written as stand-alone papers for publication in a journal. Chapter 7 contains an overview of how the developments and results have been incorporated into the development of a SCS-SA CSM for DFE in South Africa. A comparison of the results of the different approaches developed and tested in the study is included in Chapter 8. Chapter 9 contains a discussion on the study and includes conclusions and recommendations for further research.

CHAPTER 2: AN ASSESSMENT OF THE PERFORMANCE OF PUBLISHED AND DERIVED SCS CURVE NUMBERS FOR DESIGN FLOOD ESTIMATION IN SOUTH AFRICA

U Maharaj, JC Smithers and TJ Rowe

This chapter provides a summary of the progress made in meeting the first objective, listed in Chapter 1, i.e. deriving South African-specific curve numbers. Full details of the study are provided in Maharaj (2020).

2.1 INTRODUCTION

The Soil Conservation Service stormflow equation was originally developed to transform a rainfall (P) frequency distribution to a runoff (Q) frequency distribution (Hjelmfelt, 1991). The curve numbers used for the transformation are generally obtained from published tables and are the CNs associated with average antecedent moisture conditions (AMC II). They represent the central tendency of the CNs derived from observed data. However, the accuracy of the CN values that were published ($CN_{published}$) by the SCS is unknown (Woodward et al., 2002; Woodward, 2017), and empirical evidence suggests that with the current $CN_{published}$ values and hydrologic systems are over-designed (Schneider and McCuen, 2005). It is important to recognise that certain aspects of CNs are not perfect. Therefore, numerous studies have been undertaken to verify the SCS-CN equation and $CN_{published}$ values (Hjelmfelt, 1991; Ponce and Hawkins, 1996; Hawkins et al., 2009; Tedela et al., 2011).

Hawkins (1975) stressed the importance of accurate CN estimates because the SCS-CN model is more sensitive to errors in CNs than rainfall. Therefore, estimation of stormflow should focus on the accurate determination of CNs, or the use of thoroughly verified CNs. Errors in stormflow estimations are particularly sensitive in low rainfall and runoff conditions (Hawkins, 1975), because these situations tend to have a bias toward high data-derived CNs. The majority of the files and supporting data that were used to develop the SCS-CN method in 1954 were not published (Mishra and Singh, 2003; Hawkins et al., 2009). Consequently, the CN method did not undergo critical review after it was made available for use (Hawkins et al., 2009; Woodward, 2017). The $CN_{published}$ values should, therefore, only serve as a guide, and users of the method should seek to determine CN values using local P-Q data to account for any deviations from the $CN_{published}$ values (Hawkins et al., 2009). However, in practice in South Africa, guidelines on the use of the SCS-SA model recommend the use of the CNs derived by the United States Department of Agriculture (USDA)'s SCS (Schulze et al., 2004; SANRAL, 2013). The availability of observed runoff data is limited. Dlamini (2019) developed and evaluated an ensemble joint probability approach (JPA) using the SCS-SA model. His results showed that both the ensemble and single-event SCS-SA models, when applied with a one-day duration design rainfall and published CNs as an input, performed poorly in terms of estimating the observed design runoff volume and design peak discharge. These results confirm the need to assess the performance of the published CNs in South Africa.

According to Hawkins (2014), the CN concept was established in the "quiet past" and is not adequate for the "stormy present" of hydrologic engineering. The currently available published CN tables are based on soil and land-cover information that does not represent South African soil and land-cover classifications. With the uncertainty surrounding the origin and development of the CN values, and the sensitivity of the simulated hydrological responses to the CNs used, it is vital to use a CN that best represents the land cover, soil type and hydrologic condition of the catchment of interest.

Given the availability of spatially explicit information on land cover and soil types in South Africa, the aim of this study is to evaluate the currently available published CNs and to select a suitable method to derive CNs using observed or simulated rainfall-runoff data for South African catchments. The aim of the study reported in this chapter is to investigate whether published CNs from the SCS-SA manual or data-derived CNs result in better estimates of runoff when using the SCS-CN equation, and to propose a CN derivation technique that is suitable to determine CNs for land-cover classes and soil classification groups used in South Africa using the results from CSM. The specific objectives of this study are to do the following:

- Briefly review the SCS-CN method, and the importance of accurate CN estimates
- Review methods that are used in South Africa and internationally to derive CNs
- Assess the performance of different CN derivation methods with observed and simulated runoff values to calculate CNs for South African catchments and compare the calculated CNs to the currently available published CNs for each catchment
- Assess if simulated runoff values could be used to determine CNs for land cover and soil combinations specific to South Africa
- Determine whether the currently available published CNs or the data-derived CNs result in more accurate estimates of runoff when using the SCS-CN equation to estimate runoff

2.2 BACKGROUND AND METHODOLOGY

The SCS-CN method has been retitled the Natural Resource Conservation Service CN (NRCS-CN) method. It was formulated in 1954 for environmental conditions dominant in the USA (Rezaei-Sadr and Sharifi, 2018). For consistency, the name SCS-CN will be used in this report. The CN is a dimensionless parameter that ranges between 0 to 100. Three major physiographic characteristics of a catchment are accounted for by the CN (Schulze and Arnold, 1979; Mishra and Singh, 2003). These characteristics are represented by means of classes of land use, land cover and soil characteristics (Savvidou et al., 2016). The SCS-CN runoff equation, which became popular in the late 1950s, was a result of approximately 20 years of study, based on P-Q relationships that were derived using data from small agricultural catchments located in the USA (Mishra and Singh, 2003; Mishra et al., 2007).

The SCS-CN runoff equation is a simple algebraic formula that relates a runoff depth to a CN and total rainfall depth (P). When using the SCS-CN equation, for runoff to occur, the rainfall must satisfy the initial abstractions (Ia), which consist of interception, depression storage and infiltration into the soil prior to the commencement of runoff. Once the runoff begins, the quantity of actual infiltration (F) increases with increasing rainfall up to the potential maximum soil water retention (S). The actual direct surface runoff (Q) also increases with rainfall. The original SCS-CN method was formulated using the water balance equation, the proportionality equality and the Ia-S hypotheses shown in equations 2.1 to 2.3 (Schulze and Arnold, 1979; Mishra and Singh, 2003; Jain et al., 2006).

(a) The water balance equation:

$$P = I_a + F + Q \qquad 2.1$$

(b) The proportionality equality hypothesis:

$$\frac{Q}{P - I_a} = \frac{F}{S} \qquad 2.2$$

(c) The Ia-S hypothesis:

$$I_a = c \times S \qquad 2.3$$

where c = coefficient of initial abstraction (dimensionless).

The SCS-CN runoff equation was derived using equations 2.1, 2.2 and 2.3 (Schulze and Arnold, 1979; Mishra and Singh, 2003):

$$Q = \frac{(P - I_a)^2}{(P - I_a + S)} \qquad 2.4$$

The limits of Equation 2.4 are that when $P \geq cS$, then $Q > 0$, otherwise $Q = 0$ (Schulze and Arnold, 1979). The CN values may be obtained using look-up tables that have been published by various sources (USDA, 1959; Schulze and Arnold, 1979; Schulze and Schmidt, 1987; Schulze et al., 2004). The CN may then be used to calculate S (Schulze and Arnold, 1979):

$$S = \frac{25400}{CN} - 254 \qquad 2.5$$

There are numerous ways to define the CN. However, Fennessey and Hawkins (2001) used the following four definitions: array table CN, weighted design CN, best CN and asymptotic CN (CN_∞). The array table CN refers to the CN values that were published by the SCS (i.e. $CN_{published}$). When more than one land use and land cover (LULC) or hydrological soil group is identified for a catchment, a weighted CN value may be used. This is referred to as the weighted design CN. According to Fennessey (2000), the best CN is the CN that has been calibrated for selected return periods (RPs) using historical P-Q data from a gauged catchment, such that the standard error of the estimated peak discharges are minimised over the period of assessment. When using the asymptotic method of CN derivation, the equilibrium, or near-constant CN that is observed for large rainfall depths, is referred to as CN_∞.

If the CN concept were perfect, the weighted CN, determined from the CN tables, should be equal, or close to the best CN or CN_∞. Figure 2.1 shows each of these CN values derived for 60 small catchments in the USA. The catchments are labelled from 1 to 60 on the x-axis, and the CN values, on the y-axis, have been ranked by their weighted design CN for ease of observation (Fennessey and Hawkins, 2001).

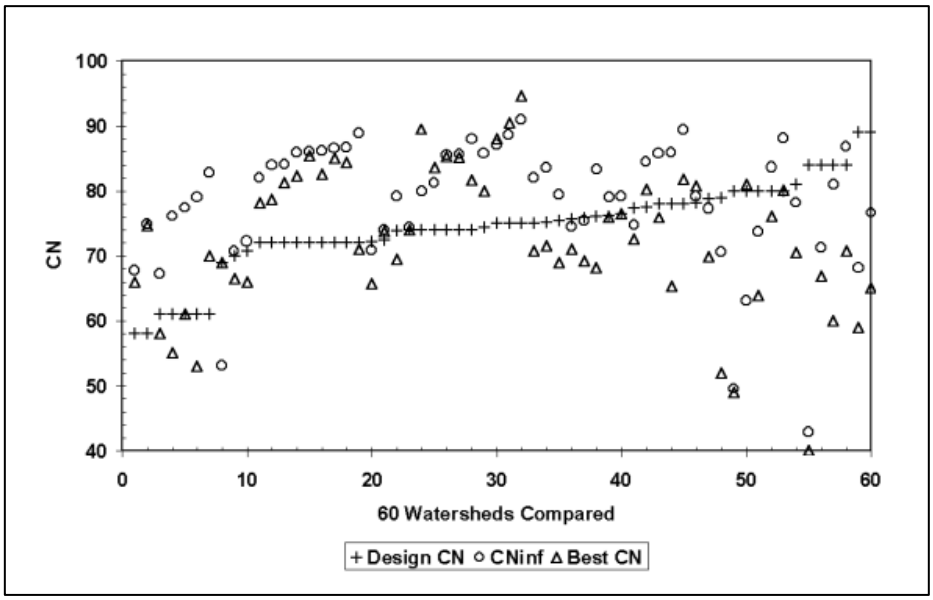

Figure 2.1 Different CNs that were calculated for 60 catchments (Fennessey and Hawkins, 2001)

From Figure 2.1, it is clear that the three CN values are not the same. On some catchments, the values vary by more than 10 CN units. There are certain cases where the three CN values are similar. However, it is more common for the best CN and CN_∞ to be similar, and for both to vary from the design CN. Numerous other researchers have found that the calculated CN values vary from the tabulated CNs (Hawkins et al., 2009; Stewart et al., 2011; Maharaj, 2020).

The uncertainty linked to the determination of CNs has been associated with three main sources: the best methodology to calibrate the CN and Ia; the procedures used to select the most representative P-Q events; and the relationship between Ia and S (Hawkins et al., 2009; Pablo et al., 2017). However, if the uncertainty when determining the CN can be reduced, it would result in more reliable estimates of CNs (Pablo et al., 2017).

Both Schulze and Schmidt (1987) and Mishra and Singh (2003) reported that, in most cases, the SCS used infiltrometer tests and daily rainfall-runoff records that corresponded to maximum annual flows from gauged catchments to compute the $CN_{published}$ values. The catchments used were from the USA, generally had a single land-cover and soil group, and the catchment sizes ranged between 0.0971 ha and 18 650 ha (Woodward et al., 2002; Hawkins et al., 2009; Tedela et al., 2011). Unfortunately, most of the original information that was used for deriving CNs was not preserved (Woodward et al., 2002; Hawkins et al., 2009). The CN for a single soil and land-cover condition was derived using the largest annual storm runoff and the associated rainfall (Woodward et al., 2002; Hawkins et al., 2009). When observed P-Qs were plotted, the CN that results in an equal number of data points on either side of the CN line was selected as the median, or "average" CN (CN_{II}) for the catchment (Schulze and Schmidt, 1987; Woodward et al., 2002).

Bonta (1997) also stated that the $CN_{published}$ values were derived from observed P-Q data. However, there is no standard technique that is used to derive CNs. Statistical theory indicates that accuracy improves with an increasing sample size (Schneider and McCuen, 2005). To reliably estimate the mean of the sample, a rule-of-thumb indicates that the sample size should be at least 30 data points. However, it is difficult to obtain data for even this relatively small sample size. Therefore, in the study by Schneider and McCuen (2005), the sample size was varied when calculating the CN. The results from three CN-derivation approaches indicated that the sample size essentially had no effect on the bias of the calculated CNs, but the accuracy of calculated CNs improved as the sample size was increased. Therefore, a large P-Q database would be required to develop a revised, more accurate CN array table (Hawkins et al., 2009). A shorter record generally has a limited data range for P and Q because large events are not expected to occur in shorter time spans (Schneider and McCuen, 2005).

Schneider and McCuen (2005) evaluated and assessed the storm event, rank order and Log-Normal frequency methods to derive CNs using both observed and simulated P-Q values. The method using concepts of the Log-Normal frequency was found to be more accurate than the storm event and rank order methods. The Log-Normal frequency method reduced the imbalance of the weights given to the P values because taking the logarithm of P depths reduced the values proportionally (Schneider and McCuen, 2005).

The SCS stormflow equation could also be applied using a frequency-matching technique. This technique equates rainfall and runoff events that have the same return period. When the chosen RP runoff is calculated from the same RP rainfall, the CN is assumed to be constant for all return periods (Hawkins, 1993). Therefore, when using the frequency-matching technique, the T-year RP rainfall must be paired with the T-year RP runoff. The storm runoff does not need to be linked to the rainfall that caused it (Hawkins, 1993). The frequency curve transformation of rainfall to runoff using the SCS-CN equations satisfies the RP matching application of the SCS-CN method, but the frequency-matching technique is not suitable in all cases. This method is not applicable in cases where the annual flood peak CN values decrease with increasing rainfall depths (Hawkins et al., 2009).

The asymptotic method builds on the frequency-matching technique and is based on the secondary relationship between the CN and P depth. With this method, a new dataset is created, with rainfall and runoff that have equal return periods. The main problem is that the runoff could be disassociated from the causative rainfall (Pablo et al., 2017). When using this method, user judgement plays a major role in determining the CN (Hawkins et al., 2009).

The method may be used with natural or ranked P-Q data, and a catchment may behave in a standard, violent or complacent pattern. However, if natural P-Q data is used, it is more difficult to observe the catchment behaviour pattern. In the standard and violent cases, if a near-constant CN is apparent at higher P values, that portion of the data is selected and the mean CN for the catchment is determined. Only the standard and violent cases are suitable for the CN definition because, with the complacent case, a single CN_∞ cannot be determined for the catchment.

In almost every case, when using natural or ranked datasets, a secondary relationship between the P depth and data-defined CNs is apparent (Hawkins, 1993). The data-defined CNs are not completely independent of the P depth and a clear decline in CNs is evident as the rainfall depth increases. This bias has been attributed to data censoring, basic errors inherent in the model or partial area effects (Hawkins et al., 2009). The decline of CNs with increasing P depths may appear to be counter-intuitive because larger Q depths are associated with higher CNs. The counter-intuitive problem can be explained using the plot of Q with P and the family of CN curves. A line of Q = C x P, an alternative P-Q model, was superimposed on the P-Q and CN plot. A C of a reasonable value, such as 0.2, could be used for the Q = C x P line, as this form occurs in nature (Hawkins, 2019). The superimposed line starts at 0 (and CN = 100) and then cuts through successively smaller CN lines with increasing P depths. Therefore, as Q increases with P, the CN reduces as shown in Figure 2.2. It is important to highlight that real catchments do not always work the way the SCS-CN equation dictates. Therefore, the decline in CNs with increasing rainfall depth may not occur in all catchments (Hawkins, 2019).

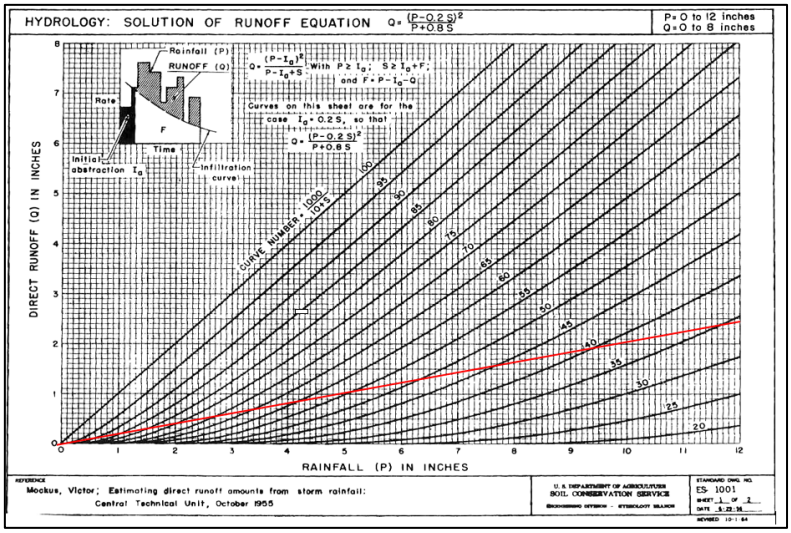

Figure 2.2 Q = C x P plotted in red superimposed on the families of CN responses (Hawkins, 2019)

2.3 CATCHMENT SELECTION AND DATA USED IN THE STUDY

Using the information from a detailed literature review of CN-derivation techniques as documented by Maharaj (2020) and summarised in Section 2.2, several CN-derivation techniques were assessed using six selected test catchments: A9H006, U2H018, U2H020, V1H015, V1H005 and W1H016. The location of the catchments used in this study is shown in Figure 2.3.

The catchments had different HSGs, hydrological conditions and LULC classes. Rowe (2019) provides a detailed account of the physical and hydrological characteristics of the six catchments. The methods reviewed to derive the CN values have been applied to the selected catchments with appropriate observed and simulated P-Q data.

Table 2.1 contains the relevant characteristics of the catchments that are required to obtain a CN from the SCS-SA CN tables.

Table 2.1: Catchment information and attributes required to derive the CN (after Rowe, 2019)

Catchment	Province	Area (km^2)	Revised SCS-SA land cover class	Treatment (class) type	Hydrological condition	SCS-SA soil group	CN
Cedara (U2H020)	KwaZulu-Natal	0.26	Unimproved (natural) grassland	2 = in fair condition	Fair	A/B	61
Cathedral Peak IV (V1H005)	KwaZulu-Natal	0.98	Unimproved (natural) grassland	3 = in good condition	Good	A/B	51
DeHoek / Ntabamhlope (V1H015)	KwaZulu-Natal	1.04	Unimproved (natural) grassland	3 = in good condition	Good	B	61
Cedara (U2H018)	KwaZulu-Natal	1.31	Forests and plantations	Humus depth > 100 mm	Loose or friable/site prep pitting	B	50
Zululand (W1H016)	KwaZulu-Natal	3.30	Unimproved (natural) grassland	3 = in good condition	Good	B	61
A9H006	Limpopo	16.00	Forests and plantations	Humus depth > 100 mm	Loose or friable/site prep pitting	B/C	56

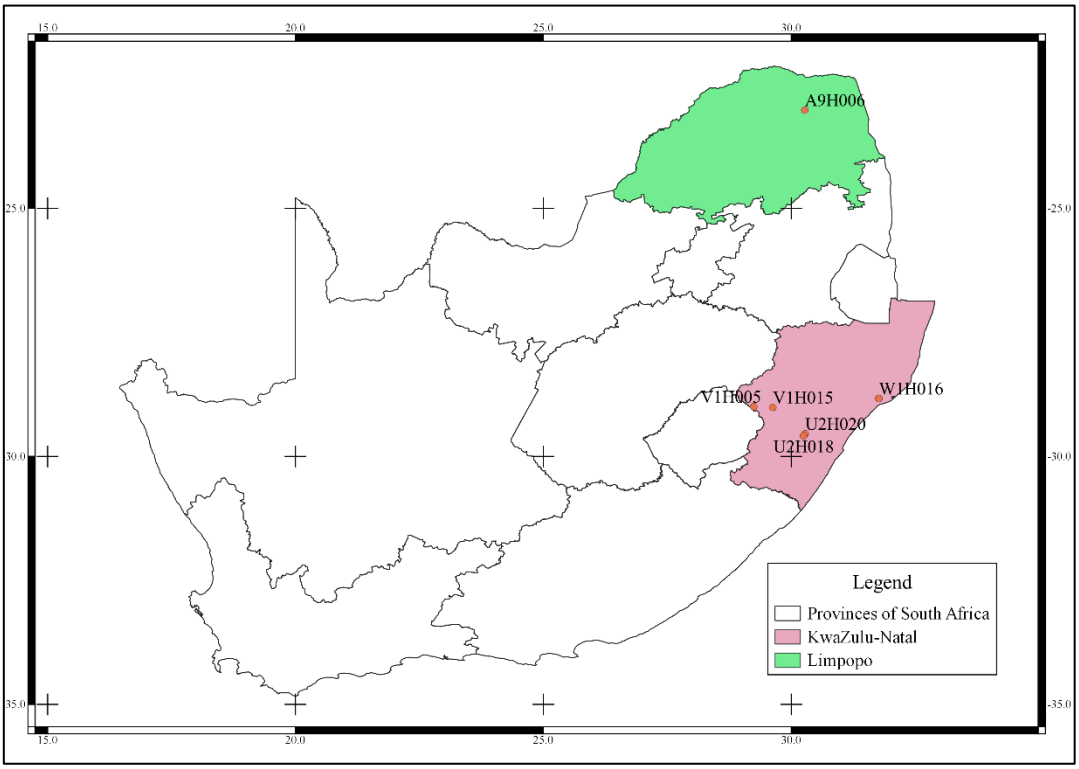

Figure 2.3 Location of the test catchments used in this study

2.4 ASSESSMENT OF METHODS TO BEST DERIVE PUBLISHED CNS

Based on a detailed review of literature undertaken by Maharaj (2020), as summarised above, several CN-derivation techniques were assessed using six catchments distributed across South Africa.

2.4.1 Observed P-Q data

Median or "average" CN values were derived using observed daily P-Q depths corresponding to the annual maximum flows from gauged catchments, as originally derived from the CN tables published in the National Engineering Handbook (NEH) (Schulze and Schmidt, 1987; Mishra and Singh, 2003). The daily annual maximum flood (AMF) depths and associated rainfall depths were used to derive CNs (AMF CN_{NEH}) for the catchments. The AMF CN_{NEH} values were obtained based on interpretations of the P-Q data that were plotted on a family of CN curves. The CN array plots were drawn using a c value of 0.1 ($CN_{NEH,0.1}$) and 0.2 ($CN_{NEH,0.2}$) to test the sensitivity of the CN_{NEH} to the c value. The CN that divided the plotted P-Q points into two halves was chosen as the AMF CN_{NEH} value. The results from applying this method to the six catchments in the study have generally shown that the AMF CN_{NEH} values were larger than the $CN_{published}$ values. In addition, the annual maximum series (AMS) of P-Q (i.e. P and Q may not be associated) was also used to derive CNs (AMS CN_{NEH}). Table 2.2 contains a summary of the CNs that were obtained and includes the mean absolute relative error between the derived and $CN_{published}$ values. The results were not conclusive when the AMF and associated P were used to derive CNs and there were large differences between the tabulated and AMF $CN_{NEH,0.1}$ and $CN_{NEH,0.2}$. The AMS $CN_{NEH,0.1}$ values were closer to $CN_{published}$ as supported by the MARE of 10%. This method, however, is very subjective because the CN_{II} is selected graphically. The choice of the CN_{II} depends entirely on interpreting the P-Q scatter plot. In certain catchments, the data points are clustered closely together, making it difficult to determine the exact CN value.

An alternative approach is to separate the observed annual maximum P-Q data into two clusters using the K-means clustering algorithm to determine the CN using AMS P-Q values (AMS $CN_{K\text{-}Mean}$). This method of data processing enabled the determination of a median CN as prescribed by the NEH (USDA, 1959) in a more objective manner. When the K-means algorithm was used to determine the median CN, the AMS $CN_{K\text{-}Mean,0.2}$ was closer to the $CN_{published}$ values in comparison to the AMS $CN_{NEH,0.2}$ values. Table 2.2 contains the CN values that were derived using the K-means algorithm and shows that when a c of 0.1 was used, the calculated CN values were much closer to the $CN_{published}$ values. Similar to the results obtained applying the NEH-4 prescribed approach, the results are not conclusive when c = 0.2 was used to calculate the CN. These initial results therefore suggest that the NEH prescribed approach and the K-means algorithm provide more consistent results when c = 0.1 is used to calculate the median CN.

Another possible improvement on the use of CNs from the handbook tables was to use frequency-matched P-Q pairs to determine the CNs. When frequency distributions were used to derive CNs as a function of RP (CN_{RP}), in general, the CN reduced as the return period increased. Taking all the catchments into consideration, the $CN_{2,0.1}$, $CN_{5,0.1}$ and $CN_{10,0.1}$ resulted in CNs that were close to the $CN_{published}$ values (low MARE), as shown in Table 2.2.

Numerous researchers have highlighted that CNs vary with rainfall depth (Hawkins, 1993; Hawkins et al., 2009). Therefore, using a single or few rainfall events, such as the annual maximum events, to calculate an average or median CN is not ideal. Hence, the asymptotic approach that uses all the rainfall values could provide reasonable CN estimates. In this study, when the method was applied, there were differences between the CN_{∞} and $CN_{published}$ values. The standard behaviour, and most common pattern according to Hawkins et al. (2009), was observed on four of the six catchments. A CN_{∞} could not be determined with the available data on only one of the six catchments (Catchment V1H005). Therefore, Catchment V1H005 could best be described as a complacent catchment because the CNs declined with increasing P depths, but did not approach a near constant CN_{∞} value.

The $CN_{\infty,0.1}$ values were closest to the $CN_{published}$ values on three of the five catchments with a MARE of 13.5% between the $CN_{\infty,0.1}$ and $CN_{published}$ values.

Based on the literature that was reviewed, there is clear evidence that high rainfall events are associated with lower CN values (Hawkins, 1993; Hawkins et al., 2009; D'Asaro et al., 2014). In this study, the highest rainfall value and the associated minimum CN (CN_{AnnMin}) for each year were extracted from the daily CNs that were calculated. The mean and median of the CN_{AnnMin} values associated with the annual maximum P were then calculated for each catchment. As shown in Table 2.2, the median of the $CN_{AnnMin,0.2}$ values were closest to the $CN_{published}$ values (low MARE).

Subsequently, the annual maximum daily P and Q depths, which may not be associated with the same event, were used to calculate CNs (CN_{AMS}). The mean CN_{AMS} values were more consistent with the $CN_{published}$ values than the use of the median CN_{AMS} values. The total error between the mean CN_{AMS} and $CN_{published}$ values was higher when c = 0.2 was used to calculate the mean CN_{AMS}, as indicated by the higher MARE shown in Table 2.2. When c = 0.1 was used to calculate the CN_{AMS}, the mean CN_{AMS} values were much closer to the $CN_{published}$ values, as supported by the MARE of 12% shown in Table 2.2. A concern with using the AMS of the P-Q depths is that the largest rainfall event may not have caused the largest runoff event. Consequently, the annual maximum daily runoff and the associated daily rainfall depths were used to calculate the CN (CN_{AMF}) representative of each catchment. The mean and median $CN_{AMF,0.1}$ and $CN_{AMF,0.2}$ values were larger than the $CN_{published}$ values on all the catchments.

In this study, CNs were also derived using the Log-Normal frequency method (CN_{LN}). The CN_{LN} values derived using c = 0.1 ($CN_{LN,0.1}$) and c = 0.2 ($CN_{LN,0.2}$) are given in Table 2.2. The $CN_{LN,0.1}$ and $CN_{published}$ values were closer (MARE of 14%) compared to the $CN_{LN,0.2}$ and $CN_{published}$ values (MARE of 19%). Taking all six catchments into consideration, the $CN_{LN,0.1}$ values were closer to the $CN_{published}$ values on four of the six catchments, compared to the $CN_{LN,0.2}$ values.

As shown in Table 2.2, there were differences between the CNs calculated using observed P-Q data and the $CN_{published}$ values. According to the literature that was reviewed, some differences between the calculated and $CN_{published}$ values were expected. Based on the initial results, the mean of the $CN_{AMS,0.1}$, $CN_{LN,0.1}$, $CN_{2,0.1}$, $CN_{5,0.1}$, $CN_{10,0.1}$, $CN_{\infty,0.1}$, mean and median of the $CN_{AnnMin,0.2}$, AMS $CN_{NEH,0.1}$ and AMS $CN_{CNK\text{-}mean,0.1}$ provided good estimates of the $CN_{published}$ values. The CNs that were derived with c = 0.2 were generally higher than the CNs derived with c = 0.1, and the CNs derived using observed data and c = 0.1 were generally closer to the $CN_{published}$ values. The methods discussed in Section 2.4.1 were then applied with simulated Q values and c = 0.1, which is consistent with the c value used with the SCS-SA model and the c used by Rowe (2019) to develop an improved CSM for DFE in South Africa. The simulated approach was used to determine whether simulated Q values may be used to derive CNs for South African land use, land cover and hydrological soil groups. The results from applying the methods listed above with simulated Q values from ACRU are provided in Section 2.4.

Table 2.2: Comparison between published CNs and CNs derived using observed P-Q data

Catchment name	$CN_{published}$	CN_{∞}		AMS $CN_{K\text{-}Mean}$		Mean CN_{AMS}		Mean CN_{AnnMin}		Median CN_{AnnMin}		AMS CN_{NEH}		CN_{LN}		CN_{10}		CN_{2}		CN_{5}	
		c = 0.2	c = 0.1	c = 0.2	c = 0.1	c = 0.2	c = 0.1	c = 0.2	c = 0.1	c = 0.2	c = 0.1	c = 0.2	c = 0.1	c = 0.2	c = 0.1	c = 0.2	c = 0.1	c = 0.2	c = 0.1	c = 0.2	c = 0.1
A9H006	56	54	47	50	40	54	45	39	27	40	28	50	45	51	42	49	42	52	44	50	42
U2H018	50	54	48	55	50	67	58	58	42	57	44	65	50	66	56	62	55	67	56	65	56
U2H020	61	80	77	75	75	69	60	59	44	61	45	70	55	65	55	71	65	70	61	71	65
VIH015	61	76	71	75	70	74	68	58	44	58	42	75	65	74	67	73	68	73	67	73	67
V1H005	51	-	-	70	60	70	63	61	49	61	49	70	60	70	62	68	61	69	61	68	61
WIH016	61	62	58	55	50	67	61	54	51	54	42	65	65	66	59	60	54	74	69	66	61
MARE (%)																					
A9H006	56	4	16	11	29	4	20	30	52	29	50	11	20	9	25	13	25	7	21	11	25
U2H018	50	8	4	10	0	34	16	16	16	14	12	30	0	32	12	24	10	34	12	30	12
U2H020	61	31	26	23	23	13	2	3	28	0	26	15	10	7	10	16	7	15	0	16	7
VIH015	61	25	16	23	15	21	11	5	28	5	31	23	7	21	10	20	11	20	10	20	10
V1H005	51			37	18	37	24	20	4	20	4	37	18	37	22	33	20	35	20	33	20
WIH016	61	2	5	10	18	10	0	11	16	11	31	7	7	8	3	2	11	21	13	8	0
MARE (%)		14	14	19	17	20	12	14	24	13	26	20	10	19	14	18	14	22	13	20	12

2.4.2 Simulated P-Q values

The ACRU model, which uses the SCS stormflow equation with a soil water budget to generate runoff, was used to simulate runoff for the six study catchments. The daily observed P and simulated Q, referred to as simulated P-Q depths, were used with c = 0.1 to calculate the CNs for each of the catchments. A prefix "S" was added to the abbreviation for the different CN-derivation methods when simulated Q values were used to derive the CN. The conventional rules to parametrise ACRU ($ACRU_{CON-P}$) and the rules developed by Rowe (2019) were used to parametrise ACRU ($ACRU_{TR-P}$). In Section 2.4.2.1, CNs derived using simulated P-Q depths from $ACRU_{TR-P}$ are discussed. The CNs derived using simulated P-Q depths from $ACRU_{TR-P}$ and $ACRU_{CON-P}$ are compared in Section 2.4.2.2.

2.4.2.1 CNs derived using simulated P-Q depths from $ACRU_{TR-P}$

The annual maximum simulated P-Q depths were plotted on a CN array, drawn using c = 0.1. In general, the plotted points were well distributed on the array. The AMS $S\text{-}CN_{NEH}$ values estimated using this method and simulated P-Q depths from $ACRU_{TR-P}$ were similar to the $CN_{published}$ values as indicated by the low MARE between the derived and published CNs (MARE = 5%). The annual maximum simulated P-Q depths, from $ACRU_{TR-P}$, were then used with the K-means clustering algorithm to obtain the AMS $S\text{-}CN_{K\text{-}Mean}$ for each catchment. The AMS $S\text{-}C_{NK\text{-}Mean}$ values were only similar to the $CN_{published}$ values in catchments U2H020 and V1H015.

Similarly, when using $ACRU_{TR-P}$ to simulate P-Q depths, the mean $S\text{-}CN_{AMS}$ resulted in good estimates of the $CN_{published}$ values. When taking all six catchments into account, the mean $S\text{-}CN_{AMS}$ values were close to the $CN_{published}$ values, and the MARE between the $CN_{published}$ and the mean $S\text{-}CN_{AMS}$ values was 5%, as shown in Table 2.3.

Subsequently, design-simulated Q depths from $ACRU_{TR-P}$ were used with design-observed rainfall depths ($P_{T,O}$) to derive $S\text{-}CN_{RP}$ values. The $S\text{-}CN_{RP}$ values decreased as the return period increased, as shown in Table 2.3, and both the $S\text{-}CN_2$ and $S\text{-}CN_5$ resulted in a MARE of 8% between the $CN_{published}$ and CN_{RP} values.

When the asymptotic method of CN derivation was applied using simulated P-Q depths, the $S\text{-}CN_\infty$ values were much easier to identify because all the catchments displayed the standard catchment behaviour pattern. The overall error was low between the $S\text{-}CN_\infty$ and $CN_{published}$ values and are given in Table 2.3.

The daily simulated P-Q depths from $ACRU_{TR-P}$ were used to calculate daily CNs. Thereafter, the annual minimum CNs were extracted from the daily CN record. The mean and median of the annual minimum CN values ($S\text{-}CN_{AnnMin}$) were then calculated and taken to be the CN representative of the catchment. As shown in Table 2.3, the mean of the $S\text{-}CN_{AnnMin}$ values were generally closer to the $CN_{published}$ values than the median of the $S\text{-}CN_{AnnMin}$ values, as indicated by the lower MARE between the mean $S\text{-}CN_{AnnMin}$ and $CN_{published}$ values.

When the Log-Normal frequency method was applied using simulated P-Q depths from $ACRU_{TR-P}$, the $S\text{-}CN_{LN}$ values were similar to the $CN_{published}$ values in three of the six catchments (MARE of 7%).

Table 2.3: Comparison between CNs derived using the conventional ACRU parameter guidelines (Con-P) and the rules developed by by Rowe (2019) (TR-P)

Catchment name	$CN_{published}$	S-CN_{∞}		AMS S-$CN_{K\text{-}Mean}$		Mean S-CN_{AMS}		Mean S-CN_{AnnMin}		Median S-CN_{AnnMin}		AMS S-CN_{NEH}		S-CN_{LN}		S-CN_{10}		S-CN_{2}		S-CN_{5}	
		Con-P	TR-P	Con-P	TR-P	Con-P	TR-P	Con-P	TR-P	Con-P	TR-P	Con-P	TR-P	Con-P	TR-P	Con-P	TR-P	Con-P	TR-P	Con-P	TR-P
A9H006	56	44	51	45	45	51	54	44	47	45	48	52	50	47	50	39	43	49	52	42	46
U2H018	50	57	52	35	30	57	50	50	47	51	48	48	50	53	48	49	45	55	51	53	48
U2H020	61	60	65	35	55	60	64	54	54	54	54	58	62	58	63	54	63	60	65	57	65
VIH015	61	54	67	55	65	56	67	49	60	49	55	54	65	54	67	50	65	55	67	52	66
V1H005	51	54	55	55	60	56	58	51	53	50	53	55	57	62	57	51	55	55	59	53	56
WIH016	61	53	66	40	75	48	61	44	54	44	54	43	60	43	60	38	57	49	65	42	61
MARE (%)																					
A9H006	56	21	9	20	20	9	4	21	16	20	14	7	11	16	11	30	23	13	7	25	18
U2H018	50	14	4	30	40	14	0	0	6	2	4	4	0	6	4	2	10	10	2	6	4
U2H020	61	2	7	43	10	2	5	11	11	11	11	5	2	5	3	11	3	2	7	7	7
VIH015	61	11	10	10	7	8	10	20	2	20	10	11	7	11	10	18	7	10	10	15	8
V1H005	51	6	8	8	18	10	14	0	4	2	4	8	12	22	12	0	8	8	16	4	10
WIH016	61	13	8	34	23	21	0	28	11	28	11	30	2	30	2	38	7	20	7	31	0
MARE (%)		11	8	24	19	11	5	13	8	14	9	11	5	15	7	17	10	10	8	15	8

2.4.2.2 Comparison between CNs derived using simulated Q depths from $ACRU_{CON-P}$ and $ACRU_{TR-P}$

$ACRU_{CON-P}$ and $ACRU_{TR-P}$ were used to simulate Q depths to calculate CNs. The same CN-derivation methods applied with simulated Q depths from $ACRU_{TR-P}$ were also applied with simulated Q depths from $ACRU_{CON-P}$. A comparison between the CNs derived using simulated Q depths from $ACRU_{CON-P}$ and $ACRU_{TR-P}$ is provided in Table 2.3. When using $ACRU_{CON-P}$ to simulate P-Q depths and derive CNs, the $S\text{-}CN_2$, the mean $S\text{-}CN_{AMS}$, $S\text{-}CN_{\infty}$ and the AMS $S\text{-}CN_{NEH}$ were closest to the $CN_{published}$ values, as indicated by the low MARE values in Table 2.3.

Based on the results shown in Table 2.3, it is evident that the CNs derived using simulated P-Q depths from $ACRU_{TR-P}$ resulted in CN values that were closest to the $CN_{published}$ values. In terms of design flood estimates, Rowe et al. (2018b) indicated that $ACRU_{CON-P}$ was sensitive to QFRESP and SMDDEP. When using $ACRU_{CON-P}$, QFRESP and SMDDEP are generally set to default values, but Schulze (1995) provided guidance on selecting SMDDEP values based on rainfall intensity, soil conditions and vegetation density. Subsequently, Rowe et al. (2018b) developed a methodology to parameterise QFRESP and SMDDEP using the $CN_{published}$ values. The calibrated QFRESP and SMDDEP parameter values from Table 11.1 in Rowe (2019) were used to set up $ACRU_{TR-P}$. Since $ACRU_{TR-P}$ was set up using QFRESP and SMDDEP, which were calibrated using the $CN_{published}$ values, it was expected that the CNs derived using simulated P-Q depths from $ACRU_{TR-P}$ would be closer to the $CN_{published}$ values. However, when using simulated P-Q depths from either $ACRU_{CON-P}$ or $ACRU_{TR-P}$, it is possible to derive mean $S\text{-}CN_{AMS}$ and AMS $S\text{-}CN_{NEH}$ values that are similar to the $CN_{published}$ values.

2.4.2.3 Comparison between best derived CNs and $CN_{published}$ values

Table 2.4 contains a summary of the CN-derivation methods that resulted in the lowest MARE between the $CN_{published}$ values and the CNs derived using observed P-Q data and simulated Q values from $ACRU_{TR-P}$ and $ACRU_{CON-P}$. As shown in Table 2.4, the CNs derived using simulated P-Q depths from $ACRU_{TR-P}$ were much closer (lower MARE) to the $CN_{published}$ values compared to the CNs derived using observed P-Q data (higher MARE). The mean $S\text{-}CN_{AMS,0.1}$ and AMS $S\text{-}CN_{NEH,0.1}$ values derived using annual maximum simulated P-Q depths from $ACRU_{TR-P}$ resulted in CNs that were most similar to the $CN_{published}$ values in the study catchments. The AMS $CN_{NEH,0.1}$ values derived using observed P-Q data performed the best in terms of replicating the $CN_{published}$ values. The mean $S\text{-}CN_{AMS,0.1}$ and AMS $S\text{-}CN_{NEH,0.1}$ values derived using simulated Q values from $ACRU_{CON-P}$ were also reasonable and were comparable to the CNs derived using observed P-Q data. From the above results and in the absence of reliable observed runoff data, it is evident that runoff simulated for specific South African land cover classes and soils using $ACRU_{TR-P}$ or $ACRU_{CON-P}$ can be used to derive CNs. The CNs derived using simulated values also provide a more objective method than the subjective interpolation that was originally done by the SCS.

Table 2.4: Comparison between CNs derived using observed P-Q data and CNs derived using simulated P-Q depths

Catchment name	$CN_{published}$	Mean $CN_{AMS,0.1}$			AMS $CN_{NEH,0.1}$		
		Observed P-Q	$ACRU_{CON-P}$	$ACRU_{TR-P}$	Observed P-Q	$ACRU_{CON-P}$	$ACRU_{TR-P}$
A9H006	56	45	51	54	45	52	50
U2H018	50	58	57	50	50	48	50
U2H020	61	60	60	64	55	58	62
VIH015	61	68	56	67	65	54	65
V1H005	51	63	56	58	60	55	57
WIH016	61	61	48	61	65	43	60
MARE (%)							

Catchment name	$CN_{published}$	Mean $CN_{AMS,0.1}$			AMS $CN_{NEH,0.1}$		
		Observed P-Q	$ACRU_{CON-P}$	$ACRU_{TR-P}$	Observed P-Q	$ACRU_{CON-P}$	$ACRU_{TR-P}$
A9H006	56	20	9	4	20	7	11
U2H018	50	16	14	0	0	4	0
U2H020	61	2	2	5	10	5	2
VIH015	61	11	8	10	7	11	7
V1H005	51	24	10	14	18	8	12
WIH016	61	0	21	0	7	30	2
MARE (%)		12	11	5	10	11	5

2.5 ASSESSMENT OF PUBLISHED AND DERIVED CNS FOR BEST DESIGN RUNOFF VOLUME ESTIMATION

In this section, the performance of design runoff estimation is assessed using published CNs, CNs derived from observed P-Q data and CNs derived from simulated P-Q depths.

2.5.1 Use of published CNs

The design runoff depth ($Q_{T,S}$), estimated using the SCS-CN equation and calculated using the $P_{T,O}$ and $CN_{published}$ values for the sites and c = 0.1, was compared to the design runoff depth ($Q_{T,O}$), calculated from the observed data using scatter plots and various statistical measures such as MARE, mean relative error (MRE) and R^2. A linear regression analysis was performed using $Q_{T,O}$ and $Q_{T,S}$ for the six study catchments for all return periods to evaluate the use of the $CN_{published}$ values collectively across the different catchments. Figure 2.4 shows the $Q_{T,O}$ and $Q_{T,S}$ that were obtained using the $CN_{published}$ values to estimate $Q_{T,S}$.

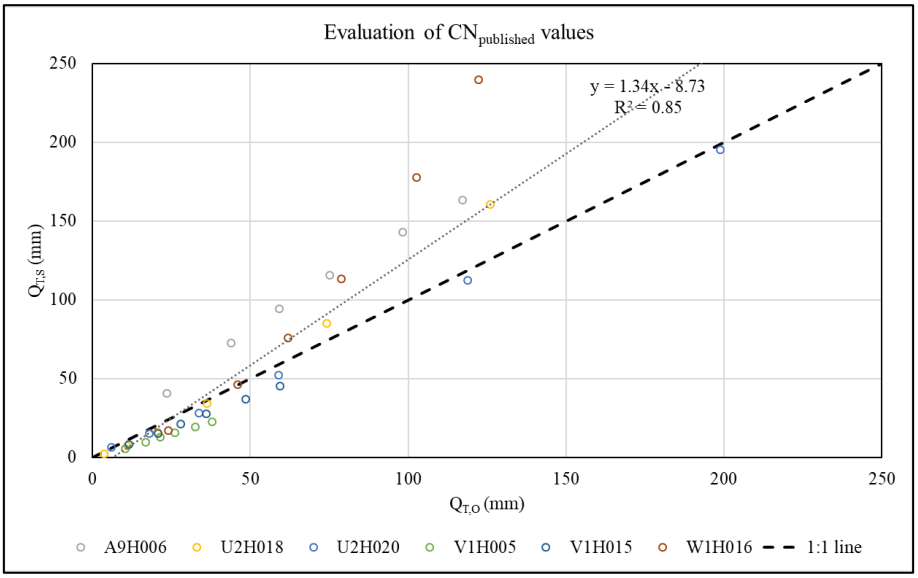

Figure 2.4: Performance of the SCS-CN method using published CNs at six study catchments and for return periods of 2, 5, 10, 20, 50 and 100 years

As shown in Figure 2.4, there is a good correlation between the $Q_{T,O}$ and $Q_{T,S}$ calculated using the $CN_{published}$ values. In general, using the $CN_{published}$ values to estimate $Q_{T,S}$ resulted in a 34% over-estimation. The over-estimation is more evident for the larger $Q_{T,O}$ values. A summary of the results from the statistical analysis of the $CN_{published}$ values is provided in Table 2.5.

Table 2.5: Evaluation of the performance of the SCS-SA model using published CNs selected for the study catchments

Catchment name	MARE	MRE
A9H006	0.56	0.56
U2H018	0.25	-0.11
U2H020	0.09	-0.08
V1H005	0.42	-0.42
V1H015	0.25	-0.25
W1H016	0.44	0.34
Mean	0.34	0.01

The MRE and MARE values that are closer to zero indicate that there is a good fit between $Q_{T,O}$ and $Q_{T,S}$. The overall best performance of the $CN_{published}$ values was in Catchment U2H020. The results presented in Table 2.5 were only acceptable in one of the six catchments. Therefore, the CNs derived using observed P-Q data were also used to calculate $Q_{T,S}$ and evaluate the performance of the SCS-CN equation. The results of the analyses are presented in Section 2.5.2.

2.5.2 Use of CNs derived from observed P-Q data

In this section, the results from using CNs derived using observed P-Q data to estimate $Q_{T,S}$ are presented. The CN-derivation methods were used to estimate $Q_{T,S}$. Linear regression analyses, R^2, MRE and MARE values were used to evaluate the performance of the SCS-CN equation. All the CN-derivation techniques were individually assessed on each catchment. As an example, the CNs derived for Catchment U2H018 using observed P-Q data and the MRE and MARE values are ranked in ascending order. A summary is provided in Table 2.6.

Table 2.6: MARE and MRE values obtained when using the $CN_{published}$ and CNs derived using observed data to estimate $Q_{T,S}$ in catchment U2H018

Published CN	Method	Derived CN	MRE	MARE	Rank
50	$CN_{10,0.1}$	55	0.13	0.18	1
	$CN_{LN,0.1}$	56	0.18	0.19	2
	$CN_{2,0.1}$				
	$CN_{5,0.1}$				
	Median $CN_{AnnMin,0.2}$	57	0.23	0.23	3
	$CN_{published}$	50	-0.11	0.25	4
	AMS $CN_{NEH,0.1}$				
	AMS $CN_{K\text{-}Mean,0.1}$				
	Mean $CN_{AnnMin,0.2}$	58	0.28	0.28	5
	Mean $CN_{AMS,0.1}$				
	$CN_{\infty,0.1}$	48	-0.19	0.29	6

In Catchment U2H018, the lowest total error between $Q_{T,O}$ and $Q_{T,S}$ was obtained when $CN_{10,0.1}$ was used to estimate $Q_{T,S}$. The MRE was less than the MARE, which indicates a combination of both an over- and under-estimation of $Q_{T,O}$.

The $CN_{2,0.1}$, $CN_{5,0.1}$ and $CN_{LN,0.1}$ resulted in similar MRE and MARE values. Both the MRE and MARE were greater than zero. This indicates that a CN of 56 resulted in a consistent over-estimation of $Q_{T,O}$. The MRE of 0.13, associated with $CN_{10,0.1}$, indicates that $CN_{10,0.1}$ resulted in a lower over-estimation of $Q_{T,O}$ than $Q_{T,S}$ estimated using $CN_{2,0.1}$, $CN_{5,0.1}$ and $CN_{LN,0.1}$.

In the different catchments, the optimum CN associated with best estimates of $Q_{T,O}$ determined from the MARE and MRE values was obtained using different CN estimation methods. Therefore, the next section contains the results from a comparison of the $Q_{T,O}$ and $Q_{T,S}$ depths that were calculated using the different derived CNs.

2.5.2.1 Performance of derived CNs on different catchments

The MARE (in ascending order) and MRE between the $Q_{T,O}$ and $Q_{T,S}$ depths, calculated using the $CN_{published}$ values, and the CNs derived using observed P-Q data were calculated. The results are given in Table 2.7. In general, $CN_{10,0.1}$, $CN_{5,0.1}$, $CN_{LN,0.1}$ and the mean $CN_{AMS,0.1}$ resulted in good estimates of $Q_{T,O}$ (low MARE and MRE). It was, however, evident that the optimum CNs, i.e. the CNs that resulted in the lowest MRE and MARE on a catchment differed from the $CN_{published}$ values. Furthermore, the optimum CNs may have been derived using different methods. As detailed in the next section, the single-best CN derivation technique was identified using the $P_{T,O}$ and $Q_{T,O}$ data from all six study sites for all return periods using the MRE, MARE and linear regression analyses.

Table 2.7: The average MARE and MRE across all the catchments when using $CN_{published}$ and CNs derived using observed P-Q data

CN derivation method	MARE	MRE
$CN_{10,0.1}$	0.12	0.05
$CN_{5,0.1}$	0.13	0.09
Mean $CN_{AMS,0.1}$	0.17	0.11
$CN_{LN,0.1}$	0.17	0.02
$CN_{2,0.1}$	0.17	0.12
Median $CN_{AMS,0.1}$	0.19	0.08
Median $CN_{AnnMin,0.2}$	0.2	-0.04
Mean $CN_{AnnMin,0.2}$	0.22	-0.05
AMS $CN_{NEH,0.1}$	0.22	0
AMS $CN_{K\text{-}Mean,0.1}$	0.23	0.05
$CN_{\infty,0.1}$	0.33	0.2
$CN_{published}$	0.34	0.01
Median $CN_{AnnMin,0.1}$	0.52	-0.5
Mean $CN_{AnnMin,0.1}$	0.54	-0.52

2.5.2.2 Identification of the single-best CN-derivation technique for all the study sites

The $Q_{T,S}$ values from all the catchments were used to identify the CN-derivation method that performed the best in terms of estimating $Q_{T,O}$, taking all the catchments into account. A summary of the statistics when assessing the CN-derivation methods on all catchments for all return periods is provided in Table 2.8. The statistics from Table 2.8 indicate that there is a strong linear relationship between the $Q_{T,O}$ and $Q_{T,S}$, calculated using $CN_{10,0.1}$, which is overall the highest ranked method.

It is also evident that the relationship between $Q_{T,S}$ and $Q_{T,O}$ was stronger when using data-derived CNs such as $CN_{10,0.1}$ instead of the $CN_{published}$ values. This is identified by the higher R^2 and smaller MARE (Table 2.8) for the $CN_{10,0.1}$, compared to the lower R^2 and higher MARE (Table 2.8) when the $CN_{published}$ values were used to calculate $Q_{T,S}$.

Table 2.8: Performance of CN-derivation methods assessed using $P_{T,O}$ and $Q_{T,O}$ data for all return periods on all the catchments

CN derivation method	MARE	MRE	Rank (MARE)	R^2	Rank (R^2)	Slope	Rank (slope)	Base constant (y-intercept)	Sum of ranks
$CN_{published}$	0.34	0.01	10	0.85	5	1.34	10	-8.73	25
Median $CN_{AnnMin,0.2}$	0.20	-0.04	6	0.87	3	1.20	3	-8.08	12
Mean $CN_{AnnMin,0.2}$	0.22	-0.05	7	0.85	5	1.18	1	-7.63	13
Mean $CN_{AMS,0.1}$	0.17	0.11	5	0.85	5	1.26	6	-3.40	16
$CN_{LN,0.1}$	0.17	0.02	3	0.82	8	1.18	1	-4.00	12
$CN_{2,0.1}$	0.17	0.12	4	0.80	9	1.32	9	-5.20	22
$CN_{5,0.1}$	0.13	0.09	2	0.87	3	1.29	8	-6.45	13
$CN_{10,0.1}$	0.12	0.05	1	0.91	2	1.23	4	-6.29	7
AMS $CN_{K\text{- Mean},0.1}$	0.23	0.05	9	0.94	1	1.26	6	-8.14	16
AMS $CN_{NEH,0.1}$	0.22	0.00	8	0.79	10	1.23	4	-5.24	22

The CNs derived using simulated P-Q depths were evaluated. Results from the analyses are provided in Section 2.5.3.

2.5.3 Use of CNs derived from simulated P-Q values

In Section 2.5.2, the CNs derived using observed P-Q data were evaluated using MARE, MRE, slope and R^2. In this section, the CNs derived using simulated P-Q depths from $ACRU_{TR\text{-}P}$ and $ACRU_{CON\text{-}P}$, as presented in Section 2.4.2, were used to estimate $Q_{T,S}$ and subsequently evaluate the performance of the CN-derivation methods. The results were analysed to determine whether the $CN_{published}$ values or the CNs derived using simulated P-Q depths resulted in more accurate estimates of $Q_{T,O}$. All the CN-derivation techniques were assessed individually on each catchment. A summary of the CNs derived for Catchment U2H020 using simulated P-Q depths from $ACRU_{TR\text{-}P}$ and the MRE and MARE, ranked in ascending order, is provided in Table 2.9.

Table 2.9: MARE and MRE values obtained when using the $CN_{published}$ and CNs derived using simulated Q ($ACRU_{TR\text{-}P}$) values on Catchment U2H020

CN	Method	MRE	MARE
64	Mean S-$CN_{AMS,0.1}$	0.03	0.07
63	S-$CN_{LN,0.1}$	-0.01	0.07
	S-$CN_{10,0.1}$		
65	S-$CN_{2,0.1}$	0.07	0.08
	S-$CN_{5,0.1}$		
62	AMS S-$CN_{NEH,0.1}$	-0.04	0.08
61	$CN_{published}$	-0.08	0.09
55	AMS S-$CN_{K\text{-}Mean,0.1}$	-0.29	0.29
54	Median S-$CN_{AnnMin,0.1}$	-0.32	0.32
	Mean S-$CN_{AnnMin,0.1}$		

The lowest total error between $Q_{T,O}$ and $Q_{T,S}$ was obtained when the mean S-$CN_{AMS,0.1}$, S- $CN_{LN,0.1}$ and S-$CN_{10,0.1}$ (MARE = 0.07) was used to calculate $Q_{T,S}$ in Catchment U2H020. When the S-$CN_{LN,0.1}$ and S-$CN_{10,0.1}$ were used to estimate $Q_{T,S}$ in Catchment U2H020, the MARE and MRE were 0.07 and -0.01, respectively, which indicates that that there was a good correlation between $Q_{T,O}$ and $Q_{T,S}$. The negative MRE shows that there was a slight tendency to under-estimate $Q_{T,O}$. However, the MRE of 0.03 associated with S-$CN_{AMS,0.1}$ = 64 indicates that there was a slight over-estimation of $Q_{T,O}$ in comparison to when the S-$CN_{10,0.1}$ or S-$CN_{LN,0.1}$ was used to estimate $Q_{T,S}$. The $CN_{published}$ value resulted in a combination of both an under- and over-estimation of $Q_{T,O}$, as indicated by the MRE that was less than the MARE. However, in general, the different CN-derivation methods performed differently in the study catchments. The MRE and MARE between the $Q_{T,O}$ and $Q_{T,S}$ calculated using the different derived CNs are provided in Section 2.5.3.1.

2.5.3.1 Differences in the performance of derived CNs on the different catchments

The optimum CNs, derived using P-Q depths simulated from $ACRU_{TR-P}$, were obtained using different methods on the different catchments. Therefore, each different CN-derivation method was assessed using the $P_{T,O}$ and $Q_{T,O}$ values from all the catchments to identify the CN-derivation method that performed the best, taking all the catchments into account. A linear regression analysis was performed using the $Q_{T,O}$ and $Q_{T,S}$ for all catchments for all return periods to evaluate the different derived CN values collectively across the different catchments. As summarised in Table 2.10, there is a strong linear relationship between the $Q_{T,O}$ and $Q_{T,S}$ calculated using S-$CN_{10,0.1}$. This is supported by the high R^2 and low MARE and MRE shown in Table 2.10.

Table 2.10: The average MARE and MRE across all the catchments when using CNs derived using Q depths simulated from $ACRU_{TR-P}$

CN-derivation method	MARE	MRE	Rank (MARE)	R^2	Rank (R^2)	Slope	Rank (slope)	Base constant (y-intercept)	Sum of ranks
$CN_{published}$	0.34	0.01	8	0.85	8	1.34	7	-8.73	23
Median S-$CN_{AnnMin,0.2}$	0.33	-0.16	7	0.86	6	1.18	2	-9.20	15
Mean S-$CN_{AnnMin,0.2}$	0.30	-0.15	6	0.86	6	1.16	1	-8.24	13
Mean S-$CN_{AMS,0.1}$	0.24	0.09	5	0.88	2	1.34	7	-6.23	14
S-$CN_{LN,0.1}$	0.22	0.03	2	0.88	2	1.29	5	-6.96	9
S-$CN_{2,0.1}$	0.23	0.12	4	0.87	5	1.37	9	-6.23	18
S-$CN_{10,0.1}$	0.21	-0.08	1	0.89	1	1.23	4	-9.04	6
AMS S-$CN_{K\text{-}Mean,0.1}$	0.36	-0.05	9	0.65	9	1.21	3	-5.25	21
AMS S-$CN_{NEH,0.1}$	0.23	0.03	3	0.88	2	1.29	5	-7.18	10

In comparison to the $CN_{published}$ values, the mean S-$CN_{AMS,0.1}$, S-$CN_{2,0.1}$, S-$CN_{5,0.1}$, S-$CN1_{0,0.1}$, S-$CN_{LN,0.1}$ and AMS S-$CN_{NEH,0.1}$ resulted in improved estimates of $Q_{T,O}$ in the study catchments. The S-$CN_{10,0.1}$ resulted in improved estimates of $Q_{T,O}$ on five of the six catchments in comparison to the $CN_{published}$ values. Overall, S-$CN_{10,0.1}$ performed best in terms of estimating $Q_{T,O}$, as indicated by the lowest sum of rank (SOR) value in Table 2.10.

In addition to $ACRU_{TR-P}$, $ACRU_{CON-P}$ was also used to simulate Q depths that were used to calculate CNs using the CN-derivation techniques mentioned in Section 2.5.2. The R^2, MARE and MRE between $Q_{T,O}$ and $Q_{T,S}$, calculated using the $CN_{published}$ values, and the CNs derived using simulated Q depths from $ACRU_{CON-P}$ were calculated. The results are given in Table 2.11.

Table 2.11: The MARE and MRE between $Q_{T,O}$ and $Q_{T,S}$ depths calculated using CNs derived using Q depths simulated from $ACRU_{CON-P}$

CN-derivation method	MARE	MRE	Rank (MARE)	R^2	Rank (R^2)	Slope	Rank (slope)	Base constant (y-intercept)	Sum of ranks
$CN_{published}$	0.34	0.01	5	0.85	8	1.34	9	-8.73	22
Median $S\text{-}CN_{AnnMin,0.1}$	0.35	-0.26	8	0.89	5	1.10	3	-11.01	16
Mean $S\text{-}CN_{AnnMin,0.1}$	0.34	-0.25	7	0.90	4	1.11	4	-11.10	15
Mean $S\text{-}CN_{AMS,0.1}$	0.28	0.06	3	0.89	5	1.27	8	-6.25	16
$S\text{-}CN_{LN,0.1}$	0.25	-0.11	1	0.91	2	1.12	5	-7.35	8
$S\text{-}CN_{2,0.1}$	0.27	-0.08	2	0.90	3	1.22	6	-9.33	11
$S\text{-}CN_{10,0.1}$	0.36	-0.33	9	0.92	1	1.01	2	-11.06	12
AMS $S\text{-}CN_{K\text{-}Mean,0.1}$	0.34	-0.26	6	0.77	9	0.92	1	-3.67	16
AMS $S\text{-}CN_{NEH,0.1}$	0.29	-0.04	4	0.89	5	1.25	7	-8.32	16

The high MARE values in Table 2.11 indicate that no single CN-derivation method performed consistently well when $ACRU_{CON-P}$ was used to simulate P-Q depths and derive CNs. In terms of $Q_{T,S}$ estimates, the MARE is worse (higher) when using $CN_{published}$ compared to $S\text{-}CN_{LN,0.1}$ (lowest MARE), and the R^2 is better (closer to 1) when using $S\text{-}CN_{LN,0.1}$ compared to the $CN_{published}$ values. The MRE was higher and positive for $CN_{published}$, compared to the negative, lower value for both $S\text{-}CN_{LN,0.1}$ and $S\text{-}CN_{10,0.1}$, indicating a greater tendency for $S\text{-}CN_{LN,0.1}$ and $S\text{-}CN_{10,0.1}$ to under-estimate $Q_{T,O}$. Overall, when using $ACRU_{CON-P}$ to simulate Q and derive CNs, the $S\text{-}CN_{LN,0.1}$ resulted in the best estimates of $Q_{T,O}$, as indicated by the lowest SOR in Table 2.11.

2.5.3.2 Comparison between CNs derived using observed P-Q data and simulated Q depths from $ACRU_{CON-P}$ and $ACRU_{TR-P}$

In this section, $Q_{T,O}$ and $Q_{T,S}$, calculated using CNs derived using observed P-Q data and simulated P-Q depths from $ACRU_{CON-P}$ and $ACRU_{TR-P}$, are compared. The comparison was done to determine whether the CNs derived using simulated P-Q depths from $ACRU_{CON-P}$ or $ACRU_{TR-P}$ resulted in better estimates of $Q_{T,O}$ compared to the $Q_{T,S}$ calculated using CNs derived from observed P-Q data.

As shown in Section 2.5.3.1, when $ACRU_{TR-P}$ was used to simulate P-Q depths and derive CNs, the overall best performance of the SCS-CN method was achieved when $S\text{-}CN_{LN,0.1}$ and $S\text{-}CN_{10,0.1}$ values were used to estimate $Q_{T,S}$. Subsequently, the $Q_{T,O}$ and $Q_{T,S}$ calculated using CNs derived using simulated P-Q depths from $ACRU_{TR-P}$ and $ACRU_{CON-P}$, were compared. When $S\text{-}CN_{10,0.1}$ values, derived using simulated P-Q depths from $ACRU_{TR-P}$ and $ACRU_{CON-P}$, were compared, $S\text{-}CN_{10,0.1}$ performed better than the $CN_{published}$ values as mentioned in sections 2.5.3.1 and 2.5.3.2. Overall, $S\text{-}CN_{10,0.1}$, derived using simulated P-Q depths from $ACRU_{TR-P}$ (MARE = 0.21 across all catchments), performed better than $S\text{-}CN_{10,0.1}$ derived using simulated P-Q depths from $ACRU_{CON-P}$ (MARE = 0.36 across all catchments).

As indicated above, the optimum CNs, i.e. the CNs that resulted in the best correlation between $Q_{T,O}$ and $Q_{T,S}$ with minimal over- or under-simulation, were derived using different methods in the study catchments. This was also the case when using observed P-Q data, as mentioned previously. However, in general, the CNs derived using $ACRU_{CON-P}$ were lower than the CNs derived using $ACRU_{TR-P}$. Furthermore, no single method performed well on all catchments when using P-Q depths simulated by $ACRU_{CON-P}$ to calculate CNs, but the $S\text{-}CN_{10,0.1}$ derived using P-Q depths from $ACRU_{TR-P}$ resulted in good estimations of $Q_{T,O}$ on five of the six study catchments.

The ability of $ACRU_{TR-P}$ to account for different hydrological responses that are used to parametrise the SMDDEP and QFRESP in ACRU was identified as a major advantage over $ACRU_{CON-P}$. Although the QFRESP and SMDDEP parameters that were used to set up $ACRU_{TR-P}$ were calibrated using the $CN_{published}$ values, the $S\text{-}CN_{10,0.1}$ calculated using P-Q depths simulated using $ACRU_{TR-P}$ resulted in improved estimates of $Q_{T,O}$ compared to the $Q_{T,S}$ estimated using $CN_{published}$ or the CN values that were derived using P-Q depths simulated from $ACRU_{CON-P}$.

Table 2.12 contains a comparison of the $Q_{T,O}$ and $Q_{T,S}$ values calculated using the $CN_{published}$ values, the $CN_{10,0.1}$ values derived using observed data and the $S\text{-}CN_{10,0.1}$ values derived using simulated Q depths from $ACRU_{TR-P}$ and $ACRU_{CON-P}$.

Table 2.12: Comparison between $CN_{10,0.1}$ values derived using observed P-Q data and simulated P-Q depths ($ACRU_{TR-P}$ and $ACRU_{CON-P}$)

Catchment	$CN_{10,0.1}$		$S\text{-}CN_{10,0.1}$ ($ACRU_{CON-P}$)		$S\text{-}CN_{10,0.1}$ ($ACRU_{TR-P}$)		$CN_{published}$	
	MRE	**MARE**	**MRE**	**MARE**	**MRE**	**MARE**	**MRE**	**MARE**
A9H006	-0.02	0.03	-0.14	0.14	0.02	0.03	0.56	0.56
U2H018	0.13	0.18	-0.15	0.27	-0.31	0.35	-0.11	0.25
U2H020	0.07	0.08	-0.32	0.32	-0.01	0.07	-0.08	0.09
V1H005	-0.03	0.04	-0.42	0.42	-0.28	0.28	-0.42	0.42
V1H015	0.01	0.03	-0.58	0.58	-0.11	0.11	-0.25	0.25
W1H016	0.11	0.37	-0.37	0.43	0.21	0.40	0.34	0.44
Mean	0.05	0.12	-0.33	0.36	-0.08	0.21	0.01	0.34
Slope	1.23		1.01		1.23		1.34	
R^2	0.91		0.92		0.89		0.85	

As shown in Table 2.12, the $CN_{10,0.1}$ values resulted in improved estimates of $Q_{T,O}$ in all six catchments in comparison to the $CN_{published}$ values. In addition, the results given in Table 2.12 show that the $S\text{-}CN_{10,0.1}$ values derived using $ACRU_{TR-P}$ resulted in better estimates of $Q_{T,O}$ (an MRE closer to zero and a lower MARE) compared to the $S\text{-}CN_{10,0.1}$ values derived using $ACRU_{CON-P}$. However, the R^2 and slope for $S\text{-}CN_{10,0.1}$ ($ACRU_{CON-P}$) were closer to one than the R^2 and slope for $S\text{-}CN_{10,0.1}$ ($ACRU_{TR-P}$). Based on the results obtained from the study catchments, it is evident that the best derived CNs, i.e. $CN_{10,0.1}$ and $S\text{-}CN_{10,0.1}$ ($ACRU_{TR-P}$ and $ACRU_{CON-P}$), resulted in improved estimates of $Q_{T,O}$ compared to the $Q_{T,S}$ calculated using the $CN_{published}$ values. In Section 2.6, the observed design peak discharge for each study catchment is compared to the design peak discharge estimated using the SCS-SA model.

2.6 ASSESSMENT OF PEAK DISCHARGE ESTIMATED USING PUBLISHED AND DATA-DERIVED CNS

The peak discharge estimated using the SCS model is a function of catchment area, runoff depth, effective storm duration and catchment lag. In the original SCS lag equation, the catchment lag was based on physical catchment characteristics. The estimation of catchment lag has frequently been attributed to being a source of error when estimating peak discharge using the SCS model (Schulze and Schmidt, 1984). In the original SCS peak discharge equation, the calculation of peak discharge is done using a dimensionless unit hydrograph, where the catchment response time is only related to catchment physiographic factors (Schulze, 1984; Schulze and Schmidt, 1984). This introduces linearity to the response factor.

The incorporation of non-linear processes in unit hydrograph theory with an adjustment of the unit hydrograph according to storm magnitude is particularly important in small catchments where the peak discharge rates are subject to varying intensities of rainfall (Schulze, 1984). Therefore, Schulze and Schmidt (1984) attempted various procedures to estimate peak flow rates more realistically when using the SCS model. Schulze and Schmidt (1984) obtained improved estimates of lag time for ungauged catchments when indices of regional rainfall characteristics and climate were incorporated into an empirical lag equation (Schmidt-Schulze lag equation). In addition, Schulze (1984) stated that the distribution of rainfall is one of the key inputs for hydrological models used for design purposes in small catchments.

The performance of the SCS-SA model using $CN_{published}$ values and derived CNs is evaluated in this section using data from the following eight catchments: A9H006, V1H005, V1H015, V1H032, V7H003, U2H018, U2H020 and W1H016. Design peak discharge values were estimated using the conventional SCS-SA model as it is currently applied in practice. The $CN_{published}$ values, as well as the CN_{10} values derived by Maharaj (2020), were used with the SCS-SA model. For all the different cases ($CN_{published}$ or CN_{10} derived using observed or simulated data), the Schmidt-Schulze lag equation was applied, and the generalised extreme value (GEV) was used to estimate the design-observed peak discharges and design-observed rainfall depths ($P_{T,O}$) for the 2-, 5-, 10-, 20-, 50- and 100-year return periods. The design peak discharge calculated using the $P_{T,O}$, $CN_{published}$ and CN_{10} values derived using observed and simulated values for the sites, and c = 0.1 was compared to the observed design peak discharge values using MARE. Figure 2.5 shows the average MARE between the observed and simulated peak discharge for the 2, 5, 10-, 20-, 50- and 100-year return periods for each of the eight catchments.

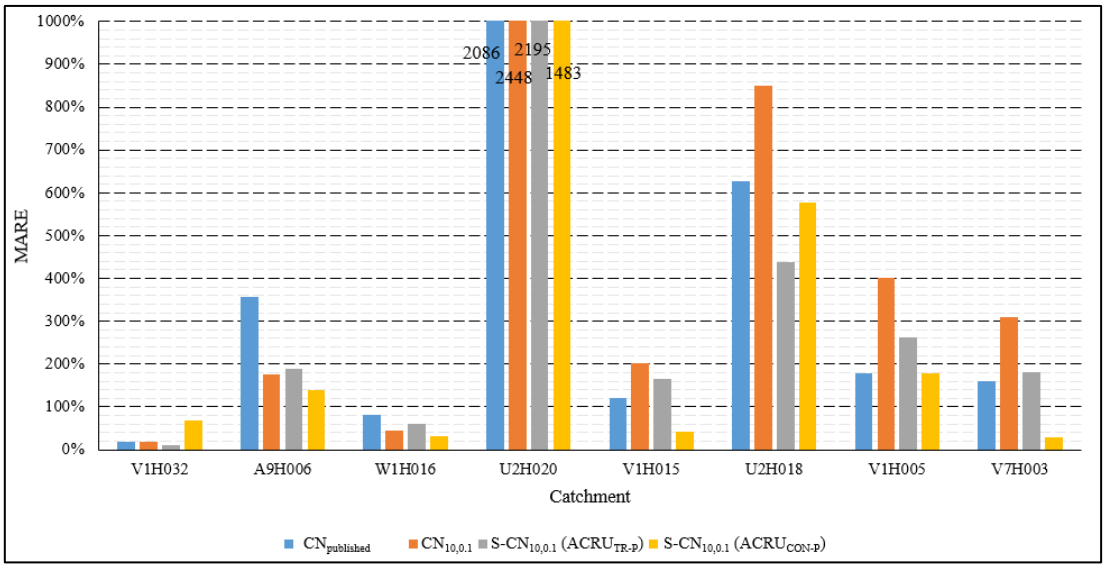

Figure 2.5: MARE between the design-observed and estimated peak discharge values computed for the 2-, 5-, 10-, 20-, 50- and 100-year return periods

For the results shown in Figure 2.5, the simulated peak discharges were computed using the currently utilised SCS-SA model. The model was set up using the catchment areas, slope, mean annual precipitation (MAP) and rainfall region from Table 2.1. Four different simulations were done using $CN_{published}$, CN_{10} calculated using observed P-Q data, CN_{10} calculated using Q depths from $ACRU_{CON-P}$ and CN_{10} calculated using Q depths simulated from $ACRU_{TR-P}$. It is interesting to note that the different CNs resulted in good estimates of the observed design peak discharges in Catchment V1H032, which was the largest catchment (67.8 km^2). The MARE between the observed and calculated peak discharge was averaged using the results for each catchment. The results from the analyses are summarised in Table 2.13.

Table 2.13: Average MARE between observed and estimated design peak discharge values

CN estimation method	Average MARE (%)
$CN_{published}$	453
$CN_{10,0.1}$	556
S-$CN_{10,0.1}$ ($ACRU_{TR-P}$)	437
S-$CN_{10,0.1}$ ($ACRU_{CON-P}$)	319

When the design peak discharges were calculated, overall, S-$CN_{10,0.1}$ ($ACRU_{CON-P}$) resulted in the lowest MARE (averaged across all catchments) between the observed and design peak discharge. However, S-$CN_{10,0.1}$, calculated using Q depths from $ACRU_{CON-P}$, generally resulted in an under-estimation of $Q_{T,O}$ (Maharaj, 2020) and the $CN_{10,0.1}$ derived using observed P-Q data. The S-$CN_{10,0.1}$ calculated using Q depths simulated from $ACRU_{TR-P}$ resulted in the best estimates of $Q_{T,O}$ (Maharaj, 2020). The peak discharge estimated using the SCS peak discharge equation is directly proportional to runoff volume (Schulze, 1984). However, as shown in Figure 2.5, the peak discharge calculated using derived CNs that resulted in good estimates of runoff volumes (Table 2.12) did not result in good estimates of peak discharge.

2.7 DISCUSSION AND CONCLUSIONS

The SCS-CN equation is an empirical equation that transforms a rainfall depth to a runoff depth. Various CN tables have been published in the literature, but information regarding the background and details about the calibration of CNs in these tables is rarely provided. This creates misunderstandings regarding the quality of data and degree of subjective interpolation used to derive the $CN_{published}$ values. There are numerous different approaches to derive CNs using observed or simulated P-Q depths. However, the CN values derived using the different methods may be dissimilar and could lead to different fundamental definitions of the CN. Additionally, the selected data series (ordered or natural, annual maximum series or daily event data) may also result in different CNs. Based on the CNs derived using P-Q values from the catchments used in this study, it is apparent that not all CN-derivation techniques perform well on all the catchments. The differences between the data-derived CNs in different catchments when using different methods is evident. The c value also plays a role in the magnitude of the calculated CN. The inverse relationship between c and the CN is evident from the results, where the data-derived CNs were lower when c = 0.1 was used compared to c = 0.2 to derive the CNs.

One aim of this study was to determine the best method to replicate the $CN_{published}$ values that were selected for each study catchment. If observed P-Q data is available, the most suitable method currently identified to replicate the published CNs is AMS $CN_{NEH,0.1}$, which resulted in the lowest MARE (10%) between the $CN_{published}$ and derived CNs. The CNs derived using simulated Q values from $ACRU_{CON-P}$ were comparable to the CNs derived using observed P-Q data (similar MARE values). As expected, the CNs derived using $ACRU_{TR-P}$ resulted in CNs closest to the published CNs. This was expected because the $CN_{published}$ values were used to calibrate some of the parameters used with $ACRU_{TR-P}$. Therefore, if observed Q data is not available, the mean S-$CN_{AMS,0.1}$ and AMS S-$CN_{NEH,0.1}$ (derived using simulated P-Q depths from $ACRU_{TR-P}$) resulted in derived CN values that were similar to the published CNs with the least error (the MARE between the published and derived CNs was 5%). Therefore, if the user of the SCS-CN model has confidence in the published CNs, the methods that were identified to replicate the published CNs will be useful to derive CNs on catchments with land-cover classes that are not currently available in the published CN tables. The user should remove the subjective interpolation when no observed data is available for a given LULC and HSG combination.

One of the significant issues that emerged from these findings is that the CN is sensitive to c. The results from this study indicate that the c value also plays a role in the magnitude of the calculated CN. The inverse relationship between c and the CN is evident from the results, where the data-derived CNs were lower when c = 0.1 was used compared to c = 0.2 to derive the CNs. The CNs derived using observed data and c = 0.1 were generally closer to the $CN_{published}$ values. This was unexpected, because the $CN_{published}$ values were derived using c = 0.2. It is also important to note the inconsistency of the recommendation to use c = 0.1 for South Africa with $CN_{published}$ values that were derived with c = 0.2. This finding has important implications for developing an updated CN table for South Africa, because the c used with the SCS-CN equation to estimate $Q_{T,S}$ must be consistent with the c used to derive the CN. Therefore, future research should focus on the calibration of the c and the CN. In addition to c = 0.1 and c = 0.2, experimentation with the use of different c values when calculating CNs using observed P-Q data is required.

An additional aim of this study was to assess the $Q_{T,S}$ values calculated using the CNs derived using observed P-Q data or simulated Q depths. The use of the $CN_{published}$ values to estimate Q_T was also evaluated by comparing the $Q_{T,O}$ and $Q_{T,S}$ depths. In general, the $CN_{published}$ values resulted in poor estimates of runoff with high MARE values between $Q_{T,O}$ and $Q_{T,S}$ on five of the six catchments. Initially, each CN-derivation technique was evaluated separately on each catchment. The different CN-derivation techniques resulted in different CNs being derived for the same catchment. This led to different $Q_{T,S}$ values being estimated for the same catchment. However, the best fit for $Q_{T,O}$ in most catchments was achieved with the data-derived $CN_{10,0.1}$ values. The $CN_{10,0.1}$ resulted in a lower MARE between $Q_{T,O}$ and $Q_{T,S}$ than the $CN_{published}$ values in all six of the study catchments. The $S\text{-}CN_{10,0.1}$ calculated using P-Q depths simulated for all RPs from $ACRU_{TR\text{-}P}$ also resulted in a lower MARE between $Q_{T,O}$ and $Q_{T,S}$ than the $CN_{published}$ values in five of the six study catchments. However, in some catchments, the CNs derived using other methods resulted in a better fit (lower MARE) to the observed data than $CN_{10,0.1}$ or $S\text{-}CN_{10,0.1}$. Therefore, the optimum CNs were identified for each catchment. Each of the optimum CN-derivation techniques were assessed using the $P_{T,O}$ and $Q_{T,O}$ data from all the study catchments to identify the single-best CN-derivation technique. When the CN-derivation methods were assessed using $P_{T,O}$ and $Q_{T,O}$ values from all the catchments, the $CN_{10,0.1}$ resulted in the best estimates of $Q_{T,O}$ with the lowest overall MARE and a high R^2. When using Q depths simulated from $ACRU_{TR\text{-}P}$, the overall best performance of the SCS-CN method was also achieved when the $S\text{-}CN_{10,0.1}$ values were used to estimate $Q_{T,S}$. When using Q depths simulated from $ACRU_{CON\text{-}P}$, the overall best performance of the SCS-CN method was achieved when $S\text{-}CN_{LN,0.1}$ values were used to estimate $Q_{T,S}$.

A common misconception is that the published CNs are credible and applicable in all situations. The basis for this statement is that the published CN values seem to generally be estimates or judgements based on soil and vegetation in the absence of local P-Q data. The most consistent CN-derivation technique that can replicate published CNs with the least error was identified. The performance of the SCS-CN equation using $CN_{published}$ and derived CNs was evaluated by comparing $Q_{T,S}$ and $Q_{T,O}$ using different statistics. The $CN_{published}$ values only performed well in one of the study catchments. In general, when using the $CN_{published}$ values to estimate $Q_{T,S}$, the larger $Q_{T,O}$ values were over-estimated and there was a better correlation between the lower $Q_{T,O}$ and $Q_{T,S}$ values. A possible reason for this could be that the CNs were derived using P-Q data from catchments in the USA with P-Q patterns that are not applicable to local catchments. The results from this study indicate that the $CN_{published}$ values are not suitable for use in South Africa. Therefore, the different CNs derived using observed P-Q data were also assessed to determine whether the data-derived CNs result in better estimates of $Q_{T,O}$.

From the results presented in this chapter, it is evident that CNs are more accurately defined by observed P-Q data or simulated Q values for a specific catchment and not from published CN tables. Therefore, it is recommended that the methods that resulted in the lowest MRE and MARE between the $Q_{T,O}$ and $Q_{T,S}$, such as the $CN_{10,0.1}$ value derived using observed P-Q data, be used to derive CNs for catchments with observed P-Q data in South Africa.

Furthermore, in the absence of reliable P-Q data, the results from this study indicate that the S-$CN_{10,0.1}$ values calculated using simulated Q depths from $ACRU_{TR-P}$ and the S-$CN_{LN,0.1}$ calculated using Q depths from $ACRU_{CON-P}$ resulted in improved estimates of $Q_{T,O}$ compared to the $Q_{T,S}$ values estimated using $CN_{published}$ values.

When the design peak discharges were calculated using the SCS-SA model, overall, S- $CN_{10,0.1}$ ($ACRU_{CON-P}$) resulted in the lowest MARE (averaged across all catchments) between the observed and design peak discharge values. The $CN_{published}$ and $CN_{10,0.1}$ values only performed well in terms of estimating design peak discharges in Catchment V1H032. However, in terms of estimating runoff depths, the $CN_{10,0.1}$ values resulted in improved estimates of $Q_{T,O}$ in all the study catchments in comparison to the $CN_{published}$ values. In addition, the S-$CN_{10,0.1}$ values derived using Q depths simulated using $ACRU_{TR-P}$ resulted in better estimates of $Q_{T,O}$ (an MRE closer to zero and a lower MARE) compared to the S- $CN_{10,0.1}$ values derived using $ACRU_{CON-P}$. The S-$CN_{10,0.1}$ calculated using Q depths from $ACRU_{CON-P}$ generally resulted in an under-estimation of observed Q depths (Maharaj, 2020). In addition, Rowe (2019) stated that “the results indicated a tendency of the default implementation of the ACRU model to under-estimate daily streamflow volumes and design streamflow volumes”. However, the S-$CN_{10,0.1}$ values (calculated using simulated Q depths from $ACRU_{CON-P}$), which were much smaller than the published and other derived CNs, resulted in the best estimates of design peak discharge values.

From the results obtained in this study, it is evident that the use of both published and derived CNs resulted in a large over-estimation of design peak discharges when using the SCS-SA model. This indicates that there may be an issue with the model in terms of converting a runoff volume/depth to a peak discharge. According to Schulze (1984), the estimates of peak discharge are highly sensitive to the rainfall distribution curves used with the SCS-CN model. Therefore, the poor estimates of peak discharge obtained in this study may be attributed to the inputs into the peak discharge equation or the peak discharge equation used to translate a runoff depth to a peak discharge value. Therefore, the peak discharge equation, and the methods used to estimate lag time and effective storm duration, need to be analysed and updated if needed.

CHAPTER 3: DEVELOPMENT AND ASSESSMENT OF AN IMPROVED CONTINUOUS SIMULATION MODELLING SYSTEM FOR DESIGN FLOOD ESTIMATION IN SOUTH AFRICA USING THE ACRU MODEL

TJ Rowe, JC Smithers, U Maharaj and NS Dlamini

3.1 INTRODUCTION

The assessment of flood risk by associating the magnitude of a flood event with the probability of an exceedance or return period is the standard approach to design flood estimation in most countries (Smithers, 2012; Kang et al., 2013). Smithers (2012) and Smithers et al. (2013) categorise DFE techniques used in South Africa into two groups: the analysis of observed flow data, and rainfall run-off-based methods. Most of the methods used for design flood estimation in South Africa were developed in the 1970s and 1980s with the resources and hydrological data available at the time. With the extended hydrological records currently available, advances in technology and knowledge, and a number of extreme events exceeding previous records, the need to update these methods has been well documented in the literature (Alexander, 2002; Smithers and Schulze, 2002; Görgens, 2007; Smithers, 2012; Van Vuuren et al., 2013). Consequently, a National Flood Studies Programme, aimed at updating and modernising the various approaches to DFE used in South Africa, has been proposed and initiated (Smithers et al., 2016).

One of the recommendations contained in the plan for the NFSP is the development and assessment of a continuous simulation modelling approach to DFE. Due to the limited availability of streamflow data in South Africa, both in terms of the number of gauges and record length, and/or errors and inconsistencies in the data, rainfall-runoff methods for DFE are often required and applied in preference to, or in combination with, methods based on the analysis of observed flow data. Rainfall records, on the other hand, are available from a denser network of gauges, are generally of a better quality, and have longer records compared to streamflow data (Schulze, 1989; Smithers and Schulze, 2002; Smithers, 2012). Therefore, based on the advantages of the CSM approach alluded to above, the rationale for the further development and assessment of a CSM approach for DFE in South Africa is evident.

A CSM approach, like many of the rainfall-runoff methods used in South Africa, is generally applicable and well suited to small catchments (0–100 km^2). However, it is not limited to this size range. A CSM approach to DFE was applied in a pilot study in the 29 036 km^2 Thukela catchment (Smithers et al., 2013). According to Smithers et al. (2016), the majority of the catchments (55%) for which design floods are required in South Africa are relatively small (< 15 km^2). In South Africa, the daily timestep ACRU agrohydrological model (Schulze, 1995) has provided reasonable results for DFE in several pilot studies and investigations (Smithers et al., 1997; 2001; 2007; 2013; Chetty and Smithers, 2005). The model is a physical conceptual model, since it is made up of idealised concepts, and is physically based, i.e. physical processes are explicitly represented (Schulze et al., 1994). The model is not a parameter-fitting or optimising model (Schulze et al., 1994). Therefore, parameters are not directly calibrated. Instead, they are assigned based on physical catchment characteristics, as estimated or obtained in the field. The performance of the model is verified against observed data (if available). Based on the verification results, specific parameters may be adjusted based on a sound conceptual understanding of the hydrological processes within a catchment.

The CSM approach to DFE may be particularly suited to South Africa for the following reasons. In South Africa, climate varies significantly across the country, and significant rainfall variability within relatively small areas is common. Therefore, a CSM approach that accounts for spatial differences in rainfall would be beneficial and appropriate in South Africa. Although promising results have been obtained applying a CSM approach to DFE, no comprehensive CSM methodology applicable at a national scale has been developed, such as is available for the event-based SCS-SA model. The SCS-SA event-based method was adopted from the CN method of the Soil Conservation Service (SCS, 1956; 1972) and adapted to South African conditions (Schmidt and Schulze, 1987). The SCS-SA approach (Schmidt and Schulze, 1987; Schulze et al., 1992; 2004) is widely used in practice in South Africa for DFE (Smithers, 2012; SANRAL, 2013; Smithers et al., 2016) and is generally recommended for use on small catchments (0–30 km^2). Rowe (2015) initiated preliminary investigations towards the development of a national-scale CSM methodology for DFE in South Africa using the ACRU model, and identified significant similarities and links between the SCS-SA and ACRU models, including the fact that both models use the SCS (1956) runoff equation.

A comprehensive review of CSM for DFE developments to date and potential for application in South Africa is provided in Rowe and Smithers (2018). Table 3.1 provides a summary of the steps required to develop and establish a national-scale CSM approach for DFE in South Africa. In terms of developing a useable system for practitioners, the most critical components from Table 3.1 are steps 3 and 4. As identified from the review of the developments towards a national CSM approach in the United Kingdom (Savvidou et al., 2016; Calver et al., 2005), and as highlighted by Lamb et al. (2016), this was the critical step that was not achieved. Therefore, the successful adoption of this approach will rely on the development of a final software tool, with all the necessary inputs and required national-scale databases. The idea, as alluded to in Table 3.1, is to base the system (particularly in terms of the user interface and options) on the already widely used SCS-SA event-based approach, which will assist in the adoption of the approach in practice.

The aim of the study reported in this chapter is to further develop and assess the performance of a comprehensive CSM system that can be used to consistently and reliably estimate design flood discharges in small catchments (0–100 km^2) throughout South Africa, and which can be easily applied by practitioners. Specific objectives include the following:

- Review CSM for DFE from both the international and local literature; this has been published (Rowe and Smithers, 2018c)
- Develop a comprehensive CSM system, including the definition of a structure and rules on how to implement the system, define a land-cover and soil classification to apply with the system, and assign default input information to use with the system
- Assess the performance of the above CSM system on selected catchments and, based on the results, perform any refinements or additional investigations to improve on the CSM system
- Assess the impact of model configuration and application on the performance of the CSM system that was developed and, based on the results, propose a final CSM system for DFE in South Africa
- Assess and compare the performance of the final CSM system proposed to that of the conventional SCS-SA model and associated antecedent soil water adjustment procedures

Full details of the results summarised in this chapter can be found in Rowe (2019).

Table 3.1: Flow chart of the necessary steps required to develop a comprehensive useable CSM approach for DFE in South Africa (Rowe and Smithers, 2018)

STEP 1
Further development, validation and verification of the ACRU continuous simulation model in terms of the following: • Input data (climate, soil, land cover), model structure in terms of process representation, and how best to set up or package the model in terms of ease of use, while still providing outputs of high quality and certainty, i.e. level of detail required • Accurate simulations of both day-to-day flows and extreme values in terms of volumes, peak discharges (lag time) and complete hydrographs • The inclusion of a methodology to account for uncertainty in model parameterisation
STEP 2
Further development, assessment and inclusion of national stochastic rainfall generation and/or disaggregation techniques: • These methods will introduce the ability to account for uncertainty in model time-series inputs, as well as increase confidence in estimates of high return-period events (100 years and above) • The methods should also provide options to estimate projected climate change scenarios. Alternatively, an additional set of rainfall models should be established for this. These techniques will be of significant benefit to both the CSM approach and other event-based simulation approaches.
STEP 3
• Compile all these steps and additional models into a user-friendly, simple software tool that is attractive to consultants and government organisations (e.g. Department of Water and Sanitation (DWS) and the South African National Roads Agency Limited (SANRAL)) • Training courses, workshops and user manuals are critical to the successful adoption of the approach. However, if the model options are similar to a tool that is already widely used, i.e. the SCS-SA model, this will greatly facilitate the adoption of the approach in practice.
STEP 4
• The approach must be continually updated, refined and improved, including, for example, flood routing routines and flood forecasting. • Close collaboration is needed between practitioners and model developers (researchers).

3.2 DEVELOPMENT OF AN IMPROVED COMPREHENSIVE CONTINUOUS SIMULATION MODELLING SYSTEM FOR DESIGN FLOOD ESTIMATION IN SOUTH AFRICA USING THE ACRU MODEL

To date, reasonable results have been obtained applying the daily timestep ACRU agrohydrological continuous simulation model (Schulze, 1995) in a number of pilot studies (Smithers et al., 1997; 2001; 2007; 2013; Chetty and Smithers, 2005). More recently, Rowe et al. (2018a) developed an approach to parameterise the ACRU continuous simulation model for DFE within South Africa to explicitly represent land-management practices and hydrological conditions for a range of land-cover classes defined in the SCS-SA land-cover classification, which are not represented, or not adequately represented, in the ACRU land-cover classification.

The most comprehensive land-cover classification available for use with the ACRU model is the COMPOVEG database (Schulze, 1995; Smithers and Schulze, 2004b). The COMPOVEG database contains the default assigned parameter values required by the ACRU model to represent five land-cover categories: urban land uses, agricultural crops, natural vegetation, aquatic systems and commercial forests, as classified by Schulze and Hohls (1993). The land-cover classification does not account for land-management practices associated with agricultural crops, as accounted for in the SCS-SA classification. Since the ACRU model is a daily timestep continuous simulation model, the land-cover classification accounts for different crop development stages, i.e. from planting to harvest and seasonal changes, and accounts for regional differences in planting dates for specific dominant crops cultivated extensively in different parts of the country, such as maize and wheat. The classification also distinguishes between commercial and subsistence crops. However, it does not explicitly represent the land-management practice and hydrological condition for crops. In terms of natural vegetation, the classification includes classes to represent good, fair and poor hydrological conditions for selected land-cover classes such as veld (grassland). This is, however, not consistently represented for all natural land-cover classes. Furthermore, Rowe et al. (2018a) identified that the ACRU model is insensitive to the parameters used to represent the different hydrological condition classes in terms of design flood estimates. This was particularly concerning, based on the comparative changes in runoff response simulated by the SCS-SA model for similar changes in hydrological condition and for similar land-cover classes. Rowe et al. (2018a) therefore performed a sensitivity analysis of the model to selected parameters to identify which parameters would more adequately represent the change in runoff response for different land-management practices and hydrological conditions. Since the CNs in the SCS-SA model were calibrated using observed data for a range of land-cover conditions, the results simulated by the SCS-SA model were used as a surrogate for observed data to simulate similar magnitudes and changes in runoff response in ACRU. This approach was adopted due to the limited observed runoff data from small catchments in South Africa and with only a limited range of land-cover and soil combinations. Rowe et al. (2018a) identified two flood-sensitive parameters in the ACRU model: the quick-flow response coefficient (QFRESP), which partitions stormflow into a same-day response fraction and a subsequent delayed stormflow response; and the critical hydrological response depth of the soil (SMDDEP). These parameters are currently set to recommended default values and have no direct physical meaning (Schulze, 1995). Rowe et al. (2018a), however, developed a methodology to estimate these two parameters using SCS-SA CNs. Thus, these parameters were related to soil and land-cover characteristics of the catchment via the CN.

3.2.1 Parameterisation of the ACRU model for DFE

Rowe et al. (2018a) used the design runoff volumes simulated by the SCS-SA model as a surrogate for observed data. The first step was to identify how to represent SCS-SA soil groups (A–D) in the ACRU model. Three attempts were made using tabulated soil textural properties to represent SCS-SA soil groups. However, these attempts alone were unsuccessful. Manual calibration of the QFRESP and SMDDEP parameter values, corresponding to a SCS-SA soil group and land-cover class, was undertaken, and used to represent that land-cover class in ACRU. This was achieved by adjusting the QFRESP and SMDDEP parameters in the ACRU model until similar runoff volumes to those simulated by the SCS-SA model were obtained for the equivalent land-cover class in ACRU.

Applying a multiple linear regression, a strong relationship between these two ACRU parameters and SCS-SA CN values was obtained and consequently preliminary rules and equations were developed to represent SCS-SA land-cover classes and soil groups in ACRU. However, the multiple linear regression was skewed by the results obtained for SCS-SA soil group C/D. Therefore, a separate multiple linear regression analysis was performed for soil group C/D. Equation 3.1 was derived from the multiple linear regression for all SCS-SA land-cover classes for all SCS-SA soil groups, excluding SCS-SA soil group C/D, to estimate “predicted” CN (CN_p) values for given QFRESP and SMDDEP combinations as calibrated against actual tabulated SCS-SA CN values.

$$CN_p = 43.91(QFRESP) - 75.52(SMDDEP) + 53.78 \quad 3.1$$

The CN_p values were then compared to the actual tabulated SCS-SA CN values. Based on the strong relationship obtained between the CN_p values and the actual tabulated SCS-SA CN values, Equation 3.1 was used to develop rules to estimated QFRESP and SMDDEP parameter values for tabulated SCS-SA CN values. These rules, for all SCS-SA soil groups excluding SCS-SA soil group C/D, are provided in Table 3.2.

Table 3.2: Rules developed for all SCS-SA soil groups, excluding SCS-SA soil group C/D

Rules	CN 40–48	CN 48–79	CN > 79
	QFRESP = 0.3	SMDDEP = 0.25	QFRESP = 1
Input CN	46	79	82
Rearrange Equation 3.1 to solve for SMDDEP or QFRESP	SMDDEP	QFRESP	SMDDEP
Calculated value	0.28	1.00	0.21

Equation 3.2 was derived to estimate CN_p values for given QFRESP and SMDDEP combinations for all SCS-SA land-cover classes for SCS-SA soil group C/D:

$$CN_p = 32.92(QFRESP) - 48.28(SMDDEP) + 63.91 \quad 3.1$$

In addition, the rules presented in Table 3.3 were determined for SCS-SA soil group C/D and are interpreted in the same manner as the results from Table 3.2.

Table 3.3: Rules developed for SCS-SA soil group C/D only

Rules	CN 57–62	CN 62–85	CN > 85
	QFRESP = 0.3	SMDDEP = 0.25	QFRESP = 1
Input CN	62	85	88
Rearrange Equation 3.2 to solve for SMDDEP or QFRESP	SMDDEP	QFRESP	SMDDEP
Calculated value	0.24	1.01	0.18

The rules defined by Rowe et al. (2018a) were only developed and assessed using design runoff volumes and not peak discharges. Furthermore, the results were not verified against observed data. Therefore, Rowe et al. (2018a) recommended the further development and assessment of the approach. This included the further development of a comprehensive CSM system for DFE in South Africa, and the verification of the system performance against observed data in terms of both simulated streamflow volumes and peak discharges. The next section addresses the first recommendation listed above, i.e. the further development of a comprehensive CSM system for DFE in South Africa using the ACRU model. This includes defining a complete structure of the system, default datasets and classifications to use with the system, and model options.

3.2.2 Development of a comprehensive CSM system for DFE using the ACRU model

In order to establish a comprehensive CSM system for DFE using the ACRU model, the following steps were required (Rowe, 2019):

1. Select and define default model input information to use with the ACRU CSM system for DFE. Consequently, the following default datasets were selected:
    a. Rainfall and climate files: The default input rainfall and climate data assigned per quinary, and stored in the quinary catchments database (Schulze, 2013) was selected. Alternatively, high-quality rainfall data from other sources such as research catchments and the Lynch (2003) database should be used.
    b. Soil: Soil is represented by the SCS-SA soil groups, as applied in the SCS-SA method, and obtained from sources such as the following:
        - The literature, i.e. where detailed soils analyses have been conducted (generally restricted to research catchments)
        - The land-type maps (SIRI, 1987)
        - Maps of the SCS-SA soil groups for South Africa, as developed by Schulze (2012), and an updated map, developed by Schulze and Schütte (2018), which factors in terrain units. Due to their national coverage, these data sources were selected as the default. However, comparison with the other data sources, where available or feasible, will be performed as this provides a way of validating the accuracy of the maps.
    c. Land cover: The National Land Cover (NLC) dataset of 2000 (ARC and CSIR, 2005), referred to as NLC 2000, and an updated 2013/14 version (DEA and GTI, 2015), referred to as NLC 2013/14, are the most comprehensive coverages of actual land cover in South Africa. This land-cover information is a suitable baseline and is used in the CSM system as the default land-cover information, unless more detailed information is available, i.e. information that is particularly relevant to research catchments, where the vegetation coverage has been explicitly described and documented.

2. Using the default land-cover data, a comprehensive land-cover classification for use with the ACRU model, similar to the SCS-SA classification, with the parameters required to model each of the NLC 2000 and NLC 2013/14 land-cover classes, was developed as follows:
    a. Based on the rules developed by Rowe et al. (2018a), a final land-cover classification for use with the ACRU model was established. The classification was adopted from the SCS-SA land-cover classification (Schulze et al., 2004) with modifications to make the classification more compatible with the NLC 2000 and NLC 2013/14 land-cover classes.
    b. Appropriate land-cover classes from the final ACRU land-cover classification were assigned to each of the 49 different land-cover classes of the NLC 2000 dataset and 72 classes of the NLC 2013/14 dataset in order to model these selected default land-cover classes.

3. A structure of how to apply the model, i.e. level of detail and model options, was established to provide a consistent methodology to implement the approach.

Further details on the development of a CSM for DFE using the ACRU model are provided in Rowe (2019).

3.3 PERFORMANCE ASSESSMENT OF THE IMPROVED CONTINUOUS SIMULATION MODELLING SYSTEM DEVELOPED COMPARED TO THE CURRENT DEFAULT ACRU MODEL CONFIGURATION

In the previous section, an improved CSM system for DFE in South Africa was defined. The system was developed to consistently and explicitly represent land-management practices and hydrological conditions as represented in the SCS-SA model, which are not adequately represented in the current default implementation of the ACRU model.

3.3.1 Streamflow and peak discharge computation in the ACRU model

In the ACRU model, several algorithms and parameters are used to transform rainfall into total streamflow, i.e. both stormflow and baseflow. This includes partitioning rainfall into the various hydrological processes, such as interception, stormflow, infiltration, evapotranspiration and baseflow. It is not practical to describe all the details of each of these processes in this section. However, specific processes that are particularly relevant to this study, which are needed to understand the methodology applied and results obtained, are summarised below. For further details on the information described below, refer to Schulze (1995).

At the heart of the ACRU model is the SCS (1956) runoff equation, which is used to estimate stormflow, referred to as STORMF in the ACRU model. In summary, once interception has been abstracted, the gross daily precipitation (P), referred to as RFL in the ACRU model, is converted into STORMF, based on the soil water deficit (S) and the regression coefficient (c), referred to as the coefficient of initial abstraction (COIAM) in the ACRU model. The multi-layer soil water budgeting approach used in the ACRU model determines the value of S on a day-by-day basis. This is calculated for a selected critical response depth of the soil (SMDDEP). The STORMF generated on a specific day is added to the stormflow store (STORMF STORE), which is partitioned into a same-day response fraction (UQFLOW), and a subsequent delayed stormflow response, i.e. applying a quick-flow response coefficient (QFRESP), which is a surrogate for interflow. The delayed stormflow response is retained in the STORMF STORE, to which the next day's STORMF is added, if any, which is then again partitioned based on the QFRESP coefficient.

In the current publicly available versions of the ACRU model, all the STORMF (Q) generated on the day is used to estimate the peak discharge. The peak discharge calculation is derived from the SCS (1956) incremental triangular unit hydrograph stormflow peak discharge equation. In the standard ACRU model, incremental triangular unit hydrographs are only used if the hydrograph routing option is evoked. When the hydrograph routing option is not selected, which is generally the default option, a single triangular unit hydrograph is used to calculate stormflow peak discharge, and the effective storm duration (ΔD) is assumed to be equal to the catchment's time of concentration (T_c), which is empirically related to lag time (L). Based on this assumption and combining the incremental triangular unit hydrograph stormflow peak discharge lag time equations simplifies to:

$$q_p = 0.2083 \left(\frac{A\ Q}{1.83\ L} \right) \qquad 3.2$$

Equation 3.3 is the default option in ACRU and was used in this section to estimate the stormflow contribution to peak discharge. The simulated baseflow from the model is then added to the ordinates of the surface runoff hydrograph, i.e. to provide a complete hydrograph (Schulze, 1995). Rowe (2019) provides further details regarding the baseflow contribution to peak discharge. The baseflow contribution to peak discharge is, however, generally very small in small catchments where the surface and groundwater catchment areas are assumed to be the same.

3.3.2 Methodology

The following methodology was applied in this section:

- Eleven catchments, which included seven research catchments and four DWS-gauged catchments (Figure 3.1), with quality-controlled, observed rainfall and streamflow data, were selected to assess and compare the performance of the improved CSM system that was developed to that of the current default implementation of the ACRU model.

- Catchment characteristics such as soil and land-cover information were identified for each verification catchment, and were used to parameterise the ACRU model applying both the current default implementation of the ACRU model and the improved CSM system that was developed.
- After setting up the ACRU model with all the required inputs for both scenarios, daily streamflow and peak discharge were simulated for all verification catchments for both scenarios.
- Graphical comparisons of the simulated versus observed daily streamflow and peak discharge results were performed. Summary statistics were calculated, including least-square linear regression analysis to determine the best-fit regressions for the simulated versus observed results, along with the coefficient of determination (R^2). In addition, the Nash-Sutcliffe Efficiency ratio of the observed versus simulated daily streamflow and peak discharge values was calculated.
- The annual maximum series was then extracted from both the daily observed and simulated streamflow volumes and peak discharges. The GEV distribution was fitted, using L-moments (Hosking and Wallis, 1997), to the AMS of the observed and simulated flows to compare how well the model simulated the design flood events, i.e. for the 2-, 5-, 10-, 20-, 50- and 100-year return periods. For comparison, and to summarise the differences between the observed and simulated design values across all return periods, both the MRE and the MARE were used. The MRE indicates general over- or under-simulation, while the MARE indicates the total error, which complements the MRE and indicates if there is consistent under- or over-simulation, or a combination of the two.

After applying the above methodology, poorly simulated design peak discharges were obtained for both scenarios assessed. Therefore, further analysis was performed of the computation of peak discharge in the ACRU model.

3.3.3 Catchments used for verification

The 11 catchments selected to verify and compare the performance of the CSM system that was developed to that of the default implementation of the ACRU model are located as shown in Figure 3.1. These include seven research catchments monitored by the Council for Scientific and Industrial Research (CSIR), formerly Forestek, and the University of KwaZulu-Natal (UKZN), and four DWS-gauged catchments. DWS-gauged catchments are indicated with blue dots in Figure 3.1 and research catchments are indicated with red dots. There are two catchments located at the Cedara and DeHoek/Ntabamhlope research catchment sites (Figure 3.1).

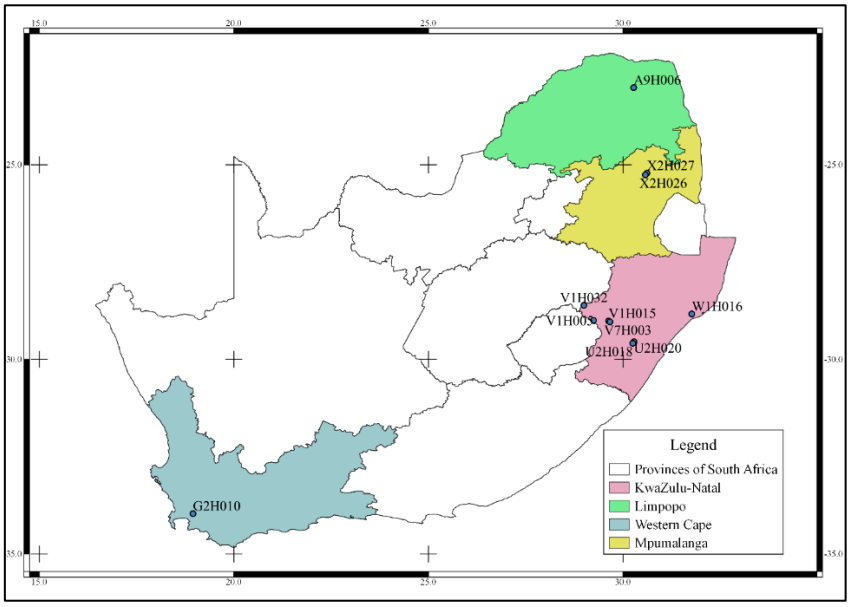

Figure 3.1: Location of catchments used for verification

Rowe (2019) provides a detailed discussion of the general climatic and physiographical characteristics of the study catchments. In addition, Rowe (2019) provides further details pertaining to data availability, collection and processing.

3.3.4 Results and discussion

Rowe (2019) provides a detailed example of the typical performance and results obtained from both the CSM system that was developed and the default ACRU model configuration for two of the verification catchments used in the study: Cathedral Peak IV (V1H005) and DeHoek/Ntabamhlope (V1H015).

However, in terms of the peak discharge, the model currently uses all the STORMF generated for the rainfall event on the day in the stormflow peak discharge equation. as shown in Equation 3.3, which represents contribution of the stormflow (surface runoff) to the total peak discharge (QPEAK). However, the STORMF generated on the day does not represent the actual fraction of stormflow that exits the catchment on the day, since this is partitioned into UQFLOW and a delayed STORMF response, conceptualised as interflow, as described above. This is therefore conceptually incorrect and results in inconsistent volumes between the UQFLOW volume released on the day, i.e. after applying QFRESP to the STORMF STORE, and the volume of STORMF used to calculate the contribution of stormflow to peak discharge for the day. In this study, this resulted in a significant over-simulation of QPEAK compared to the observed value.

To improve on the over-simulation of QPEAK and to correct the inconsistency between the UQFLOW volume released on a particular day, i.e. after applying QFRESP to the STORMF STORE, and the volume of STORMF used to calculate QPEAK for the day, the following revision was applied by introducing an additional output variable: UQFLOW ON THE DAY (UQFLOW OTD). Conceptually, UQFLOW OTD represents the fraction of STORMF generated on the day that actually exits the catchment on the day as surface runoff, i.e. calculated as STORMF x QFRESP = UQFLOW OTD. Based on this revised conceptualisation, the use of STORMF in Equation 3.3 was replaced with UQFLOW OTD, which represents the fraction of STORMF generated on the day that actually exits the catchment on the day as surface runoff. The difference between UQFLOW and UQFLOW OTD, which is conceptualised as interflow, is then calculated and added to the baseflow component of the peak discharge computation, however, conceptualised as interflow.

Applying the revised ACRU peak discharge computation corrects the volume inconsistency currently applied in the peak discharge estimation and ensures that the same volume of total simulated streamflow (USFLOW) on a particular day is used to calculate the total peak discharge for the day, i.e. the contributions of both stormflow and baseflow/interflow to peak discharge. In addition, the revised stormflow volumes (UQFLOW OTD) used in the stormflow peak discharge equations are conceptually correct since these equations, derived from the original SCS (1956) stormflow equations, estimate the contribution of surface runoff to peak discharge.

The results obtained for all verification catchments, as presented for Cathedral Peak IV (V1H005) and DeHoek/Ntabamhlope (V1H015), excluding the Lambrechtsbos B (G2H010) catchment, are summarised in figures 3.2 to 3.5. Due to particularly poor results obtained for the Lambrechtsbos B (G2H010) catchment and challenges associated with modelling this catchment, it was excluded from the analysis. As indicated in Figure 3.2, the CSM system provides the most accurate results overall in terms of daily streamflow volumes for all verification catchments (excluding the Lambrechtsbos B (G2H010) catchment), with NSE, R^2 (RSQ) and regression slope values all being higher than those obtained for the default implementation of the ACRU model. In terms of daily peak discharges (Figure 3.3), it is evident that extremely poor NSE values and high regression slope values are obtained for both the CSM system and default implementation of the ACRU model when applying the current peak discharge computation procedure.

In terms of the revised peak discharge computation, however, the NSE and regression slope values are slightly better for the default implementation of the ACRU model compared to the CSM system. The results are, however, similar (Figure 3.3). In terms of design streamflow volumes (Figure 3.4), the MARE is worse (higher) for the default implementation of the ACRU model compared to the CSM system. However, the MRE is lower and negative (-0.08) for the default implementation of the ACRU model compared to the higher positive value (0.14) obtained for the CSM system, indicating a greater tendency for the default implementation of the ACRU model to under-simulate design streamflow volumes (Figure 3.4). This trend is directly translated to the MARE/MRE values in terms of design peak discharges shown in Figure 3.5. The results confirm that the current peak discharge computation procedure is inadequate and produces extremely over-simulated design peak discharges for both scenarios.

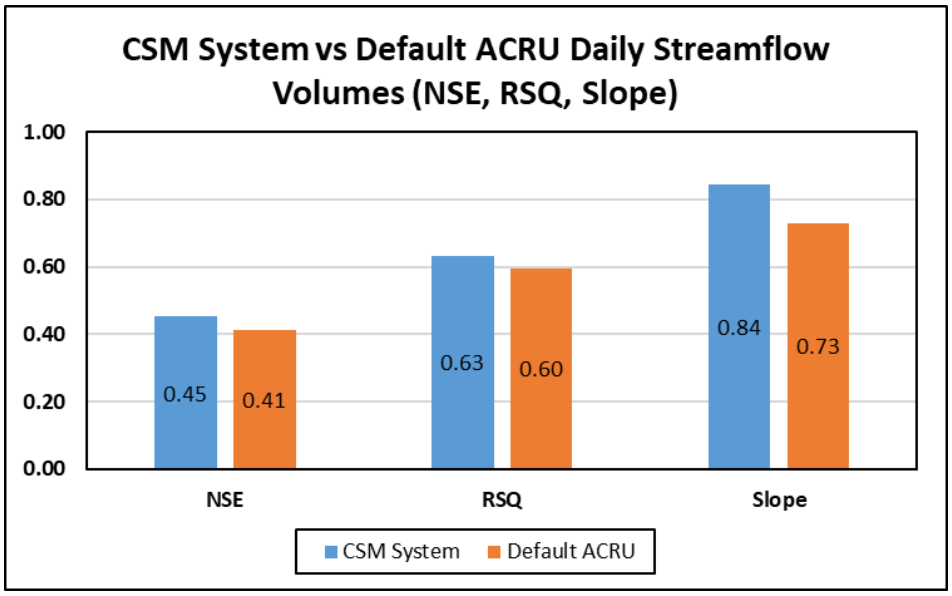

Figure 3.2: Summary of NSE, RSQ and regression slope values obtained for all verification catchments, excluding Lambrechtsbos B (G2H010), for simulated versus observed daily streamflow volumes

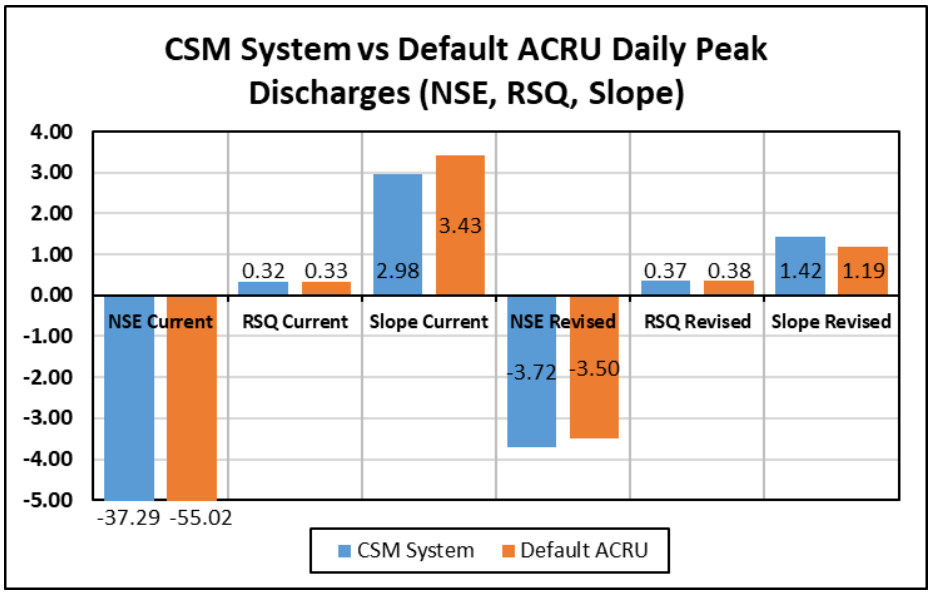

Figure 3.3: Summary of NSE, RSQ and regression slope values obtained for all verification catchments, excluding Lambrechtsbos B (G2H010), for simulated versus observed daily peak discharges, applying both the current and revised peak discharge computation procedure

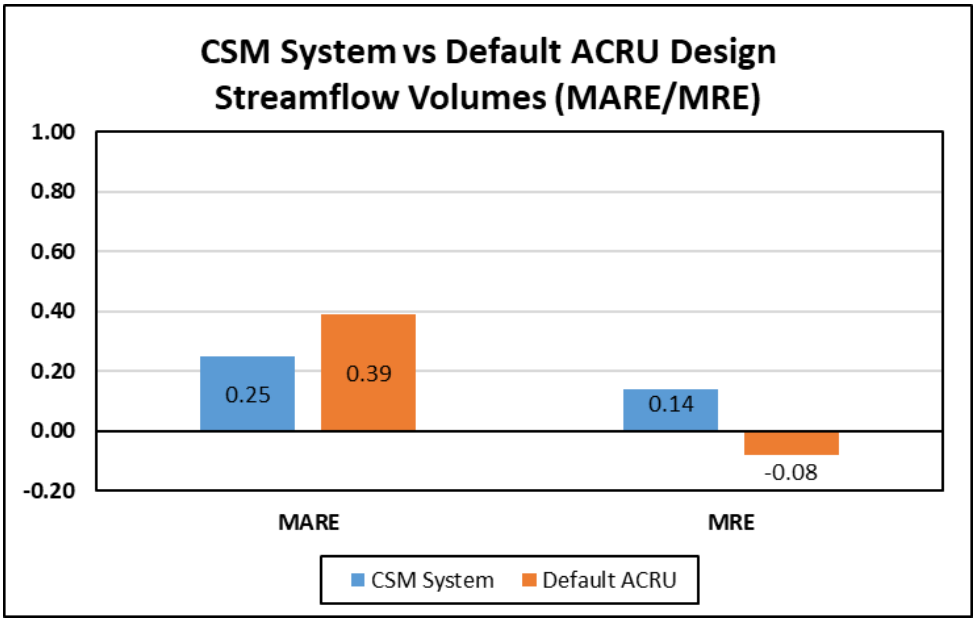

Figure 3.4: Summary of MARE and MRE values obtained for all verification catchments, excluding Lambrechtsbos B (G2H010), for simulated versus observed design streamflow volumes

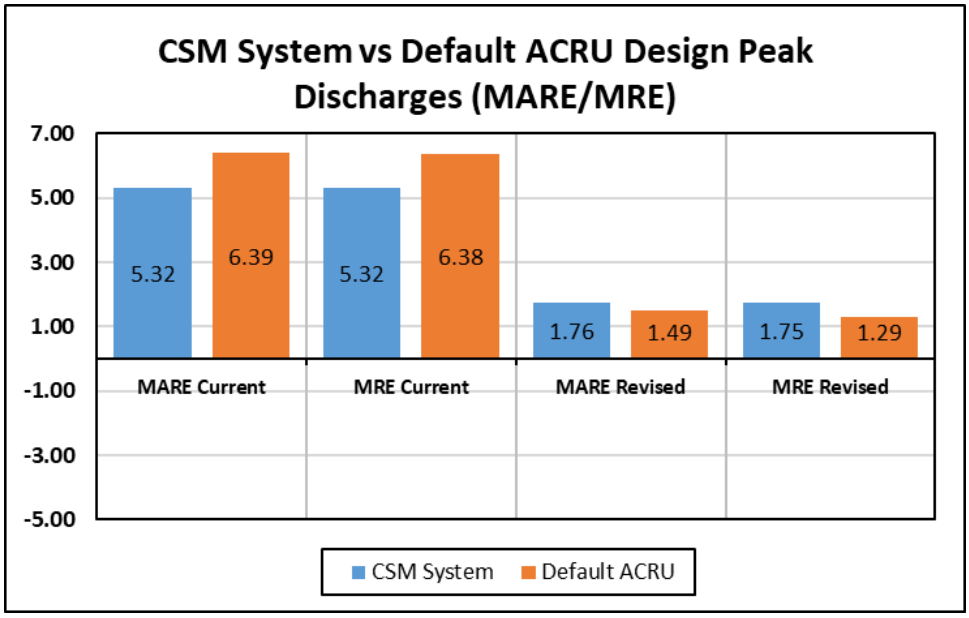

Figure 3.5: Summary of MARE and MRE values obtained for all verification catchments, excluding Lambrechtsbos B (G2H010), for simulated versus observed design peak discharges, applying both the current and revised peak discharge computation procedure

3.3.5 Conclusions and recommendations

The initial results indicated that reasonable daily and design streamflow volumes are simulated when applying both the CSM system that was developed and the default implementation of the ACRU model within the current ACRU structure and computational procedures. However, daily and design peak discharges were significantly over-simulated. Further investigation of the computation of peak discharge in the current ACRU model structure highlighted an inconsistency between daily simulated stormflow volumes and the volume of stormflow used in the daily stormflow peak discharge equation.

Therefore, revisions were made to the calculation of peak discharge in the model, correcting the volume imbalance, which significantly improved the results. Overall, considering both daily and design streamflow volumes and peak discharges, the CSM system was identified as providing the most accurate results.

This motivates the further development and assessment of the CSM system. In conclusion, however, regardless of how the QFRESP and SMDDEP parameter values are estimated, the revision applied to the ACRU peak discharge computation in this section should be applied in all future applications of the ACRU model to provide more realistic and accurate peak discharge estimates. The simulation of daily streamflow from a catchment in the ACRU model is very sensitive to these parameters. It is therefore essential to obtain a best estimate of these parameters. This should be considered carefully.

3.4 PERFORMANCE AND SENSITIVITY ANALYSIS OF THE SCS-BASED PEAK DISCHARGE ESTIMATION IN THE ACRU MODEL

This section assesses the performance and sensitivity of the SCS-based peak discharge estimation procedures, as implemented in the ACRU model, for two case study catchments. It includes an assessment and comparison of both the single and incremental unit hydrograph approaches.

3.4.1 Methodology

The two case study catchments used in this section are the Cathedral Peak IV catchment (Gauging Weir V1H005), located on the Little Berg plateau of the Drakensberg mountain range, KwaZulu-Natal, near the town of Winterton, and the DeHoek/Ntabamhlope catchment (Gauging Weir V1H015), also located in KwaZulu-Natal approximately 20 km from the town of Estcourt in the foothills of the Drakensberg.

The following methodology was applied in this section:

- The Flood Hydrograph Extraction Software, EX-HYD, developed by Görgens et al. (2007) and provided by Gericke (2018), was used to extract complete flood hydrographs from the primary streamflow data of the two selected catchments.
- For Cathedral Peak IV (V1H005), where only a short record of overlapping and consistent streamflow and sub-daily rainfall data was available, i.e. 1974–1979, the largest event for each year on record was first extracted. This was followed by the second-largest event, the third-largest event, etc. until a reasonable sample of 20 events had been obtained. For DeHoek/Ntabamhlope (V1H015), the same procedure was followed. However, the record length was significantly longer, i.e. 1979–1993. Therefore, the majority of the events selected were the annual maximum events. Seventeen events were finally extracted.
- A Hydrograph Analysis Tool (HAT), developed in Microsoft Excel by Gericke and Smithers (2017), was used to further analyse and process each of the events extracted using EX-HYD.
- The ACRU simulation results obtained from the assessment of the CSM system, i.e. applying the revised peak discharge computation procedure, were used to provide the simulated stormflow volumes, i.e. UQFLOW OTD, that were required as input into the ACRU stormflow peak discharge equations.
- The Schmidt and Schulze (1984) (S&S) lag time equation was used to estimate the average catchment lag time for the two case study catchments.
- Using all the information above, the performance of the single UH approach, i.e. the default option in the ACRU model, was firstly investigated (Step 1). The following procedure was followed:
  Step 1.1: The simulated UQFLOW OTD from the ACRU model was used as input to the single UH approach, along with the estimated S&S lag time, to estimate the contribution of stormflow to the peak discharge for the day, i.e. for each of the events extracted for the two case study catchments.

  Step 1.2: Repeat Step 1.1. However, replace the estimated S&S lag time, i.e. the time that remains constant for each event, with the observed lag time estimated for each event, extracted from the observed event hydrographs.

Step 1.3: Use both the observed stormflow volume and observed lag time for each event to calculate the contribution of stormflow to peak discharge.

- The same procedure was followed to assess the performance of the incremental UH approach (Step 2). However, in this case, the temporal distribution of daily rainfall was required. Therefore, the procedure was as follows:

  Step 2.1: The simulated UQFLOW OTD from the ACRU model was disaggregated into incremental stormflow volumes, based on hyetographs generated using the daily rainfall and one of four SCS-SA synthetic regionalised rainfall distributions applicable to each catchment. Incremental triangular UHs were then generated for each increment of stormflow volume, using the estimated S&S lag time. The incremental UHs were then superimposed onto each other to provide a composite surface runoff hydrograph and final stormflow peak discharge estimate.

  Step 2.2: Repeat Step 2.1. However, replace the synthetic regionalised rainfall distributions with the observed rainfall hyetographs for each event, and replace the estimated S&S lag time with the observed lag time for each event.

  Step 2.3: Use the observed stormflow volume, the observed rainfall hyetographs and the observed lag time for each event to calculate the contribution of stormflow to peak discharge.

  Step 2.4: Use the UQFLOW OTD as the input for stormflow and keep this fixed. Then use the observed rainfall hyetographs and the estimated S&S lag time for one set of computations. Then change this to the synthetic regionalised rainfall distributions and the observed lag time.
- The results from each of the above analyses are summarised for each catchment using both MRE and MARE.

3.4.2 Results and discussion

The results obtained from the assessment of both the single and incremental UH approaches are presented in this section. A detailed example of the results from the application of the single UH approach, for a single event, is provided in Figure 3.6.

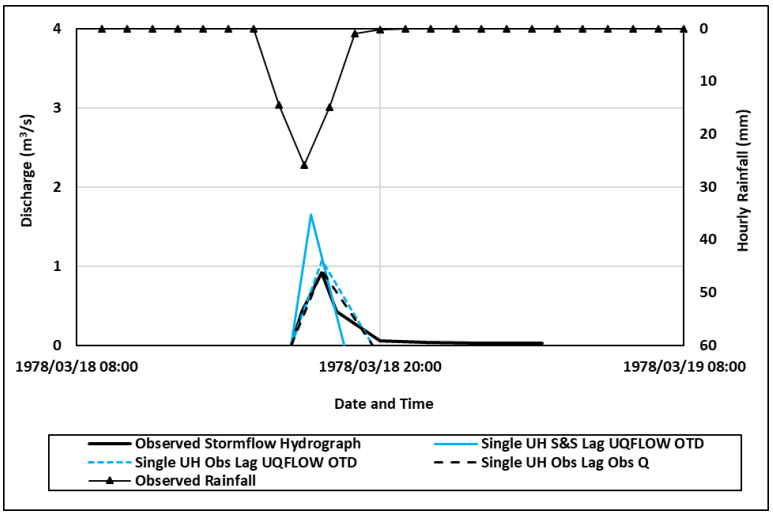

Figure 3.6: Observed stormflow hydrograph and simulated stormflow hydrographs obtained for a single event at Cathedral Peak IV (V1H005) applying the single UH approach

From Figure 3.6, it is evident that using UQFLOW OTD and the estimated S&S lag time results in an over-simulation of the stormflow peak discharge for this event (the solid blue line), i.e. compared to the observed stormflow hydrograph (the solid black line). An improvement is observed when UQFLOW OTD and the observed lag time are used (the dashed blue line). This result is very similar to that obtained when both the observed stormflow and the observed lag time are used (the dashed black line). The results indicate that UQFLOW OTD is a reasonable estimate of the stormflow volume for this event, and that the single UH approach is sensitive to catchment lag time.

A detailed example of the results obtained from the application of the incremental UH approach, i.e. applying the methodology, is depicted in Figure 3.7 using the same event as that used for the single UH approach described above. The incremental UH approach was used to develop the composite stormflow hydrographs depicted in Figure 3.7, based on either the regionalised synthetic rainfall distribution defined for the region, i.e. Type 4 rainfall distribution in this case, referred to as Rain T4, or the observed rainfall hyetograph. Observed stormflow, observed lag time and the S&S lag time are as defined above for the single UH approach.

As investigated for the single UH approach, the performance of the incremental UH approach was assessed using both observed and simulated (UQFLOW OTD) stormflow volumes, and observed and estimated S&S lag time for the catchment. However, in this case, the distribution of daily rainfall was also accounted for. From Figure 3.7, it is evident that using UQFLOW OTD, the estimated S&S lag time and Rain T4 results in an over-simulation of the stormflow peak discharge for this event (the solid blue line), i.e. compared to the observed stormflow hydrograph (the solid black line). An improvement is observed when UQFLOW OTD, the observed lag time and observed rainfall are used (the dashed blue line). This result is very similar to that obtained when all the observed inputs are used, i.e. observed stormflow, observed lag and observed rainfall (the dashed black line). The results once again indicate that UQFLOW OTD is a reasonable estimate of the stormflow volume for this event, and that the incremental UH approach is sensitive to catchment lag time.

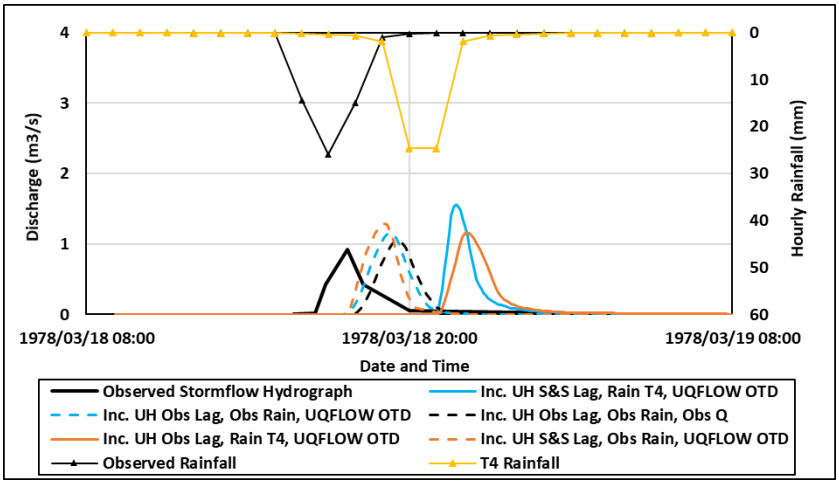

Figure 3.7: Observed stormflow hydrograph and simulated stormflow hydrographs obtained for a single event at Cathedral Peak IV (V1H005) applying the incremental UH approach

The final two simulated stormflow hydrographs compare the sensitivity of the incremental UH approach to lag time. When the distribution of daily rainfall individually, i.e. if the simulation where UQFLOW OTD is used in combination with the observed lag time and observed rainfall (the dashed blue line) is considered and the observed rainfall is replaced with Rain T4 (the solid orange line), there is no noticeable change in the stormflow peak discharge. However, there is a slight increase when the observed lag time is replaced with the estimated S&S lag time (the dashed orange line).

Therefore, in this case and for this specific event, the incremental UH approach is more sensitive to the estimated S&S lag time than Rain T4, i.e. the synthetic rainfall distribution. This is, however, as a result of the observed rainfall distribution being very similar to the synthetic T4 rainfall distribution for this particular event. The detailed results provided above for both the single UH approach and the incremental UH approach, for this single event in the Cathedral Peak IV (V1H005) catchment, provide a graphical example of how the peak discharges and stormflow hydrographs were generated for each of the respective approaches.

The results obtained from both catchments were summarised using MARE and MRE values. The results for Cathedral Peak IV (V1H005) and DeHoek/Ntabamhlope (V1H015) are summarised in figures 3.8 and 3.9, respectively. The results when using UQFLOW OTD and observed stormflow are both provided for comparison.

The performance of the single UH approach was assessed using both observed and simulated (UQFLOW OTD) stormflow volumes, with estimated S&S lag time or observed catchment lag times.

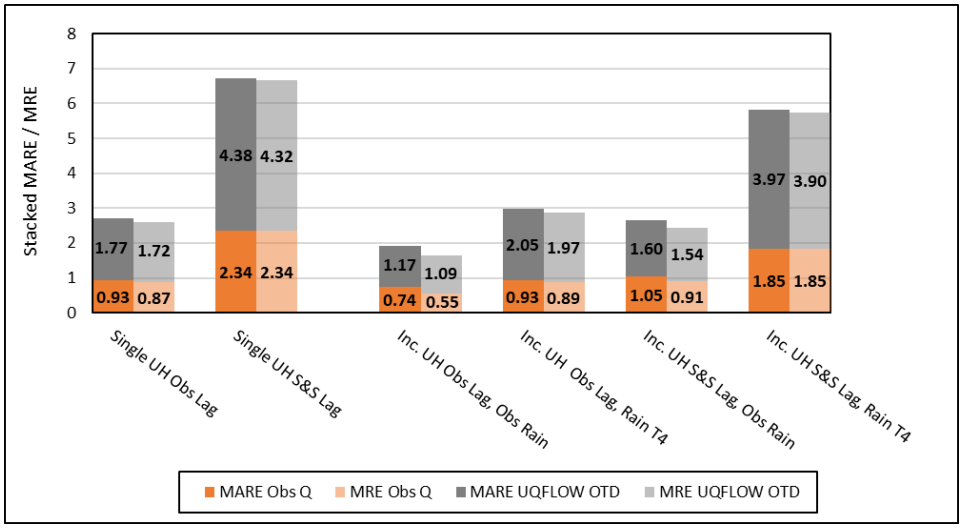

Figure 3.8: Cathedral Peak IV: MARE and MRE between observed and simulated stormflow peak discharges for both the single and incremental UH approaches

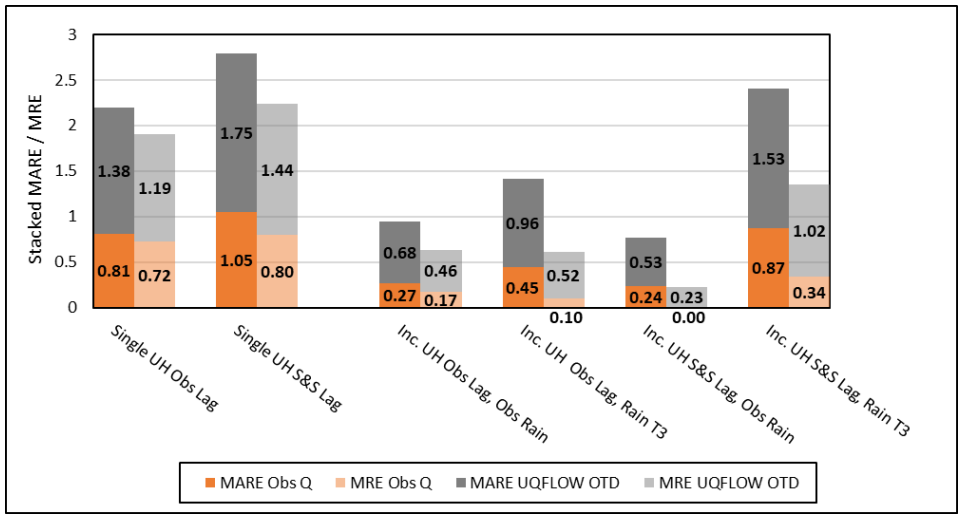

Figure 3.9: DeHoek/Ntabamhlope: MARE and MRE between observed and simulated stormflow peak discharges for both the single and incremental UH approaches

As indicated by the results presented in figures 3.8 and 3.9, the combinations where all the observed data was used as input into each of the respective approaches produce the lowest MARE values. This is logical and was expected since the observed data is the best estimate of the input parameters required for each approach. In addition, there is generally a consistent over-estimation of the peak discharges for all scenarios, i.e. the MARE and MRE values are generally the same or very similar (Figure 3.8). Similarly, for the DeHoek/Ntabamhlope catchment, when applying the single UH approach, MARE is lowest when using the observed runoff and observed lag (0.81). When applying the incremental UH approach, however, the MARE is lowest when using observed stormflow, S&S lag time and observed rainfall (0.24). This is, however, only slightly lower than that obtained when using observed stormflow, observed lag and observed rainfall (0.27).

The average percentage increase in MARE for both catchments, for both the single and incremental UH approaches when replacing observed inputs with estimated and/or synthetic inputs, is provided in Table 3.4. The results when using both observed stormflow and UQFLOW OTD indicate that the single UH approach is particularly sensitive to catchment lag time with the MARE increasing by 91% and 87%, respectively, when the observed lag is replaced with the S&S lag time. In terms of the incremental UH approach, the results indicate that, on average, the approach is more sensitive to the distribution of daily rainfall compared to catchment lag time. The average increase in MARE when observed rainfall is replaced with synthetic rainfall distributions (Rain T3/T4) is 46% (observed stormflow) and 58% (UQFLOW OTD), and only 27% (observed stormflow) and 29% (UQFLOW OTD) when the observed lag is replaced with the S&S lag time, keeping all other inputs fixed. When simultaneously replacing both observed rainfall and observed lag with synthetic rainfall distributions (Rain T3/T4) and the S&S lag time, the average increase in MARE is 186% (observed stormflow) and 182% (UQFLOW OTD), which is substantially higher than the combined percentage changes from the individual replacements of each of the two observed estimates, i.e. 46% + 27% = 73% (observed stormflow) and 58% + 29% = 87% (UQFLOW OTD).

The results thus indicate a compounding of the error when both the rainfall distribution and catchment lag time are not accurately estimated. The average percentage increase in MARE of Q_p estimates between the results obtained from the incremental and single UH approaches, when using both observed versus estimated and/or synthetic inputs, is also provided in Table 3.4. On average, when using the estimated and/or synthetic inputs in both the single and incremental UH approaches, MARE is 24% (observed stormflow) and 12% (UQFLOW OTD) higher for the single UH approach compared to the incremental UH approach. When using the observed inputs in both the single and incremental UH approaches, MARE is 113% (observed stormflow) and 77% (UQFLOW OTD) higher for the single UH approach compared to the incremental UH approach.

Table 3.4: Average percentage increase in MARE for both the single and incremental UH approaches when replacing observed inputs with estimated and/or synthetic inputs, and between the results obtained from the single and incremental UH approaches

From	To	Average percentage increase in MARE
Single UH observed lag, observed stormflow	Single UH observed lag, UQFLOW OTD	80
Including UH observed lag, observed rainfall, observed stormflow	Including UH observed lag, observed rainfall, UQFLOW OTD	105

From	To	Observed stormflow	UQFLOW OTD
Single UH observed lag	Single UH S&S lag	91	87
Including UH observed lag, observed rainfall	Including UH observed lag, Rain T3/T4	46	58
Including UH observed lag, observed rainfall	Including UH S&S lag, observed rainfall	27	29
Including UH observed lag, observed rainfall	Including UH S&S lag, Rain T3/T4	186	182
Including UH S&S lag, Rain T3/T4	Single UH S&S lag	24	12
Including UH observed lag, observed rainfall	Single UH observed lag	113	77

3.4.3 Conclusions and recommendations

In this study, the influence of three parameters that directly influence the simulation of the contribution of stormflow to peak discharges in the ACRU model has been investigated for two methods of hydrograph generation.

The first method, which is the default option applied in the ACRU model, uses the design stormflow peak discharge equation (the single UH approach) and relies only on the simulated stormflow volume and estimated catchment lag time. The second method, the incremental UH approach, also requires an estimate of both stormflow volume and catchment lag time, as well as the temporal distribution of daily rainfall, where a fixed regionalised synthetic rainfall distribution is generally assumed for application in South Africa. The lack of reliable sub-daily rainfall data, particularly consistent and accurate short-duration rainfall data, was a significant challenge to this study. This resulted in the use of only two pilot study catchments. Both the single and incremental UH approaches are sensitive to stormflow volume. Although the UQFLOW OTD is a reasonable estimate of the daily stormflow volume, it still tends to over-estimate stormflow in general. The single UH approach, which does not account for the distribution of daily rainfall, was particularly sensitive to estimated lag time, which varies significantly from event to event. However, the incremental UH approach is sensitive to both the estimated lag times and daily rainfall distributions used, which vary significantly from event to event.

Based on the results obtained for the two case study catchments, however, the incremental UH approach was identified as being more sensitive to the distribution of daily rainfall used. When applying the incremental UH approach, and incorrectly estimating both the daily rainfall distribution and the catchment lag time, a compounding of the error obtained is observed. The S&S lag equation was identified to provide a relatively good estimate of the average catchment response time. Although less satisfactory, the synthetic daily rainfall distributions provided a reasonable average representation of the typical rainfall distribution observed in the catchments. The incremental UH approach provides more accurate peak discharge estimates compared to the single UH approach, i.e. both when using parameters obtained from observed events and when using estimated and synthetic information. The results are, however, much improved when using parameters derived from the observed data. This indicates the importance of accounting for the variation in daily rainfall distribution and catchment lag time on a day-to-day basis. Therefore, to improve on the results obtained from the incremental UH approach, methods need to be developed to account for these variations. Lastly, the results highlight that accurate simulations of peak discharge may be obtained when applying both the single and incremental UH approaches when accurate inputs to the equations are used, validating that the model concepts and structure are reasonable to use in practice.

3.5 IMPACT OF MODEL CONFIGURATION AND PARAMETER ESTIMATION ON THE PERFORMANCE OF THE CONTINUOUS SIMULATION MODELLING SYSTEM DEVELOPED AND THE ESTABLISHMENT OF A FINAL SYSTEM

This section assesses the impact of model configuration and parameter estimation, i.e. using different sources of input information, such as land cover and soil, on the performance of the CSM system developed and assessed in the previous sections.

3.5.1 Methodology

This section outlines the methodology applied and results obtained to determine if the incremental UH approach with the estimated S&S lag time and synthetic daily rainfall distribution (Weddepohl, 1988) consistently performs better than the single UH approach, also using the estimated S&S lag time, for all verification catchments (Section 3.3.3). These include operational catchments where short-duration rainfall data is not available, which is generally the case when estimating design floods in practice in South Africa, due to the scarcity of short-duration sub-daily rainfall data in South Africa.

The results obtained from the assessment of the CSM system that was developed, i.e. with revision to the volume used in the peak discharge computation (UQFLOW OTD), and applying the single UH approach, are compared to those obtained when applying the incremental UH approach with synthetic rainfall distribution (Weddepohl, 1988) applicable to each catchment. In both cases, the same input information was used, and only the peak discharge computation procedure was changed.

3.5.2 Results and discussion

In terms of overall model performance, as indicated by the NSE values for all verification catchments (summarised in Table 3.5), it is evident that the incremental UH approach performed better than the single UH approach (due to the higher NSE values) for nine catchments. It had slightly lower NSE values in catchments V1H032 and X2H027, which are considerably larger than the other catchments. Therefore, the results may suggest that the performance of the incremental UH approach deteriorates with catchment size, i.e. for catchments outside the recommended size range (< 50 km^2) defined for the ACRU model (Schulze, 1995). However, the results for these two catchments are only slightly worse than those obtained from the single UH approach, whereas, for the remaining catchments, in most cases, substantial improvements were obtained when using the incremental UH approach compared to the single UH approach. Therefore, in general, the incremental UH approach provides better results compared to the single UH approach. The general poor performance of the model with predominantly negative NSE values for both the single and incremental UH approaches used to simulate peak discharge can be attributed to the simulated stormflow volume on any given day not being representative of the observed stormflow volume for that day, variations in the sub-daily temporal distribution of daily rainfall from day to day, and variations in lag time from day to day. Therefore, on a day-to-day basis, the simulated versus observed comparisons are relatively poor. However, the predominant or most typical conditions are accounted for.

Table 3.5: Comparison of NSE results between observed versus simulated daily peak discharges when applying the single and incremental UH approaches

Catchment	Area (km^2)	NSE daily peak discharges – Single UH approach	NSE daily peak discharges – Incremental UH approach
U2H020	0.26	-1.89	-1.20
V7H003	0.52	-1.12	-0.49
G2H010	0.73	-23.70	-3.14
V1H005	0.98	-10.53	-7.47
V1H015	1.04	-1.24	-0.41
U2H018	1.31	-10.02	-5.59
W1H016	3.30	-0.70	0.27
X2H026	13.82	-6.57	-4.68
A9H006	16.00	-1.43	-0.83
V1H032	67.80	0.17	-0.01
X2H027	77.16	-3.91	-4.49

A comparison of the MRE values between observed and simulated design peak discharges for return periods ranging from two to 100 years when applying both the single and incremental UH approaches is given in Figure 3.10. The results, similar to the NSE values, indicate that improved design peak discharges are obtained for all verification catchments (delivering lower MRE values) when using the incremental UH approach, except – once again – for catchments V1H032 and X2H027. However, the results for Catchment V1H032 are very similar when applying the two approaches, and the results obtained when applying the incremental UH approach are only slightly worse for Catchment X2H027 than when applying the single UH approach. The MARE was not presented here since the values are identical to the MRE values, i.e. both methods consistently over-estimate the observed design peak discharges. Therefore, from the NSE and MRE values obtained, it may be concluded that, in general, the incremental UH approach provides better results and should be used as the default option in the CSM system.

Consequently, the incremental UH approach will be used in all subsequent investigations and assessments in the sections to follow. In addition, there is room for improvement in the results when using this approach if the actual distribution of daily rainfall or an improved method of disaggregating the daily rainfall into a hyetograph on a day-to-day basis is developed and used. Furthermore, relationships between rainfall intensity and catchment lag time have been identified. Therefore, lag time may possibly be adjusted based on the distribution of daily rainfall in the future development of the system.

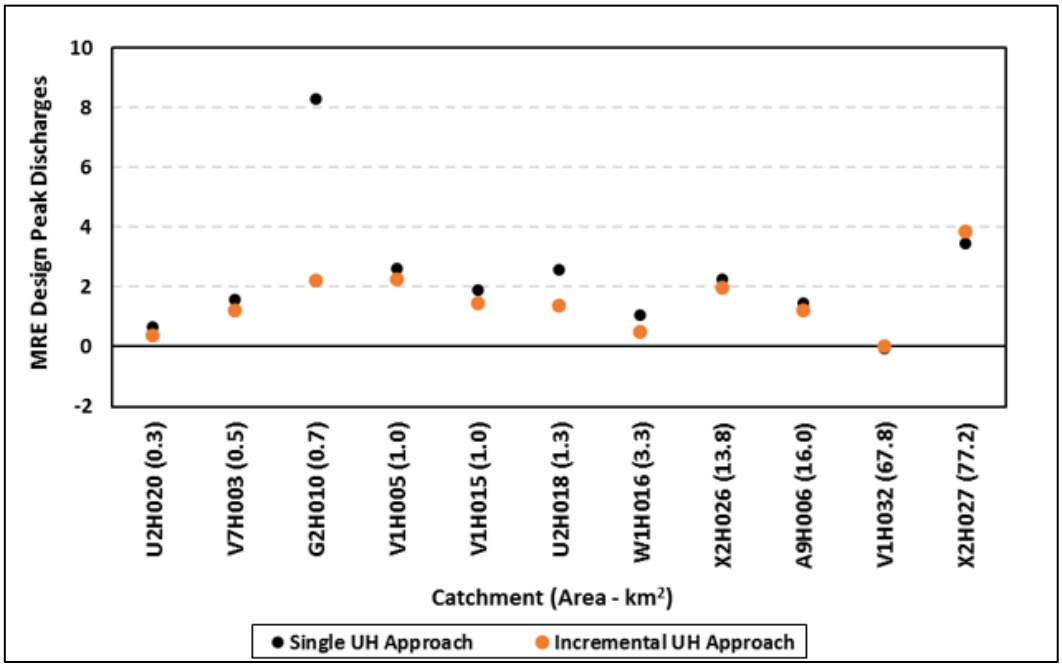

Figure 3.10: MRE between observed and simulated design peak discharges (two- to 100-year return period) when applying the single versus the incremental UH approach

3.5.3 Conclusions and recommendations

The aim of this section was to assess the impact of model configuration and parameter estimation on the performance of the CSM system that was developed and assessed. The objective was to identify if the incremental UH approach with the estimated S&S time lag and synthetic daily rainfall distribution (Weddepohl, 1988) consistently performs better than the single UH approach, also using the estimated S&S lag time for all verification catchments used in the assessment of the CSM system. The results indicated that the incremental UH approach generally performs substantially better than the single UH approach, or at least very similarly to the single UH approach, and should be used as the default peak discharge computation procedure in the CSM system.

The results indicate that the current CSM system, i.e. with site-specific land-cover and soil information, and the estimated S&S lag time, produced the best results. The S&S lag time equation produced substantially better results compared to the SCS lag time equation (SCS, 1972) and must therefore be used to estimate lag time in the CSM system.

It can be concluded that the incremental UH approach should be applied with the CSM system as the default option to simulate peak discharges. Site-specific information related to land cover and soil should be used in preference to national land-cover and soil maps, where available. If national soils maps are used, the Schulze and Schütte (2018) SCS Soil Map must be used to estimate the SCS-SA soil group. When using the NLC maps, validation of the land-cover classes should be performed using globally available imagery such as Google Earth or other means to identify the most accurate land-cover class for the catchment of interest. The S&S lag time equation should be used as the default lag time equation in the CSM system.

It is acknowledged that the CSM system has relied heavily on the SCS-SA land-cover classification. In the absence of observed data, the assumption has been made that the hydrological responses from the SCS-SA model for these soil and land-cover classes are reasonable. Consequently, it is possible that the ACRU CSM system and event-based SCS-SA model may provide similar results. Therefore, an assessment is needed of how the results from the CSM system developed compared to those obtained from the SCS-SA model.

3.6 A COMPARATIVE PERFORMANCE ASSESSMENT OF THE FINAL CONTINUOUS SIMULATION MODELLING SYSTEM ESTABLISHED IN RELATION TO THE TRADITIONAL SCS-SA MODEL

This section contains a comparison of the performance of the final CSM system that was established above with the performance of the traditional SCS-SA model and associated antecedent soil moisture adjustment procedures.

3.6.1 Introduction

In the previous section, a final CSM system for DFE in South Africa was established using the ACRU model (Schulze, 1995). In the absence of observed data, the development of the method relies extensively on the SCS-SA land-cover classification, i.e. in terms of representing hydrological responses from specific combinations of soil types, land-cover classes, land-cover conditions and land-management practices. Consequently, the ACRU CSM system has been modified to use the SCS-SA land-cover classification. In addition, there are striking similarities between the ACRU and SCS-SA models. Hence, there is a need to compare the performance of the two models for DFE. This is essential to identify if the ACRU CSM system provides better DFE estimates compared to the traditional SCS-SA model and, if so, whether it justifies the further development and implementation of the ACRU CSM system. It also provides the opportunity to assess the performance of the SCS-SA model when applying the initial catchment CN (CN-II), the median condition method (MCM) and the joint association method.

3.6.2 Methodology

This section summarises the methodology applied in this section. Rowe (2019) provides a detailed breakdown of the methodology used to compare the CSM developed with the traditional SCS-SA model. The first step was to set up both the ACRU and SCS-SA models.

In terms of the ACRU model, the same setup was used as was applied in the final CSM system. This information was used to simulate continuous time-series of daily simulated streamflow volumes and peak discharges.

When setting up the SCS-SA model (Schulze et al., 2004) the same input information was used to determine the CN, whereas for the ACRU model, the QFRESP and SMDDEP parameter values were used, which were derived from the SCS-SA CNs based on the rules developed by Rowe et al. (2018a). In terms of both models, the S&S lag time equation and the incremental UH approach (Schulze, 1995) were used with the synthetic rainfall distribution identified for each catchment, as defined by Weddepohl (1988). The difference again was that the peak discharges were simulated on a daily basis in the ACRU model, and an extreme value analysis was performed to determine the design values. For the SCS-SA model, with the exception of the joint association method, the design stormflow volumes simulated were used to simulate design peak discharges. In the case of the JAM, however, simulated stormflow volumes at specific non-exceedance percentiles were used to simulate corresponding peak discharges. The average MRE and MARE, averaged across all verification catchments for each model simulation, i.e. the final ACRU CSM system, the SCS-SA model using CN-II, the SCS-SA model applying the MCM, and the SCS-SA model applying the JAM, was then used to assess the overall performance of both models.

3.6.3 Results and discussion

It is important to emphasise that the ACRU model simulates total streamflow, which includes both stormflow (surface runoff) and interflow/baseflow. The SCS-SA model, on the other hand, only simulates stormflow (surface runoff). Both models, however, use simulated stormflow to simulate the contribution of stormflow to peak discharge. In the ACRU model, the baseflow/interflow volume is uniformly distributed throughout the day and converted to a constant flow rate, which is added to the simulated stormflow peak discharge. However, this contribution to the peak discharge is negligible, particularly for design events. It should be noted, however, that the ability of the ACRU model to explicitly account for antecedent soil moisture also contributes to the differences observed between the design streamflow volumes simulated by the ACRU model and those simulated by the SCS-SA model. The overall performance of the ACRU CSM system and the SCS-SA model for all verification catchments, excluding the Lambrechtsbos B (G2H010) Catchment, is summarised in Figure 3.11. For consistency, the results from the Lambrechtsbos B (G2H010) Catchment were excluded due to challenges associated with modelling this catchment and associated poorly simulated results.

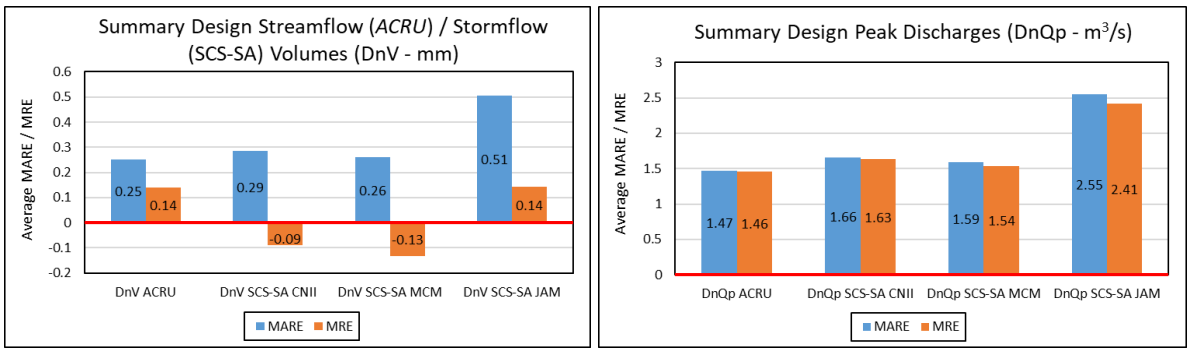

Figure 3.11: Average MARE and MRE values obtained for simulated versus observed design streamflow/stormflow volumes (DnV) and design peak discharges (DnQp), averaged across all verification catchments, excluding Lambrechtsbos B (G2H010), for both the ACRU and SCS-SA models

When comparing the average MARE and MRE values in terms of design streamflow (ACRU) and design stormflow (SCS-SA) volumes, it is evident that the ACRU CSM system produced the lowest MARE (0.25) with a positive MRE (0.14), indicating a general tendency to over-estimate observed design streamflow volumes. The MARE for the SCS-SA model when using CN-II is only slightly larger (0.29) than for the ACRU CSM system. However, the MRE is significantly lower (-0.09), indicating a greater tendency to under-estimate the observed design streamflow.

When using the SCS-SA model applying the MCM, both the MARE and MRE are only slightly lower, 0.26 and -0.13, respectively, compared to those obtained for the SCS-SA model using CN-II. Therefore, in general, the SCS-SA model does not seem to be very sensitive to changes in antecedent soil moisture for the catchments assessed.

The SCS-SA model applying the JAM produced the highest MARE (0.51), with a positive MRE of 0.14. This indicates that, in general, there is an over-estimation of the observed design streamflow. However, in many cases, there is also significant under-estimation, i.e. as indicated by the relatively lower MRE compared to MARE. Overall, however, the JAM did not perform well. As alluded to above, this can be attributed to the use of historically assigned rainfall stations with limited record lengths, and the use of frequency analyses and not extreme value analyses in the development of the approach and results generated.

In terms of the design peak discharges, the ACRU CSM system and the SCS-SA model using CN-II and applying the MCM provided similar results (Figure 3.11). This again indicates that, in terms of design stormflow volumes, both the ACRU CSM system and the SCS-SA model are producing similar values.

Therefore, similar design peak discharges are obtained. There are, however, more significant differences between the design streamflow and design stormflow volumes from each model, since the ACRU model includes the contribution of the interflow/baseflow to the total streamflow. Both the ACRU CSM system and the SCS-SA model using CN-II and applying the MCM generally over-estimate design peak discharges, with the ACRU CSM system producing the lowest MARE (1.47) and MRE (1.46), and the SCS-SA model using CN-II producing the highest MARE (1.66) and MRE (1.63) values, i.e. when comparing the results from these three scenarios, excluding those from the SCS-SA model applying the JAM. The slightly better results obtained for the ACRU CSM system compared to the SCS-SA using CN-II and applying the MCM can be attributed to the explicit accounting of antecedent soil moisture and an extreme value analysis being performed on the AMS extracted from continuous simulations of daily peak discharges. The general over-estimation of the observed design peak discharges can be attributed to one or a combination of the following: inaccurate simulations of stormflow volumes for certain design values; poor approximation of the actual daily rainfall distribution for design events by the synthetic rainfall distribution selected; and inaccurate estimation of the catchment lag time, i.e. as explained in the analysis of the results from catchment V1H005 and V7H003 above. Once again, the SCS-SA model applying the JAM produced the highest MARE (2.55) and MRE (2.41) in terms of design peak discharges.

3.6.4 Conclusions and recommendations

In summary, the results indicated that the ACRU CSM system performed best in terms of simulating design peak discharges, particularly design streamflow volumes. It was highlighted that the ACRU model simulates total streamflow, i.e. stormflow and interflow/baseflow, while the SCS-SA model only simulates stormflow. The contribution of interflow/baseflow to total streamflow for certain catchments was identified as being significant. Therefore, the results indicate the benefit of using the ACRU CSM system over the SCS-SA model. The results of the SCS-SA model using CN-II and applying the MCM were reasonable and highly comparable. However, the SCS-SA model using CN-II and applying the MCM design streamflow volumes were under-estimated, in general, across all catchments (MRE = -0.09 and -0.13, respectively), compared to the ACRU CSM system, i.e. where a general over-estimation of design streamflow volumes was observed (MRE = 0.14). In terms of the design peak discharges, with the exception of the SCS-SA model applying the JAM, similar estimates were obtained, on average, for all catchments, with the ACRU CSM system producing results slightly better than the SCS-SA when using CN-II and applying the MCM. This can be attributed to the explicit accounting of antecedent soil moisture and performing extreme value analyses on continuous flow sequences. However, the similarity in the design peak discharge results indicates that the design stormflow volumes simulated by the ACRU CSM system and the SCS-SA model using CN-II and applying the MCM are similar, which was expected since the ACRU CSM system was calibrated against the SCS-SA model's CN-II values.

The SCS-SA model applying the JAM performed particularly poorly in terms of simulating both design stormflow volumes and design peak discharges. It was noted, however, that the results from the JAM are not directly comparable to the results from the ACRU simulations and the other two SCS-SA simulations since the method does not use the same rainfall data, and the results are based on a frequency analysis performed on simulated flows and not an extreme value analysis. Conversely, the CN-II and MCM SCS-SA simulations, and those from the ACRU model are based on results obtained from the same rainfall data and from design values obtained from extreme value analyses. The results of the SCS-SA model applying the JAM are particularly poor for the 20-year return period, since only approximately 20 years of rainfall data was available when developing and applying the approach. In addition, for this reason, the method only provides results up to the 20-year return period. Therefore, from the results presented in this section, the SCS-SA model using CN-II and applying the MCM should be used in preference to the model applying the JAM. However, it is recommended that the ACRU CSM system be used to obtain the most accurate results.

CHAPTER 4: ASSESSING THE PERFORMANCE OF TECHNIQUES FOR DISAGGREGATING DAILY RAINFALL FOR DESIGN FLOOD ESTIMATION IN SOUTH AFRICA

R Ramlall and JC Smithers

Abstract

Design flood estimation methods are used to limit the risk of failure and ensure the safe design of hydrological and related infrastructure and for water resources management. In order to improve DFE methods, which are based on event-based or continuous simulation rainfall-runoff models, it is generally necessary to use sub-daily rainfall data. However, sub-daily rainfall gauges are relatively sparse and have shorter record lengths than daily rainfall gauges in South Africa. Rainfall temporal disaggregation techniques can be used to produce finer-resolution data from coarser-resolution daily rainfall data. Several RTD approaches have been developed and are used in South Africa. However, there is a need to review and assess the performance of the available RTD methods. This chapter contains an overview of selected RTD approaches on different sets of rainfall data in South Africa and the performance of the methods. Temporal distributions of rainfall were represented by dimensionless Huff curves, which served as the basis for comparison of observed and disaggregated rainfall. In the case study, it was found that the SCS-SA distributions and the Knoesen model approaches performed considerably better than the other approaches in the pilot study. The RTD approaches were further assessed using data from 14 additional rainfall stations. For the additional stations, the Knoesen model and SCS-SA disaggregated rainfall generally provided the most realistic temporal distributions.

4.1 INTRODUCTION

The occurrence of floods has numerous negative impacts on society. These include economic losses due to infrastructure damage, loss of productive time, injuries and loss of human life (Ward et al., 2016). Therefore, the management of flood risk is important to maintaining the overall wellbeing of society (Parkes and Demeritt, 2016). Design flood estimation comprises the assessment of flood risk by determining the exceedance probability, commonly referred to as return period, of extreme events that are potential hazards (Rowe et al., 2018b). This technique is necessary for the planning and design of hydraulic and related infrastructure and to ensure that the management of water resources is carried out taking safety into consideration (Rowe and Smithers, 2018).

Rainfall is a highly variable driver of the hydrological cycle, and is a key input in many DFE techniques (Smithers et al., 2002). Rainfall data is utilised to determine hyetographs and subsequently hydrographs from which peak discharges are obtained, both of which are required for the design of hydraulic structures (Arnaud et al., 2007; Hassini and Guo, 2017; Rowe and Smithers, 2018). The temporal distribution of rainfall intensity within storms influences both the magnitude and timing of peak discharges within a catchment and, as a result, the flood-generation potential of the event (Knoesen and Smithers, 2008).

Design flood estimation can be determined from gauged runoff data where this is available, but is generally performed utilising daily rainfall data due to the scarcity of observed runoff data and the relative abundance and longer record lengths of daily rainfall as opposed to sub-daily rainfall data (Pui et al., 2012). However, such data may not adequately represent the important characteristics of rainfall processes occurring at hourly and sub-hourly scales (Smithers and Schulze, 2000; Pui et al., 2012).

Therefore, in order to obtain adequate data at finer temporal resolutions, RTD techniques are often employed (Pui et al., 2012). RTD methods disaggregate coarser-resolution data, such as daily data, to produce data of a finer resolution, such as hourly data (Koutsoyiannis et al., 2003). The finer-resolution data can more accurately represent the rainfall hyetographs required for modelling runoff and DFE (Koutsoyiannis et al., 2003). RTD techniques have been successfully applied under South African conditions to obtain finer-resolution rainfall data (Adamson, 1981; Lambourne and Stephenson, 1987; Weddepohl, 1988; Knoesen, 2005; Knoesen and Smithers, 2008). However, the performance of these RTD methods needs to be assessed to determine the need for updating RTD methods as a number of newer approaches have been developed and successfully applied internationally (Smithers et al., 2002). Hence, there is a need to assess the feasibility of new methods for application in South Africa and subsequently update the toolbox of RTD techniques.

The overall aim of this study was to assess the performance of selected RTD methods and to recommend the adoption or adaptation of one or more of these approaches for application under South African conditions. The study was part of the research conducted for a Master of Science degree at the University of KwaZulu-Natal. This chapter provides a brief review of disaggregating coarser-level rainfall data into a finer-resolution hyetograph, assessing the performance of selected RTD methods. It also makes recommendations for RTD methods to be used in practice and for further research to be undertaken. Full details of the study reported are contained in Ramlall (2020).

4.2 A REVIEW OF METHODS FOR RAINFALL TEMPORAL DISAGGREGATION

The RTD approaches identified through a review of the literature are broadly classified as either rainfall distribution curves or disaggregation models, as shown in Figure 4.1 (Knoesen, 2005). When applied, a disaggregation approach should ideally result in a finer timestep hyetograph, which can give a realistic representation of sub-daily rainfall (Smithers and Schulze, 2000). The applied approach should disaggregate the daily values to sub-daily timesteps, while maintaining the characteristics of the rainfall process and the sum of the sub-daily values to the daily total.

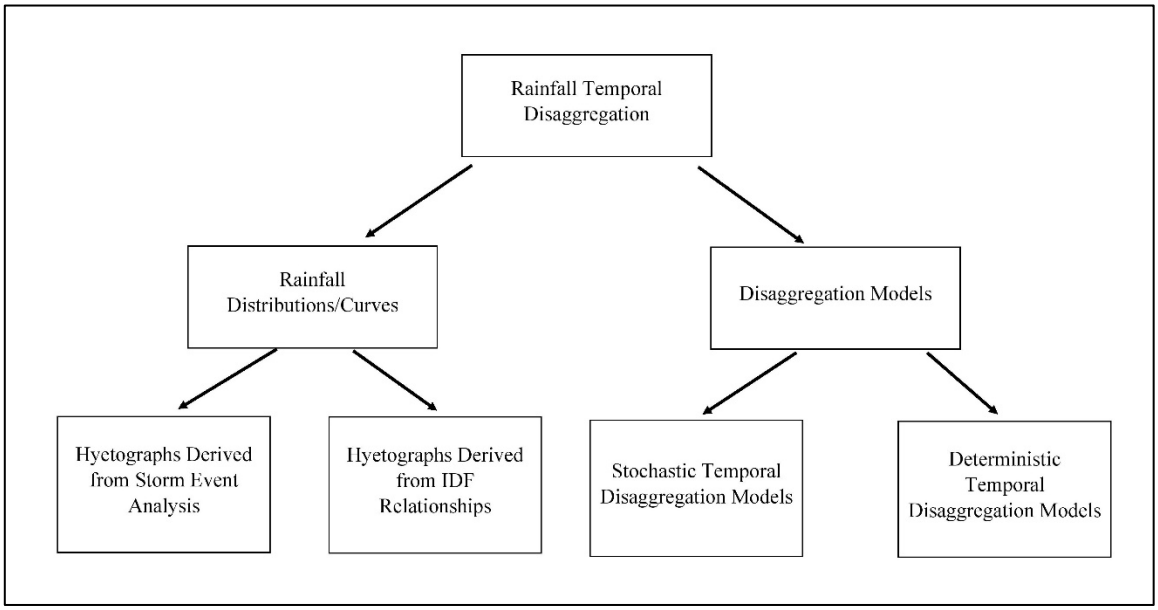

Figure 4.1: Categorisation of rainfall temporal disaggregation approaches (after Knoesen, 2005)

Rainfall distributions are used in design and modelling applications to determine the distribution of rainfall depths or intensities throughout the duration of a storm. These synthetic distributions may be used to derive hyetographs and determine the location of peak discharges within the storm duration (Chow et al., 1988; Weddepohl, 1988).

The RTD approaches could be adapted for use with observed daily data with short record lengths. Furthermore, approaches such as Huff curves (Huff, 1967; Huff and Angel, 1992; Bonta, 2004) and the average variability method (AVM) (Green et al., 2005; Bhuiyan et al., 2010) have shown potential for regionalisation. Therefore, disaggregation curves could be developed and possibly regionalised based on general storm patterns for use in disaggregating daily rainfall into sub-daily hyetographs as developed by Weddepohl (1988) and Knoesen (2005) in South Africa.

Stochastic modelling approaches generally simulate sub-daily values using statistical parameters derived from observed daily data. An element of randomness is included in sampling procedures (Rodriguez-Iturbe et al., 1987; Smithers, 1998; Koutsoyiannis and Onof, 2001). Rainfall processes are, by nature, complex, and it is unlikely that a model will be able to describe event characteristics completely and accurately. Hence, the use of stochastic models that may produce results similar to observed data is justifiable (Kossieris et al., 2018). Furthermore, such approaches are highly applicable to continuous simulation modelling, where the aim is to simulate potential outcomes for rainfall event processes (Smithers et al., 2002).

Deterministic model RTD approaches are less commonly applied than stochastic models or distribution approaches, due to their parameters being more physically related to rainfall processes, which in some cases are difficult and time-consuming to derive (Ormsbee, 1989; Hingray and Ben Haha, 2005). Therefore, the variety of models identified was comparatively limited. Given that the rainfall process is highly complex, dynamic and difficult to accurately represent with limited data, an approach that considers deterministic chaos may more accurately represent physical rainfall characteristics than a purely stochastic or deterministic method (Sivakumar et al., 2001).

Approaches that have been successfully applied in South Africa include the SCS-SA distributions (Schulze, 1984; Smithers et al., 2002), triangular distributions (Lambourne and Stephenson, 1987), Huff curves (Smithers, 1998), stochastic Bartlett-Lewis rectangular pulse (BLRP) models (Smithers, 1998; Smithers et al., 2002) and an adapted semi-stochastic regionalised disaggregation model (Knoesen, 2005). These approaches are categories of rainfall distributions and stochastic models. A summary of the various approaches that were reviewed and their performance in case studies can be seen in Table 4.1.

Table 4.1: Summary of approaches reviewed and key findings

Category	Approach	Reference	Location	Key findings
Hyetographs derived from storm event analysis	Huff curves	Huff and Angel (1992)	Nine states in the USA	• Curves developed from a dense rain gauge network were applicable over nine states because of similar climate and rainfall.
		Bonta (2004)	USA	• Curves can be developed using point data. • Potential for regionalisation; a single set can be applied over a large area.
	Triangular distribution	Lambourne and Stephenson (1987)	Vanderbiljpark, South Africa	• Triangular hyetograph was adequate for design applications. • More accurately represents natural storms than Chicago and uniform distributions.

Category	Approach	Reference	Location	Key findings
	Average variability method	Green et al. (2005)	Australia	• An unsmoothed, single-design pattern AVM temporal distribution for design flood applications should be based on the 10 highest events for a duration • The approach is still applicable for estimating probable maximum floods despite higher-intensity distributions being available.
		Bhuiyan et al. (2010)	Australia	• AVM for determining design rainfall temporal patterns successfully showed climate change-related changes in regional rainfall temporal patterns since original derivation.
	Monobe model	Na and Yoo (2018)	Seoul, Korea	• Model over-estimates rainfall peaks in comparison to the alternating block method (ABM), Huff curves and the Instantaneous Intensity Method (IIM). • May be useful in design calculations where over-design is intended for safety, but requires testing under different climatic conditions.
Hyetographs derived from intensity-duration-frequency relationships	Alternating block method	Na and Yoo (2018)	Seoul, Korea	• This approach was best suited for the estimation of annual maximum rainfall events that closely matched observed rainfall data.
	Instantaneous Intensity Method	Marsalek and Watt (1984)	Canada	• Unrealistic temporal distribution due to the assumption that the design storm contains all the maximum intensities for the various durations. • The design hyetograph should consider antecedent conditions during computation. • Inadequate for application for the development of design storms for Canadian rainfall data.
		Na and Yoo (2018)	Seoul, Korea	• In comparison to the ABM, Huff curves and the Monobe model, the approach was the most accurate in producing peak values close to observed data.
Stochastic models	Bartlett-Lewis rectangular pulse model	Koutsoyiannis and Onof (2001)	London, UK Arizona, USA	• The model could generate hourly-level data capable of aggregating to observed daily totals. • The approach was applicable in cases where limited hourly data was available for fitting. • Performed well in maintaining statistical properties of the rainfall process, including proportions of dry and wet periods, coefficients of variation and skewness of rainfall intensities.

Category	Approach	Reference	Location	Key findings
	Bartlett-Lewis rectangular pulse gamma and modified Bartlett-Lewis rectangular pulse gamma models	Smithers et al. (2002)	South Africa	• Historical data statistics were well replicated by both models. • Design rainfall events estimated by the Bartlett-Lewis rectangular pulse gamma (BLRPG) model were more accurate. • Derivation of BLRPG parameters using only available daily data allows for the estimation of short-duration data values down to one-hour time frames.
	Neyman-Scott rectangular pulse model	Frost et al. (2004)	Multiple Australian cities	• Model adequately reproduced rainfall characteristics of observed pluviograph data records. • Less capable of reproducing wet spells and dry spells, possibly due to the range of statistics for which it is calibrated.
	Random multiplicative cascade model	Güntner et al. (2001)	Brazil, UK	• Highly accurate in reproducing rainfall characteristics at an hourly timestep, with performance being generally better for semi-arid tropical rainfall. • Extreme values were accurately estimated in Brazil, while over-estimated in the UK's temperate climate.
	Random multiplicative cascade, microcanonical and canonical models	Pui et al. (2012)	Australia	• For daily to hourly disaggregation, the canonical approach under-estimated extreme rainfall values, while the microcanonical approach generally over-estimated them. • Models performed reasonably well in simulating statistical rainfall properties such as the mean values and dry periods, but not as well as the Method of Fragments (MOF).
	Method of Fragments	Pui et al. (2012)	Sydney, Perth, Caims and Hobart in Australia	• For daily to hourly disaggregation, MOF performed better than other models, such as the RMC and randomised Bartlett-Lewis model (RBLM) in preserving important rainfall event statistical characteristics, as well as estimating extreme values.
		Li et al. (2018)	Singapore, China	• MOF approaches were capable of reproducing characteristics of site-specific historical rainfall data. • Regionalised and multi-site approaches were found to better represent annual extremes and antecedent precipitation values, making them more viable for capturing the variability in historical rainfall data.

Category	Approach	Reference	Location	Key findings
Deterministic models	Constant model	Hingray and Ben Haha (2005)	Lausanne, Switzerland	• Under-estimates rainfall variability and extremes. • Over-estimates autocorrelations and occurrence probability.
	Ormsbee discrete disaggregation model	Hingray and Ben Haha (2005)	Lausanne, Switzerland	• Under-estimates rainfall variability and extremes. • Over-estimated autocorrelations at 10-minute timesteps. • Model may be unsuitable when these need to be maintained at high-resolution timesteps.
	Ormsbee continuous disaggregation model	Ormsbee (1989)	West Virginia and Kentucky, USA	• Model adequately predicts the first three rainfall moments. • Performance is improved with 15-minute data. • Employing synthetic distributions instead of average distributions produced more accurately predicted peak-flow frequencies.
	Chaotic approach	Sivakumar et al. (2001)	Mississippi, USA	• The model was found to yield reasonable disaggregation results. • The chaotic framework seemed to be more suitable for modelling temporal-scale transformation dynamics than a stochastic framework.

4.3 METHODOLOGY

Rainfall data was obtained through the research catchments database housed at the Centre for Water Resources Research (CWRR) at the University of KwaZulu-Natal, which includes data extracted from breakpoint digitised autographic rainfall charts from historical research sites and historical data previously supplied by the SAWS (Smithers and Schulze, 2001). One station was randomly selected from each of the 15 relatively homogenous extreme rainfall clusters identified by Smithers (1998) and Smithers and Schulze (2000). The data for each station was inspected to determine if the record was of sufficient length and relatively continuous without extensive periods of missing values. When a selected station was found to be unsuitable, another station was randomly selected for the cluster. This was repeated until 15 stations had been obtained, as shown in Figure 4.2.

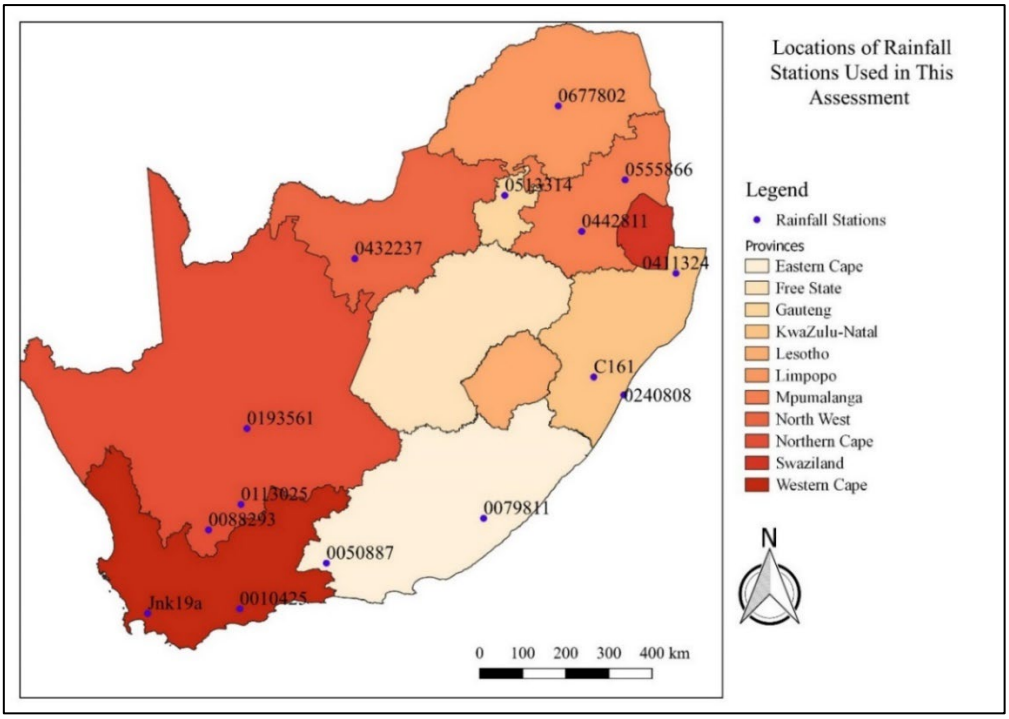

Figure 4.2: Locations of rainfall stations utilised in this study

A pilot study was initially undertaken to develop procedures to apply the methods and develop performance indices to assess and compare the performance of the methods. In the pilot study, rainfall data from Station C161 (Cedara) in the UKZN research catchments database was utilised to develop the methodology for the application of the approaches and assessment of the results. Thereafter, the RTD approaches were applied to daily rainfall data from the additional 14 stations using the same methodology utilised in the pilot study. Details of the rainfall stations are summarised in Table 4.2.

Table 4.2: Characteristics of rainfall stations used in this assessment

Station number	SCS-SA rainfall region	Short-duration homogenous cluster (Smithers, 1998)	Longitude	Latitude	Available record (years)
0513314	3	1	28° 10' 59.9"	-25° 43' 59.9"	29
0555866	2	2	30° 58' 59.9"	-25° 25' 59.9"	20
C161	3	3	30° 13' 37.9"	-29° 35' 12.8"	15
0193561	3	4	21° 49' 00.1"	-30° 21' 0."	35
0677802	2	5	29° 27' 00.0"	-23° 52' 00.1"	39
Jnk19a	2	6	18° 56' 56.0"	-33° 58' 2"	52
0411324	2	7	32° 10' 59.9"	-27° 24' 00.0"	16
0240808	2	8	30° 57' 00.0"	-29° 58' 00.1"	36
0010425	2	9	21° 15' 00.0"	-34° 4' 59.9"	12
0050887	2	10	23° 30' 00.0"	-33° 16' 59.9"	37
0442811	3	11	29° 58' 00.1"	-26° 31' 00.1"	28
0113025	3	12	21° 31' 00.1"	-31° 55' 00.1"	40
0079811	2	13	27° 28' 00.1"	-32° 31' 00.1"	33
0432237	3	14	24° 37' 59.9"	-26° 57' 00.0"	36
0088293	3	15	20° 40' 00.1"	-32° 22' 59.9"	38

4.3.1 Characteristics of rainfall data for all stations

Days with rainfall were identified from the 15-minute data available for the selected rainfall stations. Daily rainfall was computed for periods between 08:00 and 08:00 the next day, as per the standard timeframe for daily rainfall used in South Africa. Furthermore, following the methodologies in studies such as Huff (1967) and Walker and Tsubo (2003), rainfall days with total depths less than 10 mm were excluded from the assessment. Rainfall days were sorted into depth ranges. The distribution of rainfall days in each depth range per station can be seen in Figure 4.3.

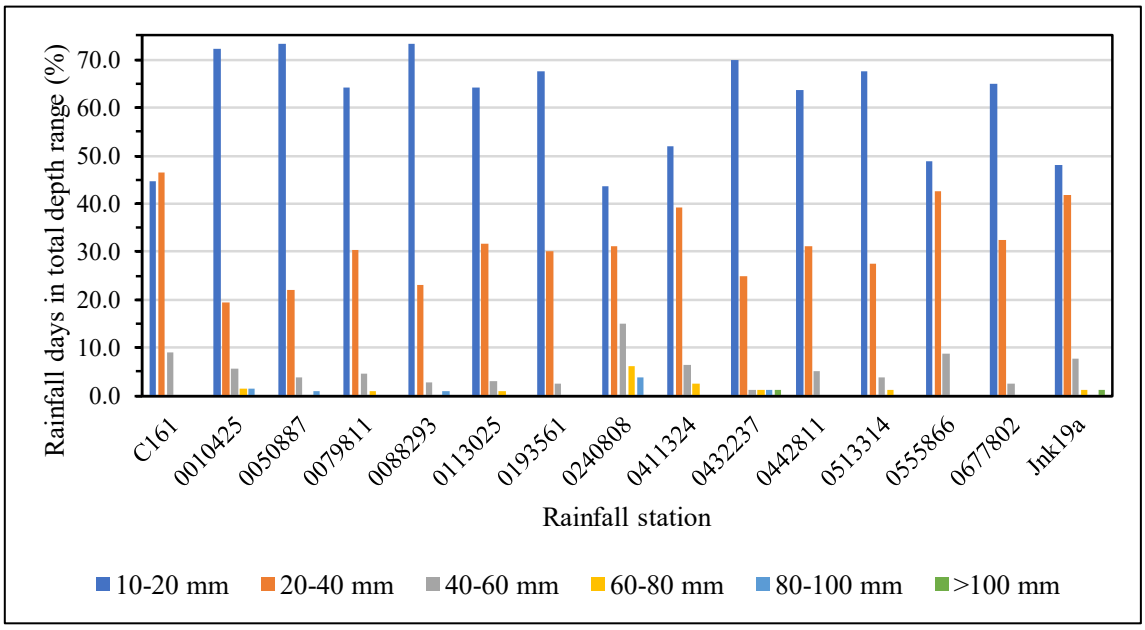

Figure 4.3: Distribution of rainfall days with daily total depths in each range per station

It can be seen that the majority of rainfall days have total depths in the 10–20 mm and 20–40 mm ranges for all stations. The temporal distributions of rainfall on these rainfall days will therefore have a greater influence on the generalised temporal distributions produced for each rainfall station.

The quartile in which the peak of the rainfall occurs is a representation of the period of the rainfall day in which the highest rainfall intensity occurs. The quartiles can be determined by dividing the total duration into four quarters, giving the first, second, third and fourth quartiles. Early rainfall days would display a peak intensity in the first or second quartiles, while later-peaking rainfall days would display peaks in the third or fourth quartiles. The distribution of the percentage of rainfall days that displays peaks in each quartile thus influences the shape of the set of dimensionless Huff curves produced. The distribution of rainfall days with peak intensities in each quartile for each station can be seen in Figure 4.4.

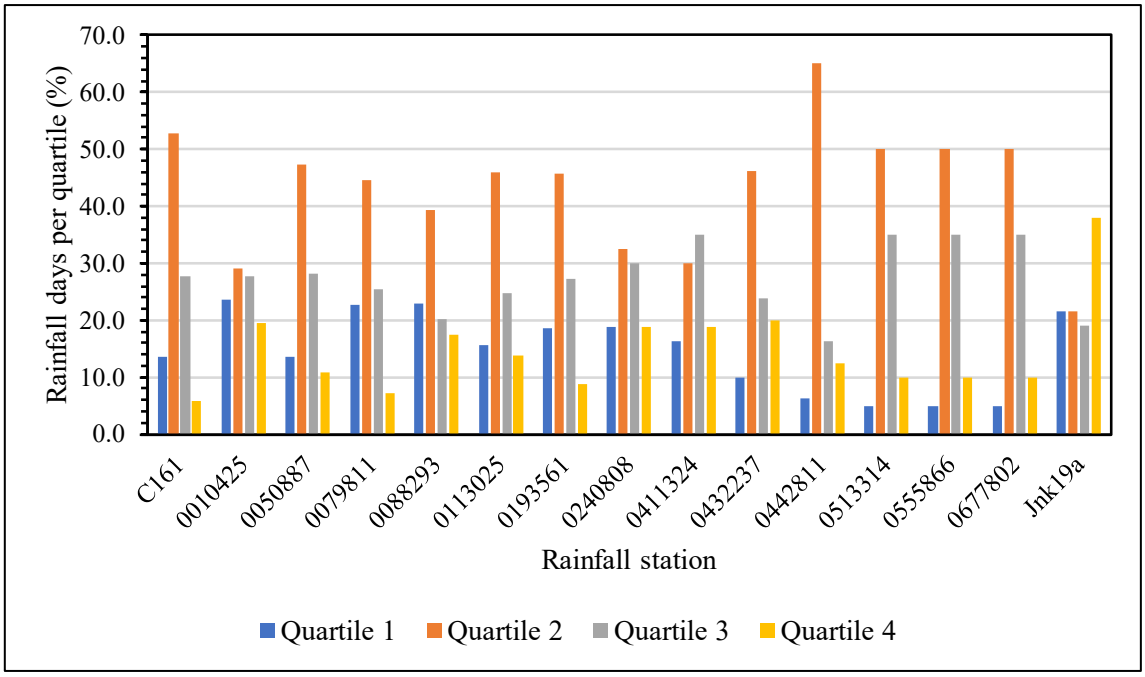

Figure 4.4: Distribution of rainfall days with peak intensities in each quartile per rainfall station

The majority of rainfall days for the selected stations displays peaks in the second quartile of their respective durations. The second-highest concentration is in the third quartile. Hence, the generalised temporal distributions of rainfall produced are likely to display a higher proportion of rainfall in the middle to later sections of the duration.

4.3.2 Rainfall data used in the pilot study

Daily rainfall was computed from the 15-minute rainfall data, and daily totals of < 10 mm were excluded from the analysis, as described above. Trends in the relationships between daily rainfall parameters can be seen in figures 4.5 and 4.6.

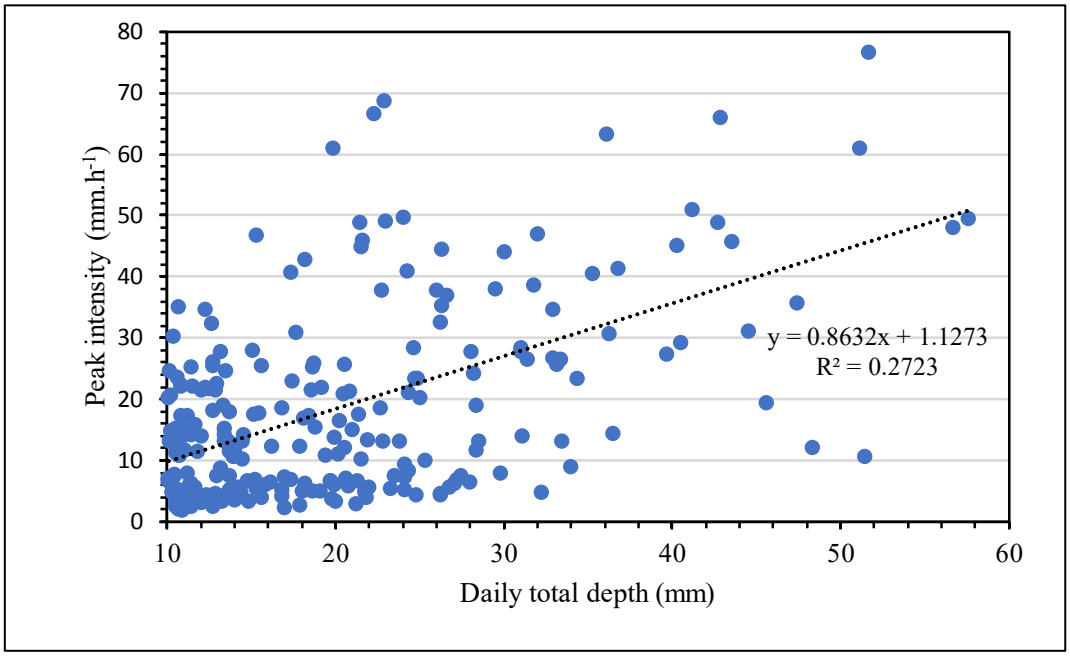

Figure 4.5: Relationship between peak intensity and daily total depth for Station C161's rainfall days

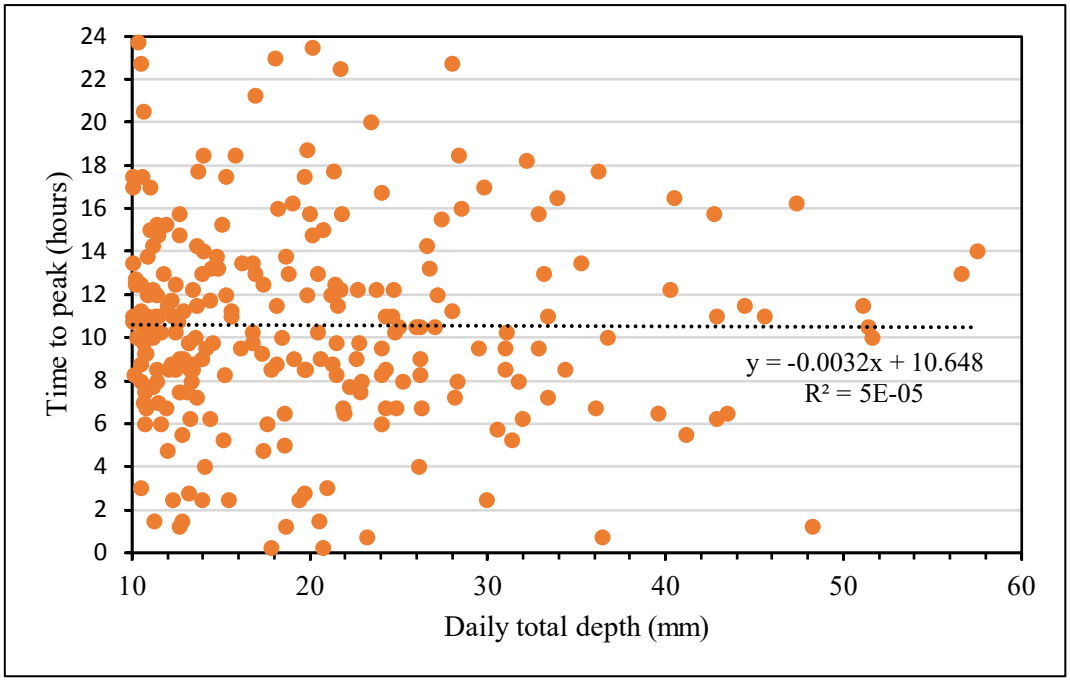

Figure 4.6: Relationship between time to peak and daily total depth for Station C161's rainfall days

Key trends in the analysis of daily rainfall showed a low correlation between peak intensity and total depth. It should be noted that the highest rainfall intensity in a 15-minute duration for the 24-hour daily rainfall period was used as the peak intensity for the day. Hence, this peak is not the same as the actual peak for the rainfall event. Rainfall events may occur across multiple rainfall days or occur multiple times within a 24-hour daily period.

4.3.3 Selection of RTD approaches

RTD approaches were selected from those identified from the literature review on the basis of the ease of application with the available data in terms of the number of input parameters required, reported performance in case studies, and potential for regionalisation in South Africa. The following RTD models and distributions were selected for assessment in this study:

- Huff curves as a means of comparing observed and disaggregated distributions
- SCS-SA rainfall distributions
- HRU 1/72 24-hour distribution
- Triangular distribution
- Average variability method
- Knoesen semi-stochastic disaggregation model

4.3.4 Assessment of performance of approaches

The performance of the disaggregation approaches was determined by analysing the Huff curves produced using the observed 15-minute data and disaggregated daily data. Huff curves were developed according to the methodology outlined in Bonta (2004). Percentiles are generalised probabilistic representations of dimensionless rainfall events or daily rainfall durations (for 24-hour periods) plotted against the corresponding dimensionless accumulated depths. For example, the 90th percentile curve shows that 90% of the accumulated event or daily rainfall has occurred. Therefore, 90% of all other rainfall temporal distribution profiles lie below this curve (Bonta, 2004). An example of a set of Huff curves can be seen in Figure 4.7.

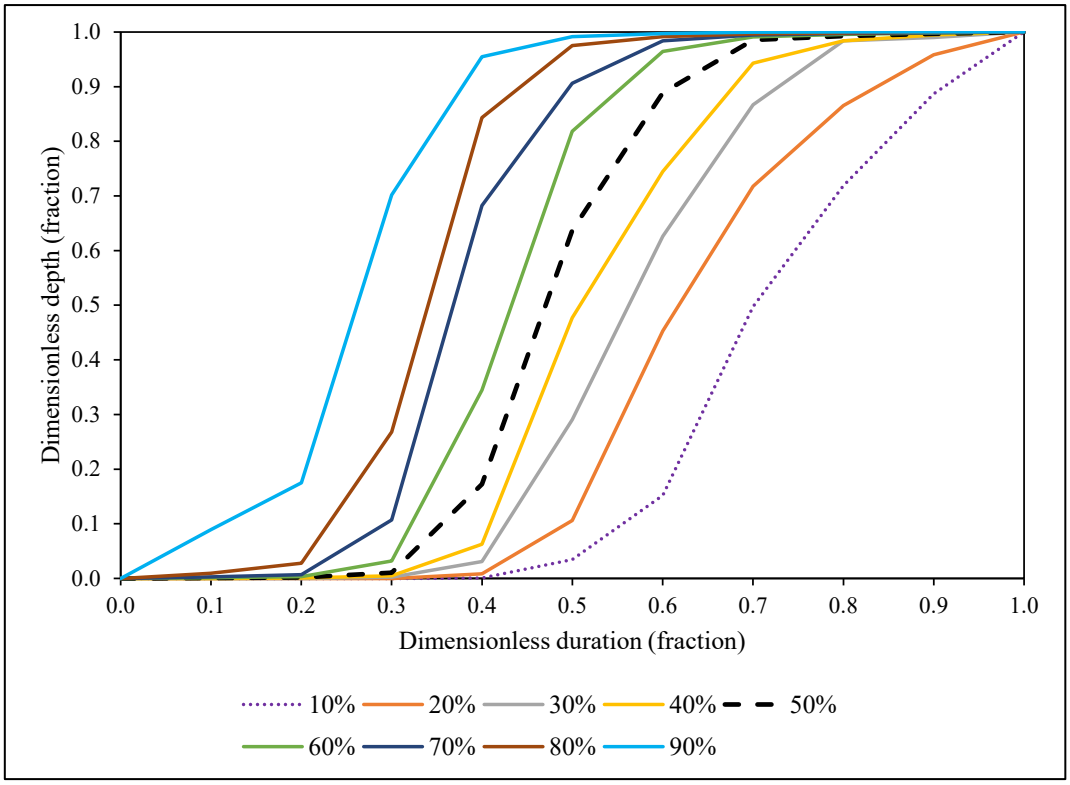

Figure 4.7: Huff curves for rainfall days greater than 10 mm from Station C161

The mean absolute relative error, a single value that quantifies the performance of disaggregation approaches and distributions, was used to measure the difference between a percentile Huff curve generated from the disaggregated daily data and the percentile curve derived from the observed 15-minute data, as shown in Equation 4.1. The total MARE ($\sum$MARE) represents the total value for all percentiles and is given by Equation 4.2.

$$\text{MARE}_{\text{j}}(\%) = \frac{\sum_{n=0.1}^{S} |X_n - D_n|}{S} \times 100 \qquad 4.1$$

$$\sum\text{MARE}\ (\%) = (\text{MARE}_{10\text{th}} + \text{MARE}_{20\text{th}} + \cdots + \text{MARE}_{90\text{th}}) \qquad 4.2$$

where:

j = percentile (10th, 20th, …, 90th)
X_n = observed dimensionless depth at dimensionless time = n
n = dimensionless duration fraction (0.1, 0.2, … 1.0)
D_n = disaggregated dimensionless depth at dimensionless timestep = n
S = number of dimensionless duration fraction values

The Nash-Sutcliffe efficiency value is a normalised statistic that can be used to indicate how well the plot of observed versus simulated data fits the 1:1 line (Moriasi et al., 2007). The NSE is utilised in addition to the MARE to determine the performance of the disaggregation approaches by comparing observed and disaggregated Huff curve increments. The NSE ranges between -∞ and 1.0, with a value of 1.0 being the optimal value. Values between 0.0 and 1.0 are considered acceptable levels of performance (Moriasi et al., 2007). The NSE is determined using Equation 4.3.

$$\text{NSE} = \left[\frac{\sum_{i=1}^{n}\left(Y_i^{obs} - Y_i^{sim}\right)^2}{\sum_{i=1}^{n}\left(Y_i^{obs} - Y^{mean}\right)^2}\right] \qquad 4.3$$

where:

Y_i^{obs} = the i[th] observation for the constituent being evaluated

Y_i^{sim} = the i[th] simulated value for the constituent being evaluated

Y^{mean} = the mean of observed data for the constituent being evaluated

n = the total number of observations

4.3.5 Application of rainfall temporal disaggregation approaches

A summary of the differences between the application of RTD approaches to daily rainfall is detailed below. It should be noted that some of the disaggregation approaches were modified for application on daily rainfall. The modifications were based on the following assumptions:

- Data that was provided in the digitised database was accurate. It was evident that long periods of low rainfall values displayed may be an artefact of the digitisation and interpolation procedure between two digitised points used for the derivation of the rainfall depths from the original rainfall chart data.
- It is acknowledged that not all the RTD approaches selected for application are designed for application on daily rainfall data as obtained from the rainfall stations used in this study. Therefore, the methods were either applied directly or in a modified manner, as detailed in Section 4.3.4.
- Huff curves provide smoother distributions than actual rainfall temporal distributions.

4.3.5.1 Huff curves

Huff curves were developed using the depths of rainfall at each 15-minute interval of the 24-hour (08:00 to 08:00) duration for each rainfall day.

4.3.5.2 SCS-SA

Dimensionless depth fractions provided by each distribution were used to produce a distribution of the total daily rainfall depth over a 24-hour duration (SCS-SA distributions). It is acknowledged that the correct approach for applying the SCS-SA method is to select a single appropriate distribution for a rainfall station based on the SCS-SA rainfall region. However, in this study, all the SCS-SA distributions were applied to assess if a distribution from another region provides a better fit to the distribution of the observed data at the site. A comparison of the four SCS-SA distributions and Huff curves for Site C161 is shown in Figure 4.8.

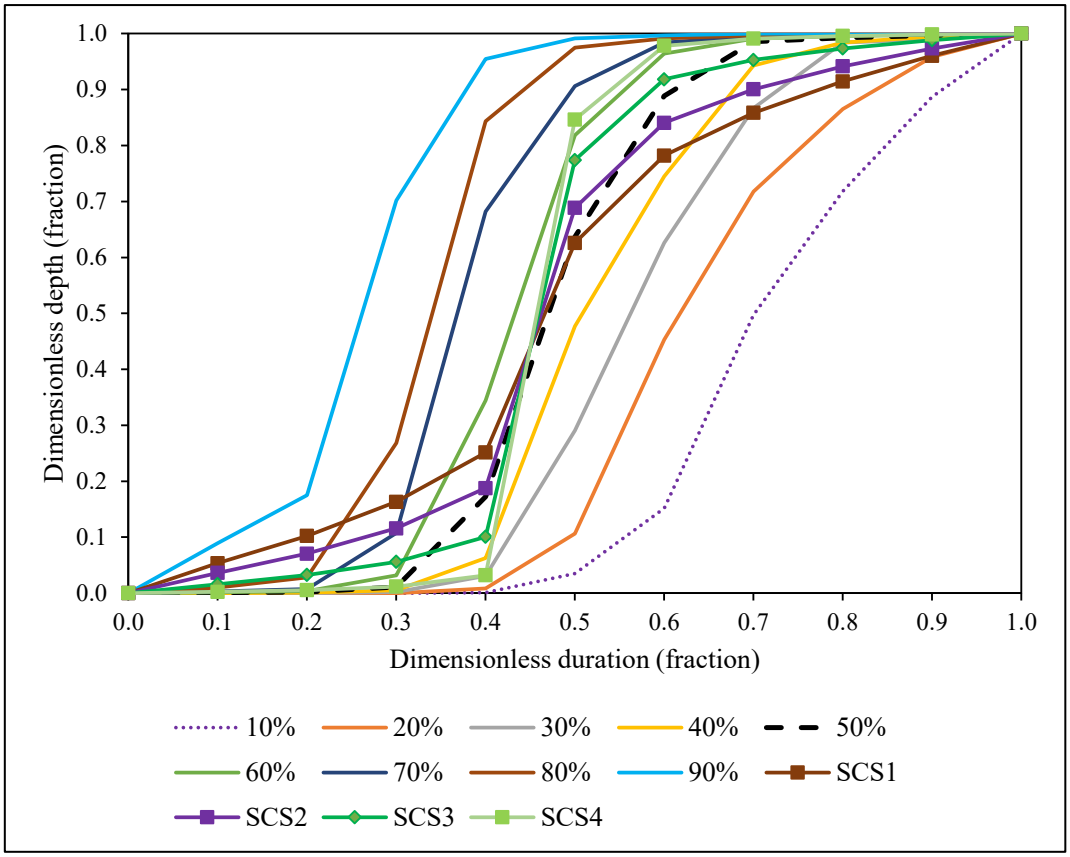

Figure 4.8: Comparison of SCS-SA distribution curves and observed daily rainfall Huff curves

4.3.5.3 Hydrological Response Unit 1/72

The HRU 1/72 distributions were selected from the range of two-hour to 24-hour distributions provided in the HRU 1/72 report for characterising design storms (HRU, 1972). The distributions associated with the approach each provide a dimensionless distribution of percentage of total depth per corresponding percentage of total duration. In order to obtain the fraction of event total for each 15-minute incremental timestep, a 10th order polynomial equation was fitted to the cumulative curves. This followed the methodology used by Bonta (2004) in the application of Huff curves. For daily rainfall, the HRU 1/72 24-hour distribution was used to disaggregate daily total depths.

4.3.5.4 Triangular distribution

The methodology described in Lambourne and Stephenson (1987) and Chow et al. (1988) was followed for application of the triangular distribution. In the first approach in the pilot study, triangular distributions for daily rainfall were determined using the available daily rainfall total depth, 24-hour duration and observed time to peak (TP) to calculate the peak intensity for a rainfall day (triangular ObsTP approach). In a second approach, the median time to peak derived from the observed rainfall days was determined and used to derive distributions (triangular median TP approach). The use of the median value time to peak was adopted, given the weak relationship between time to peak and total depth, thus making it difficult to estimate the time to peak for each rainfall day

4.3.5.5 Average variability method

A modified version of the AVM described in Chapter 2 was utilised in this assessment, which did not involve an analysis of intense bursts of rainfall. Literature and case studies reviewed described the application of the approach for rainfall events. In this assessment, the approach was modified to be more suitable for application with the available daily rainfall data.

The 24-hour rainfall days were divided into four sections of six hours in duration and the method derivation of the AVM temporal pattern, as given in Bhuiyan et al. (2010), was followed. Rainfall data for Station C161 was ranked to identify the highest daily rainfall totals in each year on record. Full details on the adopted method are contained in Ramlall (2020).

4.3.5.6 Modified average variability method (AVM-B)

The methodology used for the initial derivation of the AVM distribution used in this assessment displays a limitation relating to the six-hour sections of daily rainfall depths utilised. The use of four six-hour sections of rainfall results may not result in disaggregated daily depths with similar peak values to the observed rainfall. Therefore, the second approach (AVM-B), which modified the AVM distribution used in this study, was developed using 96 sections of 15 minutes in duration, which is the same resolution as the observed daily rainfall.

4.3.5.7 Knoesen semi-stochastic disaggregation model

The Knoesen model was developed for application on 24-hourly data (00:00 to 00:00). The software developed by Knoesen (2005) was utilised to generate 24-hour distributions of total daily rainfall depths. For the pilot study, it was determined that Station C161 falls within Range III of the regionalised distribution map of R values associated with the model (Knoesen, 2005). The range category (Range III) and daily total depths were used as input into the programme to generate 15-minute rainfall depths distributed over 24 hours. The stochastic nature of the model results in a different distribution with each successive run. For purposes of this assessment, a single distribution was generated for each respective rainfall day. The total depth of each rainfall day was used as input into the model to stochastically generate a distribution of depths over 24 hours.

4.4 RESULTS

The RTD approaches were applied to disaggregate daily rainfall depths at Site C161 in the pilot study and then at the additional 14 rainfall stations. The approaches were assessed for their performance in approximating the observed temporal distribution of rainfall, as represented by the Huff curves developed, using MARE, ∑MARE and NSE values.

4.4.1 Pilot study

The Huff curves for two of the worst-performing methods can be seen in figures 4.9 and 4.10.

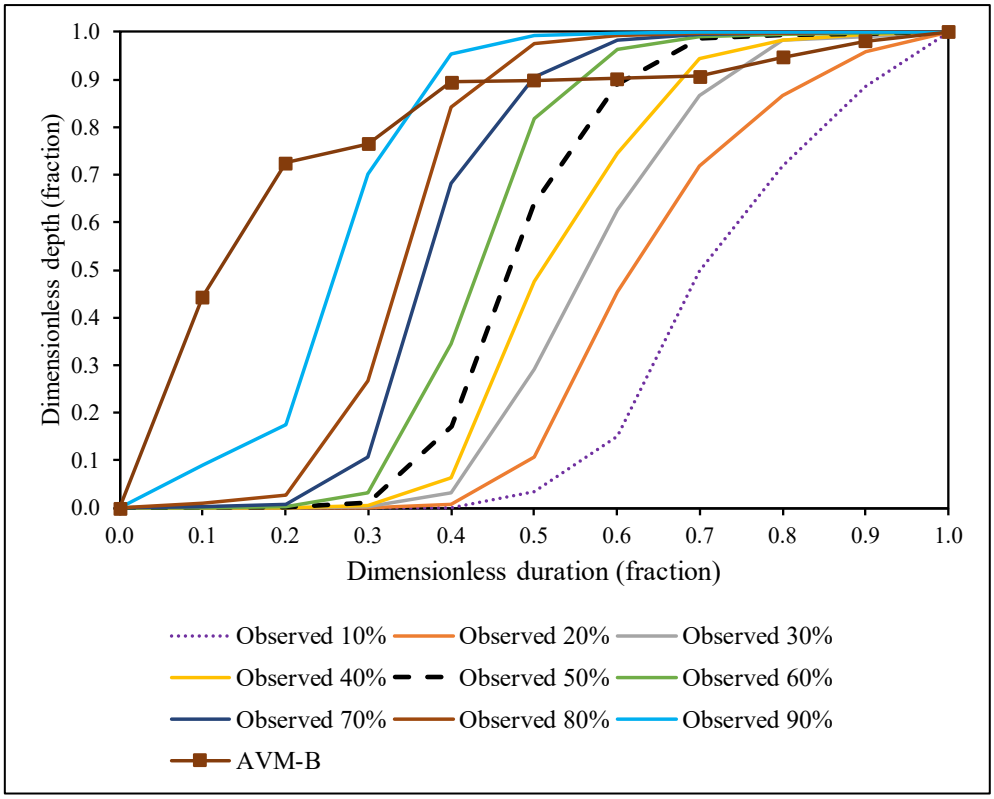

Figure 4.9: Comparison of observed daily rainfall Huff curves to AVM-B curve for Station C161

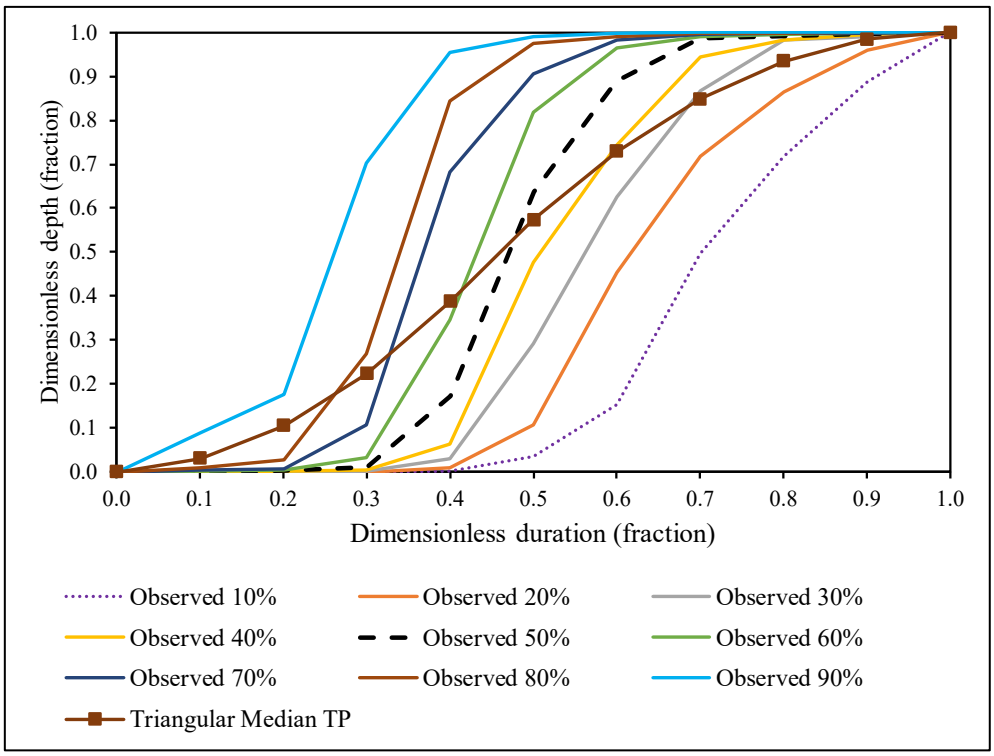

Figure 4.10: Comparison of observed daily Huff curves and median time-to-peak triangular distribution curve for Station C161

The ∑MARE values for comparisons of observed daily rainfall Huff curves and Huff curves derived from daily rainfall depths disaggregated using each RTD approach can be seen in Figure 4.11.

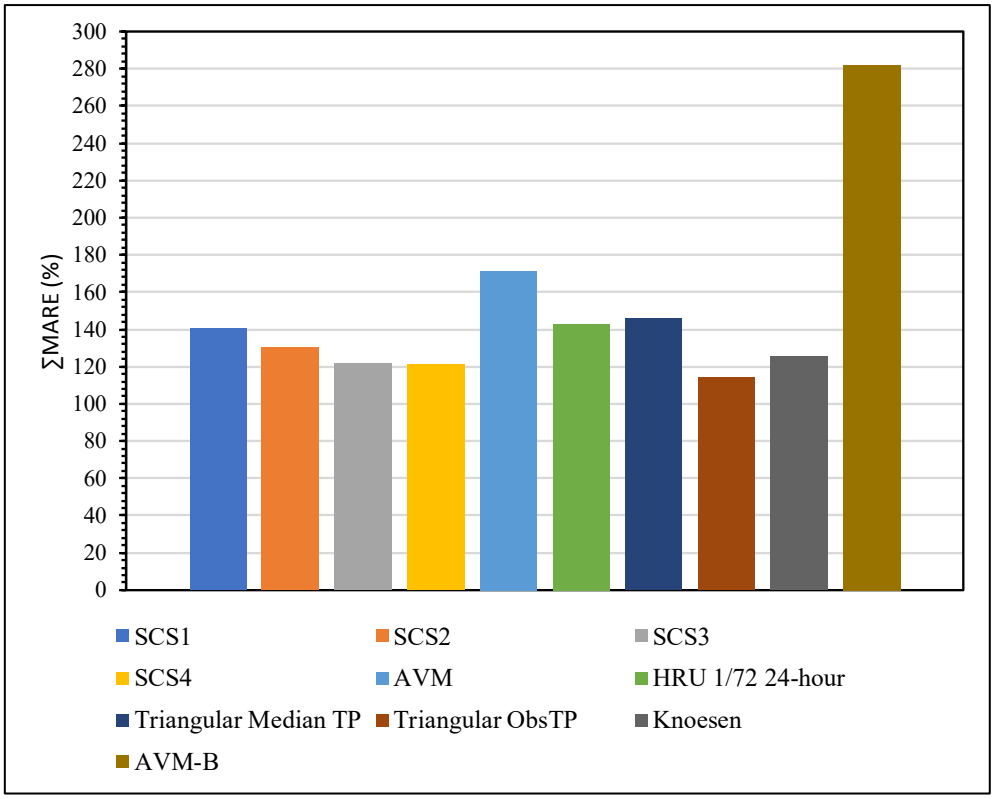

Figure 4.11: Total MARE for RTD approaches applied to daily rainfall data at Station C161

The triangular ObsTP appears to perform the best out of the RTD approaches. However, it should be noted that the approach was developed using observed total rainfall depths and the observed time to peak, which likely accounts for the good performance. The triangular median TP distribution, which was developed using the median time to peak value for all rainfall days and the total daily depth, does not perform as well. Considering these factors, the Knoesen model performs the best out of the approaches that are not fixed distributions or use observed parameters. The SCS3 and SCS4 distributions are quite similar in performance. However, the SCS4 distribution performs the best, despite the rainfall station from which the observed data was obtained falling within an SCS3 region.

The NSE values between the observed and disaggregated Huff curves were determined and can be seen in Table 4.3. This serves as an additional assessment of how similar the distributions displayed by the disaggregated rainfall curves are to those of the observed rainfall curves.

Table 4.3: NSE values for comparison of observed and disaggregated Huff curves

RTD approach	NSE for each percentile									Mean
	10th	20th	30th	40th	50th	60th	70th	80th	90th	
SCS1	**0.36**	**0.73**	**0.89**	**0.95**	**0.97**	**0.94**	**0.84**	**0.73**	**0.42**	**0.76**
SCS2	**0.26**	**0.69**	**0.88**	**0.96**	**0.99**	**0.96**	**0.85**	**0.73**	**0.38**	**0.74**
SCS3	**0.10**	**0.60**	**0.84**	**0.94**	**0.99**	**0.97**	**0.83**	**0.69**	**0.29**	**0.70**
SCS4	**-0.05**	**0.51**	**0.79**	**0.91**	**0.97**	**0.96**	**0.80**	**0.65**	**0.20**	**0.64**
AVM	0.46	0.72	0.81	0.85	0.86	0.84	0.79	0.72	0.45	0.72
AVM-B	-1.29	-0.59	-0.20	-0.02	0.16	0.30	0.45	0.55	0.73	0.01
HRU 1/72 24-hour	0.18	0.61	0.81	0.89	0.93	0.95	0.92	0.85	0.63	0.75
Triangular ObsTP	0.75	0.88	0.92	0.93	0.93	0.92	0.89	0.86	0.77	0.87
Triangular median TP	0.36	0.72	0.87	0.91	0.93	0.92	0.86	0.78	0.52	0.76
Knoesen	0.52	0.46	0.55	0.60	0.63	0.61	0.77	0.97	0.96	0.68

It can be seen that relatively high NSE values are displayed for each approach, particularly for the higher percentiles. An exception to this is the AVM-B approach, which displays values indicative of overall poor performance. The results characterised by the NSE values are slightly different to those of the MARE and ∑MARE values previously shown, especially by the mean NSE values. The Knoesen model is shown to be the second-least accurate RTD approach, based on approximation of the Huff curve temporal distributions, according to the NSE values. This is despite the result shown by the MARE values, which indicated that the Knoesen model was the best-performing model. However, the NSE values provide a fair indication that there is a discernible difference between the observed Huff curves and the Huff curves derived from the disaggregated rainfall produced by each approach.

4.4.2 Daily rainfall disaggregation at all sites

The daily rainfall data for 14 additional rainfall stations, with one station selected from each of the 15 homogenous rainfall clusters, was used for the application of RTD approaches using the same methodologies from the pilot study. This was undertaken to further assess the performance of the selected approaches for the disaggregation of rainfall data in different climatic locations in South Africa.

The ∑MARE values were calculated for RTD approaches applied at each station to determine the overall performance of each approach. The station-specific ∑MARE values for each approach were summed across all the rainfall stations, as shown in Figure 4.12. The value for SCS-SA indicates the total when the MARE values are applied for the appropriate SCS-SA distribution for each station, i.e. based on the appropriate SCS-SA region for each station.

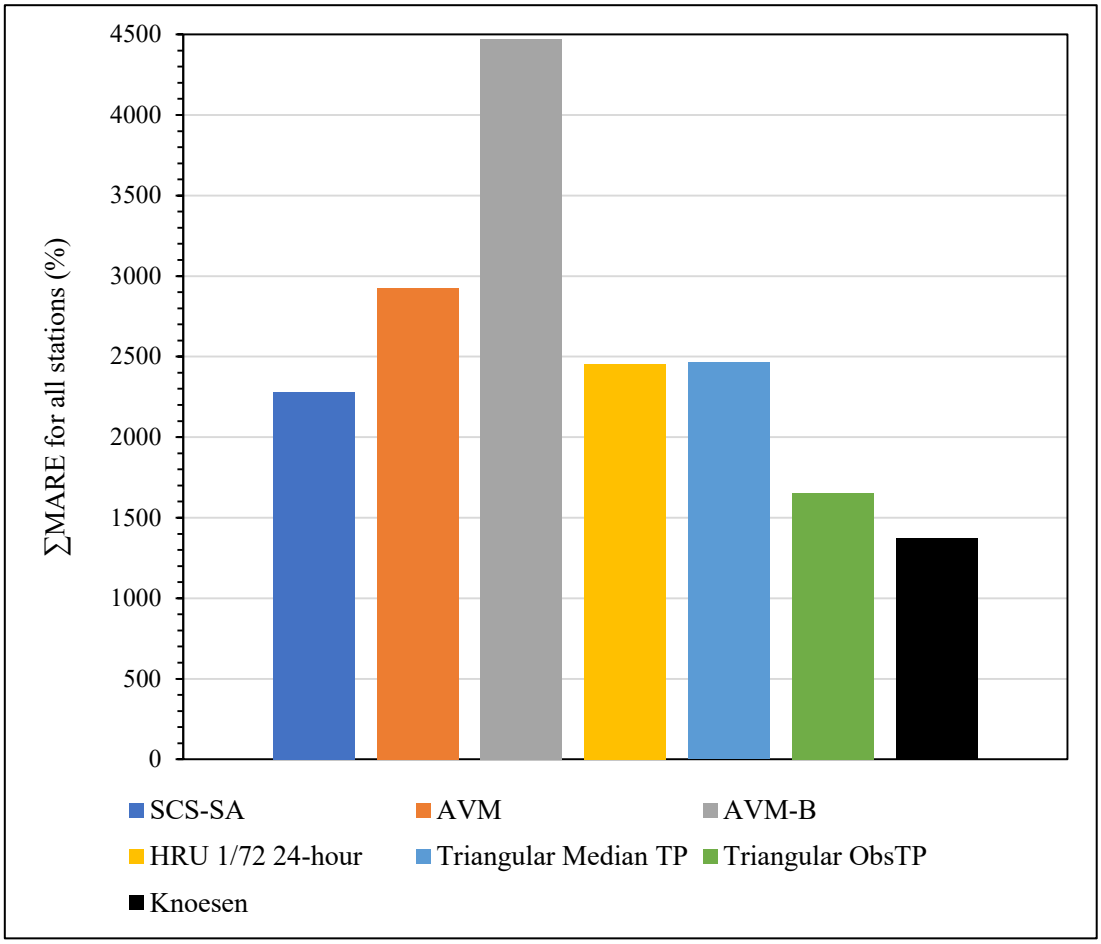

Figure 4.12: ∑MARE values for RTD approaches summed across all stations

The approach that provides the least realistic rainfall temporal distribution in terms of Huff curves appears to be the AVM-B approach, followed by the AVM distribution. It can be seen that, for all the rainfall stations, the approaches that generally display the lowest ∑MARE values are the Knoesen, triangular ObsTP and SCS-SA approaches. It is acknowledged that the good performance of the triangular ObsTP can be attributed to the methodology used in its application. The approach was applied using available timing peak intensity for each application, which improves the performance in approximating the observed daily rainfall temporal distribution. The version of the approach that utilises a generalised timing of the peak intensity value and hence removes this bias, the triangular median TP distribution, does not perform as well and often displays relatively high ∑MARE values. Given the abovementioned factors, it can be said that the RTD approach that results in the best overall performance for the disaggregation daily rainfall totals into realistic temporal distributions is the Knoesen semi-stochastic disaggregation model, followed by the SCS-SA.

Table 4.4: Mean NSE values for each approach for each rainfall station

Rainfall station	Mean NSE for each method										
	SCS1	SCS2	SCS3	SCS4	SCS-SA	AVM	AVM-B	HRU 1/72 24-hour	Triangular ObsTP	Triangular median TP	Knoesen
C161	0.76	0.74	0.70	0.64	0.70	0.72	0.01	0.75	0.87	0.76	0.68
0010425	0.52	0.46	0.35	0.24	0.46	0.52	0.35	0.53	0.46	0.56	0.96
0050887	0.70	0.68	0.62	0.55	0.68	0.62	-0.54	0.68	0.84	0.70	0.77
0079811	0.72	0.69	0.61	0.53	0.69	0.53	0.31	0.73	0.97	0.74	0.97
0088293	0.54	0.50	0.41	0.31	0.41	0.48	-0.18	0.55	0.96	0.57	0.96
0113025	0.58	0.54	0.47	0.39	0.47	0.54	0.38	0.58	0.79	0.59	0.83
0193561	0.66	0.64	0.58	0.52	0.58	0.48	-0.05	0.67	0.83	0.67	0.64
0240808	0.53	0.47	0.37	0.26	0.47	0.49	-0.61	0.53	0.81	0.55	0.77
0411324	0.64	0.61	0.54	0.46	0.61	0.42	-0.43	0.61	0.81	0.66	0.85
0432237	0.54	0.50	0.42	0.34	0.42	0.20	0.32	0.51	0.78	0.56	0.78
0442811	0.78	0.77	0.74	0.69	0.74	0.61	-0.06	0.78	0.87	0.78	0.61
0513314	0.74	0.73	0.69	0.63	0.69	0.66	0.26	0.72	0.85	0.74	0.77
0555866	0.51	0.46	0.35	0.25	0.46	0.53	-0.35	0.50	0.80	0.55	0.76
0677802	0.51	0.46	0.37	0.28	0.46	0.46	-0.05	0.48	0.79	0.53	0.86
Jnk19a	0.39	0.30	0.14	-0.02	0.30	-0.01	0.22	0.34	0.83	0.49	0.91

The mean NSE values shown in Table 4.4 are reflective of the results that have previously been shown by the ∑MARE values. Overall, the Knoesen model is the RTD approach that provides the temporal distributions that are most similar to those of the observed daily rainfall data. The four SCS-SA distributions also perform relatively well for stations in their respective recommended regions. However, some exceptions noted previously are seen in cases where an SCS-SA distribution not recommended for the region may outperform the recommended distribution. It should also be noted that relatively fair performance is shown by the triangular median TP approach, which outperforms other approaches in some instances and for certain percentiles.

4.5 DISCUSSION AND CONCLUSIONS

DFE generally utilises daily rainfall data that is abundantly available in South Africa. Many event-based and continuous simulation models require rainfall data to be available in finer timestep resolutions. Hence, there is a need for sub-daily timestep rainfall data. Sub-daily rainfall stations are relatively sparse and have shorter record lengths compared to daily rainfall stations, both in South Africa and internationally.

Therefore, a means of disaggregating daily rainfall data into sub-daily rainfall hyetographs is required. RTD approaches may be utilised to disaggregate daily rainfall data into shorter temporal resolutions from higher temporal resolution data. Several RTD approaches have been applied in South Africa, including the SCS-SA distributions, Huff curves, the Knoesen semi-stochastic disaggregation model and triangular distribution. However, application of RTD approaches locally is relatively limited compared to those developed and applied internationally. The overall aim of this study was to assess the performance of selected RTD methods and to recommend the adoption or adaptation of one or more of these approaches for application under South African conditions.

A pilot study was used to develop procedures to apply the methods and develop performance indices. Huff curves were utilised for comparison of the observed and disaggregated rainfall depths. Furthermore, the MARE, ∑MARE and NSE values served as an index for quantifying the difference between curves derived from observed and disaggregated rainfall.

The Huff curves developed from daily rainfall disaggregated using the Knoesen model, SCS3, SCS4 and triangular distribution performed well in approximating the observed Huff curves for the pilot study. The good performance of the triangular ObsTP distribution was attributed to the inclusion of observed parameters in its application. However, the triangular median TP did not perform as well. The triangular median TP was developed using a generalised timing of the peak and observed durations in order to remove part of the performance bias of the triangular ObsTP. Overall, the best-performing approach for disaggregating daily rainfall was SCS4, despite the station falling within a SCS3 region

The results of the assessment of the RTD approaches according to ∑MARE and NSE values, as shown in Section 4.4.2, were different to those seen in the pilot study. The best-performing RTD approaches were found to be the SCS-SA distributions and the Knoesen model when the triangular ObsTP is appropriately excluded. However, the triangular median TP displayed fair performance and shows potential for further investigation into general use. Overall, the Knoesen model provided the lowest ∑MARE values and most appropriate NSE values across all stations. It can therefore be considered the most suitable approach for disaggregating daily rainfall into realistic temporal distributions. An additional finding was that, in certain cases, the recommended SCS-SA distribution for a station was outperformed by one that was recommended for a different region. This may be explained by some of the stations being located at the edge of one region and in close proximity to another region.

The AVM and AVM-B approaches, which were adapted from the original application of the AVM in literature, performed exceptionally poorly and are therefore not recommended for use in disaggregation in the forms utilised in this assessment. However, it is noted that the AVM is no longer recommended as a temporal distribution in Australia due to limitations relating to the averaging of the distribution and use of high rainfall periods in its construction.

The triangular distribution approaches, including the triangular ObsTP and triangular median TP, have shown considerable potential for providing a similar temporal distribution to observed daily rainfall in terms of the shape of the distribution when the observed value for the timing of the peak is utilised. Therefore, it is recommended that the approach be further developed using generalised values for the timing of the peak. This will require relationships between depths and time to peak to be derived at + levels.

CHAPTER 5: AN ASSESSMENT OF SIMPLE CONTINUOUS SIMULATION MODELLING APPROACHES FOR DESIGN FLOOD ESTIMATION IN SOUTH AFRICA

N Mabila, TJ Rowe and JC Smithers

This chapter provides a summary of the study undertaken by Mabila (2019) to address the fourth objective listed in Chapter 1: Select and assess the performance in South Africa of a simpler, parameter-sparse continuous simulation model applied internationally and compare the performance with the ACRU continuous simulation model that was developed.

5.1 INTRODUCTION

The use of continuous simulation modelling for design flood estimation (DFE) has received increasing attention in local and international literature as an approach that has potential for DFE and which explicitly simulates the antecedent moisture conditions and joint association of rainfall and runoff (Schulze, 1989; Calver and Lamb, 1995; Calver et al., 1999; Cameron et al., 1999; Reed, 1999; Boughton and Droop, 2003; Smithers and Schulze, 2003; Chetty, 2010; Smithers, 2012; Rowe, 2015). Thus, many limitations of the conventional event-based methods are overcome with the application of CSM. Unlike event-based methods, in the CSM method, a complete hydrograph is obtained and AMC are directly accounted for (Boughton and Droop, 2003; Chetty and Smithers, 2005; Smithers, 2012). In addition, stochastically generated rainfall can be used to generate long sequences of streamflow hydrographs, which further motivate the use of CSM methods over event-based methods.

Schulze (1989), Smithers and Schulze (2003) and Smithers (2012) advocated for the CSM approach in South Africa, highlighting the advantages it has over event-based methods. The CSM approach to DFE has been applied with acceptable success in selected catchments in South Africa (Schulze, 1989; Smithers and Schulze, 2003; Chetty and Smithers, 2005; 2011; Chetty, 2010; Smithers, 2012; Smithers et al., 2013; Rowe, 2015). All these studies used the physically based conceptual ACRU model, which is a comprehensive parameter and data-intensive model. Although the results found using the ACRU model were reasonable and consistent, input data requirements, the time and expertise required to set up the model remain a challenge to many of the model's users. The use of simple models over comprehensive ones has been suggested as a promising approach to represent the processes governing runoff generation within a catchment (Nash and Sutcliffe, 1970; Jakeman et al., 1990; Beven, 1993; Jakeman and Hornberger, 1993; 1994; Dye and Croke, 2003). Therefore, there is a need to evaluate the use of simple CS models for DFE, which have fewer parameters and which are less data demanding. In addition, only a limited number of studies have compared comprehensive and simple CS models (Dye and Croke, 2003). Therefore, the aim of this component of the study is to assess the performance of a selected simple CS model and compare the performance to that of the comprehensive ACRU model.

5.2 BACKGROUND AND METHODOLOGY

A detailed review of the literature focused on simple parameter-sparse CS models is contained in Mabila (2019). From this, the GR4H (hourly timestep simulation) and GR4J (daily timestep simulation) models (Le Moine, 2008), which have four parameters, were selected as the simple CS models to be applied and assessed. This section contains the details of the steps undertaken to calibrate and verify the models and how the model's performance was evaluated.

The ability of the models to reproduce flood peaks, volumes and other hydrograph characteristics was tested under different calibration scenarios. Three consistent calibration scenarios were used for both the daily and hourly models. However, an additional calibration scenario (Scenario 4) was used with the hourly model. The calibration scenarios include the following:

- Calibration Scenario 1: The models were calibrated to the full available period and verified to the same period, referred to as “Calib. All data”.
- Calibration Scenario 2: The models were calibrated to a shorter subset of the data (preferably a wet period) and verified using the rest of the period, referred to as “Calib. Wet period”.
- Calibration Scenario 3: To improve the simulation of peak discharges, the models were calibrated to flows above the 90th percentile threshold of observed flows, referred to as “Calib. Q90”.
- Calibration Scenario 4: For the hourly model (GR4H), actual streamflow hydrographs at an hourly timestep were used for calibration with the observed hourly rainfall data. Consequently, to improve the simulation of the largest peaks, calibration to a single high peaked event with high-quality rainfall and runoff data was used for calibration in Scenario 4, referred to as “Calib. Single event”.

Across all the calibration scenarios, the calibration Michel option was used and parameters were optimised automatically using the shuffle complex evolution of the American Society of Civil Engineers (ASCE)’s global optimisation algorithm (Muttil and Jayawardena, 2008; Bennett et al., 2014; Ling et al., 2015; Pokhrel et al., 2015). This algorithm uses an iterative process to provide the best set of parameters for a given catchment (Perrin et al., 2003). To reduce the challenges of initialisations, the first year of the available record was used as a warm-up period. Finally, the GEV distribution was fitted to the AMS of the observed and simulated flows using L-moments to assess the performance of the models to simulate design values, both in terms of flood volumes and peak discharges. Similar analyses were performed on the simulated results from the ACRU CSM system. However, the ACRU model is not calibrated, but rather parameterised based on physical catchment characteristics.

The airGR package (Coron et al., 2018) uses different statistical objective functions to evaluate the performance of the GR4J and GR4H models in terms of simulating observed flows for calibration and verification purposes. In addition to statistical evaluation procedures, flow data can be visually inspected using graphical plots such as flow duration curves, hydrographs and scatter plots to understand the differences in flow over time and the data distribution (ASCE, 1993; Legates and McCabe Jr, 1999; Moriasi et al., 2007; Vaze et al., 2012). For this study, the NSE objective function was applied to assess the general performance of the models. The MRE was used to assess the difference between the observed design flood values and the simulated design flood values.

5.3 RESULTS

The performance of the airGR models to reproduce the observed hydrograph and the observed flood frequency curve at both daily and hourly timesteps for two test catchments, the Cathedral Peak IV catchment (V1H005) and the Beestekraalspruit catchment (X2H026), located as depicted in Figure 3.1, are presented in this chapter. For clarity, detailed results are provided for the Cathedral Peak IV catchment. Thereafter, for brevity, the remainder of the results are summarised using the NSE for observed and simulated flows at the daily and hourly timestep, and the MRE for the design values, i.e. observed and simulated flood frequency curves. The results obtained from the ACRU model are included in this summary for comparison.

In addition to the limited spatial density of recording rainfall stations in South Africa, i.e. compared to daily rainfall stations, the record lengths are generally much shorter than those available for the daily stations. Moreover, autographic recording rainfall stations are more prone to errors and missing rainfall data.

One of the objectives outlined in the methodology is to compare the performance of the daily and hourly models. The performance of the hourly model was expected to better approximate the actual daily peak discharges, since the daily model only simulates the total runoff volume for the day. Hence, only the average daily flow can be calculated. For DFE, it is essential to estimate both design runoff volumes and peak discharges. Therefore, it was hypothesised that the hourly model would provide a better estimate of the actual peak discharge. Since the hourly rainfall records were shorter than the daily records, the daily records were constrained to the same period as the hourly data for the daily versus hourly model comparison. The limited availability of hourly rainfall data further limited the comparison to only two catchments. This was mainly due to errors and missing data (both flagged and not flagged) in the hourly record, and the inability to identify consistent and continuous periods of rainfall and runoff data at the hourly timestep at other sites.

The ability of the model to simulate the observed design values was evaluated by comparing the design observed and simulated average daily discharges (ADD), i.e. calculated from the daily observed and simulated runoff volumes for all the scenarios simulated, and the design observed and simulated hourly peak discharges (HPD) for all the scenarios simulated. Design values for the observed actual daily peak discharges (ADPD) are included to highlight that, at the daily timestep and particularly for small catchments where the hydrograph often rises and falls within a few hours, the ADD is a poor estimate of the ADPD. The MRE between the observed and simulated design values for the daily and hourly timesteps are included for comparison, i.e. after investigating the hourly and daily results individually.

5.3.1 Performance of the GR4J daily model at the Cathedral Peak catchment

The simulated and observed flow hydrographs obtained from the GR4J daily model at the Cathedral Peak IV catchment are shown in Figure 5.1. The observed volumes are well simulated in terms of timing and flow magnitudes. The peak flows are generally simulated well, with a few instances of over-simulation (Figure 5.1). Calibration to the full available record simulated the timing of the rising and receding limb of the hydrograph and some of the peak flows well, but the majority of the peak flows were under-simulated. Calibrating to a wet period resulted in a good simulation of the observed hydrograph with a slight over-simulation of most of the observed peak flows. When calibrating to flows above the 90th percentile, the low flows are slightly over-simulated, the intermediate flows are well simulated and the peaks are under-simulated.

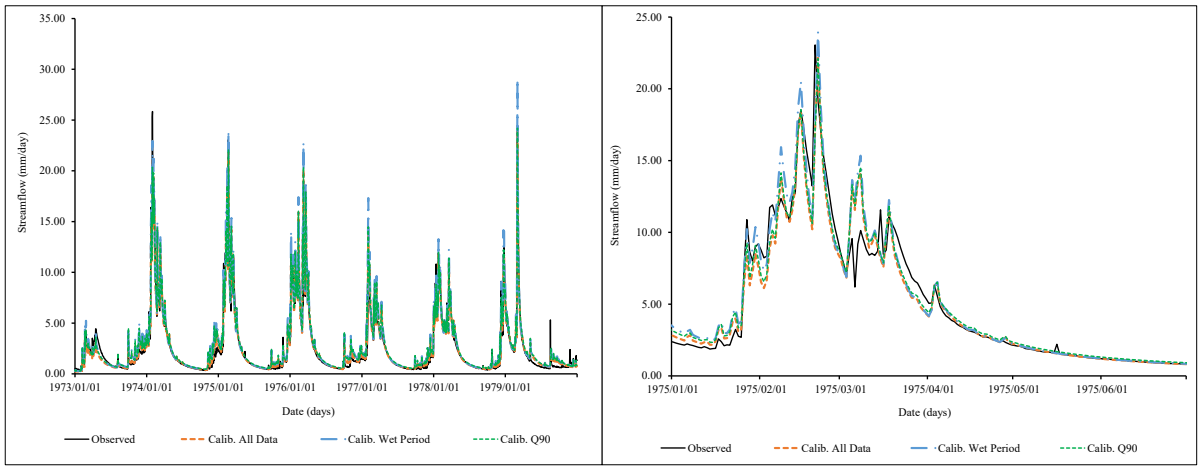

Figure 5.1: Typical hydrographs from the Cathedral Peak IV catchment (V1H005) showing the observed and simulated hydrographs for all the calibration scenarios using the GR4J daily timestep model

The correlation and frequency distribution curves at the daily timestep at the Cathedral Peak IV catchment are shown in figures 5.2 and 5.3, respectively.

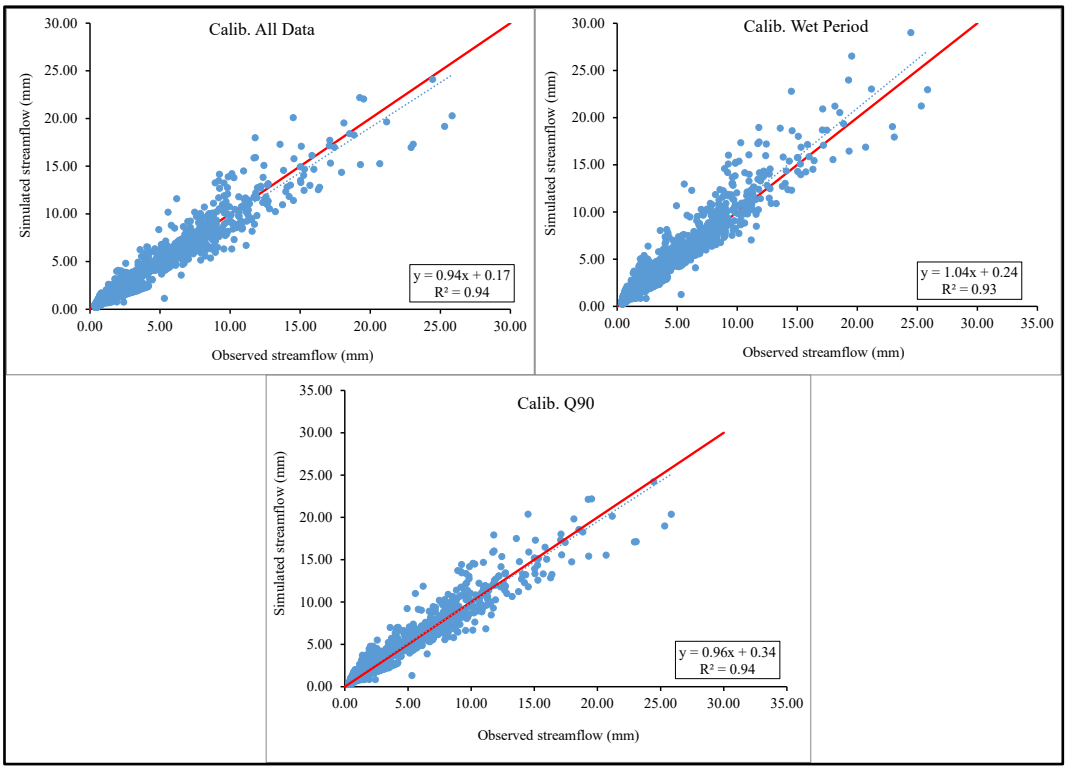

Figure 5.2: Comparison of the observed and simulated flow volumes at the Cathedral Peak IV catchment (V1H005) at a daily timestep

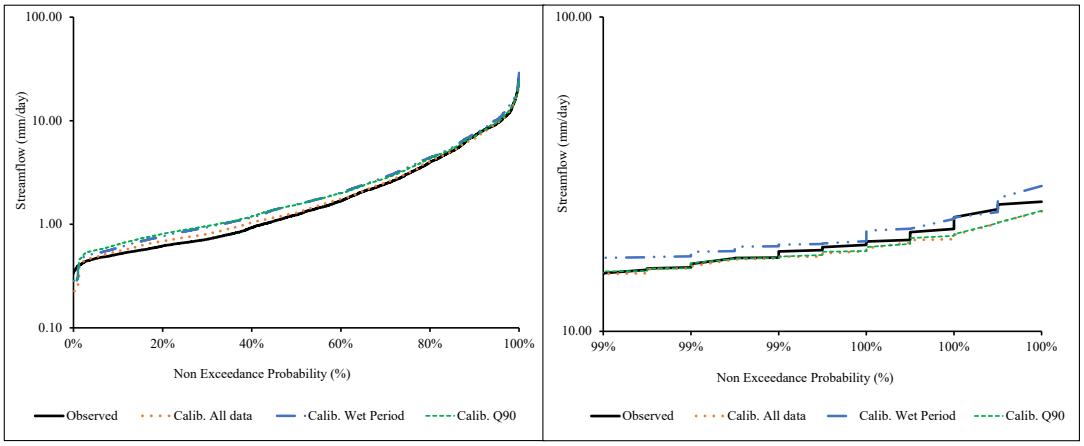

Figure 5.3: Frequency distribution of observed and simulated daily streamflow volumes at the Cathedral Peak IV catchment (V1H005)

A good representation of the observed flows was obtained with R^2 values over 0.9, and regression slopes between 0.9 and 1.05 across all calibration scenarios. The frequency distribution curves show slight deterioration of the overall flows, i.e. a slight over-simulation of the low to intermediate flows for calibration to a wet period and calibration to flows above the 90th percentile. For calibration to a wet period, however, the highest flows, i.e. peaks above the 99th percentile, are slightly better simulated with some slight over-simulation.

Figure 5.4 shows the design ADD, i.e. daily runoff volumes, for the simulated and observed data, as well as the observed ADPD at the Cathedral Peak IV catchment. The ADD values for the simulated and observed volumes at the Cathedral Peak IV catchment were very similar. A very slight over-estimation of the design values at the five-year return period was observed. Calibrating to a wet period generally resulted in the best simulation of ADD. As expected, given the daily temporal resolution used in the simulations, ADPD was significantly under-simulated across all scenarios.

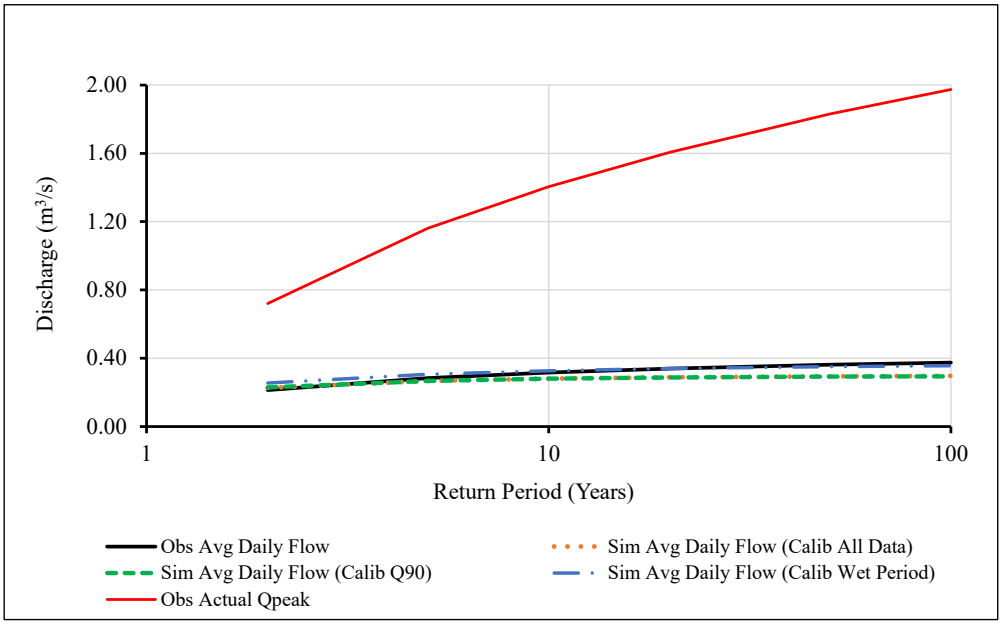

Figure 5.4: The GEV design peak discharges for the simulated scenarios and observed at the Cathedral Peak IV catchment (V1H005) at a daily timestep

5.3.2 Performance of the GR4H hourly model at the Cathedral Peak catchment

At Cathedral Peak IV, as shown in Figure 5.5, the timing of the rise and descent of the observed hydrograph is reasonably well simulated in general. However, the magnitudes are poorly simulated. This could be due to the poor quality of the observed hourly rainfall data where there is inconsistent phasing compared to the observed streamflow data, as well as missing and erroneous rainfall data that is not flagged and is not easily identified. Calibration to all data and to the wet period simulated the timing of the rising and receding limb of the hydrograph well, but under-simulated the observed peaks. Calibration to flows above the 90th percentile simulated the timing of the events well. However, in an attempt to simulate the larger events better, the hydrograph was shifted up, resulting in an over-simulation of low flows. Despite, the notable shift of the hydrograph, the peak flows were still significantly under-simulated. Calibration to a single event simulated the timing of the events poorly and still under-simulated the peak discharges in general, with the exception of the large event on the 3 March 1979, i.e. to which the model was calibrated.

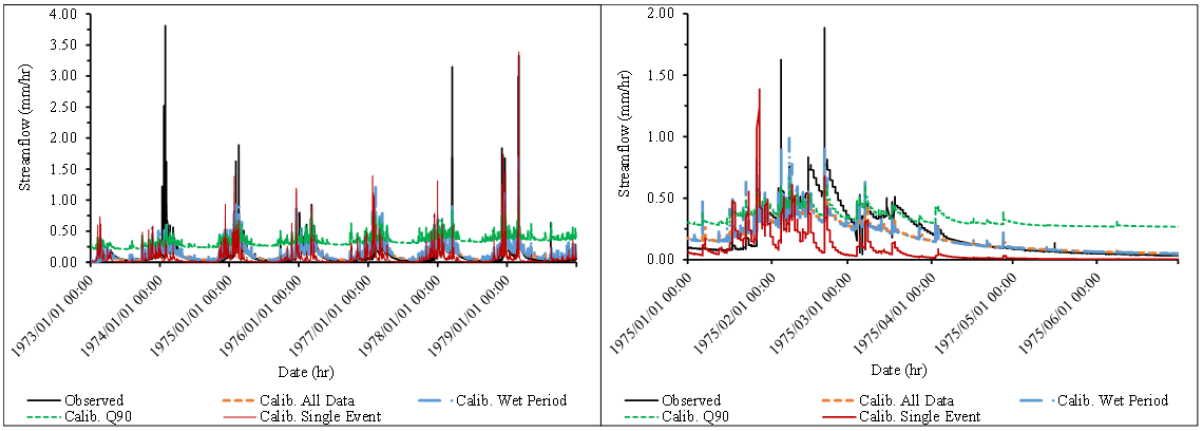

Figure 5.5: Typical hydrographs from the Cathedral Peak IV catchment (V1H005) showing the observed and simulated hydrographs for all the calibration scenarios using the GR4H model

Figures 5.6 and 5.7 further illustrate the under-simulation of the peak flows at the Cathedral Peak IV catchment. The shift of the hydrograph when calibrating to flows above the 90th percentile is clearly seen in Figure 5.7. The good simulation of the timing of events when calibrating to all data and the wet period is shown in Figure 5.6 where the regression line aligns with the 1:1 line.

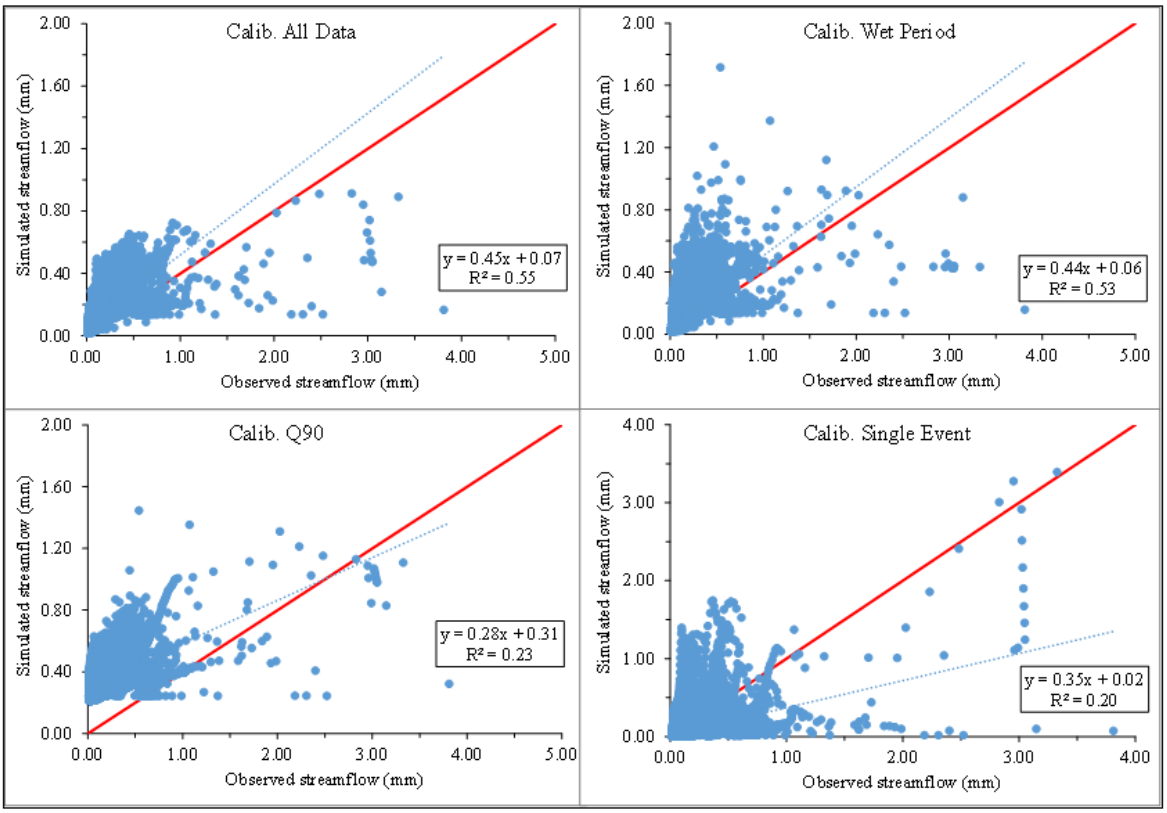

Figure 5.6: Comparison of the observed and simulated flow volumes at the Cathedral Peak catchment (V1H005) at an hourly timestep

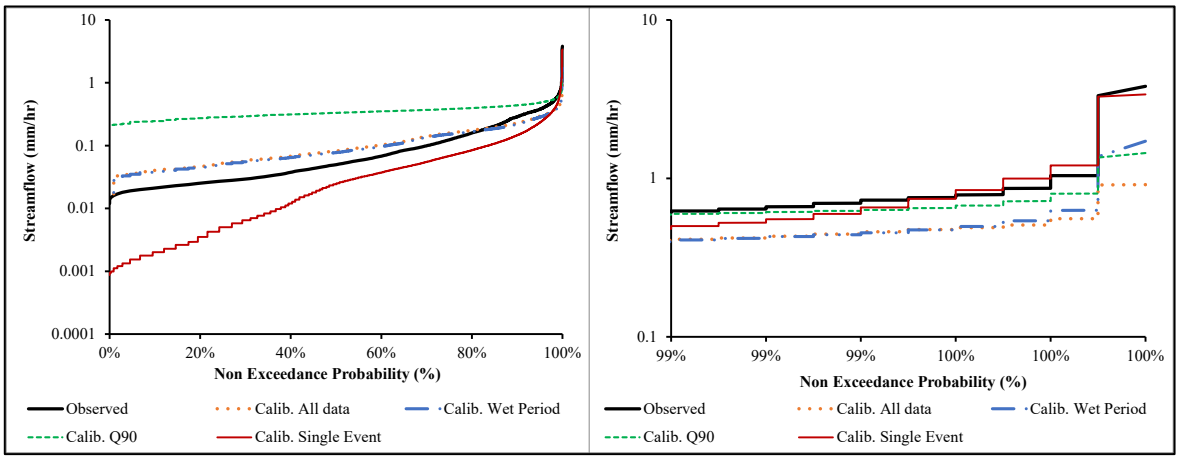

Figure 5.7: Frequency distribution of observed and simulated hourly streamflow volumes at the Cathedral Peak IV (V1H005) catchment

At Cathedral Peak IV (Figure 5.8), unlike the daily timestep, there is no consistent trend between all the scenarios for the hourly results. The design values for the observed hourly and actual peak discharges are under-simulated in general, and to a greater extent for calibration to all data and calibration to flows above the 90th percentile. Calibrating to a single large event and to a wet period results in over-simulation of the observed hourly design values from approximately the 50-year return period. However, the actual observed peak discharges are still under-simulated.

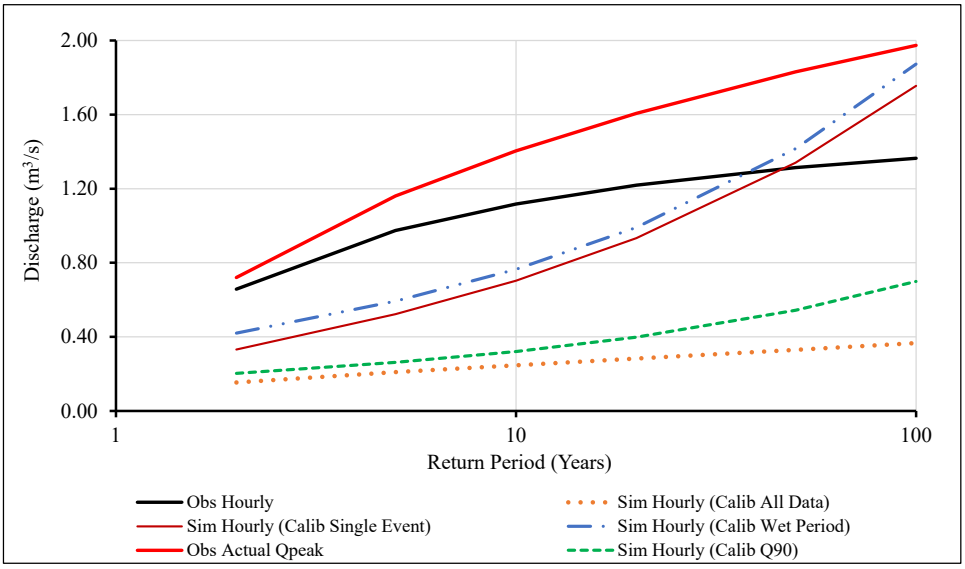

Figure 5.8: GEV design peak discharges for the simulated scenarios and observed at the Cathedral Peak IV catchment (V1H005) at an hourly timestep

5.3.3 Summary and comparison of GR4J, GR4H and ACRU model performance

Table 5.1 contains a summary of the NSE values of flow volumes obtained for the two test catchments for the GR4J, GR4H and ACRU models. In terms of the GR4J (daily) model, the NSE values for both catchments across all three calibration scenarios were reasonably good. However, there was a substantial reduction in the NSE values when calibrating to flows above the 90th percentile threshold, particularly for the Beestekraalspruit catchment (X2H026). This resulted in particularly poor NSE results during validation for the Beestekraalspruit catchment (X2H026). There were only slight differences in NSE values in terms of verification when calibrating to all the data compared to calibrating to a wet period, suggesting that the daily timestep model will give similar results when using either of these two calibration options. The calibration and verification results were, however, noticeably reduced when calibrating to flows above the 90th percentile threshold, particularly for the Beestekraalspruit catchment (X2H026), suggesting that the model is sensitive to this calibration option. It is therefore likely not the most suitable calibration option to use.

The NSE results from the GR4H (hourly) model generally remained the same or declined when compared to the daily results (GR4J model). However, the results from the GR4H model are generally still acceptable, with the exception of those obtained when calibrating to flows above the 90th percentile and calibration to a single event. Calibrating to flows above the 90th percentile threshold performed particularly poorly for the two catchments in terms of the overall flow behaviour. The poor results in calibrating to flows above the 90th percentile threshold could be because the model is now only calibrating to these higher flows and is therefore not accounting for or influenced by the low flows. It therefore simulates the low flows poorly. Moreover, poor-quality observed hourly rainfall data and the phasing of the rainfall data compared to the streamflow data may have more of an influence for these calibration scenarios, where it is likely that errors in short-duration rainfall data predominantly occur during large rainfall events. Calibration to a single event also produced poor verification results because only the response from a single peaked event is used to calibrate the model and the wide range of responses is not captured. Although these calibration scenarios reduce the overall model performance, they are more effective in improving the simulation of peak flows. The results suggest that the hourly timestep model (GR4H) is more sensitive to the calibration option selected compared to the daily model (GR4J). The model may need to be calibrated differently at an hourly timestep to obtain either accurate overall flow behaviour or accurate peak flows. Alternatively, a multi-criteria objective function may be required to simultaneously achieve both accurate general flow behaviour and accurate peaks.

The NSE values obtained from the ACRU model have been included in Table 5.1 for comparison. Since the ACRU model is a daily timestep model, the ACRU results are only comparable to those obtained from the GR4J model. The results indicate that the GR4J model provides superior results in terms of simulating daily streamflow volumes with NSE values higher than those obtained for the ACRU model, particularly for the Beestekraalspruit catchment (X2H026). This is expected since the GR4 models are calibrated using observed rainfall and runoff data, whereas the ACRU model is not calibrated, but rather parameterised based on physical catchment characteristics, and the simulated results are verified against observed data. However, the ACRU model converts the simulated streamflow volumes into peak discharges applying the SCS peak discharge equation, whereas the GR4J model does not convert volumes to peak discharges. Consequently only the ADD may be calculated. As stated previously, this may be a poor approximation of the ADPD, particularly for small catchments where the hydrograph rises and falls within a few hours.

Table 5.1: NSE values for steamflow volumes simulated by the GR4J, GR4H and ACRU models

NSE									
Catchments	**Calibration**				**Verification**				**ACRU**
	Calib All Data	**Calib Wet Period**	**Calib Q90**	**Calib Single Event**	**Calib All Data**	**Calib Wet Period**	**Calib Q90**	**Calib Single Event**	
	GR4J (daily)								
Cathedral Peak IV (V1H005)	0.94	0.91	0.69		0.94	0.91	0.94		0.76
Beestekraalspruit (X2H026)	0.71	0.71	0.36		0.71	0.71	-0.13		0.22
	GR4H (hourly)								
Cathedral Peak IV (V1H005)	0.53	0.79	0.08	0.89	0.53	0.51	-2.55	-0.02	
Beestekraalspruit (X2H026)	0.74	0.75	0.42	0.58	0.74	0.73	0.39	-0.15	

The MRE between observed and simulated design streamflow values for the two test catchments for the GR4J, GR4H and ACRU models are summarised in Table 5.2.

In terms of the GR4J model, the ADD is generally slightly under-simulated for both catchments, with similar results for all three calibration scenarios. In terms of ADPD, the MRE is significantly higher, as expected. The MRE for the ACRU model in terms of ADD is generally slightly higher than that of the GR4J model and positive, indicating a slight over-simulation.

In terms of the GR4H model the HPD and ADPD are under-simulated in both catchments and across all calibration scenarios. In addition, there is generally no significant improvement on the simulation of ADPD from the daily timestep model (GR4J). Calibrating to all data and the wet period simulated the observed flood frequency curve trends well. When calibrating to flows above the 90th percentile and a single event, an inconsistent trend of over-simulation and under-simulation was observed. The differences in the results obtained from the different calibration options further confirm that a multi-criteria objective function may be required to simultaneously achieve both the accurate simulation of general flow behaviour and accurate peaks. The ACRU model over-simulated ADPD in comparison to both the GR4J and GR4H models, which are linked to the SCS peak discharge equation and the lag time and distribution of daily rainfall used. Improving the distribution of daily rainfall is being investigated in this study, as documented in Chapter 4, with the aim of improving these estimates.

In summary, the GR4J and ACRU models performed well in terms of simulating daily design streamflow volumes, i.e. ADD. The GR4H model did not provide superior estimates of ADPD compared to the GR4J model, which was unexpected.

Table 5.2: MRE values obtained from the GR4J, GR4H and ACRU models

MRE									
Catchments	**Calib All Data**		**Calib Wet Period**		**Calib Q90**		**Calib Single Event**		**MRE ACRU ADD**
	MRE ADD	**MRE ADPD**	**MRE ADD**	**MRE ADPD**	**MRE ADD**	**MRE ADPD**	**MRE ADD**	**MRE ADPD**	
	GR4J (daily)								
Cathedral Peak IV (V1H005)	-0.12	-0.79	-0.11	-0.79	-0.08	-0.78			0.09
Beestekraalspruit (X2H026)	-0.18	-0.80	-0.32	-0.84	-0.17	-0.79			0.61
Catchments	Calib All Data		Calib Wet Period		Calib Q90		Calib Single Event		MRE *ACRU* ADPD
	MRE HPD	MRE ADPD	MRE HPD	MRE ADPD	MRE HPD	MRE ADPD	MRE HPD	MRE ADPD	
	GR4H (hourly)								
Cathedral Peak IV (V1H005)	-0.76	-0.81	-0.13	-0.34	-0.65	-0.73	-0.21	-0.40	2.26
Beestekraalspruit (X2H026)	-0.62	-0.76	-0.71	-0.82	-0.60	-0.75	0.26	-0.20	1.97

5.4 DISCUSSION AND CONCLUSIONS

The initial results obtained for the two test catchments selected indicate the potential of the GR4J model to provide accurate daily and design streamflow volumes, which were identified to be superior to those obtained from the ACRU model. The GR4J model, however, needs to be calibrated against observed data. Therefore, for the GR4J model to be applicable nationally, and particularly for ungauged catchments, a methodology would be required that could transfer parameters to ungauged locations or regionalise parameters. This is a significant task that is beyond the scope of this study. In addition, the GR4J model does not have the capabilities to estimate peak discharge for the day from simulated streamflow volumes. Consequently, the performance of the GR4H model was assessed, which was hypothesised to better approximate the ADPD. This was not the case, however, and the results from the GR4H model were generally not any better than the ADD values obtained from the GR4J model. Based on these results, and due to the challenges associated with obtaining or synthetically generating short-duration rainfall data, further experimentation with the GR4H model is not recommended.

In summary, the potential of the GR4J model for application in South Africa has been indicated. However, significant work is required to develop the model into a DFE tool that is applicable at a national scale.

CHAPTER 6: DEVELOPMENT AND ASSESSMENT OF AN ENSEMBLE JOINT PROBABILITY APPROACH USING THE SCS-SA MODEL

NS Dlamini and JC Smithers

This chapter provides a summary of the progress made to date regarding the fifth objective listed in Chapter 1: Investigate the potential to incorporate a joint probability approach into the updated version of the SCS-SA model.

6.1 INTRODUCTION

Global climate change has resulted in an increase in the severity and frequency of flooding (Charalambous et al., 2013). According to Zaman et al. (2012), reliable flood estimates can provide a foundation for dealing with floods, which will be most needed under future extreme weather regimes. According to Smithers and Schulze (2003), design flood estimation methods in South Africa are based on the statistical analysis of historical streamflow data and rainfall-based methods. According to Schulze (1989), Rahman et al. (1998) and Rauf and Rahman (2004), rainfall-based methods have the advantage of generally having longer rainfall records at more sites, with better quality, and being more available for analysis compared to streamflow records. Smithers (2012) noted that design engineers and hydrologists are most frequently faced with situations where there is no, or inadequate, streamflow data at the site of interest.

Rahman et al. (2002) pointed out that, when applying rainfall-based methods and selecting the representative input variables that are likely to produce a significant flood, there are no guidelines to guide the procedure. Thus, the random choice of fixed values for flood-producing variables, which have a probability distribution, can lead to uncertainty, inconsistencies and significant bias in design flood estimates for a given return period, and has been widely criticised (Kuczera et al., 2006; Gioia et al., 2008; Kjeldsen et al., 2010). According to Charalambous et al. (2013), the thorough treatment of the probabilistic aspects of the key input variables should be adopted to significantly improve the limitations associated with rainfall-based methods. This can be achieved by adopting a joint probability approach with a deterministic model to obtain probability distributed flood hydrographs (Rahman et al., 2002).

While a number of rainfall event-based methods of design flood estimation are used in South Africa (SANRAL, 2013), this study has selected the use of the SCS-SA model (Schulze et al., 2004). The SCS-SA model was selected for use in this study as the model is readily available, there is readily available data for the key input variables and sufficient operational support is available.

Hence, the aim of this study is to develop, apply and assess the performance of an Ensemble JPA using the SCS-SA model for design flood estimation in South Africa. Specific objectives include the selection of test catchments, the development of probability distributions for key input variables using readily available data, and the development and application of an Ensemble model configuration, details of which are summarised in the following sub-sections.

6.2 OVERVIEW OF SCS-SA MODEL

Schmidt et al. (1987) adapted the SCS method for design flood estimation in South Africa based on developments and verifications from multiple studies (Schulze, 1979; 1982; Schmidt and Schulze, 1984; Dunsmore et al., 1986). These were computerised by Schulze et al. (1992).

SANRAL (2013) recommends the SCS-SA method for application in agricultural catchments with areas less than 30 km^2. According to Smithers (2012), the SCS-SA method is now extensively applied to estimate design floods for small urban and rural catchments of less than 30 km^2 in South Africa. The advantage of using the method is that it can generate full hydrographs and not only peak discharges (SANRAL, 2013). Equations 6.1 and 6.2 indicate how the stormflow and peak discharge are estimated, respectively (Schulze et al., 2004):

$$Q = \frac{(P - I_a)^2}{P + I_a + S} \quad 6.1$$

where: Q = stormflow depth (mm)
P = daily rainfall depth (mm)
I_a = initial losses (mm)
S = potential maximum soil water retention (mm)

$$\Delta Q_p = \frac{0.2083 \times A \times \Delta Q}{\frac{\Delta D}{2} + L} \quad 6.2$$

where: ΔQp = peak discharge of incremental unit hydrograph (m^3.s^{-1})
A = catchment area (km^2)
ΔQ = incremental stormflow depth (mm)
ΔD = unit duration of time (h)
L = catchment lag (h)

A number of options to estimate catchment lag are available in the SCS-SA model. The widely used Schmidt-Schulze equation (Schmidt and Schulze, 1984) is shown in Equation 6.3:

$$L = \frac{A^{0.35} \times MAP^{1.1}}{41.67 \times y^{0.3} \times I_{30}^{0.87}} \quad 6.3$$

where: L = catchment lag (h)
A = catchment area (km^2)
MAP = mean annual precipitation (mm)
y = average catchment slope (%)
I_{30} = two-year return period 30-minute rainfall intensity (mm/h)

The potential maximum soil water retention is estimated using the curve number, which is an expression of the hydrological soil properties, land cover and land-management conditions, as well as the soil moisture status of the catchment prior to a rainfall event. The potential maximum soil water retention is expressed by Equation 6.4:

$$S = \frac{25400}{CN} - 254 \quad 6.4$$

6.3 GENERAL METHODOLOGY

The catchments used in the study are shown in Figure 6.1. Most of the catchments were selected in regions used by Gericke and Du Plessis (2012). These include the northern interior, summer coastal region, central interior and the winter coastal region. The rest of the catchments were selected from the study done by Rowe (2019).

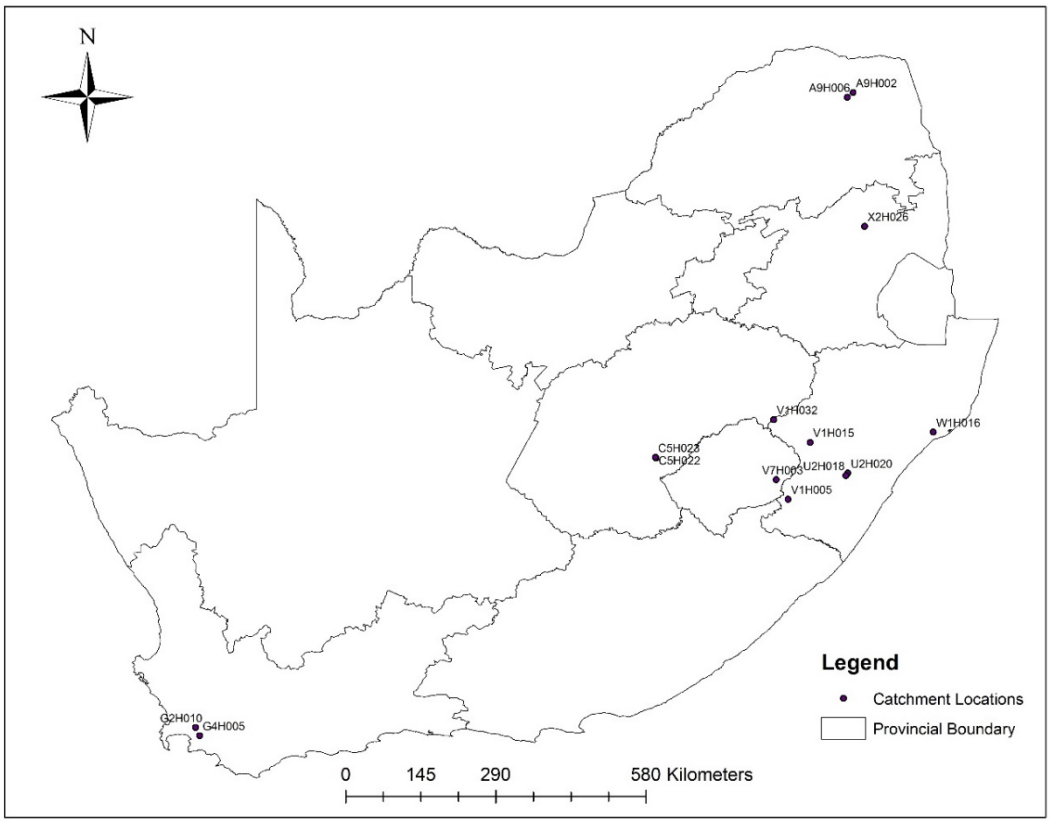

Figure 6.1: Location of catchments used in the study

6.3.1 Catchment data and information

Catchment information such as the catchment slope and altitude were obtained using ArcGIS software, and a 30 m-resolution digital elevation model (Van der Spuy and Raddemeyer, 2014) for South Africa. The NLC 2000 dataset for South Africa, provided by the Agricultural Research Council (ARC) and the CSIR (2005), was used to estimate the SCS-SA land-cover class for each of the test catchments. The mean annual precipitation for the test catchments was obtained using information provided by Smithers and Schulze (2003) for the centroid of the catchments. The SCS-SA soil group for each catchment was obtained from the national SCS-SA soil group map developed by Schulze (2012). Additional catchment soil information required by the model, such as soil depth and soil texture, were obtained from the South African Atlas of Climatology and Agrohydrology, published by Schulze (2007). The observed streamflow data used for comparison was obtained from a historical research catchment database, available from the CWRR and the Department of Water and Sanitation.

Table 6.1 contains a summary of the catchment information and data availability. The catchment area ranges in size from 0.26 km^2 to 185 km^2. Although it is recommended that the model is applicable to catchment areas up to 30 km^2, catchments with an area larger than the prescribed range were selected due to insufficient smaller catchments with reasonable observed data record lengths. Historical streamflow data was obtained from multiple sources, as summarised in Table 6.1. The observed record lengths ranged from 11 to 70 years.

Table 6.1: Summary of catchment information and observed data

Catchment	Catchment area (km^2)	Record length (years)	Period of record	Data source*
U2H020 (Cedara)	0.26	17	1978–1994	CWRR
V7H003 (Ntabamhlophe)	0.52	23	1970–1992	CWRR
G2H010 B (Jonkershoek-Lambrechtsbos)	0.73	52	1947–2006	CSIR
V1H005 (Cathedral Peak IV)	0.98	31	1950–1981	CSIR
V1H015 (Ntabamhlophe)	1.04	15	1965–1994	CWRR
U2H018 (Cedara)	1.31	19	1976–1994	CWRR
W1H016 (Zululand)	3.3	11	1976–1986	CWRR
X2H026	13.82	27	1966–1992	DWS
A9H006	16	15	1965–1979	DWS
C5H022	39	28	1980–2008	DWS
V1H032	67.8	20	1974–1993	DWS
A9H002	103	70	1931-2001	DWS
G4H005	146	57	1957–2013	DWS
C5H023	185	26	1984–2009	DWS

CSIR: Council for Scientific and Industrial Research
CWRR: Centre for Water Resources Research
DWS: Department of Water and Sanitation

6.3.2 Distribution fitting and assessment

The SCS-SA model comprises several key input variables that are required to estimate design runoff volumes and peak discharges. These include design rainfall (P), catchment response time, temporal distribution of rainfall and the antecedent soil moisture conditions, which are related to the CN. Each of these input variables has a distribution of potential values. These distributions were estimated as detailed below. Freely available software (EasyFit) was utilised to fit probability distributions to each of the key input variables. Once the distributions were fitted, 10 000 samples were generated for each of the key input variables, from which inputs were randomly sampled to generate the simulated ensemble peak discharges.

6.3.2.1 Time to peak

Gericke (2016) extracted event time to peak information from primary flow data for a number of sites in three regions of South Africa. In this study, event time to peak information was extracted for eight additional sites. Information from these studies was used to develop the probability distribution for the time to peak at each site.

Figure 6.2 is an example of the three-parameter Log-Normal probability distribution fitted to the observed time to peak data from Catchment X2H026. The histogram in blue represents the frequency of the time to peak for given intervals of duration. The orange line represents the probability density function fitted to the frequencies. The three-parameter Log-Normal probability distribution fitted the observed time to peak relatively well for Catchment X2H026.

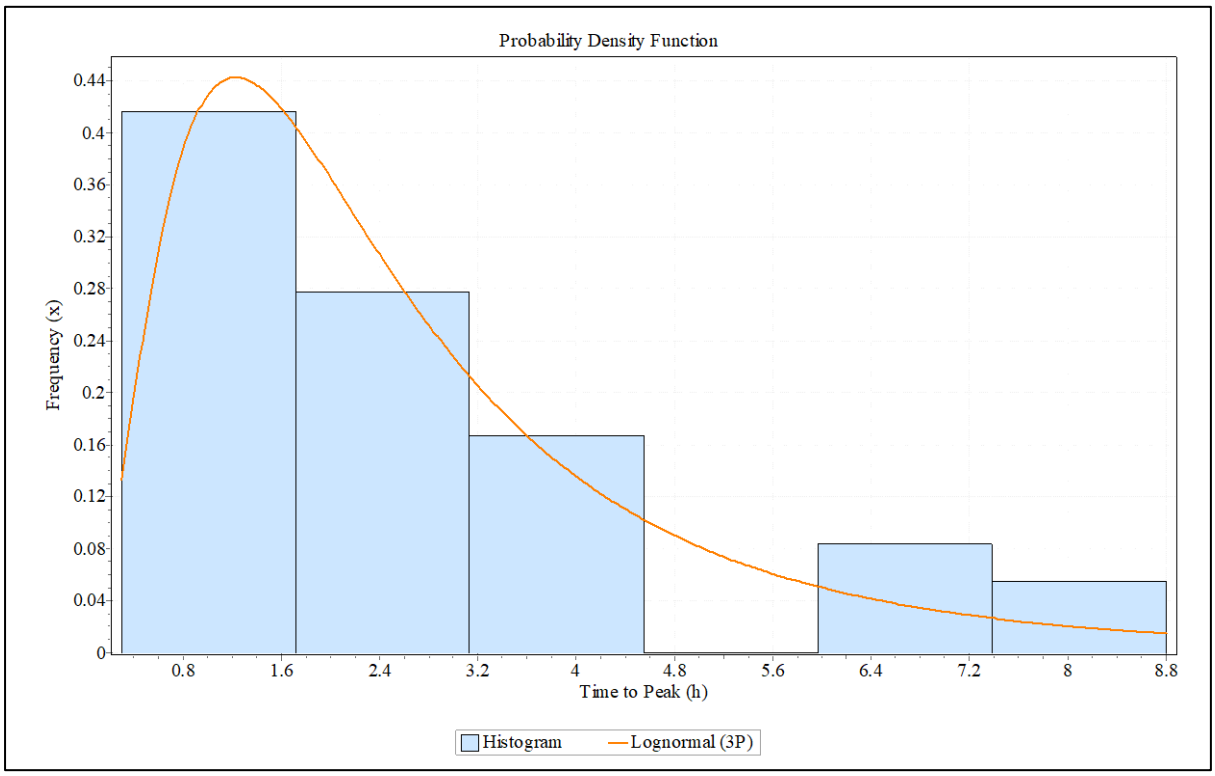

Figure 6.2: Probability distribution of time to peak data from Catchment X2H026

6.3.2.2 Antecedent soil moisture

The available data for the change in the soil moisture condition (ΔS) prior to large storm events was limited to the 20th, 50th and 80th percentile values reported by Schmidt and Schulze (1987). These values were then extrapolated to the 10th and 90th percentile values, as indicated in Figure 6.3. This was done to increase the data available for distribution fitting. A regression was then fitted to the values, and the resulting equation was used to extrapolate the data to the 10th and 90th percentile values, respectively. A probability distribution was then fitted to the five values of ΔS. Figure 6.4 illustrates a uniform probability distribution fitted to the observed data of the change in soil moisture (ΔS). The distribution indicates that samples will be selected uniformly across the range of the distribution of the change in soil moisture. This distribution is a result of the limitation in the available data.

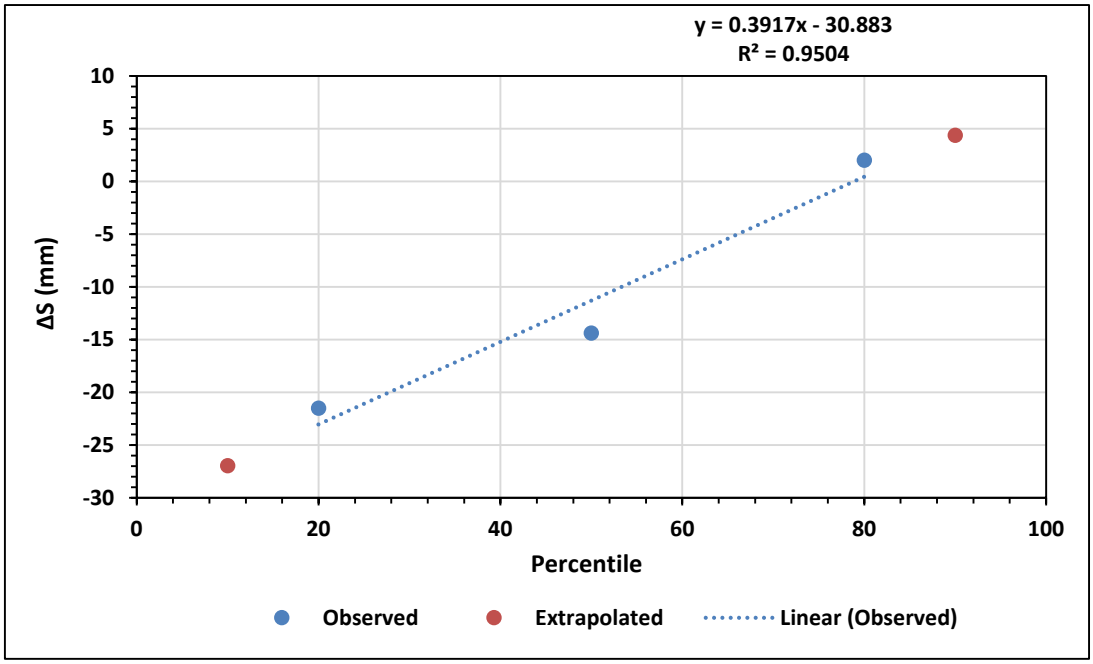

Figure 6.3: Regression analysis for ΔS data for Catchment X2H026

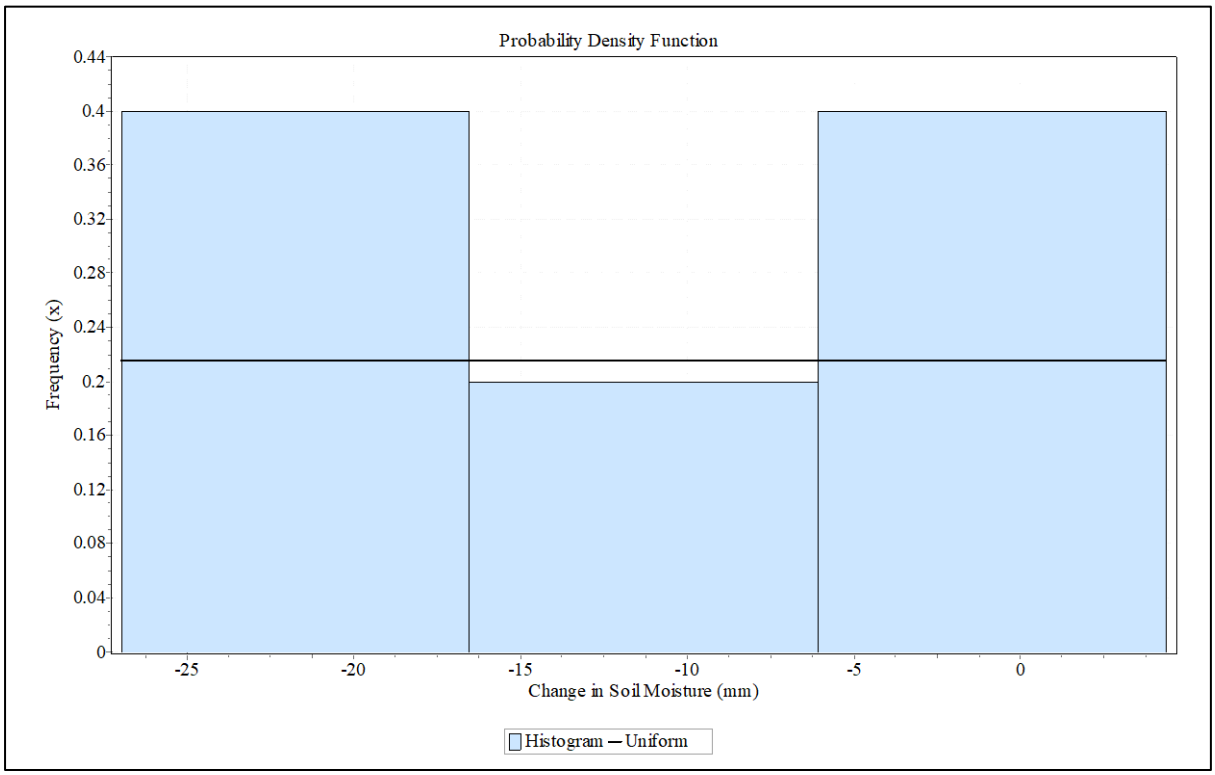

Figure 6.4: Probability distribution of change in soil moisture data for Catchment X2H026

6.3.2.3 Temporal distribution

The data for the temporal distribution was readily available and obtained from Knoesen and Smithers (2008). The temporal distributions were then incorporated into the Ensemble SCS-SA model. Figure 6.5 illustrates a sample of the 480 different temporal distributions that were incorporated into the Ensemble SCS-SA model.

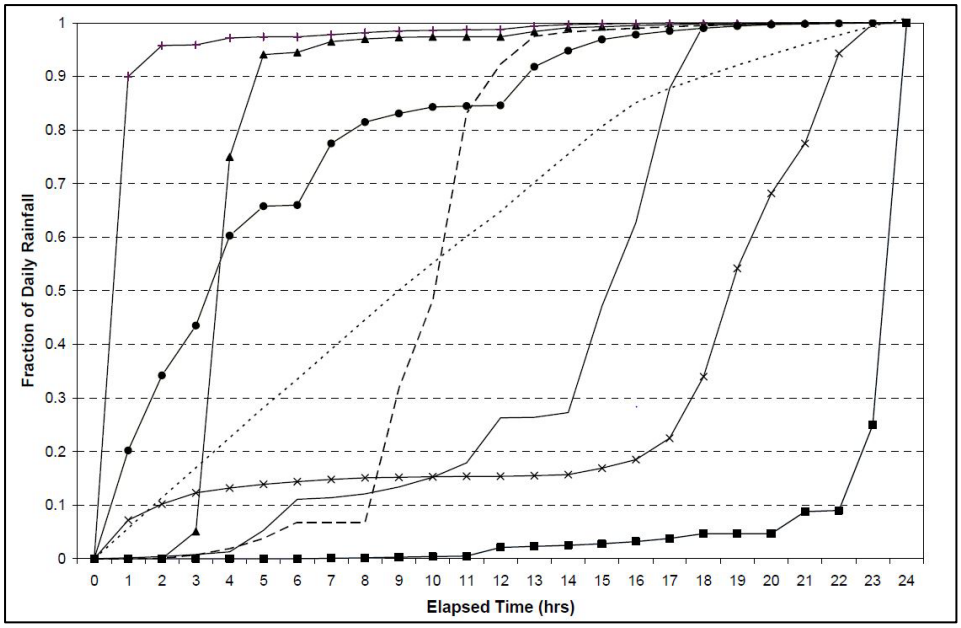

Figure 6.5: Samples of the 480 different temporal distributions (Knoesen, 2005)

6.2.3.4 One-day design rainfall

The rainfall distribution was determined by interpolating the 30th and 70th percentiles from the 10th, 50th and 90th one-day design rainfall percentiles (Smithers and Schulze, 2003). This process is illustrated in Figure 6.6, where a trend line and the resulting equations were used to determine the 30th and 70th percentiles for three return periods shown as an example. The estimation of the 30th and 70th percentiles was done to have sufficient data points to fit a probability distribution for each return period to sample from the fitted distribution.

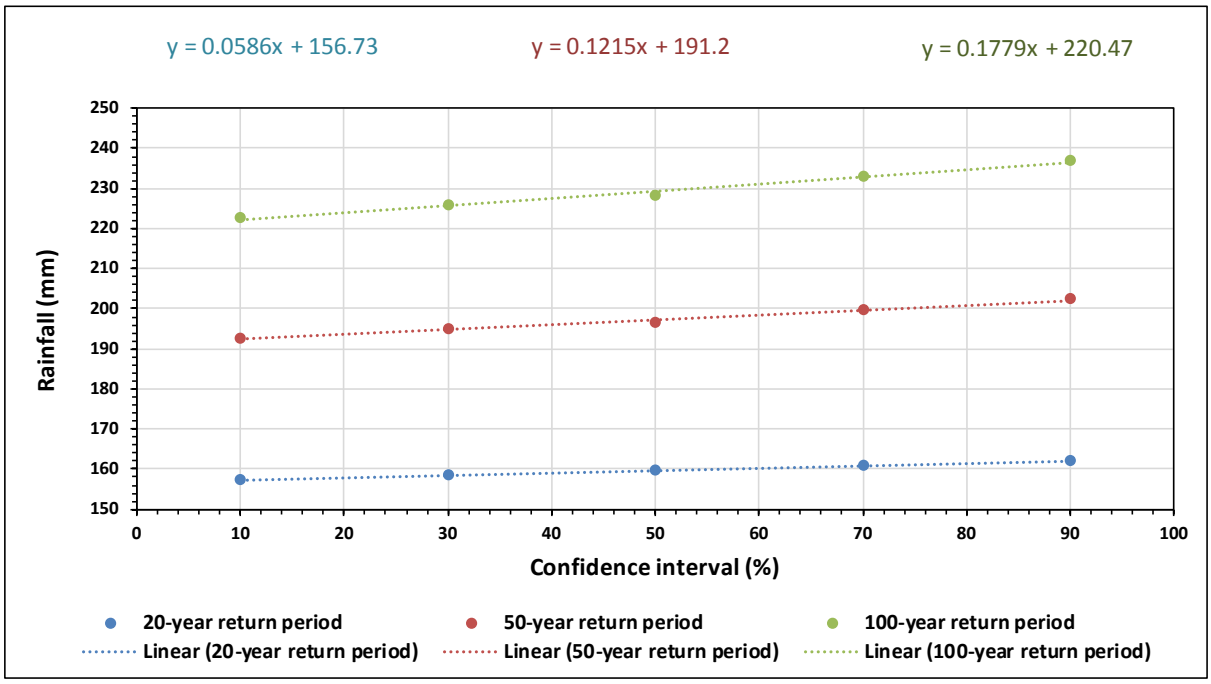

Figure 6.6: One-day design rainfall confidence intervals for different return periods for Catchment X2H026

Figure 6.7 illustrates derived depth duration frequency curves used when the duration of the input design rainfall was conditioned to the catchment response time.

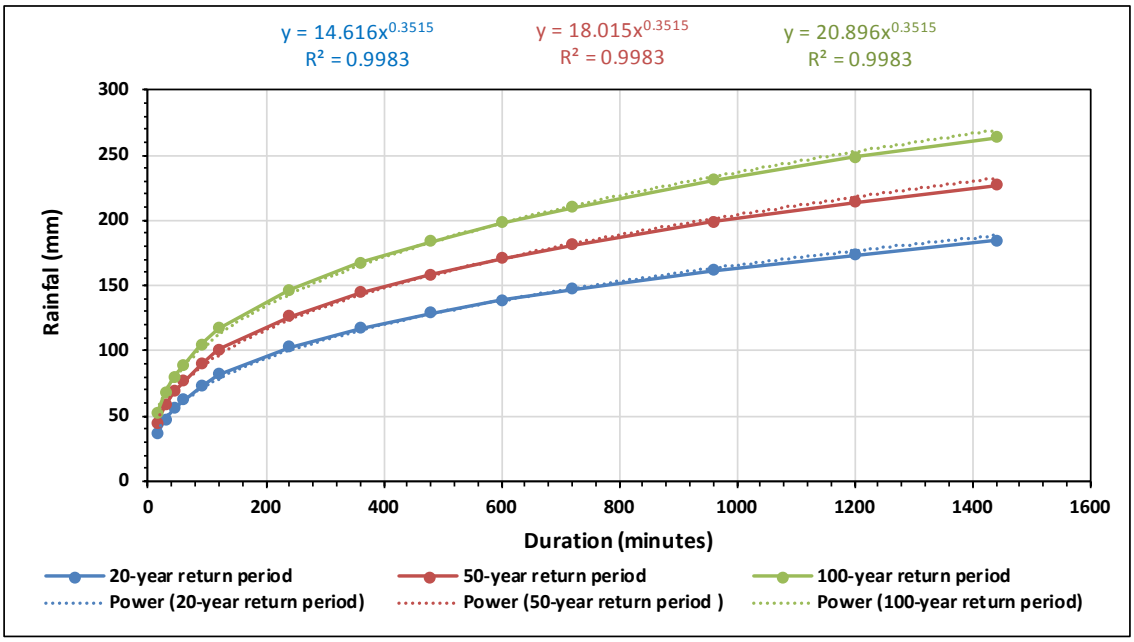

Figure 6.7: Derived rainfall depth duration frequency curves for Catchment X2H026

6.3.3 Ensemble SCS-SA model setup

Once the distributions for design rainfall, catchment response times, antecedent moisture conditions and disaggregation of daily rainfall were determined, the Ensemble SCS-SA JPA model was set up as follows. The simulation of runoff volume and peak discharge were simulated in an Excel spreadsheet. Two sheets in the spreadsheet were reserved to be used to input the relative sampled distributions and store the results of the ensemble events. Since SCS-SA is an event-based model, it had to be refined to enable it to run an ensemble of events. This was achieved by using the Visual Basic for Application (VBA) code to the model structure to include a loop function. The loop function transfers the sampled ensemble inputs into the model individually, then transfers the simulated ensemble results to the storage sheet. Once the model has completed simulating the events, VBA code was developed to sort, organise and perform statistical analyses on the ensembles. The Ensemble SCS-SA still applies the SCS-SA stormflow equation to estimate the runoff volume from an event, and the peak discharge equation to estimate the peak discharge. Once the distributions had been fitted, 10 000 samples were generated for each of the key input variables, from which inputs were randomly sampled to generate the simulated ensemble peak discharges.

6.3.4 Model evaluation criteria

To evaluate the performance of the model, the simulated results were compared to the observed design peak discharges. Statistics calculated from the simulated ensembles included the median value and the 10th and 90th percentiles. The MARE was then used to evaluate the model performance. In terms of the simulated ensembles, the median values were used to calculate the MARE. The MARE is a measure of the difference between two continuous variables and is an average of the absolute error. The MARE (percentage) is expressed by Equation 6.5 (Smithers et al., 2015):

$$MARE = \frac{100}{n}\sum_{i=1}^{n}\frac{|Q_i - Q_o|}{Q_o} \qquad 6.5$$

where: Q_i = simulated peak discharge ($m^3.s^{-1}$)
Q_o = observed peak discharge ($m^3.s^{-1}$)
n = number of observations

6.4 RESULTS

The results obtained are summarised in the following sections.

6.4.1 Ensemble and single-event SCS-SA models using one-day duration design rainfall input for Catchment U2H020

The Ensemble SCS-SA (one-day duration) initially included fitting a probability distribution to the one-day design rainfall using the 90% confidence intervals for each return period. The standard SCS-SA (one-day duration) model uses the one-day design rainfall as input. The probability distributions were derived for the other key input variables (antecedent moisture conditions, time to peak and temporal distribution). Random samples were generated from the fitted distributions. As an example, Figure 6.8 shows the simulated and observed design peak discharges for Catchment U2H020. It is evident that both the Ensemble SCS-SA (one-day duration) and standard SCS-SA (one-day duration) models are consistently over-simulating the observed design peak discharge for all return periods at Catchment U2H020. The observed design flood estimates also consistently lie outside the 10th and 90th percentiles, indicating poor confidence in the estimated design peak discharges.

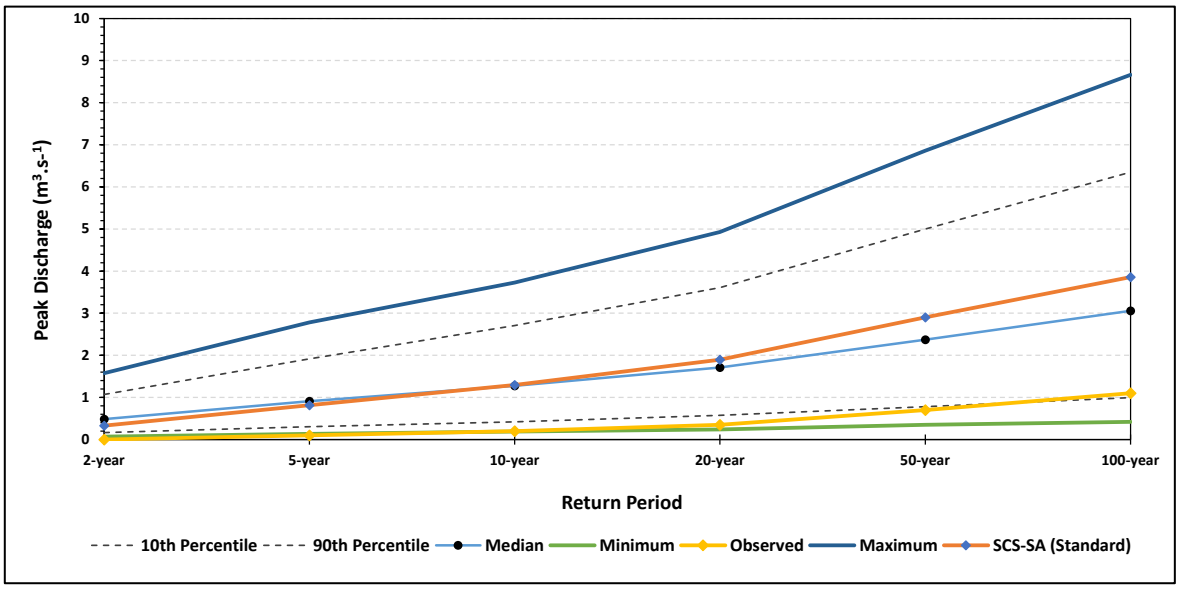

Figure 6.8: Simulated and observed design peak discharges for Catchment U2H020 using the Ensemble and standard SCS-SA (one-day duration)

It is evident that both the standard SCS-SA (one-day duration) and Ensemble SCS-SA (one-day duration) models are performing relatively poorly in terms of simulating the observed design peak discharge using one-day design rainfall. However, the results obtained show that the Ensemble SCS-SA model framework works and provides an estimate of the confidence limits for all return periods. Since the models did not perform well using one-day rainfall, the analyses were repeated using design rainfall depths associated with the catchment response time, i.e. design rainfall with a duration equal to the time to peak, as detailed in the next section.

6.4.2 Ensemble and single-event SCS-SA models using design rainfall duration equal to the catchment response time for Catchment U2H020

Figure 6.9 shows the estimated and observed design peak discharge at Catchment U2H020 when the duration of the design rainfall input to the Ensemble SCS-SA (time to peak) and standard SCS-SA (time to peak) model was conditioned to the catchment response time (time to peak) using a derived relationship between the design rainfall depth and a range of durations.

It is evident from Figure 6.9 that the Ensemble SCS-SA (time to peak) simulates the observed peak discharges relatively well for all the return periods. The standard SCS-SA (time to peak) model also simulates the observed peak discharges for the lower return periods relatively well. In addition, all the observed peak discharge estimates were within the 10th and 90th percentiles, which provides confidence in the simulated peak discharges provided by the Ensemble SCS-SA model. The median design peak discharges from the simulated ensembles are also relatively similar to the observed design peak discharge. Thus, the median peak discharge estimates are the recommended design values to use. The single-event SCS-SA (time to peak) model performed poorly in terms of estimating the observed peak discharge as it consistently under-simulated the peak discharge for all return periods. However, the results improved when selecting design rainfall duration equivalent to the catchment response time.

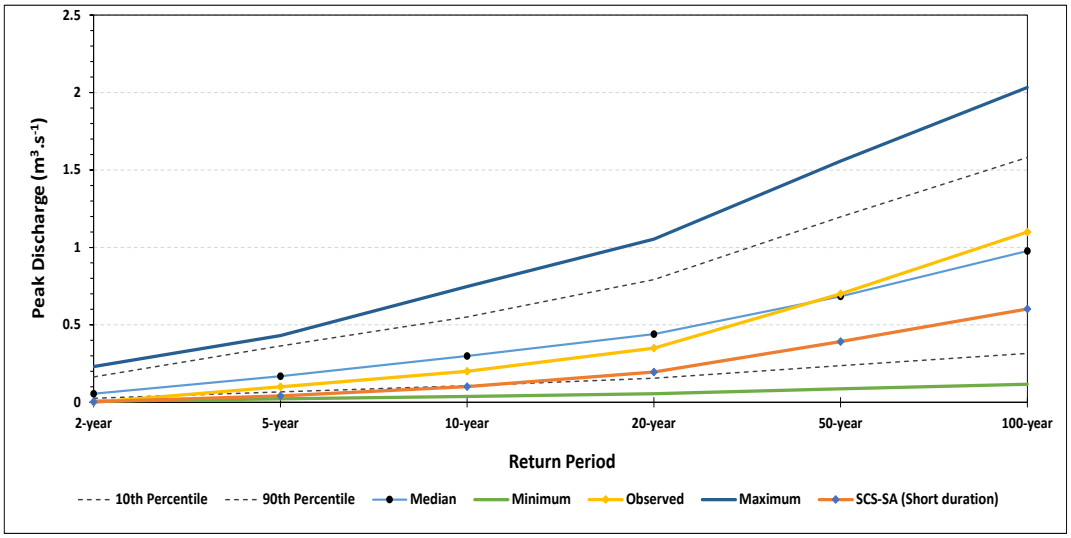

Figure 6.9: Simulated and observed design peak discharges for Catchment U2H020 using Ensemble and standard SCS-SA (time to peak)

6.4.3 Performance of Ensemble and single-event SCS-SA on all selected catchments

As shown in the example in Section 6.4.2, it was found that using a design rainfall duration equal to the catchment time to peak has, for both the Ensemble SCS-SA (time to peak) and standard SCS-SA (time to peak) models, significantly improved the model's performance for the peak discharge estimation. With the improvements and satisfactory model performance, the models were applied to all selected catchments to assess their performance over a wider range of catchments in different climatic regions in South Africa. A total of four model applications were performed on the rest of the catchments. These include the standard SCS-SA (one-day duration), standard SCS-SA (time to peak), Ensemble SCS-SA (one-day duration) and Ensemble SCS-SA (time to peak) models. These model applications are variations between using the design rainfall duration equivalent to one day and the design rainfall duration equivalent to time to peak.

Figure 6.20 illustrates the MARE of the peak discharge for all the catchments in the order of the catchment size (0.26 to 185 km^2). The MARE averaged across all catchments is shown in Figure 6.11. It can be seen that the Ensemble SCS-SA (time to peak) model generally has a lower MARE value than the other model applications, and the MARE values of the Ensemble SCS-SA (time to peak) model are generally less than 50% for the majority of the catchments. The Ensemble SCS-SA (one-day duration) and standard SCS-SA (one-day duration) models produced the highest MARE for the majority of the catchments, indicating a poor performance in the model for design flood estimates when adopting the one-day duration for design rainfall.

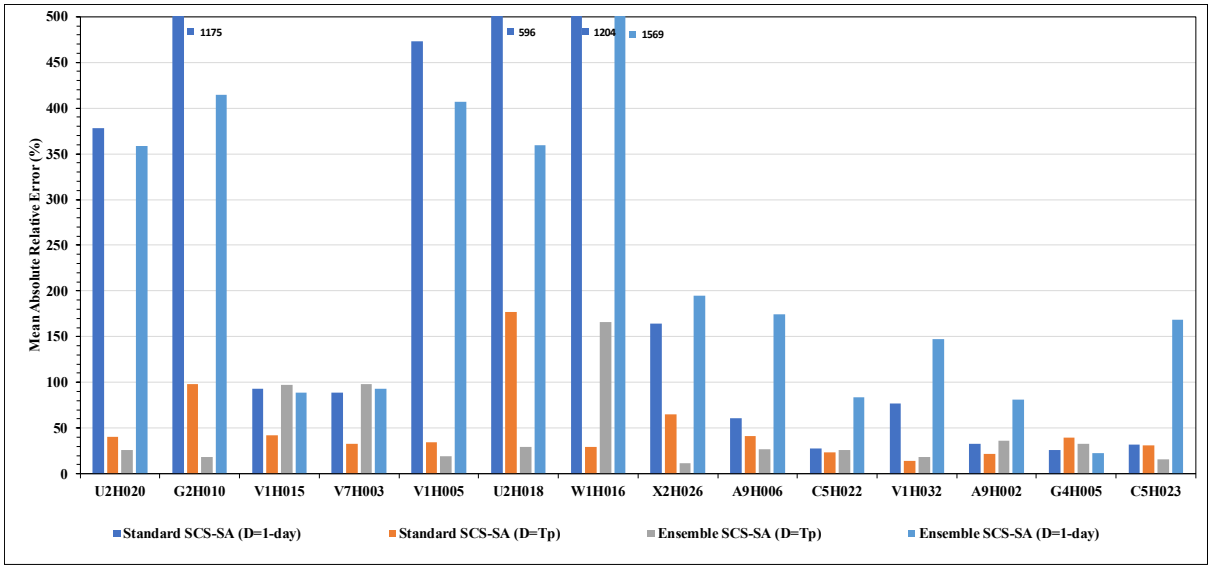

Figure 6.10: Mean absolute relative error of the estimated peak discharge for all the catchments used in the study

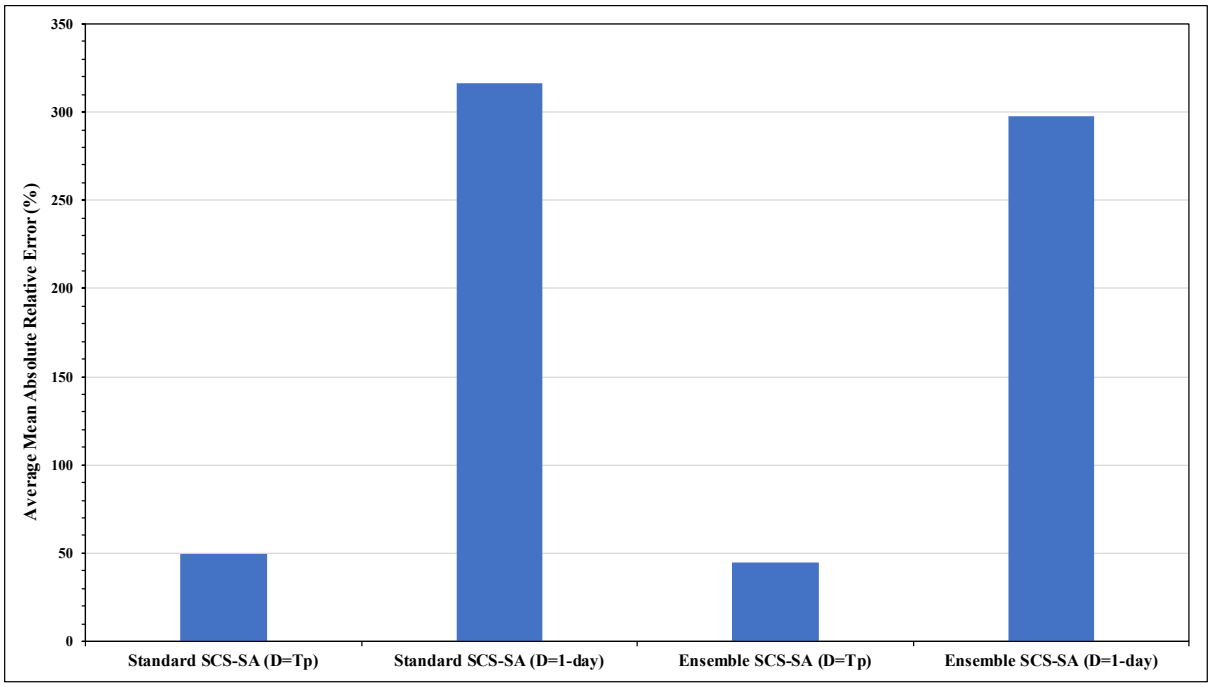

Figure 6.11: Average mean absolute relative error of the peak discharge across all the catchments used in the study

6.4.4 Performance of Ensemble and standard SCS-SA models on larger catchments

The MARE relative to the catchment area was assessed to see if there was any deterioration in the performance of the models with increasing catchment area size. This was done for the same catchments presented above. Figure 6.12 illustrates the relationship between MARE and catchment area, where it is evident that both models seem to be performing relatively well as the catchment area increases and the performance of the models does not deteriorate as the recommended maximum catchment area (30 km^2) for the models is exceeded.

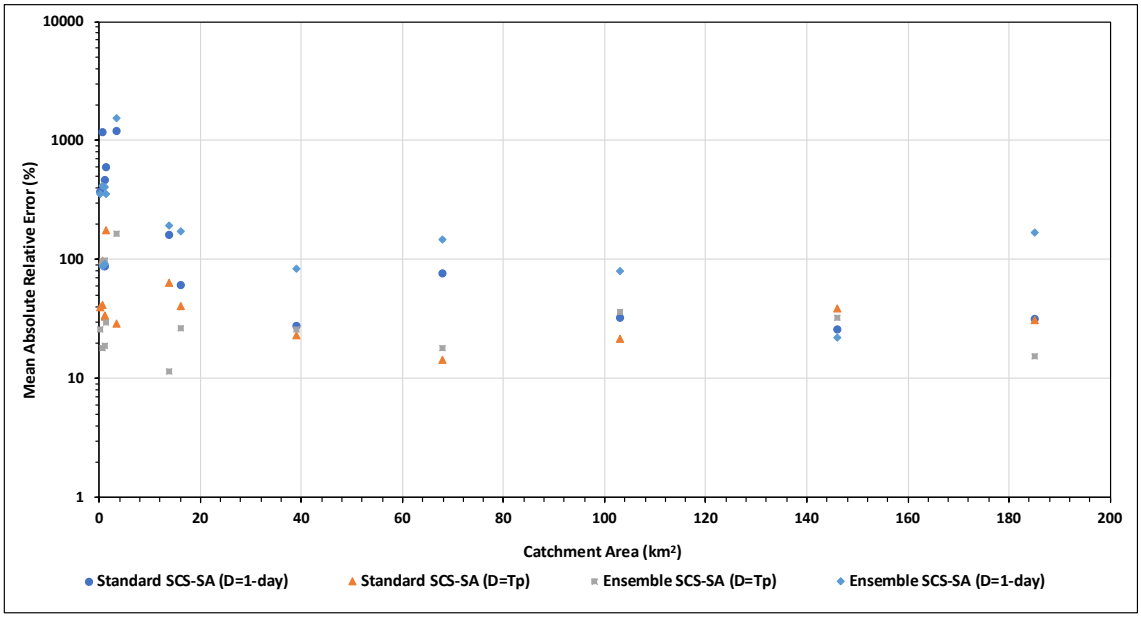

Figure 6.12: MARE of peak discharge estimation versus catchment area

6.5 DISCUSSION AND CONCLUSIONS

The results produced by applying both Ensemble SCS-SA (one-day duration) and standard SCS-SA (one-day duration) models using the one-day duration design rainfall as input, as is the norm when using the SCS-SA model, indicated that the models were performing relatively poorly in terms of estimating both the observed design runoff volume and design peak discharge for all the selected catchments. Even though the probability distributions for the other key input variables are included in the Ensemble SCS-SA model, the Ensemble SCS-SA (one-day duration) model still significantly over-estimated the observed design runoff volume and design peak discharge for all the return periods. The observed design peak discharge estimates consistently fell outside the 10th and 90th percentiles simulated with the Ensemble SCS-SA (one-day duration) model, indicating a very low confidence in the design peak discharges. The standard SCS-SA (one-day duration) model performed similarly to the Ensemble SCS-SA (one-day duration) model, where the model also performed poorly and generally over-estimated both the observed design runoff volume and the design peak discharge.

When short-duration rainfall was adopted, the Ensemble SCS-SA (time to peak) and standard SCS-SA (time to peak) models generally simulated the observed design peak discharges relatively well for all the return periods for all catchments. Although the standard SCS-SA (time to peak) estimates of the observed design peak discharge generally improved compared to the SCS-SA (one-day duration) model, it still performed poorly compared to the Ensemble SCS-SA (time to peak) model estimates. These results are also supported by the MARE values of the estimated design peak discharges from the Ensemble SCS-SA (time to peak) model. It is evident that the Ensemble SCS-SA (time to peak) and standard SCS-SA (time to peak) models generally have MARE values less than 40% and 50%, respectively for the estimated design peak discharges. This indicates that the Ensemble SCS-SA (time to peak) model generally has lower errors in estimating the observed design peak discharges.

When the Ensemble SCS-SA (time to peak) and standard SCS-SA (time to peak) models were tested on larger catchments than the recommended range, the model showed promising results as it estimated the observed design peak discharge reasonably well for all the catchments. The MARE of the simulated design peak discharges did not increase with an increase in catchment area either, indicating that the performance of the Ensemble SCS-SA (time to peak) and standard SCS-SA (time to peak) models do not generally decrease as the catchment area increases.

This study has demonstrated how a JPA can be applied using ensemble event simulation by adapting the single-event SCS-SA model in South Africa. Even though the JPA was generally developed using only readily available data to determine the probability distributions, the use of these distributions in the application of the Ensemble SCS-SA model showed how it can reproduce the observed design flood estimates with reasonable accuracy over a wide range of return periods and for catchments larger than the recommended sizes. The Ensemble SCS-SA model has also shown potential and flexibility to deal with uncertainty by accounting for the distributed nature of the input variables and taking on values across the full range of their distribution in the modelling process, thus avoiding the potential bias that can occur when adopting a single set of predetermined input values.

An unexpected result from this study is the much-improved performance of both the single-event and Ensemble SCS-SA models when the duration of the input design rainfall was changed from one day to the catchment response time. This could have potential consequences for the application of the SCS-SA model in practice. It is recommended to derive more detailed information to fit the probability distributions and to develop the Ensemble JPA for other deterministic event-based models for design flood estimation in South Africa.

CHAPTER 7: DEVELOPMENT AND ASSESSMENT OF THE SCS-SA CSM SYSTEM FOR DESIGN FLOOD ESTIMATION

JC Smithers and NS Dlamini

7.1 INTRODUCTION

Continuous simulation modelling for design flood estimation (DFE) estimation is a developing field in hydrology and takes hydrological processes into account that are not possible in an event model, but requires complex rainfall-runoff models and the availability of long continuous and reliable time series of hydrological variables (Aronica and Candela, 2007). CSM is the most comprehensive tool to account for joint probabilities in flood frequency estimation, and is emerging as a practical tool (Kuczera et al., 2006). The advantages of using CSM for DFE have been shown in a number of studies, both internationally and in South Africa.

For catchments with limited gauged flow data, the use of CSM to determine flood frequency is an alternative to direct frequency analysis (Blazkova and Beven, 2009) and has been used in many studies (e.g. Calver and Lamb, 1995; Blazkova and Beven, 1997; 2002; 2004; Calver et al., 1999; 2000; 2001; Cameron et al., 1999; 2000; Lamb, 1999; Lamb and Kay, 2004; Chetty and Smithers, 2005; Cameron, 2006; Smithers et al., 2007; 2013). Both historical rainfall (e.g. James, 1965) and stochastic rainfall models (e.g. Beven, 1987) have been used in CSM to estimate flood frequencies. The use of a CSM approach simulates the joint association of rainfall and antecedent moisture conditions explicitly. Thus, these distributions do not need to be estimated (Kjeldsen et al., 2014).

The motivation for using CSM is the better representation of physical processes and to overcome restrictive assumptions required for the application of other methods (Lamb et al., 2016), but the cost of using a CSM approach is more than other approaches and needs to be offset against its advantages (Lamb et al., 2016). Advantages of the CSM approach include the estimation of design flows at any simulation point and not just at the catchment outlet, no assumptions need to be made about a design event and hydrograph shapes, and it is possible to assess the frequency of flow volumes and peak discharges (Faulkner and Wass, 2005).

From the literature reviewed, Vogel et al. (2005) concluded that only three to five parameters are necessary for a parsimonious rainfall-runoff model. Models with more than five parameters are used for detailed engineering and scientific catchment process studies, but calibration and uncertainty analysis are much more challenging (Vogel et al., 2005). Lamb et al. (2016) concluded that integrated simulations are possible with a CSM approach. They concluded that the approach remains useful in special cases and requires standardised data, resources and models to be more widely applied.

Given developments in computing technologies, the use of CSM has been shown to be a feasible alternative for flood frequency estimation. For example, the Simulation of Hydrographs for flood frequency estimation – REGionalised (SHYREG) model was found to result in more stable estimates of flood quantiles in France than statistical distributions fitted to the observed data (Arnaud and Lavabre, 2002). The SHYREG approach was also applied successfully to 1 535 catchments in France (Odry and Arnaud, 2017). For a catchment in the United Kingdom where the Flood Estimation Handbook (FEH)'s methods could not be adequately applied, Faulkner and Wass (2005) used a stochastic rainfall model to generate 1 000 years of hourly rainfall data, which was used as input to the semi-distributed conceptual Probability Distributed Model (PDM) rainfall-runoff model.

Parameters from hydrologically similar catchments were transferred to the ungauged catchment and the simulated series at the gauged sites was adjusted to improve the correlation of simulated and observed flood frequency curves. Costa and Fernandes (2017) successfully used a bounded stochastic daily rainfall generator and the 13-parameter Rio Grande rainfall-runoff model in a Bayesian framework to derive the flood frequency in the 4 820 km^2 American River catchment. A thousand runs of a 10 000-year series was used to estimate the median frequency curves. They achieved 95% confidence intervals and accurate estimates for most return periods with smaller uncertainty than other approaches. An additional advantage of the CSM approach was the improved understanding of the dynamic factors that result in floods (Costa and Fernandes, 2017).

Sources of uncertainty when using a CSM approach include rainfall data, parameter uncertainty and the calibration metric used (Ball, 2013). When calibrating the CSM model for flood estimation, Ball (2013) found it necessary to censor the calibration data to exclude low-flow events. The spatial averaging of rainfall was found to impact on more frequent events. The variability of the estimated frequency relationship was also found to be larger than a direct frequency analysis of the flow data. Lamb (1999) found that calibrating the PDM using squared errors resulted in biased simulated flood frequency distributions, but the simulated distributions were acceptable when a range of objective and subjective measures was used in the calibration, particularly when the objective function was weighted towards to the peak discharges. When using the hydrologic modelling system (HEC-HMS) to simulate three catchments in Germany, the best results were obtained when using stochastic rainfall and using the probability distribution of the observed peak flows for model calibration. This also gave reasonable simulations for general hydrological conditions (Haberlandt and Radtke, 2013).

In South Africa, the ACRU agrohydrological model has been used in a number of pilot studies to estimate design floods using a CSM approach (Smithers et al., 1997; 2001; 2007; 2013; Chetty and Smithers, 2005). From literature reviewed by Smithers (2012), and more recently by Rowe and Smithers (2018), the potential for using a CSM approach to DFE in South Africa is evident. However, Rowe et al. (2018b) concluded that significant developments were still required before a CSM system for DFE can be widely used by practitioners in South Africa. They recommended a number of steps to do this. Rowe (2019) further refined and developed the ACRU model for DFE, including modifications to the ACRU CSM to improve verification of DFEs. The assessment of the performance of the ACRU CSM using site-specific information derived from national land cover and soil maps showed that the performance of the CSM approach was better than the event-based SCS-SA model for DFE in South Africa. The next section contains a summary of the CSM that was developed in this study.

7.2 SYSTEM DEVELOPMENT AND OVERVIEW

The SCS-SA CSM system has been developed using Excel as a front-end GUI to input user information. It uses Visual Basic code to run compiled executable Fortran code, imports results and generates hydrographs. A schematic overview of the system is shown in Figure 7.1. A number of CSV input files contain the information to run the system. Hence, the source file containing the parameter value for a particular variable can be specified by an expert user. However, this is not required for the general use of the system.

The data input GUI screens are shown in Figure 7.2. Allowance is made for up to 10 HRUs to be simulated per catchment. To run the system, the user is required to do the following:

- Enter the catchment area
- Enter the average catchment slope and mean annual precipitation
- Select the lag time estimation method
- Select the method to disaggregate the daily rainfall into a hyetograph
- Select the quinary catchment number for each HRU

- Select the vegetation class, treatment and condition for each HRU
- Select either the catchment-specific soil texture and depth or the soil texture and depth parameters in the quinary catchments database for each HRU

Typical results from a simulation are shown in Figure 7.3 and the disaggregated hyetograph and simulated hydrograph are shown in Figure 7.4. Based on results of Dlamini (2019) and summarised in Chapter 6, who found that the SCS-SA model performed better when the duration of rainfall used as input to the model was equal to the time of concentration of the catchment. Options for the user to select a duration of either one day or time of concentration are currently built into the model. When the time of concentration option is selected for the symmetrical SCS-SA rainfall distributions, the portion of the hyetograph with the maximum rainfall intensity for this duration is used to generate the hydrograph.

Rowe (2019) showed that the total runoff from a catchment simulated by the ACRU model (CELRUN) results in unrealistic volumes used in the estimation of peak discharges. Hence, an option was provided to select either CELRUN or DSTORM, which is the daily stormflow generated by the ACRU model, which runs off from the catchment on the same day as the rainfall.

Thus, in the beta version of the SCS-SA CSM, the user can select to use either the DSTORM or CELRUN runoff depths simulated by the ACRU model. The user can also select to use either one day or time to peak as the duration of the hydrograph to estimate the peak discharge.

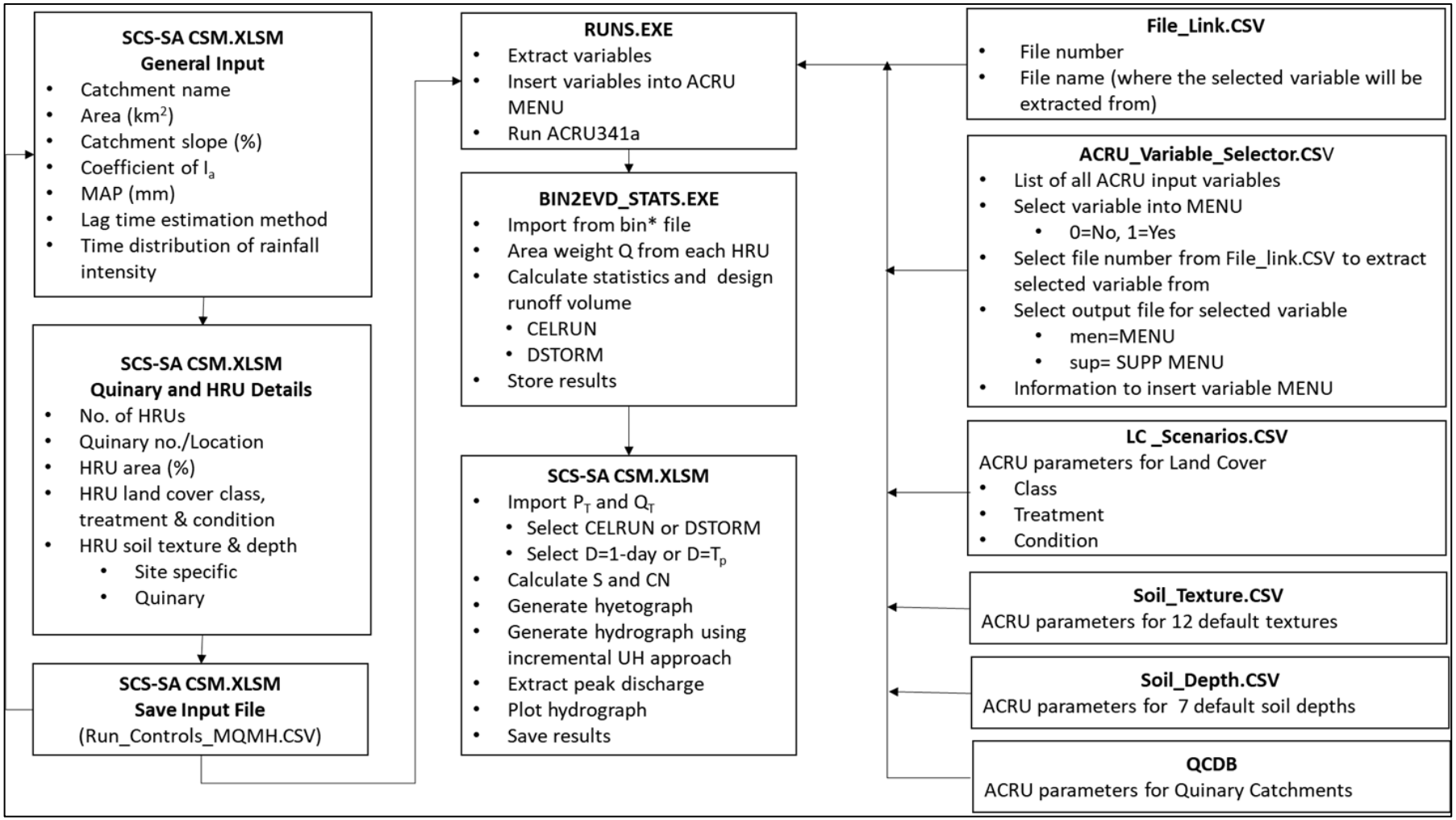

Figure 7.1: SCS-SA CSM system overview

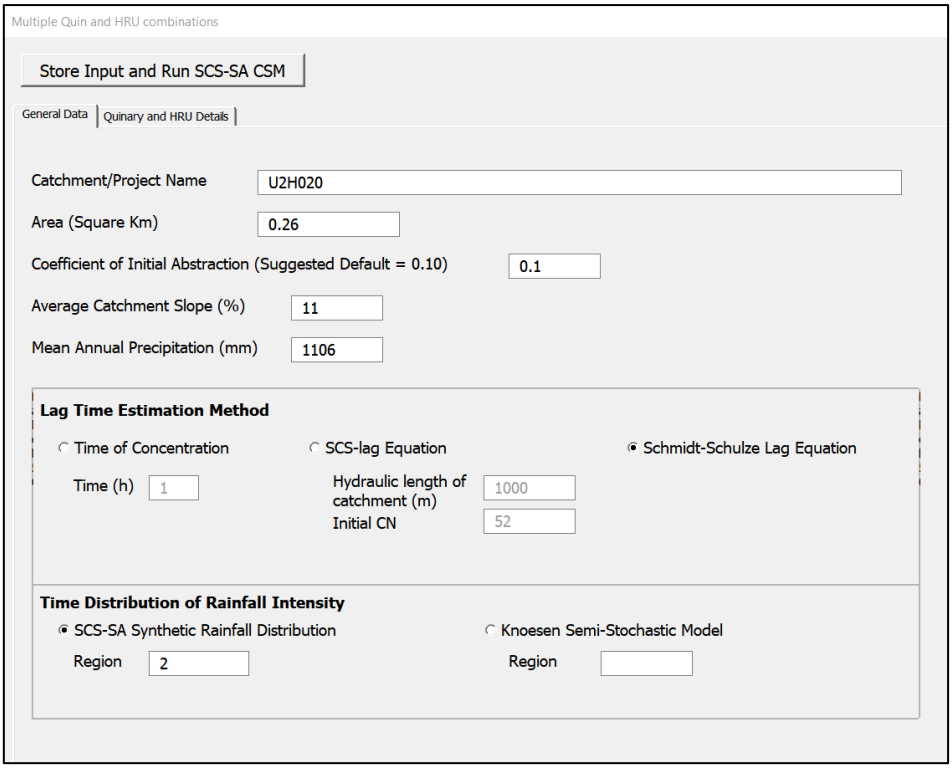

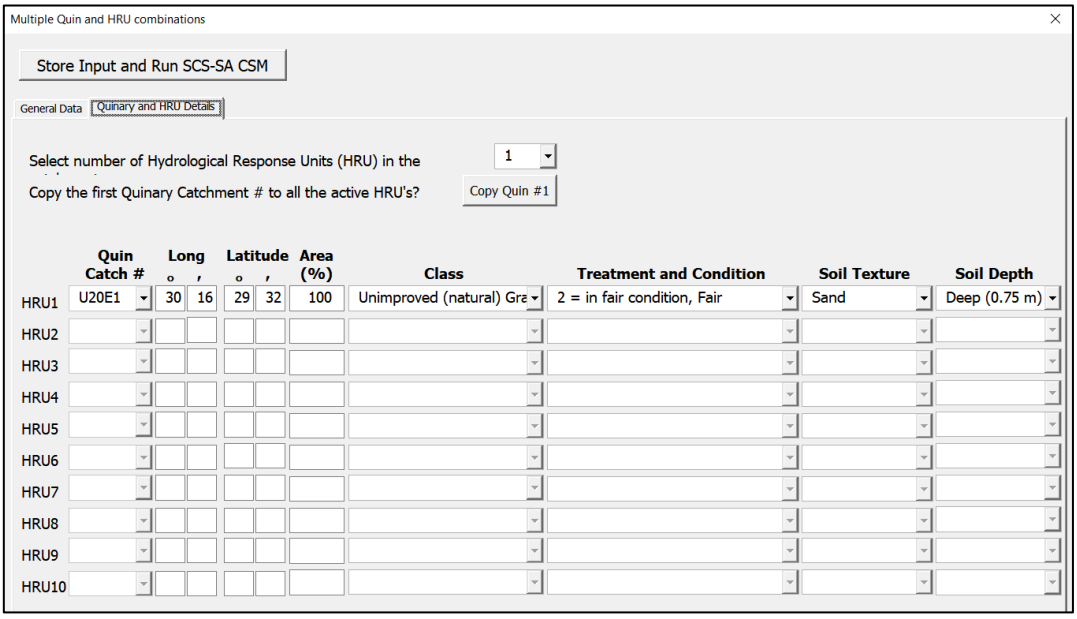

Figure 7.2: Data input screens

Peak Discharge Estimation and Hydrograph Generation: Load Menu

'Time of Concentration'	0.60 (h)						
'SCS-lag Equation'	0.53 (h)						
'Schmidt-Schulze Lag Equation'	0.44 (h)						
Catchment Lag	0.44 (h)						
Δt (h)	0.08						
Tp (h)	0.48						
Select storm duration	D = 1-day	Select CELRUN or DSTORM			CELRUN		
Return Period (years)	**2**	**5**	**10**	**20**	**50**	**100**	**200**
Design Rainfall (mm): D=1-day	62.7	88.8	111.5	138.3	182.5	224.4	275.4
Design Rainfall (mm): D=Tp	26.0	36.8	46.2	57.4	75.7	93.1	114.2
Design Rainfall Used (mm)	62.7	88.8	111.5	138.3	182.5	224.4	275.4
Design Total Runoff (mm)	4.6	10.1	16.1	24.6	41.7	61.3	89.5
Computed S (mm)	258.4	292.0	316.3	338.8	365.1	380.3	388.6
Computed CN	50	47	45	43	41	40	40
Peak Discharge ($m^3.s^{-1}$)	0.1	0.3	0.6	0.9	1.6	2.4	3.6

Figure 7.3: Example of computed output

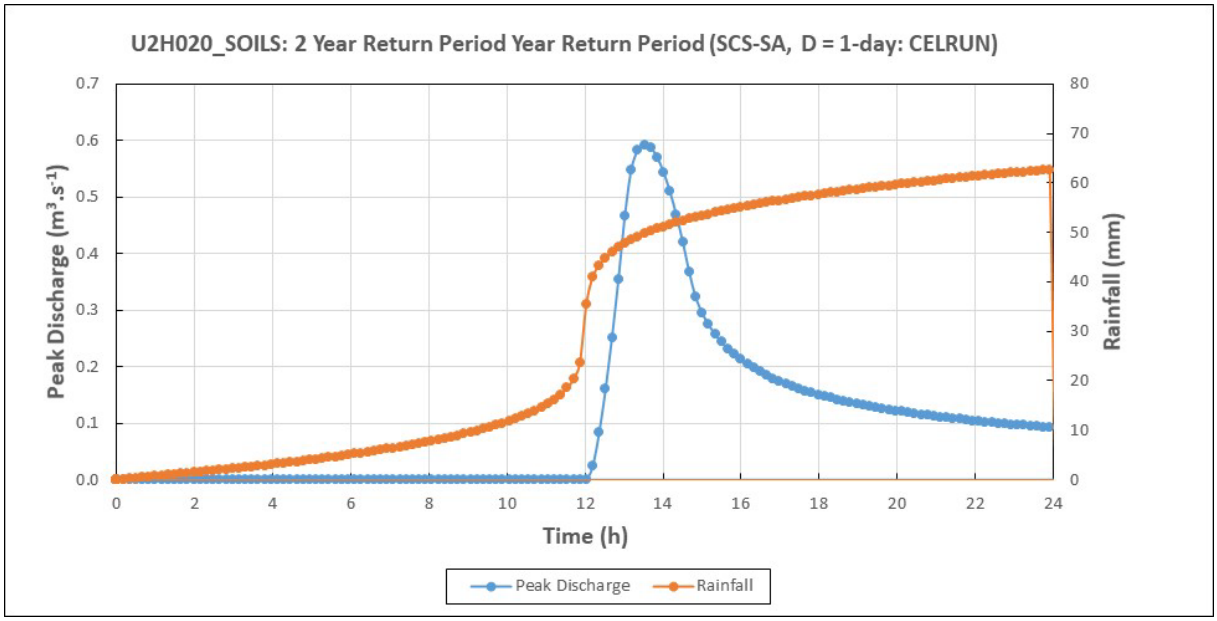

Figure 7.4: Example of generated hyetograph and simulated hydrograph

The use of the ACRU model as the CSM to simulate runoff volumes makes the need to account for antecedent soil moisture in an event-based simulation of runoff response redundant, i.e. the median condition method for CN adjustment in the current version of the SCS-SA model is not required as the soil moisture balance is computed on a daily timestep in the model, and more runoff is generated when the soil is wet compared to when the soil is drier. The next section addresses the performance of the SCS-SA CSM.

7.3 PERFORMANCE OF THE SCS-SA CSM

In this section, a brief methodology and the results obtained in the study are provided.

7.3.1 Methodology

The test-version SCS-SA CSM, as described in Section 7.2, currently incorporates a number of ways to model the design peak discharge. Table 7.1 contains a summary of the possible combinations, which include using the following:

- Catchment-specific soil (Catchment Specific), soil for the dominant quinary in the catchment (Quinary – dominant) or each quinary in the catchment modelled as an HRU using the quinary soil information for each HRU (Quinary – HRU)
- One-day-duration design rainfall or short-duration rainfall equivalent to time to peak
- The “CELRUN” or “DSTORM” design volumes, as described in Section 7.2
- Land cover specific to the catchment

The simulation scenarios that are run to assess the performance of the SCS-SA CSM are referred to as Run 1 to Run 12. These represent the corresponding variable or parameter combinations that were adopted. The model runs were performed on a total of 19 catchments, as detailed in the above chapters for the various studies undertaken. The MARE for all catchments was averaged for each scenario to determine the general trend in the performance of the model when selecting different options and combinations of variables or parameters.

Table 7.1: Simulation matrix for the SCS-SA CSM model runs

Simulation runs	Parameters or variables			
	Soils	Rainfall duration	Runoff	Land cover
Run 1	Catchment-specific	one day	CELRUN	Catchment-specific
Run 2	Catchment-specific	one day	DSTORM	Catchment-specific
Run 3	Catchment-specific	time to peak	CELRUN	Catchment-specific
Run 4	Catchment-specific	time to peak	DSTORM	Catchment-specific
Run 5	Quinary – dominant	one day	CELRUN	Catchment-specific
Run 6	Quinary – dominant	one day	DSTORM	Catchment-specific
Run 7	Quinary – dominant	time to peak	CELRUN	Catchment-specific
Run 8	Quinary – dominant	time to peak	DSTORM	Catchment-specific
Run 9	Quinary – HRU	one day	CELRUN	Catchment-specific
Run 10	Quinary – HRU	one day	DSTORM	Catchment-specific
Run 11	Quinary – HRU	time to peak	CELRUN	Catchment-specific
Run 12	Quinary – HRU	time to peak	DSTORM	Catchment-specific

It is evident from Table 7.1 that runs 1 to 4 use both catchment-specific soils and land-cover information, whereas runs 5 to 8 use soil information from the quinary catchments database and catchment-specific land-cover information. Where there was more than one quinary overlapping a catchment, two scenarios were simulated: the information from the dominant quinary catchment in terms of catchment area was selected (Quin – dominant), and each quinary in the selected catchment was simulated as an HRU (Quinary – HRU). These are represented by runs 9 to 12.

The parameter values from the quinary catchments database were used in the ACRU model, i.e. default values as conventionally used. The calibrated ACRU parameter values described in Chapter 3 were not used in this assessment.

7.3.2 Results, discussion and conclusions

Figure 7.5 illustrates the MARE of design peak discharges averaged for all catchments and for each simulation run. From the general trends shown in Figure 7.5, the following conclusions are drawn:

- Generally better performance is obtained when using the DSTORM compared to CELRUN volume as is evident by comparing Run 1 to Run 2, Run 3 to Run 4, Run 5 to Run 6, Run 7 to Run 8, and Run 9 to Run 10. This is supported by the consistently lower MARE values. Although, Run 11 and Run 12 do not follow this trend, the differences in MARE values are small.
- Generally better performance is obtained when using time to peak compared to one-day duration, as is evident by comparing Run 1 to Run 3, Run 2 to Run 4, Run 5 to Run 7, Run 6 to Run 8, Run 9 to Run 11, and Run 10 to Run 12.
- Generally better performance is found when quinary catchments are simulated as HRUs with quinary catchments' soil information compared to soil information from the dominant quinary catchment, as is evident by comparing Run 5 to Run 9, Run 6 to Run 10, Run 7 to Run 10, and Run 8 to Run 12.

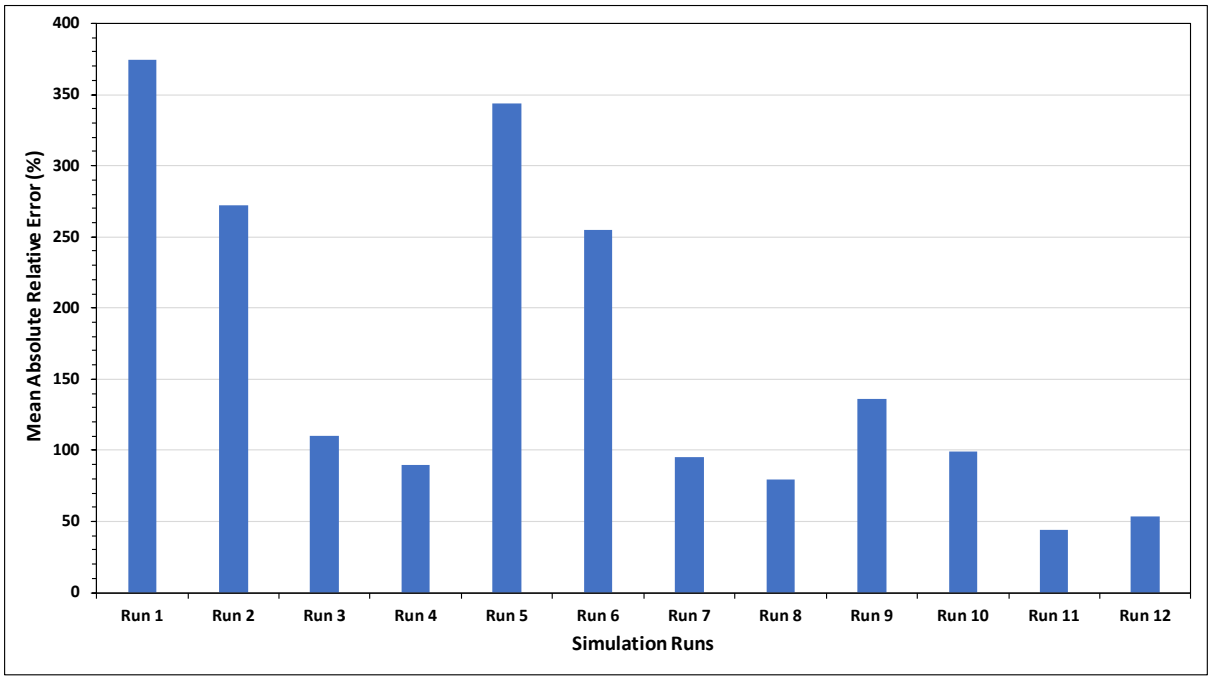

Figure 7.5: Averaged MARE of design peak discharge for each simulation run across all catchments

The average MRE and linear regression slope of the simulated vs observed design peak discharges for each simulation run are shown in Figure 7.6. From Figure 7.6, it is evident that the SCS-SA CSM simulates the observed design flood peak discharges reasonably well, and is best for Run 4 (catchment-specific soil, time to peak duration, DSTORM volume), Run 8 (quinary soil, time to peak duration, DSTORM volume), and are slightly under-simulated for Run 11 and Run 12 (Quinary – HRU, time to peak duration, and CELRUN and DSTORM volumes, respectively).

Overall, it is evident that soil information from the quinary catchment gave better results than catchment-specific soil information. This can be attributed to the source of the information used for the catchment-specific soil.

Generally, there are also improved results when the catchment is simulated as an HRU, with each HRU representing a quinary falling within the catchment. The trends in MRE and regression slope are consistent with the trends indicated by MARE values.

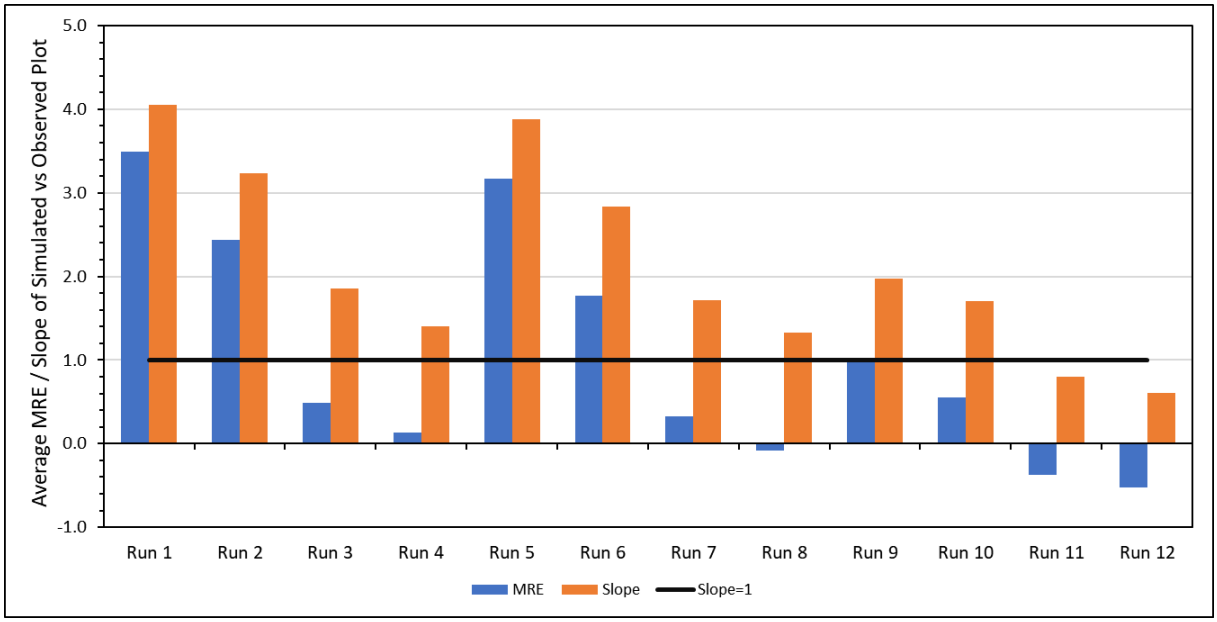

Figure 7.6: Averaged MRE and regression slope for design peak discharge for each simulation run across all catchments

To determine which simulation run performed the best in terms of having the best MARE and MRE values, the runs were ranked for both MARE and MRE values, and the ranks were summed to determine the overall rank, as shown in Table 7.2, where it can be seen that the run with the best rank is Run 8, and the run with the lowest rank is Run 1.

Table 7.2: Ranking of simulation runs using MARE and MRE values

Simulation run	MARE		MRE			Overall rank
	Value	Rank	Value	Rank		
Run 1	375	12	3.49	12		12
Run 2	272	10	2.44	10		10
Run 3	110	7	0.49	5		6
Run 4	90	4	0.13	2		3
Run 5	344	11	3.17	11		11
Run 6	255	9	1.77	9		9
Run 7	95	5	0.32	3		4
Run 8	**79**	**3**	**-0.08**	**1**		**1**
Run 9	136	8	0.98	8		8
Run 10	99	6	0.55	7		7
Run 11	44	1	-0.38	4		2
Run 12	54	2	-0.53	6		4

CHAPTER 8: COMPARISON OF RESULTS OBTAINED IN THE STUDY

NS Dlamini, JC Smithers and U Maharaj

This chapter contains a summary of results from the various studies detailed in the above chapters, including the standard and Ensemble SCS-SA models with both one-day and time to peak design rainfall durations, the comprehensive ACRU model , the parameter-sparse GR4J CSM and the SCS-SA CSM.

8.1 METHODOLOGY

The standard and Ensemble SCS-SA model were applied to 19 catchments. The SCS-SA CSM was applied to 19 catchments. The ACRU model was applied to 11 catchments. The GR4J model was applied to five catchments. The ACRU and GR4J models were applied to fewer catchments due to the lack of availability of good-quality continuous observed data. For the SCS-SA CSM, only the overall best simulation scenario (Run 8) is included in the comparison between the performance of the models.

In order to apply the Ensemble SCS-SA model at sites where event hydrographs were not available or had not been extracted (and hence the TP data for the observed events was not available), a preliminary generalised method was developed to estimate TP using the currently available TP data from selected regions. This development is detailed in Section 8.2.

The best methods to determine CNs that are similar to published CNs, or to give the best estimates of design runoff volumes, are detailed in Chapter 2. The performance of the CN-determination methods to estimate design peak discharges and the impact of different methods to estimate catchment design rainfall on the estimation of design runoff volumes are detailed in Section 8.3.

8.2 ESTIMATION OF DISTRIBUTION OF TIME TO PEAK AT UNGAUGED SITES FOR THE ENSEMBLE SCS-SA MODEL

As detailed in Chapter 6, the ensemble SCS-SA JPA model was applied at sites where event hydrographs had been extracted and the event TP has been determined. This data was used to determine the distribution of TP at the sites. In order to apply the ensemble SCS-SA JPA model at any location in South Africa, the available event TP values were scaled and used to derive a generalised regression model to estimate TP at any location in South Africa. This entailed developing a regression equation to estimate the mean TP and the standard deviation (SD) of the TP. The estimated mean and SD of TP were used with the Log-Normal distribution to generate random TP values for the selected site.

A total of 78 catchments across different climatic regions were used to develop the regression equations using the mean TP and SD of TP for each catchment extracted and used by Gericke (2016). Both the mean TP and SD of TP were scaled using the catchment area and then plotted against the catchment area, as shown in figure 8.1 and 8.2, respectively. Regression equations were then fitted to the data for both the mean and SD of TP. The equations were then used to estimate the mean and SD of TP for each catchment used in this study.

The probability distribution that best fits the observed TP is the Log-Normal distribution. The estimated mean and SD of TP were used to estimate the parameters of the Log-Normal distribution. Using the fitted Log-Normal distributions, TP values were randomly generated for each catchment and used as input to run the Ensemble SCS-SA (regional equation duration) model.

It is acknowledged that the above approach, which was developed to estimate the distribution of TP at an ungauged site, is limited by the sites used in the development, has not been independently verified, and has been applied outside the sites used in the development, but the approach was adopted as a proof of concept and for possible further development in a subsequent study.

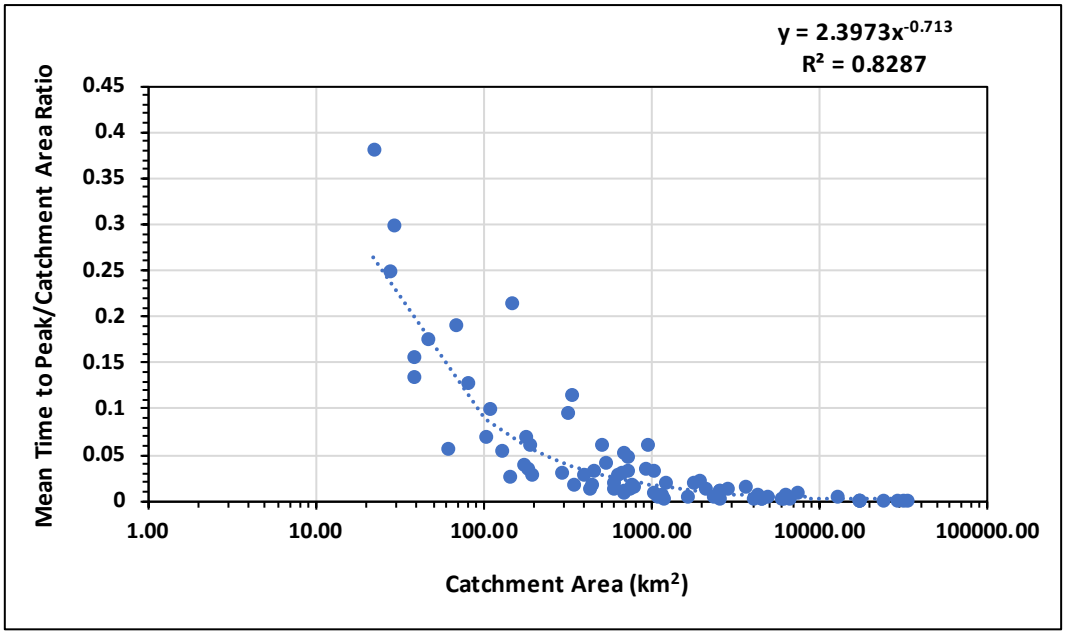

Figure 8.1: Scaled mean time to peak relative to the catchment area

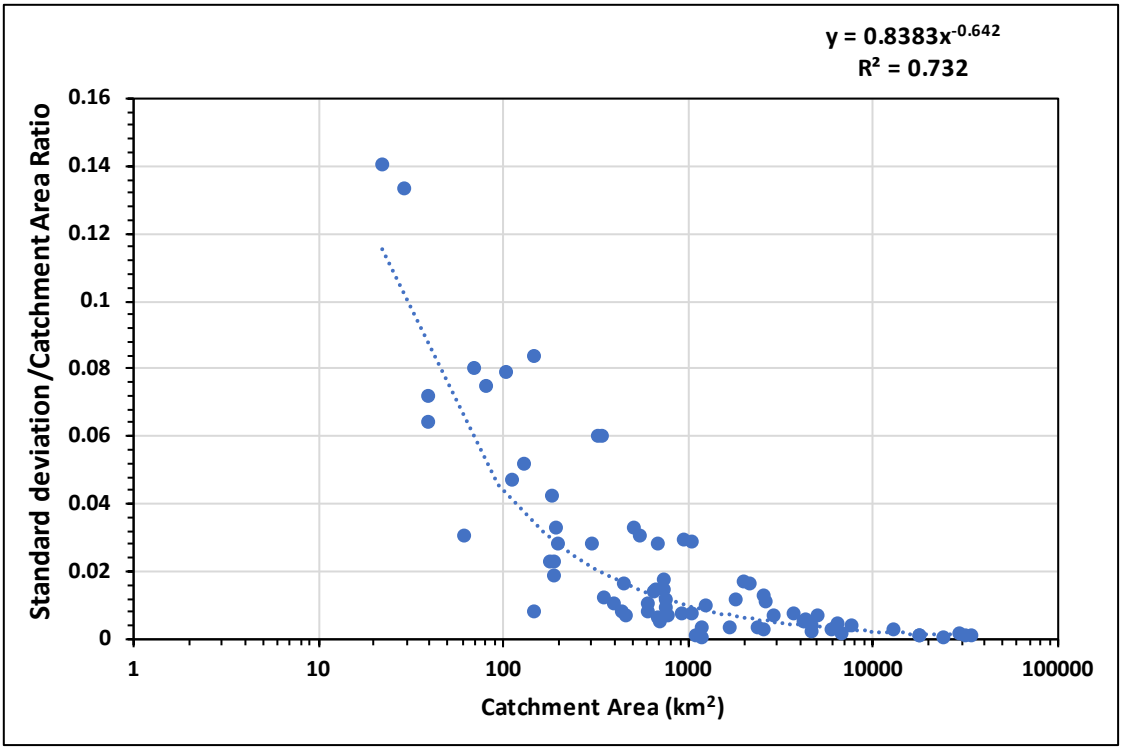

Figure 8.2: Scaled standard deviation of the time to peak relative to the catchment area

8.3 DESIGN RAINFALL ESTIMATION INPUT TO THE SCS-SA CSM FOR CN AND DESIGN PEAK DISCHARGE ESTIMATION

The results from Maharaj (2020) and summarised in Chapter 2 are expanded in this section to estimate design peak discharges and assess the impact of three methods to design rainfall estimation (DRE) on the catchment:

- DRE 1: Catchment-specific one-day design rainfall estimated from the daily rainfall data selected to represent the catchment, as used by Maharaj (2020) and summarised in Chapter 2.

- DRE 2: One-day point design rainfall estimated at the catchment centroid using the regional linear moment algorithm and scale invariance (RLMA&SI) approach (Smithers and Schulze, 2003; 2004a).
- DRE 3: Average of all one-day point design rainfalls within the catchment estimated using the gridded RLMA&SI approach.

To estimate DRE 2 and 3, ArcGIS was utilised to generate a 1 'x 1' grid of one-day design rainfall across South Africa. The Fishnet geoprocessing tool was used to generate the 1' x 1' grid with the correct specified dimensions of the cell size height and width, and coordinate system. Once the grid was generated, it was clipped to the boundary of South Africa, and the attribute table of the layer was utilised to add coordinates for each centroid of the grid using the calculate geometry option in the attribute table. Once all coordinates for the 1' x 1' grid points were obtained, the layer was used to overlay with catchment boundaries of interest and the 1' x 1' grid coordinates within the catchment boundary were extracted. At each point, the one-day point design rainfall was estimated. Thereafter the one-day point design rainfall for the catchment centroid was extracted (DRE 2) and all the values within the boundary of the catchment of interest were averaged (DRE 3).

The SCS-SA CSM model was then used to simulate the design peak discharges for the $CN_{published}$ and CN_{10} values derived using observed and simulated data for all three design rainfall estimation methods (DRE 1, DRE 2 and DRE 3). Figure 8.3 illustrates the averaged MARE for each set of scenarios when using DRE 1, DRE 2 and DRE 3 design rainfall values.

It is evident from Figure 8.3 that, when using the SCS-SA CSM to estimate the observed design peak discharge, the CN_{10} ($ACRU_{CON-P}$: DRE 2) scenario has the lowest average MARE value, indicating the best overall estimate of observed design peak discharge. Similarly, the CN_{10} values derived using $ACRU_{CON-P}$ had the lowest average MARE values for both the DRE 1 and DRE 2 design rainfall estimation methods. It is evident that, when adopting the CN_{10} values derived using the $ACRU_{CON-P}$ configuration results in the best overall estimate of observed design peak discharge compared to the other CN_{10} determination methods.

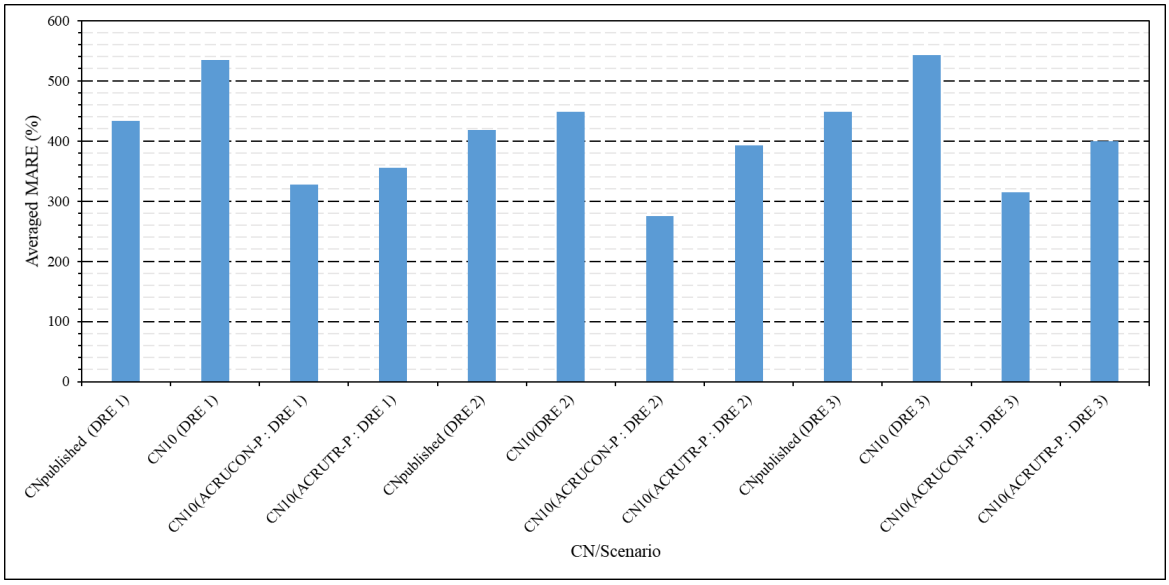

Figure 8.3: Averaged MARE for peak discharge etimation across all catchments for the different CN estimation scenarios

Figure 8.4 illustrates the MRE of peak discharge estimation for each set of scenarios for the different model applications. It can be seen from Figure 8.4 that the MRE values are relatively high positive values, indicating that there is significant over-estimation of the observed design peak discharges.

Furthermore, this can be observed across all the scenarios, indicating that the $CN_{published}$ and CN_{10} determination methods are all performing poorly in simulating the observed design peak discharges. These results are not consistent with good simulations of design runoff volumes as summarised in Chapter 2.

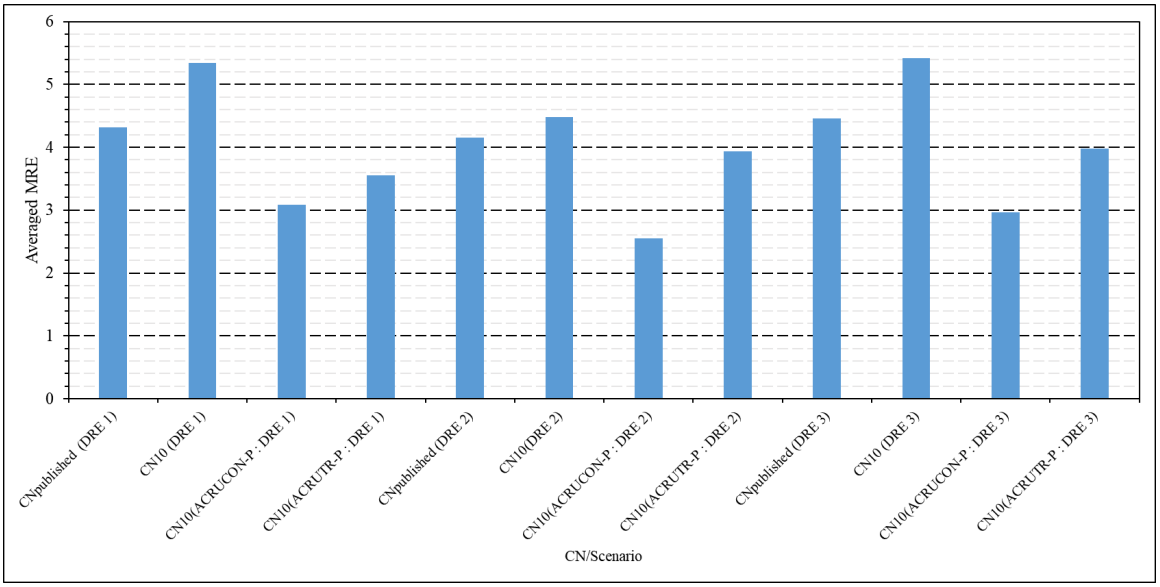

Figure 8.4: Averaged MRE for peak discharge estimation across all catchments for the different CN scenarios

8.4 OVERALL COMPARISON OF RESULTS OBTAINED IN THE STUDY

In the overall comparison of model performances, only the best simulation run (Run 8) from the SCS-SA CSM was included. It can be seen from the summary graph in Figure 8.5 that the best MARE of design peak discharges is obtained by the Ensemble SCS-SA (time to peak) model, followed by the calibrated GR4J models, SCS-SA CSM (Run 8), standard SCS-SA model (time to peak) and the Ensemble SCS-SA (regional equation duration) models, all of which have similar MARE values.

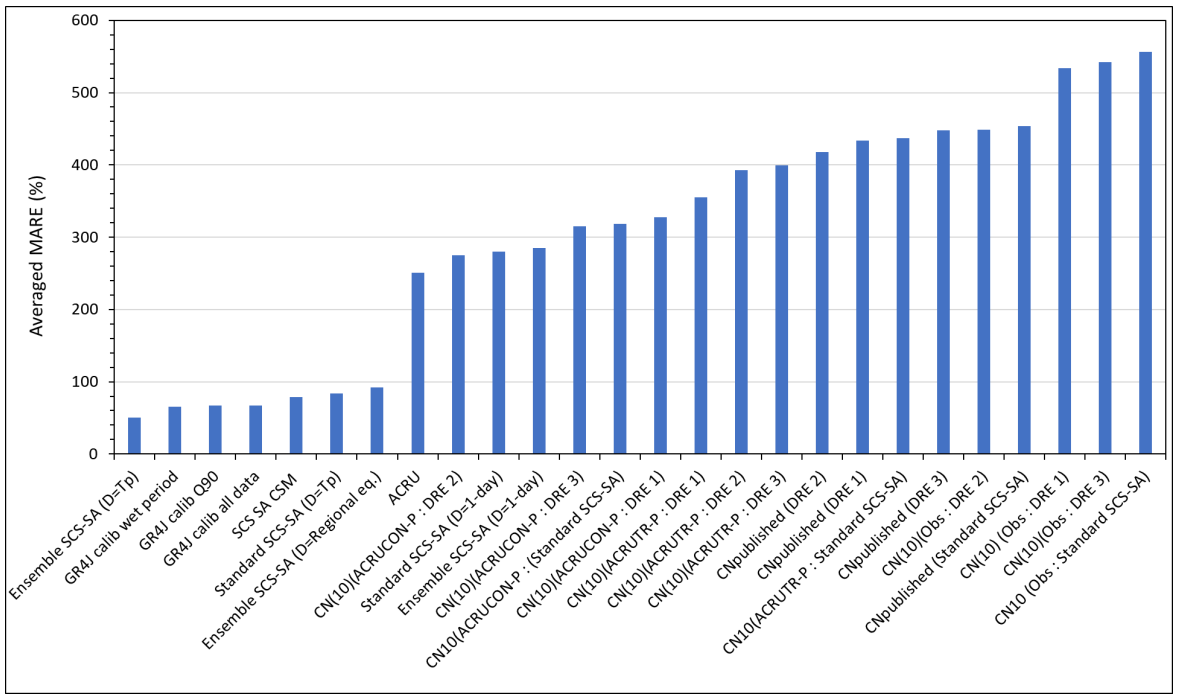

Figure 8.5: Averaged MARE for peak discharge estimation for each model application across all catchments

It is encouraging to note that some of the models developed in this study (Ensemble SCS-SA and SCS-CSM) perform better than the standard SCS-SA (one-day duration) model, which is currently used in practice.

Figure 8.6 illustrates the averaged MRE across all models and model scenarios evaluated. It can be seen from the summary graph in Figure 8.6, and similar to the MARE results, the best MRE results were obtained by the Ensemble SCS-SA (time to peak) model, followed by the SCS-SA CSM (Run 8), standard SCS-SA (time to peak) model and the Ensemble SCS-SA (regional equation duration) models, all of which have similarly low MRE values. The good performance of the Ensemble SCS-SA (regional equation duration) model, despite the limited datasets used in the derivation of the regionalised equations to estimate TP, is encouraging and requires further refinement.

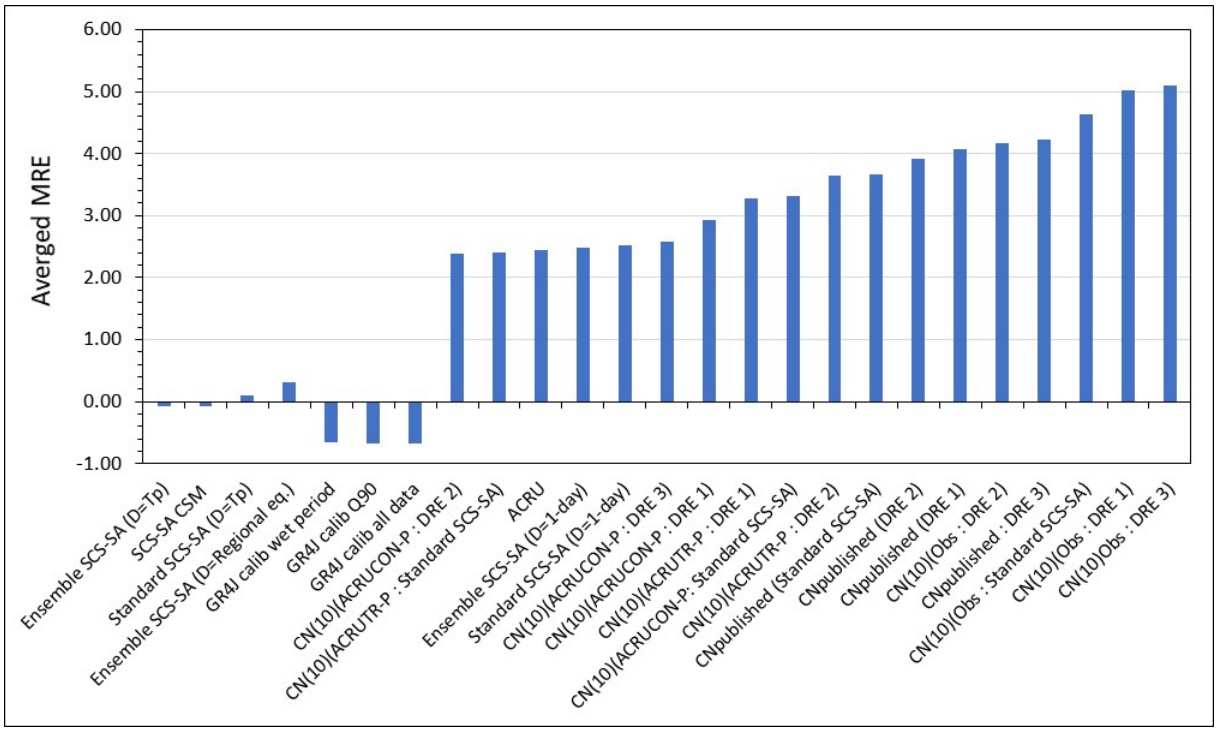

Figure 8.6: Averaged MRE for design flood estimation for all model applications across all sites

Despite the improved estimates of design peak charges by the Ensemble SCS-SA (time to peak) and SCS-SA CSM (Run 8), compared to most other models, there are some further inconsistencies in the results that require further investigation. For example, the results shown in Chapter 2 indicate that the derivation and use of $CN_{10,0.1}$ and S-$CN_{10,0.1}$ ($ACRU_{TR\text{-}P}$) resulted in reasonable estimates of design runoff volumes, but the above results for design peak discharge estimation indicate relatively poor simulations. Hence, some of the good estimations of peak discharge shown by some models used in this study may not be consistent with the estimation of design runoff volumes.

CHAPTER 9: DISCUSSION, CONCLUSIONS AND RECOMMENDATIONS

JC Smithers, NS Dlamini and U Maharaj

A list of specific objectives undertaken to meet the aims of this project are outlined in Chapter 1. The studies undertaken to achieve these objectives are discussed in the following sections.

9.1 AN ASSESSMENT OF THE PERFORMANCE OF PUBLISHED AND DERIVED SCS CURVE NUMBERS FOR DESIGN FLOOD ESTIMATION IN SOUTH AFRICA

The aim of the study reported on in Chapter 2 was to evaluate the currently available published CNs and select a suitable method to derive CNs using observed or simulated rainfall-runoff data for South African catchments. It was found that the different CN-determination methods resulted in different CN values. The CN value was also dependent on the coefficient of initial abstraction used in the derivation.

If the objective is to use a method that derives CN values closest to the published CN values, then the results show that the mean S-$CN_{AMS,0.1}$ and the AMS S-$CN_{NEH,0.1}$ (derived using simulated P-Q depths from $ACRU_{TR-P}$) resulted in derived CN values that were similar to the published CNs. These methods should be used to derive CNs on catchments with land-cover classes that are not currently available in the published CN tables.

It was found that the CNs derived using observed data and c = 0.1 were generally closer to the $CN_{published}$ values. This was unexpected, because the $CN_{published}$ values were derived using c = 0.2. Hence, future studies should focus on the calibration of both c and the CN.

This study also investigated which CN-determination methods resulted in CNs that, when used in the SCS-SA model, resulted in the best estimates of the design volumes computed from the observed data. A significant finding is that the use $CN_{published}$ values generally resulted in poor estimates of runoff, which has an impact on how the model is currently used in practice. The results from the study showed that data-derived $CN_{10,0.1}$ values generally resulted in the best design flows. This method is recommended to determine CNs.

The study also investigated how the estimated design runoff volumes from the different CN-determination methods can be used as input in the SCS model to determine design peak discharges. The design peak discharges obtained from translating the design runoff volume determined from the CNs simulated from $ACRU_{CON-P}$ parameterisation consistently resulted in better estimates of the observed design peak discharges compared to the other CN-determination methods.

The study also investigated the use of runoff simulated from two slightly different parameterisations of the ACRU model to determine CNs. The CNs determined from the runoff simulated from $ACRU_{TR-P}$ generally resulted in a better performance of the SCS model compared to when $ACRU_{CON-P}$ parameterisation was used. This result was not unexpected given that $CN_{published}$ values were used in the calibration of two sensitive parameters in the $ACRU_{TR-P}$ configuration.

From the results of this study, it is evident that CNs are more accurately defined by observed P-Q data or simulated Q values for a specific catchment and not from published CN tables. Furthermore, in the absence of reliable P-Q data, the results from this study indicate that the S-$CN_{10,0.1}$ values calculated using simulated Q depths from $ACRU_{TR-P}$ and the S-$CN_{LN,0.1}$ calculated using Q depths from $ACRU_{CON-P}$ resulted in improved estimates of design runoff volumes compared to using the $CN_{published}$ values.

A significant outcome of this study is that the simulated runoff can be used to determine CNs for a range of land-cover and soil combinations appropriate to South Africa. It is recommended that this approach be adopted in future studies.

9.2 FURTHER DEVELOPMENT AND ASSESSMENT OF THE ACRU CSM SYSTEM FOR DESIGN FLOOD ESTIMATION IN SOUTH AFRICA

The ACRU model has been successfully used in a number of pilot studies for design flood estimation. The aim of the study reported on in Chapter 3 was to further develop and assess the performance of a comprehensive CSM system that can be used to estimate design flood discharges consistently and reliably in small catchments (0–100 km^2) throughout South Africa, and which can be easily applied by practitioners. This led to the identification of some inconsistencies in the way peak discharge is calculated in the ACRU model. Some improvements were made to the volume used to estimate the peak discharge. The results also showed the improved estimates of peak discharge when the incremental unit hydrograph approach was used compared to the currently routinely applied single hydrograph approach. Based on the assumption that tabulated CNs used in the SCS model give reasonable simulations of volume, two sensitive parameters in the ACRU model were calibrated to obtain similar hydrological responses simulated by the SCS-SA model. When the above modifications were made, the revised ACRU CSM resulted in reasonable estimates of design volumes and peak discharge, and performed better than the current ACRU CSM.

A significant contribution of this study was the linking of the soil and land-cover parameters required by the ACRU model to information derived from national-scale soil and land-cover coverage. In addition, land-cover classes for the ACRU model have been extended to include management practices and cover conditions as are available for the SCS-SA model. The results from the study also showed reasonable performance when the Schmidt-Schulze lag time was used to estimate catchment response times.

A comparison of the performance of the updated ACRU CSM and SCS-SA models to estimate both design volumes and peak discharges indicated improved performance by the ACRU CSM for DFE. The comparison also highlighted the relatively small effect the median condition method of CN adjustment in the SCS-SA model had on estimated design floods and the poor performance of the joint association method as incorporated in the current SCS-SA model.

9.3 ASSESSING THE PERFORMANCE OF TECHNIQUES FOR DISAGGREGATING DAILY RAINFALL FOR DESIGN FLOOD ESTIMATION IN SOUTH AFRICA

The improved performance when using the incremental unit hydrograph approach, which requires the daily rainfall value to be transformed into a hyetograph, led to the investigation of the performance of selected RTD methods and to recommend the adoption or adaptation of one or more of these approaches for application under South African conditions. The results indicate that the use of a triangular distribution performed well when the characteristics of the observed events were available. Hence, it is recommended that this option be further investigated by developing methods to estimate event characteristics at ungauged sites.

In general, the results indicate that the Knoesen semi-stochastic disaggregation model performed the best when disaggregating daily rainfall data. This model is recommended for use in design flood estimation, particularly if ensemble joint probability approaches are used. The currently widely used SCS-SA temporal distribution was the second-best performing disaggregation method that did not rely on observed event characteristics.

9.4 ASSESSMENT OF A SIMPLER PARAMETER-SPARSE CONTINUOUS SIMULATION MODEL

Given the number of input variables and parameters required by a comprehensive CSM, such as the ACRU model, a study was undertaken to assess the performance of a selected simple CS model and

compare its performance to that of the comprehensive ACRU model. The four-parameter GR4H (hourly timestep) and GR4J (daily timestep) models were selected for assessment in this study. Several different calibration options were assessed as part of the study to improve model performance.

The initial results obtained for the two test catchments selected indicate the potential of the GR4J model to provide accurate daily streamflow volumes and design streamflow volumes that were identified to be superior to those obtained from the standard ACRU model. However, the GR4J model needs to be calibrated against observed data. Therefore, for the GR4J model to be applicable nationally, and particularly for ungauged catchments, a methodology to transfer parameters to ungauged locations or to regionalise parameters would be required, which is a significant task that is beyond the scope of this study. In addition, the GR4J model does not have capabilities to estimate the peak discharge for the day from the simulated streamflow volumes. Consequently, the performance of the GR4H model was assessed, which was hypothesised to better approximate the actual daily peak discharge. However, this was not the case. The results from the GR4H model were generally no better than the actual daily discharge values obtained from the GR4J model. Based on these results, and due to the challenges associated with obtaining or synthetically generating short-duration rainfall data, further experimentation with the GR4H model is not recommended.

In summary, the potential of the GR4J model for application in South Africa has been shown. However, significant work is required to develop the model into a DFE tool that is applicable at a national scale.

9.5 DEVELOPMENT AND ASSESSMENT OF AN ENSEMBLE JOINT PROBABILITY APPROACH USING THE SCS-SA MODEL

The aim of this study was to develop, apply and assess the performance of an ensemble joint probability approach using the SCS-SA model for design flood estimation in South Africa, using readily available data. While the Ensemble SCS-SA (one-day duration) model improved on the performance of the standard SCS-SA (one-day duration) model, the models significantly over-estimated the observed design runoff volume and design peak discharge for all the return periods. However, when short-duration rainfall was used as input to the models, both the Ensemble SCS-SA (time to peak) and standard SCS-SA (time to peak) models generally simulated the observed design peak discharges relatively well for all the return periods for all catchments, with the Ensemble SCS-SA (time to peak) performing the best.

The use of time to peak is consistent with the theory of catchment flood response, which assumes that the peak discharge at a catchment outlet will be when the duration of rainfall is at least as long as the catchment response time, i.e. runoff from the furthermost point has reached the catchment outlet, and is still remaining. However, this is not consistent with published CNs, which were derived from daily rainfall and runoff values. Hence, it is recommended that this approach be further investigated.

9.6 DEVELOPMENT AND ASSESSMENT OF THE SCS-SA CSM SYSTEM FOR DESIGN FLOOD ESTIMATION IN SOUTH AFRICA

Based on the findings of the studies undertaken in this project, a beta version of the SCS-SA CMS was developed and assessed for design flood estimation in South Africa. The system is linked to the quinary catchments database. The user can run the system using default ACRU parameter values. Currently, the ACRU parameter values calibrated by Rowe (2019) have not been included in the database.

The performance of various options of the SCS-SA CSM were assessed in 19 test catchments. Similar to the results summarised in Chapter 6, the performance of the SCS-SA CSM was better when the time to peak option was used compared to the one-day duration option. The use of the DSTORM runoff depth in the SCS-SA CSM model performed better in terms of design peak discharge estimation compared to using the CELRUN runoff depth. This is consistent with results reported in Chapter 3.

The improved performance when simulating a catchment as an HRU and not using the soil and land-cover attributes of the dominant quinary catchment is consistent with what has been found in other studies. However, it was surprising that the use of catchment-specific land-cover and soil information did not give the best results. Hence, the manner in which the catchment-specific information was derived needs to be reviewed. Based on the results obtained, it is recommended that the SCS-SA CSM model should be applied with the quinary catchments configured as HRUs, quinary catchment soil information used, duration of design rainfall (time to peak) and using DSTORM as the design volume for design peak discharge estimation in South Africa.

9.7 COMPARISON OF RESULTS FROM THE STUDY

In a comparison of results from the different studies using the sites where the models were applied, the Ensemble SCS-SA (time to peak and regional equation duration versions) and SCS-SA CSM models developed in this study generally performed best among the models evaluated in this study. These models generally show a much better performance compared to the currently used standard SCS-SA (one-day duration) model, and are hence recommended for use in practice. The relatively poor results using derived CNs for design peak discharge estimation, despite reasonable estimation of design runoff volumes, was not expected and requires further investigation.

9.8 CONCLUSIONS

The aims of this project were the following:

- Refine and update the SCS-SA model for design flood estimation to account for antecedent moisture conditions and joint association of rainfall and runoff using the results and methodology from a CSM system
- Compare the performance of the CSM system to the traditional and updated SCS-SA models.
- Further develop and assess the CSM approach, including the potential incorporation and assessment of improved daily rainfall disaggregation methods to account for the temporal distribution of daily rainfall.

As summarised in sections 9.1 to 9.7, these aims have been met and exceeded. The performance of the Ensemble SCS-SA and SCS-SA CSM models have resulted in major improvements in the estimation of design peak discharges compared to the standard SCS-SA model currently used in practice.

9.9 RECOMMENDATIONS

Based on the results from this study, the following recommendations are made:

- The performance of the models assessed in this study should be expanded to include design volume estimation and inconsistencies in the performance of the models for transforming a design volume into a design peak discharge should be investigated and resolved.
- The beta version of the SCS-SA CSM system should be further developed to include the Knoesen semi-stochastic daily rainfall disaggregation model.
- The Ensemble SCS-SA model should be further developed and refined for use in practice.
- The ensemble approach should be expanded to include other event-based flood estimation models used in South Africa.

CHAPTER 10: CAPACITY BUILDING

The students involved in this project and their roles are summarised in Table 10.1.

Table 10.1: List of students involved in the project

Name	Degree	Research topic	Status
Thomas Rowe	PhD	Development and assessment of an improved continuous simulation modelling system for design flood estimation in South Africa Using the ACRU model	PhD completed and degree awarded
Nkululeko Mabila	MSc	An assessment of simple continuous simulation modelling approaches for design flood estimation in South Africa	MSc completed and degree awarded
Nkosinathi Dlamini	MSc	Development and assessment of an ensemble joint probability event-based approach for design flood estimation in South Africa	MSc completed and degree awarded
Udhav Maharaj	MSc Eng	An assessment of the performance of published and derived SCS curve numbers for design flood estimation in South Africa	MSc Eng completed and degree awarded
Ryshan Ramlall	MSc	Assessing and updating techniques for disaggregating daily rainfall for design flood estimation in South Africa	MSc completed and degree awarded

CHAPTER 11: REFERENCES

ADAMSON PT (1981) *Southern African storm rainfall*. Department of Environment Affairs: Directorate of Water Affairs, Pretoria, South Africa.

ALEXANDER W (2002) Statistical analysis of extreme floods. Journal of the South African Institution of Civil Engineering **44 (1)** 20–25.

AGRICULTURAL RESEARCH COUNCIL (ARC) and COUNCIL FOR SCIENTIFIC AND INDUSTRIAL RESEARCH (CSIR) (2005) *National Land Cover (2000)*. Produced by a consortium of the Council for Scientific and the Industrial Research (CSIR) and the Agricultural Research Council (ARC), Pretoria, South Africa.

ARNAUD P and LAVABRE J (2002) Coupled rainfall model and discharge model for flood frequency estimation. Water Resources Research **38 (6)** 1–11.

ARNAUD P, FINE JA and LAVABRE J (2007) An hourly rainfall generation model applicable to all types of climate. Atmospheric Research **85 (2)** 230–242.

ARONICA GT and CANDELA A (2007) Derivation of flood frequency curves in poorly gauged Mediterranean catchments using a simple stochastic hydrological rainfall-runoff model. Journal of Hydrology **347** 132–142.

AMERICAN SOCIETY OF CIVIL ENGINEERS (ASCE) (1993) Criteria for evaluation of watershed models. Journal of Irrigation and Drainage Engineering **119 (3)** 429–442.

BALL JE (2013) *Estimation of design floods using continuous simulation*. Flood Managment Australia, Garden Suburb, New South Wales, Australia.

BENNETT JC, ROBERTSON DE, SHRESTHA DL, WANG Q, ENEVER D, HAPUARACHCHI P and TUTEJA NK (2014) A system for continuous hydrological ensemble forecasting (SCHEF) to lead times of 9 days. Journal of Hydrology **519** 2832–2846.

BEVEN K (1987) Towards the use of catchment geomorphology in flood frequency predictions. Earth Surface Processes and Landforms **12 (1)** 69–82.

BEVEN K (1993) Prophecy, reality and uncertainty in distributed hydrological modelling. Advances in Water Resources **16 (1)** 41–51.

BHUIYAN T, RAHMAN A and ABBEY S (2010) *Derivation of design rainfall temporal patterns in Australia's Gold Coast region*. International Conference on Information and Knowledge Engineering, IKE, Las Vegas, NV, USA, 113–119.

BLAZKOVA S and BEVEN K (1997) Flood frequency prediction for data limited catchments in the Czech Republic using a stochastic rainfall model and TOPMODEL. Journal of Hydrology **195 (1)** 256–278.

BLAZKOVA S and BEVEN K (2002) Flood frequency estimation by continuous simulation for a catchment treated as ungauged (with uncertainty). Water Resources Research **38 (8)** 14/11–14.

BLAZKOVA S and BEVEN K (2004) Flood frequency estimation by continuous simulation of subcatchment rainfalls and discharges with the aim of improving dam safety assessment in a large basin in the Czech Republic. Journal of Hydrology **292 (1/4)** 153–172.

BLAZKOVA S and BEVEN K (2009) A limits of acceptability approach to model evaluation and uncertainty estimation in flood frequency estimation by continuous simulation: Skalka catchment, Czech Republic. Water Resources Research **45 (W00B16)** 1–12.

BONTA JV (1997) Determination of watershed curve number using derived distributions. Journal of Irrigation and Drainage Engineering **123 (1)** 28–36.

BONTA JV (2004) Development and utility of Huff curves for disaggregating precipitation amounts. Applied Engineering in Agriculture **20 (5)** 641–653.

BOUGHTON W and DROOP O (2003) Continuous simulation for design flood estimation – a review. Environmental Modelling and Software **18 (4)** 309–318.

CALVER A and LAMB R (1995) Flood frequency estimation using continuous rainfall-runoff modelling. Physics and Chemistry of the Earth **20 (5-6)** 479–483.

CALVER A, LAMB R and MORRIS SE (1999) *River flood frequency estimation using continuous runoff modelling*. Paper 11883, Proceedings of the Institution of Civil Engineers – Water Maritime and Energy, Institution of Engineers, London, UK, 225–234.

CALVER A, LAMB R and CREWETT J (2000) Generalised flood frequency estimation using continuous simulation. In: Bronstert A, BISMUTH C and MENZEL L, European Conference on Advances in Flood Research. PIK Report 65, Potsdam Institute for Climate Impact Research, Potsdam, Germany, 412–421.

CALVER A, LAMB R, KAY AL and CREWETT J (2001) *The continuous simulation method for river flood frequency estimation*. Centre for Ecology and Hydrology, Wallingford, UK.

CALVER A, CROOKS S, JONES D, KAY A, KJELDSEN T and REYNARD N (2005) *National river catchment flood frequency method using continuous simulation*. R&D Technical Report FD2106/TR, Centre for Ecology and Hydrology, Wallingford, UK.

CAMERON D, BEVEN KJ, TAWN J, BLAZKOVA S and NADEN P (1999) Flood frequency estimation by continuous simulation for a gauged upland catchment (with uncertainty). Journal of Hydrology **219 (3)** 169–187.

CAMERON D, BEVEN K, TAWN J and NADEN P (2000) Flood frequency estimation by continuous simulation (with likelihood based uncertainty estimation). Hydrology and Earth System Sciences **4 (1)** 23–34.

CAMERON D (2006) An application of the UKCIP02 climate change scenarios to flood estimation by continuous simulation for a gauged catchment in the northeast of Scotland, UK (with uncertainty). Journal of Hydrology **328 (1/2)** 212–226.

CHARALAMBOUS J, RAHMAN A and CARROLL D (2013) Application of Monte Carlo simulation technique to design flood estimation: A case study for North Johnstone River in Queensland, Australia. Water Resources Management **27 (11)** 4099–4111.

CHETTY K (2010) *An assessment of scale issues related to the configuration of the ACRU model for design flood estimation*. Master's dissertation, University of KwaZulu-Natal, Pietermaritzburg, South Africa.

CHETTY KT and SMITHERS JC (2005) Continuous simulation modelling for design flood estimation in South Africa: Preliminary investigations in the Thukela Catchment. Physics and Chemistry of the Earth **30** 634–638.

CHETTY KT and SMITHERS JC (2011) An assessment of scale issues related to the configuration of the ACRU model for design flood estimation. Hydrology Research **42 (5)** 401–412.

CHOW VT, MAIDMENT DR and LARRY W (1988) *Applied hydrology*, MacGraw-Hill, New York, NY, USA.

CORON L, PERRIN C, DELAIGUE O, THIREL G and MICHEL C (2018) airGR: Suite of GR hydrological models for precipitation-runoff modelling, R package version 1.0. 15.2. https://webgr.irstea.fr/en/airGR/.

COSTA V and FERNANDES W (2017) Bayesian estimation of extreme flood quantiles using a rainfall-runoff model and a stochastic daily rainfall generator. Journal of Hydrology **554** 137–154.

D'ASARO F, GRILLONE G and HAWKINS RH (2014) Curve number: Empirical evaluation and comparison with curve number handbook tables in Sicily. Journal of Hydrology **19 (12)** 1–13.

DEPARTMENT OF ENVIRONMTAL AFFAIRS (DEA) and GEOTERRAIMAGE (PTY) LTD (GTI) (2015) *South African National Land Cover Dataset (2013/2014)*. Produced by GeoTerraImage Pty Ltd for the Department of Environmental Affairs, Pretoria, South Africa

DLAMINI NS (2019) *Development and assessment of an ensemble joint probability event based approach for design flood estimation in South Africa*. Master's dissertation, University of KwaZulu-Natal, Pietermaritzburg, South Africa.

DUNSMORE SJ, SCHULZE RE and SCHMIDT EJ (1986) *Antecedent soil moisture in design runoff volume estimation*. WRC Report No. 155/1/86, Water Research Commission, Pretoria, South Africa

DYE PJ and CROKE BF (2003) Evaluation of streamflow predictions by the IHACRES rainfall-runoff model in two South African catchments. Environmental Modelling and Software **18 (8)** 705–712.

FAULKNER D and WASS P (2005) Flood estimation by continuous simulation in the Don catchment, South Yorkshire, UK. Water and Environment Journal **19 (2)** 78–84.

FENNESSEY L and HAWKINS R (2001) *The NRCS curve number: A new look at an old tool.* Proceedings of Pennsylvania Stormwater Management Symposium, Villanova University, Pennsylvania, USA, 1–16.

FENNESSEY LA (2000) *The effect of the inflection angle, soil proximity, and location on runoff.* PhD thesis, Pennsylvania State University, Pennsylvania, USA.

FROST AJ, SRIKANTHAN R and COWPERTWAIT PSP (2004) *Stochastic generation of point rainfall data at subdaily timescales: A comparison of DRIP and NSRP*. Cooperative Reseach Centre for Catchment Hydrology, Monash University Australia, Melbourne, Australia.

GERICKE OJ and DU PLESSIS JA (2012) Evaluation of the standard design flood method in selected basins in South Africa. Journal of the South African Institution of Civil Engineering **54 (2)** 2–14.

GERICKE OJ (2016) *Estimation of catchment response time in medium to large catchment in South Africa*. Master's dissertation, University of Stellenbosch, Stellenbosch, South Africa.

GERICKE OJ and SMITHERS JC (2016) Derivation and verification of empirical catchment response time equations for medium to large catchments in South Africa. Hydrological Processes **30** 4384–4404.

GERICKE OJ and SMITHERS JC (2017) Direct estimation of catchment response time parameters in medium to large catchments using observed streamflow data. Hydrological Processes **31 (5)** 1125–1143.

GERICKE OJ (2018) Personal communication. Department of Civil Engineering, Central University of Technology, Bloemfontein, South Africa, 22 August 2018.

GIOIA A, IACOBELLIS V, MANFREDA S and FIORENTINO M (2008) Runoff thresholds in derived flood frequency distributions. Hydrology and Earth System Sciences **12 (6)** 1295–1307.

GÖRGENS A (2007) *Joint peak-volume (JPV) design flood hydrographs for South Africa*. WRC Report No. 1420/3/07, Water Research Commission, Pretoria, South Africa.

GÖRGENS A, LYONS S, HAYES L, MAKHABANE M and MALULEKE D (2007) *Modernised South African design flood practice in the context of dam safety*. WRC Report No. 1420/2/07, Water Research Commission, Pretoria, South Africa.

GREEN J, WALLAND D, NANDAKUMAR N and NATHAN R (2005) Temporal patterns for the derivation of PMPDF and PMF estimates in the GTSM region of Australia. Australian Journal of Water Resources **8 (2)** 111–121.

GÜNTNER A, OLSSON J, CALVER A and GANNON B (2001) Cascade-based disaggregation of continuous rainfall time series: The influence of climate. Hydrology and Earth System Sciences **5 (2)** 145–164.

HABERLANDT U and RADTKE I (2013) Derived flood frequency analysis using different model calibration strategies based on various types of rainfall-runoff data – a comparison. Hydrology and Earth System Sciences Discussions **10 (8)** 10379–10417.

HASSINI S and GUO Y (2017) Derived flood frequency distributions considering individual event hydrograph shapes. Journal of Hydrology **547** 296–308.

HAWKINS RH (1975) The importance of accurate curve numbers in the estimation of storm runoff. Water Resources Bulletin **11 (5)** 887–891.

HAWKINS RH (1993) Asymptotic determination of runoff curve numbers from data. Journal of Irrigation and Drainage Engineering **119 (2)** 334–345.

HAWKINS RH, WARD TJ, WOODWARD DE and MULLEM JAV (2009) *Curve number hydrology – state of practice*. ASCE, Virginia, USA.

HAWKINS RH (2014) Curve number method: Time to think anew? Journal of Hydrologic Engineering **19 (6)** 1059–1059.

HAWKINS RH (2019) Personal communication. Department of Hydrology and Water Resources, University of Arizona, Arizona, USA, 6 August 2019.

HINGRAY B and BEN HAHA M (2005) Statistical performances of various deterministic and stochastic models for rainfall series disaggregation. Atmospheric Research **77 (1-4)** 152–175.

HJELMFELT AT (1991) Investigation of curve number procedure. Journal of Hydraulic Engineering **117 (6)** 725–737.

HOSKING J and WALLIS J (1997) *Regional frequency analysis: An approach based on l-moments*, Cambridge University Press, Cambridge, UK.

HYDROLOGICAL RESPONSE UNIT (HRU) (1972) *Design flood determination in South Africa*. Report 1/72, University of Witwatersrand, Johannesburg, South Africa.

HUFF FA (1967) Time distribution of rainfall in heavy storms. Water Resources Research **3 (4)** 1007–1019.

HUFF FA and ANGEL JR (1992) *Rainfall frequency atlas of the Midwest*. Bulletin 70, Illinois State Water Survey, Champaign, IL, USA

JAIN MK, MISHRA SK, BABU PS and VENUGOPAL K (2006) On the Ia-S relation of the SCS-CN method. Nordic Hydrology **37 (3)** 261–275.

JAKEMAN A, LITTLEWOOD I and WHITEHEAD P (1990) Computation of the instantaneous unit hydrograph and identifiable component flows with application to two small upland catchments. Journal of Hydrology **117 (1-4)** 275–300.

JAKEMAN A and HORNBERGER G (1993) How much complexity is warranted in a rainfall-runoff model? Water Resources Research **29 (8)** 2637–2649.

JAKEMAN A and HORNBERGER G (1994) Reply to comment on "How much complexity is warranted in a rainfall-runoff model?" by AJ Jakeman and GM Hornberger. Water Resources Research **30 (12)** 3567–3567.

JAMES LD (1965) Using a digital computer to estimate the effects of urban development on flood peaks. Water Resources Research **1 (2)** 223–234.

KANG M, GOO J, SONG I, CHUN J, HER Y, HWANG S and PARK S (2013) Estimating design floods based on the critical storm duration for small watersheds. Journal of Hydro-Environment Research **7** 209–218.

KJELDSEN T, SVENSSON C and JONES D (2010) A joint probability approach to flood frequency estimation using Monte Carlo simulation. Proceedings of the BHS Third International Symposium: Role of Hydrology in Managing Consequences of a Changing Global Environment, British Hydrological Society, London, UK, 278–282.

KJELDSEN TR, LAMB R and BLAZKOVA S, (2014) Uncertainty in flood frequency analysis. In: BEVEN K and HALL J, *Applied uncertainty analysis for flood risk management*, Imperial College Press, London, UK, 153–197.

KNOESEN DM (2005) *The development and assessment of techniques for daily rainfall disaggregation in South Africa*. Master's dissertation, University of KwaZulu-Natal Pietermaritzburg, South Africa.

KNOESEN DM and SMITHERS JC (2008) The development and assessment of a regionalised daily rainfall disaggregation model for South Africa. Water SA **34 (3)** 323–330.

KOSSIERIS P, MAKROPOULOS C, ONOF C and KOUTSOYIANNIS D (2018) A rainfall disaggregation scheme for sub-hourly time scales: Coupling a Bartlett-Lewis based model with adjusting procedures. Journal of Hydrology **556** 980–992.

KOUTSOYIANNIS D and ONOF C (2001) Rainfall disaggregation using adjusting procedures on a Poisson cluster model. Journal of Hydrology **246 (1-4)** 109–122.

KOUTSOYIANNIS D, ONOF C and HOWARD SW (2003) Multivariate rainfall disaggregation at a fine timescale. Water Resources Research **39 (7)**.

KUCZERA G, LAMBERT M, HENEKER T, JENNINGS S, FROST A and COOMBES P (2006) Joint probability and design storms at the crossroads. Australasian Journal of Water Resources **10 (1)** 63–79.

LAMB R (1999) Calibration of a conceptual rainfall-runoff model for flood frequency estimation by continuous simulation. Water Resources Research **35** 3103–3114.

LAMB R and KAY AL (2004) Confidence intervals for a spatially generalized, continuous simulation flood frequency model for Great Britain. Water Resources Research **40 (W07501)** 1–13.

LAMB R, FAULKNER D, WASS P and CAMERON D (2016) Have applications of continuous rainfall-runoff simulation realized the vision for process-based flood frequency analysis? Hydrological Processes **30** 2463–2481.

LAMBOURNE J and STEPHENSON D (1987) Model study of the effect of temporal storm distributions on peak discharges and volumes. Hydrological Sciences Journal **32 (2)** 215–226.

LE MOINE N (2008) *Le bassin versant de surface vu par le souterrain: une voie d'amélioration des performances et du réalisme des modèles pluie-débit?* PhD thesis, UPMC, Cemagref Antony, Paris, France.

LEGATES DR and MCCABE JR GJ (1999) Evaluating the use of “goodness-of-fit” measures in hydrologic and hydroclimatic model validation. Water Resources Research **35 (1)** 233–241.

LI X, MESHGI A, WANG X, ZHANG J, TAY SHX, PIJCKE G, MANOCHA N, ONG M, NGUYEN M and BABOVIC V (2018) Three resampling approaches based on method of fragments for daily-to-subdaily precipitation disaggregation. International Journal of Climatology **38** e1119–e1138.

LING F, POKHREL P, COHEN W, PETERSON J, BLUNDY S and ROBINSON K (2015) *Revision Project 8: Use of continuous simulation models for design flood estimation*. Revision Project 12: Selection of an approach, Stage 3 Report, ARR Report Number P12/S3/008, Engineers Australia, Barton, ACT, Australia.

LYNCH S (2003) *Development of a raster database of annual, monthly and daily rainfall for southern Africa*. WRC Report No. 1156/1/03, Water Research Commission, Pretoria, South Africa.

MABILA NA (2019) *An assessment of simple continuous simulation modelling approaches for design flood estimation in South Africa*. Master's dissertation, University of KwaZulu-Natal, Pietermaritzburg, South Africa.

MAHARAJ U (2020) *An assessment of the performance of published and derived SCS curve numbers for design flood estimation in South Africa*. Master's dissertation, University of KwaZulu-Natal, Pietermaritzburg, South Africa.

MARSALEK J and WATT WE (1984) Design storms for urban drainage design. Canadian Journal of Civil Engineering **11 (3)** 574–584.

MISHRA SK and SINGH VP, (2003) SCS-CN method. In: SINGH VP, *Soil conservation service curve number (SCS-CN) methodology*, Kluwer Academic Publishers, Dordrecht, Netherlands, 84–145.

MISHRA SK, SURESH BABU P and SINGH VP (2007) *SCS-CN method revisited*, Water Resources Publications, Littleton, USA.

MORIASI DN, ARNOLD JG, VAN LIEW MW, BINGNER RL, HARMEL RD and VEITH TL (2007a) Model evaluation guidelines for systematic quantification of accuracy in watershed simulations. Transactions of the American Society of Agricultural and Biological Engineers **50 (3)** 885−900

MUTTIL N and JAYAWARDENA A (2008) Shuffled complex evolution model calibrating algorithm: Enhancing its robustness and efficiency. Hydrological Processes **22 (23)** 4628–4638.

NA W and YOO C (2018) Evaluation of rainfall temporal distribution models with annual maximum rainfall events in Seoul, Korea. Water **10 (10)** 1468.

NASH JE and SUTCLIFFE JV (1970) River flow forecasting through conceptual models Part I – a discussion of principles. Journal of Hydrology **10 (3)** 282–290.

NATHAN R and MCMAHON T (1990) Evaluation of automated techniques for baseflow and recession analyses. Water Resources Research **26 (7)** 1465–1473.

ODRY J and ARNAUD P (2017) Comparison of flood frequency analysis methods for ungauged catchments in France. Geosciences **7 (88)** 1–24.

ORMSBEE LE (1989) Rainfall disaggregation model for continuous hydrological modelling. Journal of Hydraulic Engineering **115 (4)** 507–525.

PABLO DB, GONZÁLEZ J and VALDÉS JB (2017) Sources of uncertainty in the NRCS CN model: Recognition and solutions. Hydrological Processes **31 (22)** 3898–3906.

PARKES B and DEMERITT D (2016) Defining the hundred year flood: A Bayesian approach for using historic data to reduce uncertainty in flood frequency estimates. Journal of Hydrology **540** 1189–1208.

PERRIN C, MICHEL C and ANDRÉASSIAN V (2003) Improvement of a parsimonious model for streamflow simulation. Journal of Hydrology **279 (1)** 275–289.

POKHREL P, LING F and COHEN W (2015) Testing of continuous simulation models for flood estimation. 36th Hydrology and Water Resources Symposium: The art and science of water, Engineers Australia, Hobart, Australia.

PONCE VM and HAWKINS RH (1996) Runoff curve number: Has it reached maturity? Journal of Hydrologic Engineering **1 (1)** 11–19.

PUI A, SHARMA A, MEHROTRA R, SIVAKUMAR B and JEREMIAH E (2012) A comparison of alternatives for daily to sub-daily rainfall disaggregation. Journal of Hydrology **470** 138–157

RAHMAN A, HOANG T, WEINMANN P and LAURENSON E (1998) J*oint probability approaches to design flood estimation: A review*. Report 98/8, Cooperative Research Centre for Catchment Hydrology, Department of Civil Engineering, Monash University, Australia, Melbourne, Australia.

RAHMAN A, WEINMANN PE, HOANG TMT and LAURENSON EM (2002) Monte Carlo simulation of flood frequency curves from rainfall. Journal of Hydrology **256 (3-4)** 196–210.

RAMLALL R (2020) *Assessing the performance of techniques for disaggregating daily rainfall for design flood estimation in South Africa*. Master's dissertation, University of KwaZulu-Natal Pietermaritzburg, South Africa.

RAUF A and RAHMAN A (2004) Study of fixed-duration design rainfalls in Australian rainfall-runoff and joint probability-based design rainfalls. Proceedings of the 2nd APHW Conference, Singapore.

REED D (1999) *Flood estimation handbook: Overview*, Institute of Hydrology Wallingford, Oxfordshire, UK.

REZAEI-SADR H and SHARIFI G (2018) Variation of runoff source areas under different soil wetness conditions in a semi-arid mountain region, Iran. Water SA **44 (2)** 1816–7950.

RODRIGUEZ-ITURBE I, COX DR and ISHAM V (1987) Some models for rainfall based on stochastic point processes. Proceedings of the Royal Society of London **A 410 (1839)** 269–288.

ROWE T, SMITHERS J, HORAN M and SCHULZE R (2018a) Development and assessment of rules to parameterise the ACRU model for design flood estimation. Water SA **44 (1)** 93–104.

ROWE TJ (2015) *Development and assessment of rules to parameterise the ACRU model for design flood estimation*. Master's dissertation, University of KwaZulu-Natal, Pietermartizburg, South Africa.

ROWE TJ and SMITHERS JC (2018) Continuous simulation modelling for design flood estimation – a South African perspective and recommendations. Water SA **44 (4)** 697–705.

ROWE TJ, SMITHERS JC, HORAN MJC and SCHULZE RE (2018b) Development and assessment of rules to parameterise the ACRU model for design flood estimation. Water SA **44 (1)** 93–104.

ROWE TJ (2019) *Development and assessment of an improved continuous simulation modelling system for design flood estimation in South Africa using the ACRU model.* PhD thesis, University of KwaZulu-Natal, Pietermaritzburg, South Africa.

SOUTH AFRICAN NATIONAL ROADS AGENCY LIMITED (SANRAL) (2013) *Drainage manual*, 6th ed., South African National Roads Agency Ltd, Pretoria, South Africa.

SAVVIDOU E, EFSTRATIADIS A, KOUSSIS AD, KOUKOUVINOS A and SKARLATOS D (2016) A curve number approach to formulate hydrological response units within distributed hydrological modelling. Hydrology and Earth System Sciences. DOI: 10.5194/hess-2016-627.

SCHMIDT EJ and SCHULZE RE (1984) *Improved estimation of peak flow rates using the modified SCS lag equations*. ACRU Report No. 17, Department of Agricultural Engineering, University of Natal, Pietermaritzburg, South Africa.

SCHMIDT EJ and SCHULZE RE (1987) *Flood volume and peak discharge from small catchments in Southern Africa based on the SCS technique*. WRC Report No. TT 31/87, Water Research Commission, Pretoria, South Africa.

SCHMIDT EJ, SCHULZE RE and DENT MC (1987) *Flood volume and peak discharge from small catchments in Southern Africa, based on the SCS technique*. Appendices, Water Research Commission, Pretoria, South Africa.

SCHNEIDER LE and MCCUEN RH (2005) Statistical guidelines for curve number generation. Journal of Irrigation and Drainage Engineering **131 (3)** 282–290.

SCHULZE RE (1979) *Estimation of volume and rate of runoff in small catchments in South Africa based on the SCS technique.* Department of Agricultural Engineering, University of Natal, Pietermaritzburg, South Africa.

SCHULZE RE and ARNOLD H (1979) *Estimation of volume and rate of runoff in small catchments in South Africa, based on the SCS technique*. ACRU Report No. 8, University of Natal, Pietermaritzburg, South Africa.

SCHULZE RE (1982) *Adapting the SCS stormflow equation for application to specific events by soil moisture budgeting*. University of Natal: Department of Agricultural Engineering, Pietermaritzburg, South Africa.

SCHULZE RE (1984) *Hydrological models for application to small rural catchments in Southern Africa: Refinements and development*. WRC Report No. 63/2/84, Water Research Commission, Pretoria, South Africa.

SCHULZE RE and SCHMIDT EJ (1984) *Improved estimates of peak flow rates using modified SCS lag equations.* WRC Report No. 63/1/84, Water Research Commission, Pretoria, South Africa.

SCHULZE RE and SCHMIDT EJ (1987) *Flood volume and peak discharge from small catchments in Southern Africa, based on the SCS Technique*. WRC Report No. TT 33/87, Water Research Commission, Pretoria, South Africa.

SCHULZE RE (1989) Non-stationary catchment responses and other problems in determining flood series: A case for a simulation modelling approach. In: KIENZLE SW and MAAREN H, Proceedings of Fourth South African National Hydrological Symposium, SANCIAHS, Pretoria, 135–157.

SCHULZE RE, SCHMIDT EJ and SMITHERS JC (1992) *PC-based SCS design flood estimates for small catchments in southern Africa: SCS-SA user manual.* ACRU Report No. 40, Department of Agricultural Engineering, University of Natal, Pietermaritzburg, South Africa.

SCHULZE RE and HOHLS BC (1993) A generic hydrological land cover and land use classification with decision support systems for use in models. Proceedings of the 6th South African National Hydrology Symposium, University of Natal: Department of Agricultural Engineering, Pietermaritzburg, South Africa, 547–555.

SCHULZE RE, ANGUS GR, LYNCH SD and SMITHERS JC (1994) *ACRU: Background, concepts and theory.* WRC Report No. 154/1/89, Water Research Commission, Pretoria, South Africa.

SCHULZE RE (1995) *Hydrology and agrohydrology: A text to accompany the ACRU 3.00 agrohydrological modelling system.* WRC Report No. TT 69/95, Water Research Commission, Pretoria, South Africa.

SCHULZE RE, SCHMIDT EJ and SMITHERS JC (2004) *PC-based SCS design flood estimates for small catchments in southern Africa: Visual SCS-SA user manual (Version 1.0).* ACRUcons Report No. 52, School of Bioresources Engineering and Environmental Hydrology, University of KwaZulu-Natal, Pietermaritzburg, South Africa.

SCHULZE RE (2007) *South African atlas of climatology and agrohydrology.* WRC Report No. 1489/1/06, Water Research Commission, Pretoria, South Africa.

SCHULZE RE (2012) Mapping hydrological soil groups over South Africa for use with the SCS – SA design hydrograph technique: Methodology and results. 16th SANCIAHS National Hydrology Symposium 2012, SANCIAHS, Pietermaritzburg, South Africa.

SCHULZE RE (2013) *Modelling impacts of land use on hydrological responses in South Africa with the ACRU model by sub-delineation of quinary catchments into land use dependent hydrological response units.* Internal Report, School of Agricultural, Earth and Environmental Science, University of KwaZulu-Natal, Pietermaritzburg, South Africa.

SCHULZE RE and SCHÜTTE S (2018) *Mapping SCS hydrological soil groups over South Africa at terrain unit resolution*. Internal Report, Centre for Water Resources Research, School of Agricultural, Earth and Environmental Sciences, University of KwaZulu-Natal, Pietermaritzburg, South Africa.

SOIL CONSERVATION SERVICE (SCS) (1956) *Hydrology national engineering handbook*, *Supplement A, Section 4*, Soil Conservation Service, US Department of Agriculture, Washington, DC, USA.

SCS (1972) *National engineering handbook, Section 4*, Soil Conservation Service, US Department of Agriculture, Washington, DC, USA.

SOIL AND IRRIGATION RESEARCH INSTITUTE (SIRI) (1987) *Land type series*. *Memoirs on the Agricultural Natural Resources of South Africa*, Department of Agriculture and Water Supply, Soil and Irrigation Research Institute, Pretoria, South Africa.

SIVAKUMAR B, SOROOSHIAN S, GUPTA HV and GAO X (2001) A chaotic approach to rainfall disaggregation. Water Resources Research **37 (1)** 61–72.

SMITHERS JC, SCHULZE RE and KIENZLE SW (1997) Design flood estimation using a modelling approach. In: ROSBJERG D, BOUTAYEB N, GUSTARD A, KUNDZEWICZ ZW and RASMUSSEN PF, eds, Sustainability of water resources under increasing uncertainty. The International Association of Hydrological Sciences Publication **240** 365–376.

SMITHERS JC (1998) *Development and evaluation of techniques for estimating short duration design rainfall in South Africa*. PhD thesis, University of Natal, Pietermaritzburg, South Africa.

SMITHERS JC and SCHULZE RE (2000) *Development and evaluation of techniques for estimating short duration design rainfall in South Africa*. WRC Report No. 681/1/00, Water Research Commission, Pretoria, South Africa.

SMITHERS JC and SCHULZE RE (2001) A methodology for the estimation of short duration design storms in South Africa using a regional approach based on L-moments. Journal of Hydrology **241 (1-2)** 42–52.

SMITHERS JC, SCHULZE RE, PIKE A and JEWITT GPW (2001) A hydrological perspective of the February 2000 floods: A case study in the Sabie River catchment. Water SA **27 (3)** 325–332.

SMITHERS JC, PEGRAM GGS and SCHULZE RE (2002) Design rainfall estimation in South Africa using Bartlett-Lewis rectangular pulse rainfall models. Journal of Hydrology **258 (1-4)** 83–99.

SMITHERS JC and SCHULZE RE (2002) *Design rainfall and flood estimation in South Africa.* WRC Project No. K5/1060, WRC Report No. 1060/01/03. Water Research Commission, Pretoria, South Africa.

SMITHERS JC and SCHULZE R (2003) *Design rainfall and flood estimation in South Africa.* WRC Project No. K5/1060, Water Research Commission, Pretoria, South Africa.

SMITHERS JC and SCHULZE RE (2004a) The estimation of design rainfalls for South Africa using a regional scale invariant approach. Water SA **30 (4)** 435–444.

SMITHERS JC and SCHULZE RE (2004b) *ACRU agrohydrological modelling system: User manual (Version 4)*. School of Bioresources Engineering and Environmental Hydrology, University of KwaZulu-Natal, Pietermaritzburg, South Africa.

SMITHERS JC, CHETTY KT, FREZGHI MS, KNOESEN DM and TEWOLDE MH (2007) *Development and assessment of a continuous simulation modelling system for design flood estimation.* WRC Report No. 1318/1/07, Water Research Commission, Pretoria, South Africa.

SMITHERS JC (2012) Review: Methods for design flood estimation in South Africa. Water SA **38 (4)** 633–646.

SMITHERS JC, CHETTY KT, FREZGHI MS, KNOESEN DM and TEWOLDE MH (2013) Development and assessment of a daily time-step continuous simulation modelling approach for design flood estimation at ungauged locations: ACRU model and Thukela Catchment case study. Water SA **30 (4)** 449–458.

SMITHERS JC, STREATFIELD J, GRAY RP and OAKES EGM (2015) Performance of regional flood frequency analysis methods in KwaZulu-Natal, South Africa. Water SA **41 (3)** 390–397.

SMITHERS JC, GÖRGENS A, GERICKE J, JONKER V and ROBERTS CPR (2016) *The Initiation of a national flood studies programme for South Africa.* South African National Committee on Large Dams (SANCOLD), Pretoria, South Africa.

STEWART D, CANFIELD E and HAWKINS R (2011) Curve number determination methods and uncertainty in hydrologic soil groups from semiarid watershed data. Journal of Hydrologic Engineering **17 (11)** 1180–1187.

TEDELA NH, MCCUTCHEON SC, RASMUSSEN TC, HAWKINS RH, SWANK WT, CAMPBELL JL, ADAMS MB, JACKSON CR and TOLLNER EW (2011) Runoff curve numbers for 10 small forested watersheds in the mountains of the eastern United States. Journal of Hydrologic Engineering **17 (11)** 1188–1198.

UNITED STATES DEPARTMENT OF AGRICULTURE (USDA) (1959) *National Engineering Handbook (NEH) Hydrology (Section 4)*. United States Department of Agriculture, Soil Conservation Service, Washington, DC, USA.

VAN DER SPUY D and RADDEMEYER P (2014) *Flood frequency estimation methods as applied in the Department of Water Affairs.* Department of Water Affairs, Pretoria, South Africa.

VAN VUUREN S, VAN DIJK M and COETZEE G (2013) *Status review and requirements of overhauling flood determination methods in South Africa*. WRC Project No. K8/994 (TT 563/13), Water Research Commission, Pretoria, South Africa.

VAZE J, JORDAN P, BEECHAM R, FROST A and SUMMERELL G (2012) Guidelines for rainfall-runoff modelling: Towards best practice model application. eWater Cooperative Research Centre, 2011. DOI: http://hdl.handle.net/102.100.100/102141.

VOGEL R, CHAPRA S and LIMBRUNNER J, (2005) *A parsimonious watershed model*, Watershed Models, CRC Press, 549–567.

WALKER S and TSUBO M (2003) *Estimation of rainfall intensity for potential crop production on clay soil with in-field water harvesting practices in a semi-arid area.* WRC Report No. 1049/1/02, Water Research Commission, Pretoria, South Africa.

WARD PJ, KUMMU M and LALL U (2016) Flood frequencies and durations and their response to El Niño southern Oscillation: Global analysis. Journal of Hydrology **539** 355–378.

WEDDEPOHL JP (1988) *Design rainfall distributions for southern Africa.* Master's dissertation, University of Natal, Pietermaritzburg, South Africa.

WOODWARD D (2017) *Proposed revision of NRCS curve numbers*. CWEA Storm Water Committee, ASCE-NRCS Task Group, Maryland, USA.

WOODWARD DE, HAWKINS RH, HJELMFELT A, VAN MULLEM J and QUAN QD (2002) *Curve number method: Origins, applications and limitations.* Second Federal Interagency Hydrologic Modeling Conference, US Geological Survey Advisory Committee on Water Information, Nevada, USA.

ZAMAN MA, RAHMAN A and HADDAD K (2012) Regional flood frequency analysis in arid regions: A case study for Australia. Journal of Hydrology **475** 74–83.